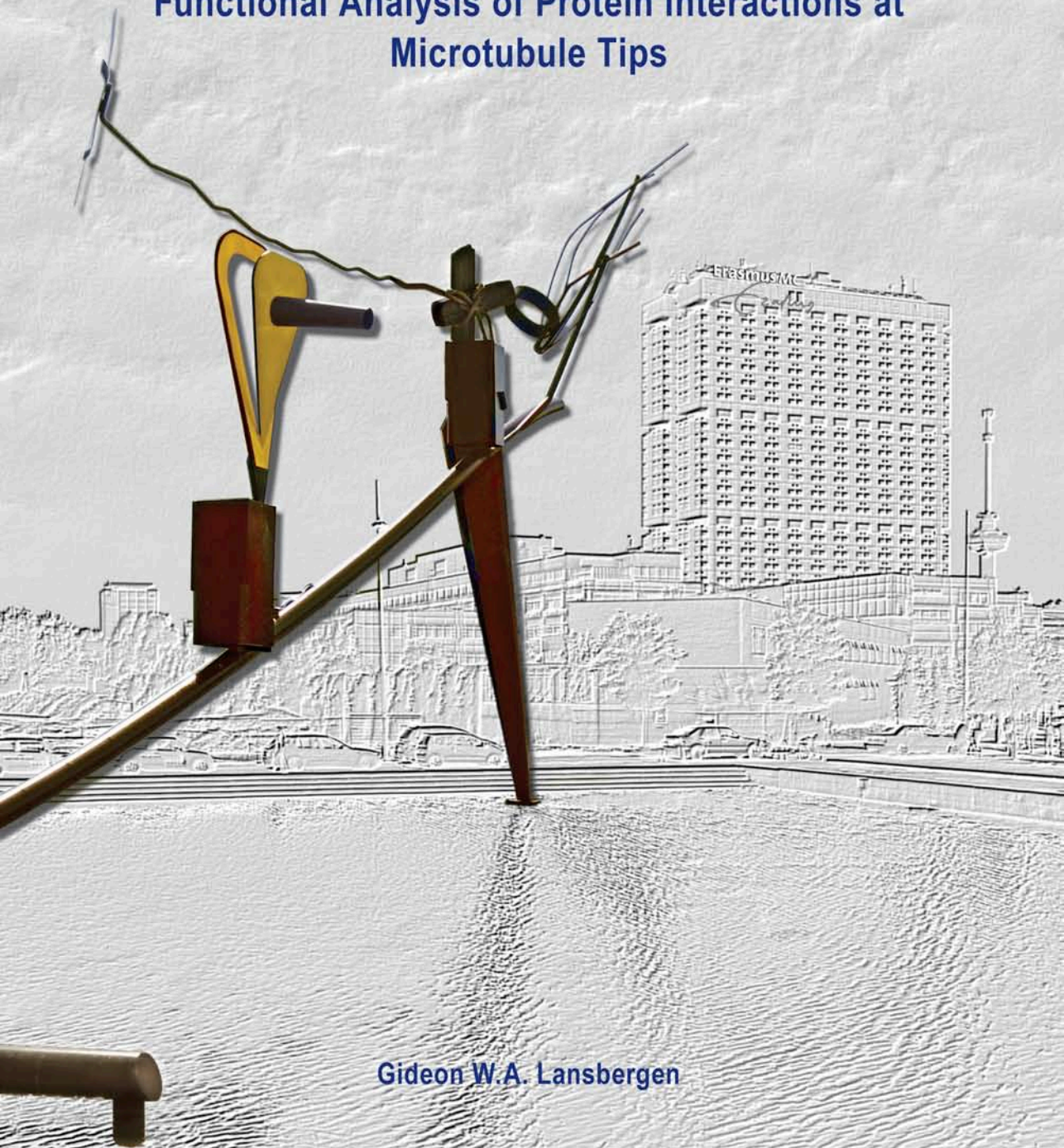


Functional Analysis of Protein Interactions at Microtubule Tips



Gideon W.A. Lansbergen



Functional Analysis of Protein Interactions at Microtubule Tips

Gideon W.A. Lansbergen

© 2005 Gideon W.A. Lansbergen

ISBN-10: 90-9020233-1

ISBN-13: 978-90-9020233-4

Thesis lay-out: Gideon Lansbergen

Graphical assistance: Tom de Vries Lentsch

Printed by PrintPartners Ipskamp, Enschede

The studies presented in this thesis were performed in the Department of Cell Biology of the Erasmus MC in Rotterdam, The Netherlands. Research performed in this thesis was supported by the Nederlandse Organisatie voor Wetenschappelijk Onderzoek (NWO).

Printing of the thesis was partially supported by the J.E. Jurriaanse Stichting and Alzheimer Nederland.

Cover: Tom de Vries Lentsch

based on sculpture 'Zonder Titel', artist: Auke de Vries.

Artwork is situated in front of Netherlands Architecture Institute near the Erasmus University Medical Center Rotterdam.

Functional Analysis of Protein Interactions at Microtubule Tips

De functionele analyse van eiwit interacties aan microtubuli uiteinden

Proefschrift

ter verkrijging van de graad van doctor aan de
Erasmus Universiteit Rotterdam
op gezag van de
rector magnificus

Prof.dr. S.W.J. Lamberts

en volgens besluit van het College voor Promoties.

De openbare verdediging zal plaatsvinden op

woensdag 25 januari 2006 om 11:45 uur

door

Gideon Willebrordus Adrianus Lansbergen

geboren te Rotterdam

Promotiecommissie

Promotor: Prof.dr. F.G. Grosveld

Overige leden: Prof.dr. J.G.G. Borst
Dr.ir. N.J. Galjart
Dr.ir. D.N. Meijer

Copromotor: Dr. A.S. Akhmanova

Voor Marieke en mijn ouders

Index:

Scope of the thesis	7
Chapter 1	
Introduction into the cytoskeleton	11
Chapter 2	
Conformational changes in CLIP-170 regulate its binding to microtubules and dynactin localization.	43
Chapter 3	
EB1 and EB3 control CLIP dissociation from the ends of growing microtubules.	57
Chapter 4	
CLASP1 and CLASP2 bind to EB1 and regulate microtubule plus-end dynamics at the cell cortex.	71
Chapter 5	
CLASPs attach microtubule plus ends to the cell cortex through a complex with LL5 β and ELKS.	87
Chapter 6	
Mass spectrometry analysis of membrane-bound protein complexes cross-linked with formaldehyde: identification of liprin- α 1 as a component of LL5 β -containing cortical clusters in HeLa cells	115
Chapter 7	
Discussion	127
Appendixes	153
Summary	160
Samenvatting	162
Curriculum Vitae & Publications	164
Dankwoord	166

Scope of the thesis

Microtubules are a part of the cytoskeleton involved in many essential processes, such as intracellular transport of cargoes, cell migration, positioning of cellular organelles and formation of the mitotic spindle for chromosome segregation. The fast growing end of microtubules (the plus-end) can interact with specific microtubule plus-end binding proteins (also known as plus-end tracking proteins, or +TIPs). +TIPs participate in microtubule interactions with different cellular structures and control microtubule dynamics. This thesis describes the functional analysis of protein interactions at the microtubule plus-ends.

Chapter 1 is an introduction into the cytoskeleton. It gives an overview of the three types of cytoskeletal filaments (intermediate filaments, actin filaments and microtubules) and diverse microtubule associated proteins (MAPs), including microtubule associated motors, general microtubule associated proteins and microtubule plus-end binding proteins.

Chapter 2 describes the microtubule plus-end tracking protein CLIP-170 (cytoplasmic linker protein of 170 kDa), which regulates its association with microtubules by changing its conformation. CLIP-170 possesses two NH₂-terminal CAP-Gly domains that are involved in the interaction with microtubules, and two COOH-terminal metal binding domains, which interact with various partners. The NH₂ terminus of CLIP-170 binds directly to the COOH terminus through its first metal-binding domain. Also the dynactin subunit p150^{Glued} and LIS1 interact with the COOH terminus of CLIP-170, but depend on the second metal-binding domain. The folded head-to-tail conformation of CLIP-170 inhibits microtubule association and also interferes with the binding of dynactin and LIS1 to the CLIP-170 COOH terminus.

Chapter 3 reports the functional relationship of CLIP-170 and CLIP-115 with the three EB family members EB1, EB2 and EB3. CLIPs bind directly to the COOH terminus of the EB proteins. This interaction contributes to CLIP-170 localization and enhances its intrinsic affinity for growing microtubule ends.

Chapter 4 shows that the two CLIP-associating proteins, CLASP1 and CLASP2 play redundant roles in regulating the density, stability and dynamics of interphase microtubules. CLASPs stabilize microtubules at the cell periphery, possibly through forming a complex with EB1 at microtubule tips. The association of CLASPs with the cortex, which is microtubule-independent, mediates interactions between microtubule plus-ends and the cell cortex.

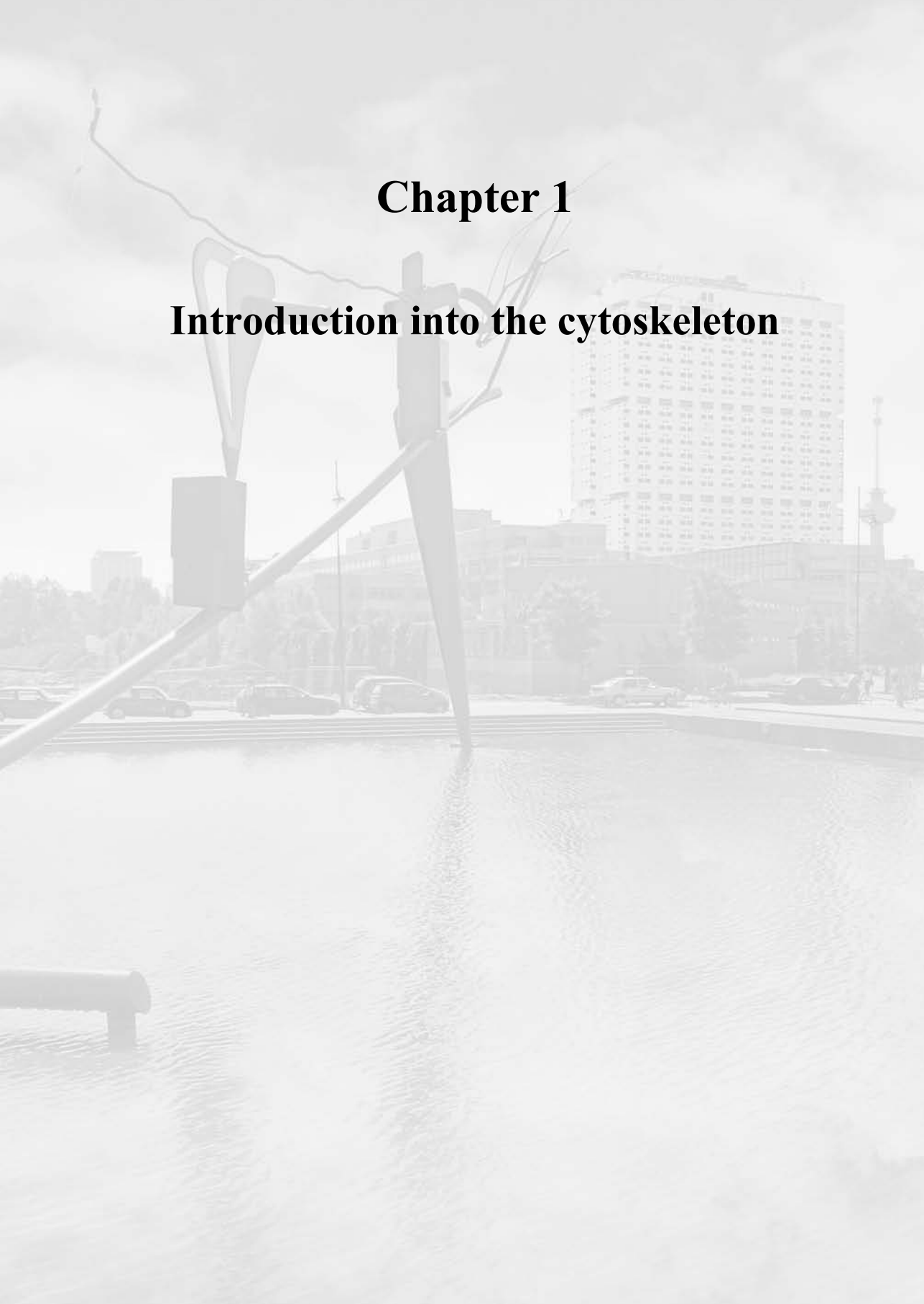
Chapter 5 describes the identification of two novel binding partners of CLASP1 and CLASP2 using pull down assays coupled to mass spectrometry. These partners, LL5 β and ELKS, are both required for the normal cortical CLASP accumulation and microtubule organisation. Since LL5 β contains a PIP3-binding pleckstrin homology (PH) domain it is

proposed that LL5 β and ELKS can form a PIP3-regulated cortical platform, to which CLASPs attach distal microtubule ends.

Chapter 6 describes an optimised procedure for using mass spectrometry to identify the components of membrane-bound protein complexes. For the cortical protein LL5 β , which is involved in attaching microtubules to the membrane, it is shown that at least one of the isolated potential partners, liprin- α 1, is indeed a component of the LL5 β clusters at the margin of HeLa cells.

Chapter 1

Introduction into the cytoskeleton



1.1 The cytoskeleton

Living cells are highly complex systems. Eukaryotic cells, such as human cells, have specialized organelles and structures with specific vital functions. For instance, mitochondria take care of the energy metabolism, the cell nucleus is the place of DNA storage and RNA transcription, the endoplasmic reticulum and the Golgi apparatus harbour the machinery for synthesis of glycoproteins and lipids and the cytoskeleton is necessary for maintaining cell morphology and intracellular transport (Fig. 1). This thesis will focuss on the last structure, the cytoskeleton. All eukaryotic cells have a cytoskeleton, from unicellular organisms such as yeasts to multicellular organisms such as plants, flies and mammals. Many cytoskeletal components are highly conserved in evolution, indicating that they are essential for the normal cell functioning.

The cytoskeleton is involved in specialized functions of diverse cell types. For example, cell migration during embryonic development, sperm cell motility, chromosome segregation during cell division, muscle contraction, intracellular vesicle transport, cell morphology and strength all depend on the cytoskeleton (Janmey 1991). Because the cytoskeleton is involved in so many essential processes, it is not surprising that its malfunctioning causes cell disorders and human diseases. Today, many diseases, such as cardiovascular syndromes, liver cirrhosis, neurodegeneration, pulmonary fibrosis, blistering skin diseases and cancer have been associated with abnormalities in cytoskeletal proteins. Research into the function, control and maintenance of the cytoskeleton is therefore of great interest. For instance, frequently used cancer therapies are based on application of anti-cytoskeletal drugs that inhibit cell division. In future, the basic knowledge about the cytoskeleton might lead to more specific drugs (Fuchs and Cleveland 1998; Benitez-King et al. 2004; Ramaekers and Bosman 2004).

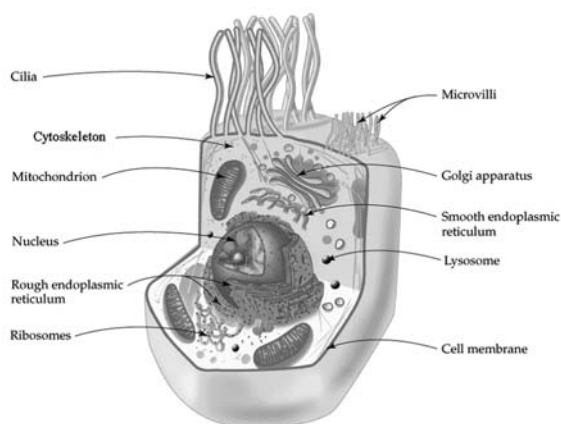


Figure 1: The major features of eukaryotic cells.

The drawing depicts an intestinal animal cell with its major organelles and structures. Microvilli and cilia, for instance, are cell structures dense with cytoskeleton filaments, especially abundant on the absorptive surface of intestinal epithelial cells.

(*Fundamentals of General, Organic, and Biological Chemistry*; McMurry and Castellion; 1999)

There are three types of cytoskeletal structures or filaments: the intermediate filaments, the microfilaments (or actin) and the microtubules (Fig. 2). All these filaments, which are constructed from smaller building blocks, play various roles within the cell. What makes them all highly important are their dynamics, their multi-functionality and their ability to cooperate with each other in different parts of the cell. Interplay between different cytoskeletal elements is regulated by a variety of proteins, protein complexes, organelles and other specific targets within the cell. Next, the cytoskeletal structures will be discussed in more detail.

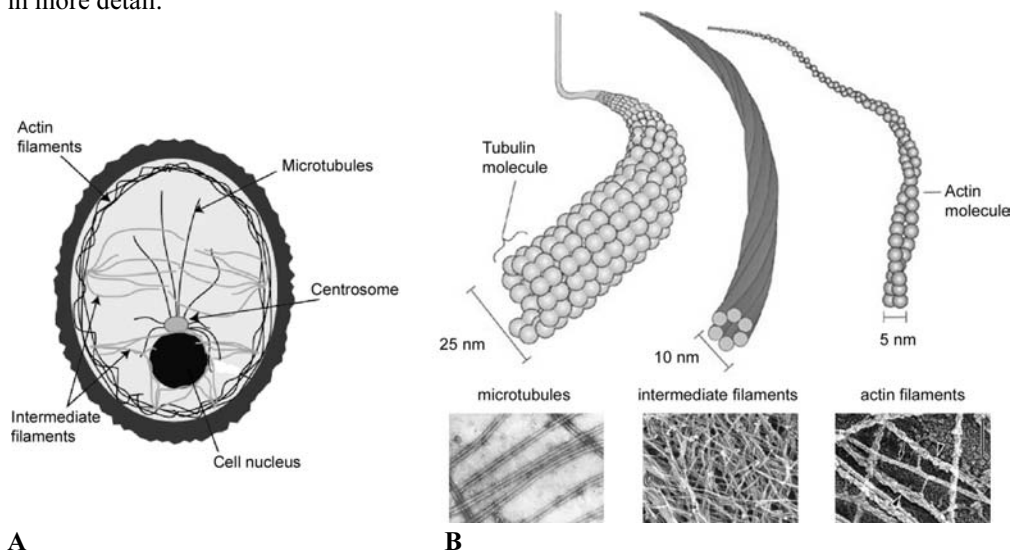


Figure 2: Components of the cytoskeleton.

(A) The cytoskeleton of a cell is constructed from three major networks: actin filaments, intermediate filaments and microtubules. Each one has its own specific function and localization within cells.

(B) Schematic representation with electron micrographs of the three types of filaments. Microtubules have the largest diameter of about 25 nm, the rope-like intermediate filaments about 10 nm and the actin filaments about 5 nm in diameter. (*Neuroscience: Exploring the Brain*, 2nd Edition 2000; <http://www.imb-jena.de/~kboehm/mt-neg.html>; <http://www.borisylab.northwestern.edu>; <http://www.sparknotes.com/biology/cellstructure/intracellularcomponents/section1.html>)

1.1.1 Intermediate filaments

Intermediate filaments are rope-like fibres with a diameter of around 10 nm (Fig. 2B). The main function of these filaments is to give cells mechanical stability and strength. A diverse group of intermediate filaments are expressed in different cell types: nuclear filaments, epithelial filaments (cytokeratins) or neurofilaments. The fibres are constructed by a large and heterogeneous family of proteins, which includes lamins, keratins and vimentins. The proteins of this family can dimerize by their extended central α -helical domains to form

parallel coiled coils. Subsequently, these dimers form anti-parallel tetramers that pack together laterally to shape a filament without polarity (Stewart 1993; Helfand et al. 2004; Herrmann and Aebi 2004; Lariviere and Julien 2004). In contrast to microtubules or actin, intermediate filaments are very stable structures that display little dynamic behaviour. This property is extremely well suited to provide mechanical strength to cells and tissues. Cytoplasmic intermediate filaments, composed of keratin and vimentin, form a complex network, which extends from the plasma membrane to the cell nucleus and is important for proper nuclear positioning and anchoring. Intermediate filaments can interact with different cellular components. A number of proteins, including plectin, bulbous pemphigoid antigen 1 (BPAG1) and desmoplakin, binds specifically to these filaments (Bousquet and Coulombe 1996). Moreover, intermediate filaments can interact with microtubules as well as actin fibres to form an integrated cytoskeletal network, which plays a role in cell migration and cell-substratum contacts (Fuchs and Yang 1999).

1.1.2 Actin filaments

Another essential component of the cytoskeleton is actin, which plays a crucial role in eukaryotic cells. Actin consists of two different forms: globular monomeric (G) actin and filamentous polymeric (F) actin. Actin monomers assemble into a polarized two-stranded rod-like helical filament of 5-7 nm in diameter (Fig. 2B). Actin polymerization can take place at a fast-growing plus-end (the barbed end) and at a slow-growing minus-end (the pointed end) and is facilitated by specific proteins that bind to the free monomers. The actin subunits are bound to adenosine triphosphate (ATP), which controls the binding affinity for the neighbouring actin subunits within filaments. As the filament matures, actin-bound ATP is hydrolysed into adenosine diphosphate (ADP), which reduces the binding affinity of actin monomers and makes them more likely to disassemble from the pointed end (Reisler 1993). Subsequently, actin monomers undergo recycling by nucleotide exchange that regenerates ATP-bound monomers for new rounds of polymerization. The continued process of G-actin assembly and disassembly at the ends of actin filaments results in a constant size of the filament. This steady state with a net flux of actin subunits through the polymer is also known as treadmilling (Cleveland 1982; Carlier 1990; Carlier 1992).

The function of actin filaments (or microfilaments) is quite diverse. For instance, they are involved in the generation and maintenance of cell morphology and polarity, endocytosis and intracellular trafficking, in motility and cell division (Furukawa and Fechheimer 1997). Actin filaments are very dynamic; they are often closely located near the plasma membrane, where they induce structures like the lamellipodia and filopodia (Luna and Hitt 1992). They can form different arrays in cells: a weblike (gel-like) network at the

cell cortex, and two types of bundles, such as the contractile stress fibres and the tight parallel bundles in filopodia. In muscles, actin filaments are the most abundant cytoskeletal structures, which together with myosin motors are responsible for the muscle contraction. They are arranged in parallel arrays and, in contrast to similar structures in non-muscle cells, are unusually stable (Rayment et al. 1993). There are also many other proteins which specifically bind to actin monomers and filaments (Hartwig and Kwiatkowski 1991; Cunningham et al. 1992; Winder and Ayscough 2005). These actin-binding proteins (or ABPs) can use microfilaments as a scaffold or regulate their dynamics. To start, there is a whole group of motors, myosins, which can move along the actin filaments using ATP hydrolysis. With the aid of myosin motors, specific cargoes can be transported or adjacent actin filaments can be moved against each other. The human genome contains almost 40 myosin genes, representing 12 different myosin classes (Mermall et al. 1998; Hodge and Cope 2000; Sellers 2000; Krendel and Mooseker 2005).

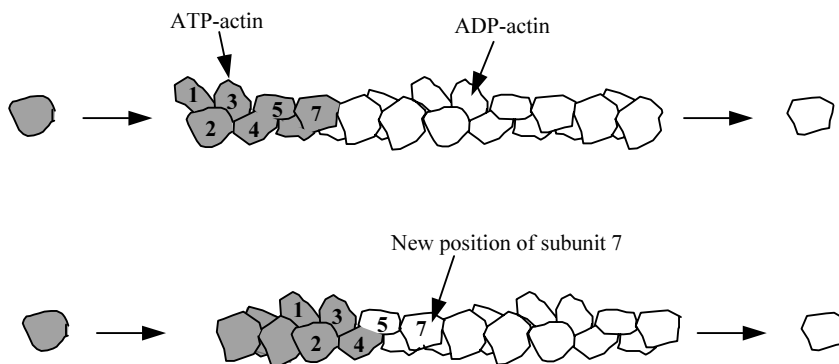


Figure 3: Treadmilling. ATP-bound actin assembles at the barbed (plus) end of the actin filament, while ADP-bound actin is released from the pointed (minus) end. This continued process results in a constant size of the filament, which means that any particular monomer recycles between the barbed end and the pointed end. This mechanism takes place in cells and is for instance responsible for the protrusion of the leading edge of moving cells.

(<http://www.bms.ed.ac.uk/research/others/smaciver/lectures/Cs2.htm>)

Another group of ABPs are proteins involved in regulating actin monomer assembly. Thymosin, for instance, binds to actin monomers and thereby prevents the assembly of the polymer. This is necessary because of the high concentration of actin monomers in the cytoplasm. Profilin, in contrast, promotes the assembly of ATP-bound actin monomers into polymerized filaments, and cofilin enhances the rate of disassembly of ADP-actin from the minus end of actin filaments (Carlier and Pantaloni 1994; Ono 2003). Finally, to start making new filaments, the Arp2/3 protein complex is involved in the nucleation of actin. When the Arp2/3 complex binds G-actin, it acts as a pointed-end-capping protein which promotes rapid growth of the filament from its barbed end (Pollard and Beltzner 2002; dos

Remedios et al. 2003; Winder and Ayscough 2005). Another family of proteins, involved in actin nucleation, are formins. This group of multi-domain proteins is defined by strongly conserved FH2 domains, which dimerize to induce nucleation of actin filaments. In contrast to the Arp2/3 complex, which is activated by existing filaments to nucleate branches from parent filaments, formins nucleate from monomers alone and generate straight filaments (Pring et al. 2003; Zigmond 2004).

Furthermore, there is a whole list of proteins involved in actin cross-linking, membrane-anchoring, filament stabilization or bundling and linking it to other cytoskeletal structures. Clearly, the actin network and its binding partners are of great importance for the regulation of cell structure and polarity.

1.1.3 Microtubules

The third cytoskeletal structure that will be discussed are microtubules. Microtubules are involved in a lot of essential processes, like intracellular transport of cargoes, cell migration, positioning of cellular organelles and formation of the mitotic spindle for chromosome segregation. Microtubules were first discovered in unicellular eukaryotes as the main component of flagella, which enable these cells to swim. Like actin filaments, microtubules are dynamic structures, which are formed by polymerization of specific monomers, tubulins. Two closely related tubulin monomers, α -tubulin and β -tubulin, can assemble into heterodimers with the help of several tubulin folding cofactors (Tian et al. 1997; Nolasco et al. 2005). The heterodimerized tubulins can subsequently polymerize in a head-to-tail fashion into linear protofilaments. Generally, 13 of these protofilaments associate laterally and with the same polarity to shape a hollow tube, the microtubule. Microtubules have a polarized structure with a diameter of 20-25 nm and, like actin, they have a fast growing plus-end and a slow growing minus-end, where the tubulin heterodimers can be incorporated (Fig. 2B) (Wade and Hyman 1997). Both α - and β -tubulin contain guanosine triphosphate (GTP), but only the β -tubulin-bound GTP can be hydrolysed. Microtubule plus-ends, the place of tubulin dimer addition *in vivo*, have β -tubulin subunits facing outside. In freshly assembled tubulin heterodimers, β -tubulin is in the GTP form. In this way the growing end of the microtubule is provided with a GTP-cap, which prevents it from shrinking. During polymerization, the α -tubulin part of the heterodimer binds to the β -tubulin at the microtubule plus-end. This binding triggers hydrolysis of β -tubulin-bound GTP to guanosine diphosphate (GDP) (Erickson and O'Brien 1992; Anders and Botstein 2001). If hydrolysis is faster than polymerisation, the microtubule will lose its GTP-cap; it will then become unstable and will start to depolymerise from the plus-end. On the other hand, if hydrolysis lags behind polymerization, the GTP-cap will form and make the microtubule

more stable. In certain cases GTP-bound heterodimers will assemble at the plus-end, while GDP-bound heterodimers are released from the minus end: a process which is comparable with treadmilling of actin filaments (Fig. 3) (Howard and Hyman 2003). Since microtubules can grow (polymerize) or shrink (depolymerize) very rapidly, the cell is able to re-arrange its microtubule network very rapidly. When a microtubule shifts from a growing phase to a shrinking phase, this is called catastrophe. The opposite transition, when a microtubule starts growing again after a phase of shrinking, is called rescue. The process of switching between these different microtubule states is called dynamic instability (Cassimeris 1993; Desai and Mitchison 1997).

In many cell types, microtubules are nucleated at the centrosome, or the microtubule organizing centre (MTOC) near the cell nucleus (Fig. 2a). The MTOC contains γ -tubulin protein complexes that form a ring-like structure and serve as templates to nucleate microtubules with 13 protofilaments. All microtubules are attached to the MTOC with their minus-ends, while the plus-ends point outward and grow toward the cell periphery (Job et al. 2003; Aldaz et al. 2005). There the microtubules can search and capture different targets within the cell. This search-and-capture process can be random in the cytoplasm, but can also be regulated by specific proteins which guide the microtubule to certain contact sites like the cell cortex (Mimori-Kiyosue and Tsukita 2003).

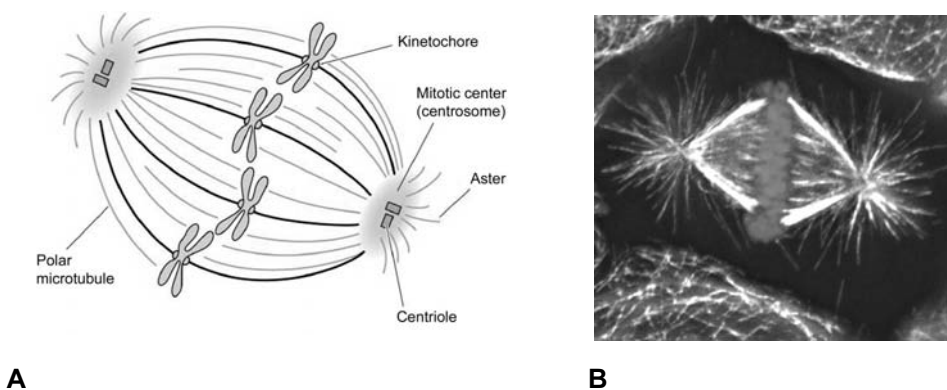


Figure 4: Mitotic spindle

(A) Diagram of the mitotic spindle in a eukaryotic cell in metaphase. The spindle consists of two opposing centrosomes or spindle poles, where the minus ends of the microtubules are anchored. The astral microtubules radiate in all directions from the centrosomes; they position the spindle and contribute to the forces that separate the poles. Polar microtubules can either be attached to chromosome kinetochores or stay unbound at the equator of the spindle to be responsible for the symmetrical, bipolar shape of the spindle. (B) A picture of a metaphase cell stained for tubulin and DNA. (Sinauer Associates 1998; http://raven.zoology.washington.edu/celldynamics/events/workshops/archive/2003/cytomod_abstracts/DCompton)

The microtubule network can also be dramatically reorganized into an important machinery that is essential for chromosome segregation during mitosis and meiosis. This so called mitotic spindle is a structure where the microtubule minus ends are centred into two spindle poles at the opposite sites of the former nucleus, while the plus-ends can be attached to chromosomes at specific binding sites, the kinetochores (Fig. 4) (Gadde and Heald 2004). Besides chromosome-bound microtubules, there are also free overlapping microtubules, which form opposite poles across the equator. These microtubules give the mitotic spindle its symmetry and provide sliding forces to push spindle poles apart during the anaphase. Outside the spindle, astral microtubules grow out of the spindle poles in all directions; they can become anchored at the cell membrane and aid the separation of the opposite poles. When all chromosomes are attached with their kinetochores to the spindle, the microtubules start to depolymerize. This process, which is under the control of specific motors and microtubule stabilizing and destabilizing proteins, finally results in the separation of the sister chromatids (Kline-Smith and Walczak 2004).

1.2 Microtubule associated proteins (MAPs)

A lot of proteins can bind specifically to microtubules to regulate dynamic instability, capture, mitotic chromosome segregation and transport along the microtubules. Proteins that specifically attach to microtubules *in vitro* as well as *in vivo* are called microtubule associated proteins (MAPs). They can be divided into two groups: motor MAPs and non-motor MAPs. In this part different MAPs will be discussed in more detail.

1.2.1 Microtubule associated motors

One of the main functions of microtubules is to aid intracellular transport of vesicles and cargoes from one part of the cell to another or from organelle to organelle. Vesicles and other cargoes are bound to specific motor proteins, which carry them along the microtubules in a specific direction (Schroer 2000). Besides intracellular transport, these motors also play a key role in chromosome movement during mitosis and meiosis (Endow 1999; Cassimeris 2004). To enable movement in two directions along microtubules, there are two different types of motor proteins (Fig. 5): dyneins, which are minus-end directed (retrograde) motors and kinesins, which are mainly plus-end directed (anterograde) motors, with the exception of KIFC kinesin motors that move oppositely (Mallik and Gross 2004). Both dynein and kinesin motors have a globular head domain, containing a microtubule binding motif with ATPase activity.

All kinesins are distantly related to myosins and show several structural similarities to these motors (e.g. kinesin-1 and myosin-V, which have a single ATP-binding site per head and hydrolyze a single ATP molecule per step during motion) (Vale and Milligan 2000; Mallik and Gross 2004). One of the best-studied members of the family, conventional kinesin (kinesin-1) is a dimer, which consists of two heavy chains containing the NH₂ terminal motor domain, central coiled-coil regions responsible for oligomerization and a tail that can interact with the light chains to enable cargo binding (Howard 1997). The position of the motor domain can vary between different kinesin superfamily proteins (KIFs): it can be located at the NH₂-terminus, in the middle, or at the COOH-terminus. So far, a total number of 45 KIFs have been identified in mammals with diverse functions (Kull 2000; Miki et al. 2001; Miki et al. 2005). In neurons, there are different KIFs that have their own function in transporting specific types of organelles, like synaptic vesicles. The specificity of the KIFs seems to lie within the cargo-binding tails of the proteins or, in the case of kinesin-1, in the light chains (Vallee and Sheetz 1996; Muresan 2000).

Dyneins can be divided into two classes: axonemal and cytoplasmic dyneins. Axonemal dyneins are involved in bending of cilia and flagella of eukaryotic cells and include heterodimers and heterotrimers, with two or three motor domain heads, respectively. Cytoplasmic dynein is a homodimer and contains, besides its heavy chains, several intermediate, light intermediate and light chains (Oiwa and Sakakibara 2005). The heavy chains of both dynein classes contain a large motor domain, bearing the sites of ATP hydrolysis and microtubule binding. Sequence analysis of dynein showed that the heavy chains are members of the AAA (ATPase associated with diverse cellular activities) superfamily of proteins. Each heavy chain has six AAA domains, of 35–40 kDa (Neuwald et al. 1999; King 2000). This makes the structure of dynein fundamentally different from that of kinesin or myosin. Cytoplasmic dynein differs from axonemal dynein by binding the multisubunit dynactin complex, which is required for dynein-driven activities and dynein's functional diversity (Karki and Holzbaur 1999). Dynactin is built up of two distinct subcomplexes: an actin-like minifilament backbone to bind the cargo and a projecting sidearm that interacts with dynein (Eckley et al. 1999). Via the p150^{Glued} subunit, a sidearm component, the dynactin complex itself is also able to bind microtubules. Hereby, dynactin helps dynein to stably interact with microtubules, which may improve its processivity (Vaughan and Vallee 1995; Schroer 2004). However, dynactin may not be essential for all types of dynein-cargo interactions. For instance, it was shown that dynein can directly bind to membrane phospholipids of vesicles and that the dynein intermediate light chain Tctex1 directly interacts with the transmembrane protein rhodopsin (Lacey and Haimo 1994; Wu et al. 2005).

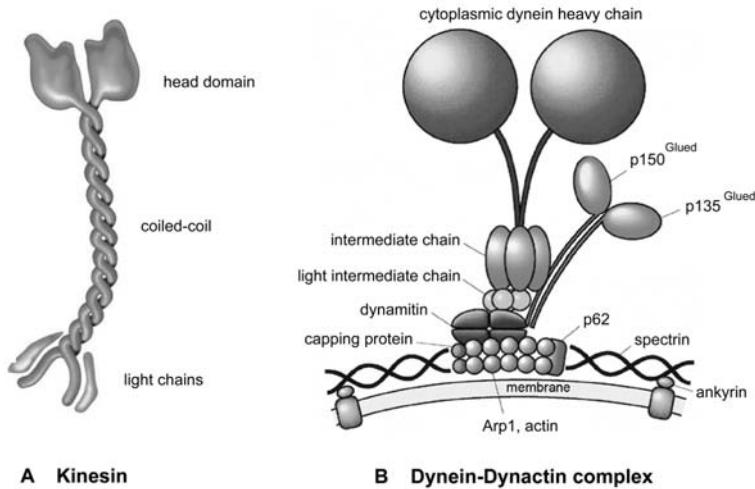


Figure 5: Microtubule motors

(A) Kinesin proteins are mostly plus-end directed microtubule motors. The conventional kinesin (kinesin-1) contains a globular head domain with the motor activity, a coiled-coil domain for dimerization and a tail interacting with two light chains to bind the cargo. (B) Dynein is a minus-end directed motor, which is functional in combination with the dynactin complex. Dynein is a large complex containing heavy chains (which harbour the motor activity), intermediate chains, light intermediate chains and light chains. Via the dynactin subunits p150/p135^{Glued}, dynein is linked to the multisubunit dynactin complex, which plays a role in the interaction with the membrane of the cargo. (Hirokawa; *Science* 1998 Vol 279, Issue 5350, 519-526)

Dynein and kinesin motors move in opposite directions on microtubules. However, this does not necessarily mean that these motors never cooperate. For example, dynein and kinesin-1 can directly interact with each other (Ligon et al. 2004). In addition, *Xenopus* kinesin-2 can be linked to dynein through a direct interaction with the dynactin subunit p150^{Glued} (Deacon et al. 2003). Obviously, this direct interaction could have several functions. For example, kinesin may be necessary to transport dynein from the cell centre back to the cell periphery, the plus-ends of the microtubules or to the end of the axon. The same might hold true for dynein-driven movement of kinesin. Furthermore, dynein and kinesin both co-localize on vesicles, which suggests that a cargo-associated motor complex may be responsible for coordinated bi-directional organelle transport. In the case of kinesin-1, the interaction with dynein may also have a regulatory role. The light chain of kinesin-1 can inhibit the motor activity of the heavy chain by an intramolecular folding back mechanism (Verhey et al. 1998). Binding of the light chain to a cargo may release this inhibition, which will activate kinesin. It might therefore be possible that the binding of dynein to the light chain provides a similar release from inhibition (Ligon et al. 2004). An *in vivo* study of GFP-labelled peroxisome movement also revealed that dynein and kinesin do not engage in a tug of war, but rather work together, producing up to 10 times the *in vitro* single-motor speed (Kural et al. 2005).

Whereas most kinesins use ATP to walk along microtubules, members of the kinesin-13 family depolymerize microtubules rather than move along them. They accumulate predominantly at both ends of microtubules and disassemble the polymerized tube in an ATP-dependent manner (Ganem and Compton 2004; Moore et al. 2005). They do not induce depolymerization by binding two adjacent protofilaments to force them apart. Instead, kinesin-13 acts on single protofilaments, inducing their curling. The conserved motor domain, which is located in the middle of kinesin-13, stabilizes the curved protofilaments of depolymerizing microtubules (Moore et al. 2002; Ovechkina and Wordeman 2003). The capacity of kinesin-13 to modulate microtubule dynamics has major implications for chromosome segregation and malignancy. For instance, human mitotic cells depleted of the kinesin-13 proteins KIF2a and MCAK lack detectable microtubule flux and frequently fail to segregate all chromosomes appropriately at anaphase (Ganem et al. 2005). Furthermore, in human cancers MCAK is overexpressed and can depolymerize paclitaxel-stabilized microtubules. Paclitaxel is a microtubule-stabilizing anticancer drug, used in several cancer treatments. MCAK can antagonize the effect of paclitaxel by stimulating microtubule dynamics. Therefore, introduction of MCAK inhibitors might be a potential strategy in treatment of paclitaxel-resistant tumours (Rowinsky 1997; Maney et al. 2001).

1.2.2 *General microtubule associated proteins*

Microtubules are dynamic structures, which can rapidly switch from growing to shrinking. This dynamic behaviour is regulated by a whole group of MAPs, which have varied and specific functions. For instance, MAP1A and MAP1B/MAP5 belong to the same family of multimeric protein complexes that are able to form cross-bridges between microtubules, regulate microtubule dynamics by stimulating rapid tubulin polymerization (Garner et al. 1990; Hirokawa 1994; Pedrotti et al. 1996). These MAPs, which are mainly expressed in the brain, contain a heavy chain and several light chains. Both their heavy and light chains contain microtubule-binding sites; the light chains also contain actin-binding domains and may help to link microtubules to actin filaments (Noiges et al. 2002).

Another MAP family has a microtubule-binding domain at the COOH-terminus, while the NH₂-terminus has a less clear function and extends into the surrounding space (“projection domain”). Proteins belonging to this family are tau, MAP2 and MAP4, which can stimulate microtubule growth and strongly suppress catastrophes (Drechsel et al. 1992). Tau and MAP2 are neuron-specific proteins that exhibit microtubule-stabilizing activities implicated in the development and maintenance of neuronal axons and dendrites. MAP4, generally absent from neurons, is present in many other tissues. MAP2/tau family proteins have a homologous COOH-terminal domain containing three or four microtubule-binding repeats which can attach along individual protofilaments and provide stabilization (Al-

Bassam et al. 2002; Dehmelt and Halpain 2005). Recently several kinases and interacting proteins have been identified that regulate the microtubule-stabilizing activity of MAP2 and tau. For instance, site-specific phosphorylation of tau by glycogen synthase kinase 3 (GSK3 β) results in detachment of tau from microtubules and in increased microtubule dynamics (Cho and Johnson 2004). Rho kinase and MT-affinity-regulating kinases MARK/PAR-1 also preferentially phosphorylate the microtubule-interacting COOH-terminus (KXGS motifs) of tau and MAP2 (Drewes et al. 1998; Amano et al. 2003).

Furthermore, it was recently found that MAP2, but not tau, is able to interact with both microtubules and F-actin through its microtubule binding domains. This is surprising, because these domains in MAP2 and tau share high sequence homology and have similar microtubule binding activities. The actin binding capacity of MAP2 might be relevant for neuromorphogenic processes, such as neurite initiation, where networks of microtubules and F-actin are rearranged (Roger et al. 2004; Dehmelt and Halpain 2005).

During peculiar circumstances aggregates can be formed of hyperphosphorylated tau, resulting in several neurodegenerative disorders such as Alzheimer's disease, Pick's disease, frontotemporal dementia, cortico-basal degeneration and progressive supranuclear palsy (Heutink 2000). In addition, tau can be cleaved near its COOH-terminus by β -amyloid-induced caspases. This results in a conformational change, which accelerates the aggregation and hyperphosphorylation of tau filaments and causes formation of insoluble neurofibrillary tangles (NFTs) (Gamblin et al. 2003; Rissman et al. 2004; Cotman et al. 2005). The abnormal hyperphosphorylation of tau abolishes its capacity to bind microtubules and promote microtubule assembly, which results in disruption of the microtubule network and in induction of neurodegenerative diseases. Strikingly, tau knockout mice are viable, appear physically normal and are able to reproduce (Dawson et al. 2001).

Besides tau and MAP2 there is another powerful microtubule stabilizer, the XMAP215(ch-TOG) protein. In *Xenopus* extracts, this MAP increases microtubule growth rate by seven to ten fold (Pryer et al. 1992). XMAP215 homologues exist in all major eukaryotic kingdoms; they all bind microtubules and localize to centrosomes and spindle pole bodies (Matthews et al. 1998; Cullen et al. 1999; Graf et al. 2000; Cassimeris and Morabito 2004; Gard et al. 2004). XMAP215 strongly modulates the catastrophe frequency by opposing the activity of microtubule destabilizers, such as Op18/Stathmin and Kinesin-13 family proteins (Holmfeldt et al. 2004; Noetzel et al. 2005). Conversely, some studies found also a destabilizing function for XMAP215 and its budding yeast homologue Stu2p (Popov and Karsenti 2003; Shirasu-Hiza et al. 2003; van Breugel et al. 2003). The mechanism of these different activities, observed for the XMAP215 family members, still remains obscure and warrants further investigation.

Another microtubule stabilizer is doublecortin (DCX), which is essential for normal brain development and is thought to maintain the correct structure of neuronal microtubules (Akhmanova and Severin 2004; Moores et al. 2004). Mutations in the human DCX gene cause the neuronal migration disorder lissencephaly (smooth brain) in males and double cortex syndrome in females. During neuronal migration, a mechanism including DCX, Lis1 and dynein pathways couples the nucleus to the centrosome and aids their translocation (Tanaka et al. 2004). Moreover, it was recently shown that DCX is able to associate with F-actin and act as a molecular link between microtubule and actin cytoskeletal filaments (Tsukada et al. 2005).

In dividing sea urchin embryos an abundant MAP was identified as the echinoderm microtubule-associated protein (EMAP). It is a 75-kDa WD repeat protein with limited sequence similarity to other well characterized MAP families (Suprenant et al. 2000; Eichenmuller et al. 2001). EMAP belongs to a large protein family conserved from nematodes to humans. EMAP-like proteins (EMLs or ELPs), such as the human ELP70, were identified as microtubule destabilizers that reduce the microtubule nucleation and growth rate and increase catastrophe frequency (Eichenmuller et al. 2002).

Recently, a new protein was identified as the ASter-Associated Protein (ASAP), which is a human MAP required for bipolar spindle assembly and cytokinesis. Because ASAP colocalizes with MTs during the whole cell cycle, it is thought to have a function in the control of MT dynamics and stabilization of the MT network during both mitosis and interphase (Saffin et al. 2005).

Finally, there are also MAPs that bind microtubules without modulating their dynamics. For instance, E-MAP-115 (ensconsin) was identified as a protein that is preferentially expressed in epithelial cells (Bulinski and Bossler 1994; Faire et al. 1999). Although it does not influence microtubule dynamics, E-MAP-115 was shown to be highly dynamic in its microtubule association, which is phosphorylation-dependent (Bulinski et al. 2001).

1.2.3 Microtubule plus-end binding proteins

So far, microtubule associated motor MAPs and general non-motor MAPs have been discussed. In addition, these two groups also comprise a particular family of proteins with a special accumulation pattern. These MAPs associate very specifically with the plus-ends of growing microtubules and are called ‘microtubule plus-end binding (tracking) proteins’ or +TIPs. They include both motor and non-motor MAPs and play an essential role in regulating dynamic instability and microtubule capture by other cellular structures (Sawin 2000; Schuyler and Pellman 2001). The tips of microtubules are of high interest because of their highly dynamic character. These sites determine the dynamic state of microtubules, as

Table 1: Microtubule plus-end binding proteins from different organisms and their structure

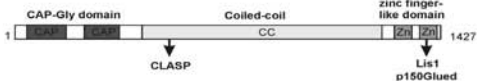
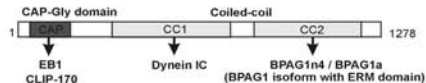
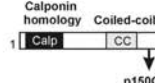
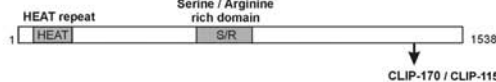
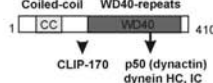
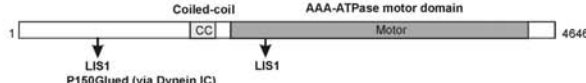
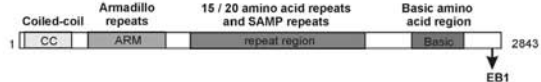
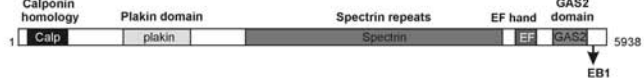

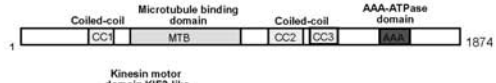
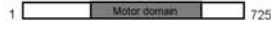
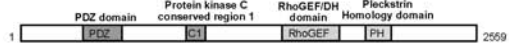

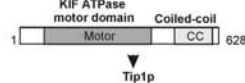
Vertebrate	Homologues	Structure
CLIP-170 / CLIP-115	D-CLIP-190 (Dm) Bik1p (Sc) Tip1p (Sp)	
Dynactin ^a (p150Glued)	Glued (Dm) Dnc-1 (Ce) Nip100p (Sc) Ssm4p (Sp) NudM (An)	
EB1,2,3	EB1 (Dm) DdEB1 (Dd) Bim1p (Sc) Mal3p (Sp)	
CLASP1,2	MAST/orbit (Dm) Cls-2/R107.6 (Ce) Stu1p (Sc)	
LIS1	Lis1 (Dm) Lis-1 (Ce) Pac1p (Sc) NudF (An)	
Dynein ^a (Dynein HC) (several isoforms)	Dhc64C (Dm) Dhc-1 (Ce) DHC (Dd) Dyn1 (Sc) Dhc1 (Sp) NudA (An)	
APC, APC2/APCL	dAPC1, E-APC/ dAPC2 (Dm) apr-1(Ce) Kar9 (Sc) ^b	
ACF7, BPAG1	Shot/Kakapo (Dm) vab10 (Ce)	
XMAP215/ ChTOG ^c	Msp (Dm) ZYG-9 (Ce) DdCP224 (Dd) Stu2p (Sc) Dis1p, Alp14p (Sp)	
Navigator-1	Unc-53 (Ce)	
MCAK / KIF2C (Kinesin-13)	K11D9 (Ce) KLP10A (Dm)	
	D-RhoGEF2 (DM) ^d	
Fission Yeast protein		
Tea1p		
Tea2p	Kip2p (Sc)	

Table 1: Microtubule plus-end binding proteins from different organisms and their structure.

The main groups of vertebrate +TIPs are listed. For groups lacking vertebrate homologues, the proteins from fission yeast are indicated. The homologues for which no published information except the sequence is available are not included in the list. The structural motifs for each protein are illustrated in the diagram (because of the large size differences, proteins are not drawn to scale). The arrows indicate protein partners, which bind directly to specific domains. When the binding domain is unknown, an arrowhead is used. The following protein sequences were used for the drawings: CLIP-170 (NP_002947), p150^{Glued} (NP_004073), EB1 (NP_036457), CLASP1 (NP_056097), LIS1 (NP_000421), Dynein Heavy Chain 1 (NP_001367), APC (NP_000029), ACF7/MACF1 (NP_149033), ch-TOG (NP_055571), Tea1p (NP_5888351), Tea2p (CAA22353), Navigator-1 (AY043013), MCAK (Q99661) and RHOGEF2 (NP_995868).

^aFor dynein and dynactin, protein complexes composed of multiple subunits, only the large, MT-binding subunits are indicated. ^bAPC and KAR9 bind to EB1 family members EB1 and Bim1p, respectively, and may have some similar functions; however they have a very limited degree of similarity. ^cThe yeast counterpart of XMAP215, Stu2p, and its *Dictyostelium* and *Drosophila* homologues have been shown to localise to the MT plus-ends; however, this behaviour may not be shared by XMAP215 itself. ^dThere are vertebrate counterparts of D-RhoGEF2; however, none of them has been shown to tip-tract yet and, therefore, they are not illustrated here. An: *Aspergillus nidulans*; Ce: *Caenorhabditis elegans*; Dd: *Dictyostelium discoideum*; Dm: *Drosophila melanogaster*; Sc: *Saccharomyces cerevisiae*; Sp: *Schizosaccharomyces pombe*. (Adapted from Current Opinion in Cell Biology 2005, 17:47-54)

well as their ability to interact with diverse cellular targets. Because of the high variety of different plus-end binding proteins, it is likely that the combination and composition of all these proteins determines the destiny of the tip and of the whole microtubule.

The first plus-end binding protein described was CLIP-170 (Perez et al. 1999). A GFP fusion of CLIP-170 was found in bright patches or comet-like structures at the growing ends of microtubules; the comets disappeared when the microtubules stopped growing (Komarova et al. 2002). Later, a whole list of +TIPs gradually emerged, including CLIP-associated proteins (CLASPs), end binding proteins (EB family), LIS1, dynein, dynactin, adenomatous polyposis coli tumor suppressor protein (APC), navigator-1, and ACF7 (see also Table 1) (Carvalho et al. 2003; Galjart and Perez 2003; Kodama et al. 2003; Akhmanova and Hoogenraad 2005; Martinez-Lopez et al. 2005).

The accumulation of +TIPs at the microtubule plus-ends depends on different mechanisms. Kinesin motors have been shown to enable transport of particular proteins, like for instance the yeast CLIP-170 homologues Bik1p (*Saccharomyces cerevisiae*) and Tip1p (*Schizosaccharomyces pombe*), towards the microtubule plus-ends (Busch et al. 2004; Carvalho et al. 2004). In mammals some +TIPs, such as CLIP-170 and EB1, are believed to accumulate at the plus-ends via a treadmilling mechanism (Fig.6). In this model, +TIPs bind with a high affinity to the freshly polymerised microtubule plus-ends by recognizing specific structural features or by co-assembling with tubulin dimers and are released from the older portions of the microtubule lattice (Diamantopoulos et al. 1999; Arnal et al. 2004; Bisgrove et al. 2004; Galjart 2005). Another way of plus-end localization is to associate with treadmilling +TIPs. This indirect microtubule association (called “hitchhiking” by Carvalho et al. 2003) is demonstrated, for instance, for the budding yeast protein Kar9p, which cannot bind microtubules by itself, but hitchhikes on the EB1 homologue Bim1p

(Miller et al. 2000). Another example of a hitchhiking +TIP is the *Drosophila* Rho-type guanine nucleotide exchange factor 2 (RhoGEF2), which was shown to localise to MT plus-ends of epithelial cells in an EB1-dependent manner (Rogers et al. 2004). Mammalian APC localizes to microtubule plus-ends possibly by using all three mechanisms: treadmilling, hitchhiking and motor-driven transport (Askham et al. 2000; Mimori-Kiyosue et al. 2000; Jimbo et al. 2002).

The release of +TIPs from the microtubule end may be caused by phosphorylation through microtubule-specific kinases, which increases the negative charge of their targets and thereby reduces their affinity for microtubules (Rickard and Kreis 1991; Schroer 2001). GSK3 β , for instance, probably regulates the microtubule affinity of CLASPs by phosphorylating their microtubule-binding domain. Conversely, the inactivation of GSK3 β results in a higher affinity of CLASP2 for microtubules (Akhmanova et al. 2001; Wittmann and Waterman-Storer 2005). However, the idea that cycles of phosphorylation and dephosphorylation drive specific plus-end localisation has not yet been proven for any +TIP.

To date, a lot of research has been done in different species to unravel the complex functioning of +TIPs with respect to the microtubule behaviour. Binding of +TIPs to microtubule ends significantly influences their dynamics, often causing microtubule stabilization. This can be achieved, for instance, by reducing the frequency of catastrophes and/or supporting repetitive rescues. The CLIP-170 family proteins were identified as rescue factors in mammalian cells (Komarova et al. 2002). The budding yeast homologue of CLIP-170, Bik1p, was found to stabilize microtubules, while the fission yeast counterpart of CLIP-170, tip1p, serves as an anti-catastrophe factor (Brunner and Nurse 2000; Carvalho et al. 2004). The importance of CLIP family proteins is underscored by the fact that a reduced amount of the brain-enriched CLIP-170 homologue, CLIP-115, is a contributing factor in the Williams-Beuren syndrome (a human neurodevelopmental disorder with mild mental retardation) (Hoogenraad et al. 2002; Hoogenraad et al. 2004).

Another +TIP is the ‘end-binding protein’ EB1 (Morrison et al. 1998), which regulates microtubule dynamics in different ways in different species. The EB1 homologues of *Drosophila* and *S. cerevisiae* both increase microtubule dynamics by increasing phases of growth and shrinkage. Loss of expression of *Drosophila* EB1 or the budding yeast homologue Bim1p was found to increase the time microtubules spend pausing and to reduce catastrophe and rescue frequencies (Tirnauer et al. 1999; Rogers et al. 2002). In contradiction, EB1 family proteins in fission yeast and *Xenopus* extracts increase the rescue frequencies and suppress the catastrophe frequencies to promote microtubule growth (Tirnauer et al. 2002; Busch and Brunner 2004). Nevertheless, all EB family proteins share a common role in preventing microtubules from pausing and decreasing the depolymerization rate.

One of the EB1 binding partners, the dynactin large subunit p150^{Glued}, has a potent effect on microtubule nucleation *in vitro* (Ligon et al. 2003). APC, another binding partner of

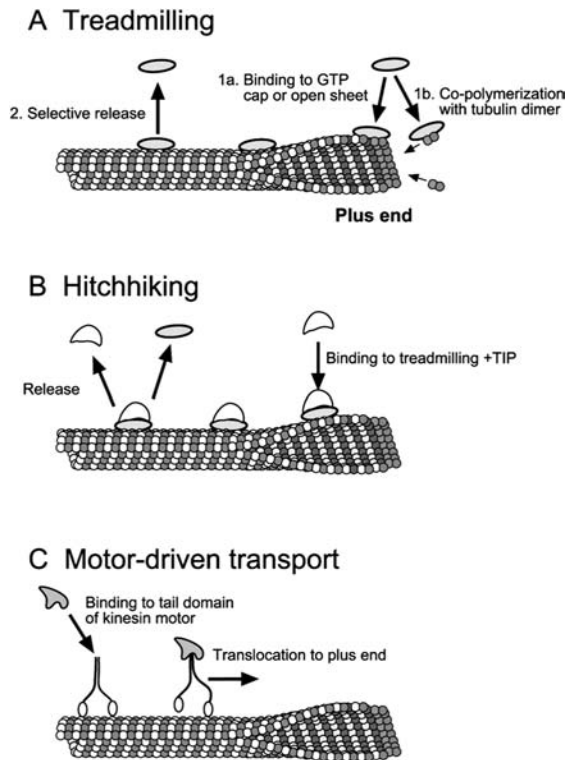


Figure 6: Mechanisms of +TIP localization.

A Treadmilling. +TIPs, like CLIP-170 and EB1, preferentially bind to the plus-ends of polymerizing microtubules and are rapidly released from the older part of the microtubule lattice.

B Hitchhiking. Various plus-end binding proteins localize to the microtubule ends by direct binding to other, treadmilling +TIPs. This mechanism results in the same localization pattern of hitchhiking and treadmilling +TIPs.

C Motor-driven transport. There are also +TIPs, such as Tip1, which attach to kinesin motor proteins to be translocated towards the plus-end. (Bisgrove et al. 2004)

EB1, plays a role in promoting microtubule polymerization and stabilization *in vitro* (Munemitsu et al. 1994; Nakamura et al. 2001; Zumbrunn et al. 2001). APC is a multifunctional tumour suppressor with a primary role in the regulation of the Wnt signalling pathway. In addition, the microtubule-related APC activities are important for proper cell division and motility; therefore, cell migration defects and chromosome instability caused by truncation mutations in the APC gene are a likely contributing factor in colorectal cancers (Nathke 2005).

A microtubule-stabilizing function was also demonstrated for CLASPs, which are conserved from animals to fungi and participate in generating polarized microtubule networks (Akhmanova et al. 2001; Mathe et al. 2003). Mammalian CLASPs and their homologues in *Drosophila* (Orbit/MAST) and *C. elegans* (Cls-2) were also shown to be essential for normal spindle formation in mitosis (Inoue et al. 2000; Lemos et al. 2000; Maiato et al. 2003; Cheeseman et al. 2005; Maiato et al. 2005).

The cytoskeletal +TIP ACF7 (actin cross-linking family-7) is a spectraplaklin homologue and helps to guide growing microtubules along polarised actin bundles, and is found to stabilize them at the leading edge of migrating cells. So, ACF7 seems to be important in controlling microtubule dynamics and reinforcing links between microtubules

and polarized F-actin. In this way cellular polarization and coordinated cell movements can be sustained (Kodama et al. 2003; Lin et al. 2005).

LIS1 is a +TIP that can associate with both CLIP-170 and dynein and seems to have its own capacity for direct microtubule binding (Sapir et al. 1997; Coquelle et al. 2002). Since LIS1 is involved in neuronal migration, it has an essential role during embryonic brain development. Mutations in the LIS1 gene cause type I lissencephaly (smooth brain), which is known as a human neuronal migration disorder (Dobyns et al. 1993; Vallee et al. 2001). LIS1 may also be involved in the regulation of microtubule dynamics, especially as its *Aspergillus nidulans* homologue NUDF causes a reduction in catastrophe frequencies *in vitro* and an increase of catastrophe frequencies *in vivo* (Sapir et al. 1997; Han et al. 2001; Coquelle et al. 2002; Xiang 2003; Liang et al. 2004). Together with dynein and dynactin, LIS1 is also required for proper cell division processes in *C. elegans* embryos and mammalian cells (Faulkner et al. 2000; Tai et al. 2002; Cockell et al. 2004).

Navigator-1 is a largely neuron-specific microtubule plus-end binding protein, which associates with the plus-ends through a novel microtubule-binding domain. Knocking down endogenous navigator-1 in mouse neurons impaired normal guidance of the leading processes, suggesting an involvement in directional neuronal migration (Maes et al. 2002; Peeters et al. 2004; Martinez-Lopez et al. 2005).

Recent studies have shown that in addition to microtubule stabilizers, kinesin-13 family members, which destabilize microtubules, can also accumulate at the microtubule tips. For instance, the potent microtubule depolymerizer MCAK was shown to associate in a phosphorylation-dependent manner with the tips of growing microtubules without inducing their depolymerization (Moore et al. 2005). Other destabilising kinesins associate with microtubule plus-ends indirectly: a *Drosophila* kinesin-13, KLP10A, accumulates at the growing microtubule tips via EB1 (Mennella et al. 2005; Sproul et al. 2005) the budding yeast kinesin-14, Kar3, attaches to the plus-ends via Cik1 (Mennella et al. 2005; Sproul et al. 2005).

In conclusion, microtubule tips are highly enriched for various stabilizing and destabilizing factors, which play a key role in fundamental processes such as cell division, cell motility and morphogenesis. Many microtubule-related proteins are affected in human diseases, such as Alzheimer disease, Williams-Beuren syndrome and various cancers. Future investigations will elucidate their cellular functioning and their importance for human health.

1.3 Microtubules at the cellular cortex

Growing microtubules explore the cytoplasm and target different organelles such as mitochondria, the Golgi apparatus, the endoplasmic reticulum (ER) and the plasma membrane (Cole and Lippincott-Schwartz 1995). Interactions between microtubules and the plasma membrane are important for diverse cellular processes, including mitosis, migration, vesicle transport and polarization. During mitosis, the mitotic spindle is anchored to the plasma membrane via astral microtubules to enable chromosome separation. Positioning of the mitotic spindle defines the plane of cell division and plays an essential role in formation of many tissues, such as epithelia. Moreover, alterations of the microtubule and actin array near the plasma membrane can change cell shape and polarization or enable cell migration (Etienne-Manneville 2004). Microtubules are also involved in the intracellular transport of different vesicles between the ER, the Golgi apparatus and the plasma membrane. During exocytosis, vesicles can fuse with the membrane in order to secrete cellular products, such as neurotransmitters from neurons or insulin from pancreatic β cells. Microtubule interactions with the plasma membrane may play a role in defining the sites of exocytosis.

The interaction between microtubules and the cell cortex is thus essential for the normal functioning of different cell types. It is therefore not surprising that this interface is well conserved from yeasts to animals.

Since microtubules do not bind to the plasma membrane by themselves, there are diverse mechanisms that generate such a connection. Obviously, +TIPs play here a major role, since they accumulate specifically at microtubule plus-ends to control their dynamics and the targeting of different structures. Some +TIPs are conserved between different species and have similar functions regarding to the microtubule capture at the cortex.

In general, +TIPs can interact either with each other or with microtubule plus-ends. However, most of them are incapable of anchoring directly at the cell cortex, since they lack membrane-binding domains. To enable cortical localization, +TIPs need to bind to other proteins that can associate with the membrane. For instance, APC can interact with the tumor suppressor gene product Dlg1 to localize at the plasma membrane of the leading edge of migrating fibroblasts (Etienne-Manneville et al. 2005). Dlg1 is an orthologue of *Drosophila* Discs large protein, which is involved in the establishment of epithelial polarity (Woods et al. 1996). In addition, some +TIPs are able to target microtubules to the cell periphery by interacting with the cortical actin network, like ACF7, which binds to actin directly (Karakesisoglou et al. 2000) or CLIP-170 and APC, which may interact with actin filaments through IQGAP1 (Fukata et al. 2002; Watanabe et al. 2004). Still, the knowledge on the composition of protein complexes that control the cortical microtubule attachment remains fragmentary. A part of this thesis describes the involvement of +TIPs in the cortical capture of microtubules, and an attempt to search for their membrane-bound partners.

References

- Akhmanova, A. and C. C. Hoogenraad (2005). "Microtubule plus-end-tracking proteins: mechanisms and functions." Curr Opin Cell Biol **17**(1): 47-54.
- Akhmanova, A., C. C. Hoogenraad, K. Drabek, T. Stepanova, B. Dortland, T. Verkerk, W. Vermeulen, B. M. Burgering, C. I. De Zeeuw, F. Grosveld and N. Galjart (2001). "Clasps are CLIP-115 and -170 associating proteins involved in the regional regulation of microtubule dynamics in motile fibroblasts." Cell **104**(6): 923-35.
- Akhmanova, A. and F. Severin (2004). "Thirteen is the lucky number for doublecortin." Dev Cell **7**(1): 5-6.
- Al-Bassam, J., R. S. Ozer, D. Safer, S. Halpain and R. A. Milligan (2002). "MAP2 and tau bind longitudinally along the outer ridges of microtubule protofilaments." J Cell Biol **157**(7): 1187-96.
- Aldaz, H., L. M. Rice, T. Stearns and D. A. Agard (2005). "Insights into microtubule nucleation from the crystal structure of human gamma-tubulin." Nature **435**(7041): 523-7.
- Amano, M., T. Kaneko, A. Maeda, M. Nakayama, M. Ito, T. Yamauchi, H. Goto, Y. Fukata, N. Oshiro, A. Shinohara, A. Iwamatsu and K. Kaibuchi (2003). "Identification of Tau and MAP2 as novel substrates of Rho-kinase and myosin phosphatase." J Neurochem **87**(3): 780-90.
- Anders, K. R. and D. Botstein (2001). "Dominant-lethal alpha-tubulin mutants defective in microtubule depolymerization in yeast." Mol Biol Cell **12**(12): 3973-86.
- Arnal, I., C. Heichette, G. S. Diamantopoulos and D. Chretien (2004). "CLIP-170/tubulin-curved oligomers coassemble at microtubule ends and promote rescues." Curr Biol **14**(23): 2086-95.
- Askham, J. M., P. Moncur, A. F. Markham and E. E. Morrison (2000). "Regulation and function of the interaction between the APC tumour suppressor protein and EB1." Oncogene **19**(15): 1950-8.
- Benitez-King, G., G. Ramirez-Rodriguez, L. Ortiz and I. Meza (2004). "The neuronal cytoskeleton as a potential therapeutical target in neurodegenerative diseases and schizophrenia." Curr Drug Targets CNS Neurol Disord **3**(6): 515-33.
- Bisgrove, S. R., W. E. Hable and D. L. Kropf (2004). "+TIPs and microtubule regulation. The beginning of the plus end in plants." Plant Physiol **136**(4): 3855-63.
- Bousquet, O. and P. A. Coulombe (1996). "Cytoskeleton: missing links found?" Curr Biol **6**(12): 1563-6.
- Brunner, D. and P. Nurse (2000). "CLIP170-like tip1p spatially organizes microtubular dynamics in fission yeast." Cell **102**(5): 695-704.
- Bulinski, J. C. and A. Bossler (1994). "Purification and characterization of ensconsin, a novel microtubule stabilizing protein." J Cell Sci **107** (Pt 10): 2839-49.
- Bulinski, J. C., D. J. Odde, B. J. Howell, T. D. Salmon and C. M. Waterman-Storer (2001). "Rapid dynamics of the microtubule binding of ensconsin in vivo." J Cell Sci **114**(Pt 21): 3885-97.
- Busch, K. E. and D. Brunner (2004). "The microtubule plus end-tracking proteins mal3p and tip1p cooperate for cell-end targeting of interphase microtubules." Curr Biol **14**(7): 548-59.

- Busch, K. E., J. Hayles, P. Nurse and D. Brunner (2004). "Tea2p kinesin is involved in spatial microtubule organization by transporting tip1p on microtubules." Dev Cell **6**(6): 831-43.
- Carlier, M. F. (1990). "Actin polymerization and ATP hydrolysis." Adv Biophys **26**: 51-73.
- Carlier, M. F. (1992). "Nucleotide hydrolysis regulates the dynamics of actin filaments and microtubules." Philos Trans R Soc Lond B Biol Sci **336**(1276): 93-7.
- Carlier, M. F. and D. Pantaloni (1994). "Actin assembly in response to extracellular signals: role of capping proteins, thymosin beta 4 and profilin." Semin Cell Biol **5**(3): 183-91.
- Carvalho, P., M. L. Gupta, Jr., M. A. Hoyt and D. Pellman (2004). "Cell cycle control of kinesin-mediated transport of Bik1 (CLIP-170) regulates microtubule stability and dynein activation." Dev Cell **6**(6): 815-29.
- Carvalho, P., J. S. Tirnauer and D. Pellman (2003). "Surfing on microtubule ends." Trends Cell Biol **13**(5): 229-37.
- Cassimeris, L. (1993). "Regulation of microtubule dynamic instability." Cell Motil Cytoskeleton **26**(4): 275-81.
- Cassimeris, L. (2004). "Cell division: eg'ing on microtubule flux." Curr Biol **14**(23): R1000-2.
- Cassimeris, L. and J. Morabito (2004). "TOGp, the human homolog of XMAP215/Dis1, is required for centrosome integrity, spindle pole organization, and bipolar spindle assembly." Mol Biol Cell **15**(4): 1580-90.
- Cheeseman, I. M., I. MacLeod, J. R. Yates, 3rd, K. Oegema and A. Desai (2005). "The CENP-F-like proteins HCP-1 and HCP-2 target CLASP to kinetochores to mediate chromosome segregation." Curr Biol **15**(8): 771-7.
- Cho, J. H. and G. V. Johnson (2004). "Primed phosphorylation of tau at Thr231 by glycogen synthase kinase 3beta (GSK3beta) plays a critical role in regulating tau's ability to bind and stabilize microtubules." J Neurochem **88**(2): 349-58.
- Cleveland, D. W. (1982). "Treadmilling of tubulin and actin." Cell **28**(4): 689-91.
- Cockell, M. M., K. Baumer and P. Gonczy (2004). "lis-1 is required for dynein-dependent cell division processes in *C. elegans* embryos." J Cell Sci **117**(Pt 19): 4571-82.
- Cole, N. B. and J. Lippincott-Schwartz (1995). "Organization of organelles and membrane traffic by microtubules." Curr Opin Cell Biol **7**(1): 55-64.
- Coquelle, F. M., M. Caspi, F. P. Cordelieres, J. P. Dompierre, D. L. Dujardin, C. Koifman, P. Martin, C. C. Hoogenraad, A. Akhmanova, N. Galjart, J. R. De Mey and O. Reiner (2002). "LIS1, CLIP-170's key to the dynein/dynactin pathway." Mol Cell Biol **22**(9): 3089-102.
- Cotman, C. W., W. W. Poon, R. A. Rissman and M. Blurton-Jones (2005). "The role of caspase cleavage of tau in Alzheimer disease neuropathology." J Neuropathol Exp Neurol **64**(2): 104-12.
- Cullen, C. F., P. Deak, D. M. Glover and H. Ohkura (1999). "mini spindles: A gene encoding a conserved microtubule-associated protein required for the integrity of the mitotic spindle in *Drosophila*." J Cell Biol **146**(5): 1005-18.
- Cunningham, C. C., J. B. Gorlin, D. J. Kwiatkowski, J. H. Hartwig, P. A. Janmey, H. R. Byers and T. P. Stossel (1992). "Actin-binding protein requirement for cortical stability and efficient locomotion." Science **255**(5042): 325-7.

- Dawson, H. N., A. Ferreira, M. V. Eyster, N. Ghoshal, L. I. Binder and M. P. Vitek (2001). "Inhibition of neuronal maturation in primary hippocampal neurons from tau deficient mice." *J Cell Sci* **114**(Pt 6): 1179-87.
- Deacon, S. W., A. S. Serpinskaya, P. S. Vaughan, M. Lopez Fanarraga, I. Vernos, K. T. Vaughan and V. I. Gelfand (2003). "Dynactin is required for bidirectional organelle transport." *J Cell Biol* **160**(3): 297-301.
- Dehmelt, L. and S. Halpain (2005). "The MAP2/Tau family of microtubule-associated proteins." *Genome Biol* **6**(1): 204.
- Desai, A. and T. J. Mitchison (1997). "Microtubule polymerization dynamics." *Annu Rev Cell Dev Biol* **13**: 83-117.
- Diamantopoulos, G. S., F. Perez, H. V. Goodson, G. Batelier, R. Melki, T. E. Kreis and J. E. Rickard (1999). "Dynamic localization of CLIP-170 to microtubule plus ends is coupled to microtubule assembly." *J Cell Biol* **144**(1): 99-112.
- Dobyns, W. B., O. Reiner, R. Carrozzo and D. H. Ledbetter (1993). "Lissencephaly. A human brain malformation associated with deletion of the LIS1 gene located at chromosome 17p13." *Jama* **270**(23): 2838-42.
- dos Remedios, C. G., D. Chhabra, M. Kekic, I. V. Dedova, M. Tsubakihara, D. A. Berry and N. J. Nosworthy (2003). "Actin binding proteins: regulation of cytoskeletal microfilaments." *Physiol Rev* **83**(2): 433-73.
- Drechsel, D. N., A. A. Hyman, M. H. Cobb and M. W. Kirschner (1992). "Modulation of the dynamic instability of tubulin assembly by the microtubule-associated protein tau." *Mol Biol Cell* **3**(10): 1141-54.
- Drewes, G., A. Ebner and E. M. Mandelkow (1998). "MAPs, MARKs and microtubule dynamics." *Trends Biochem Sci* **23**(8): 307-11.
- Eckley, D. M., S. R. Gill, K. A. Melkonian, J. B. Bingham, H. V. Goodson, J. E. Heuser and T. A. Schroer (1999). "Analysis of dynactin subcomplexes reveals a novel actin-related protein associated with the arp1 minifilament pointed end." *J Cell Biol* **147**(2): 307-20.
- Eichenmuller, B., D. P. Ahrens, Q. Li and K. A. Suprenant (2001). "Saturable binding of the echinoderm microtubule-associated protein (EMAP) on microtubules, but not filamentous actin or vimentin filaments." *Cell Motil Cytoskeleton* **50**(3): 161-72.
- Eichenmuller, B., P. Everley, J. Palange, D. Lepley and K. A. Suprenant (2002). "The human EMAP-like protein-70 (ELP70) is a microtubule destabilizer that localizes to the mitotic apparatus." *J Biol Chem* **277**(2): 1301-9.
- Endow, S. A. (1999). "Microtubule motors in spindle and chromosome motility." *Eur J Biochem* **262**(1): 12-8.
- Erickson, H. P. and E. T. O'Brien (1992). "Microtubule dynamic instability and GTP hydrolysis." *Annu Rev Biophys Biomol Struct* **21**: 145-66.
- Etienne-Manneville, S. (2004). "Actin and microtubules in cell motility: which one is in control?" *Traffic* **5**(7): 470-7.
- Etienne-Manneville, S., J. B. Manneville, S. Nicholls, M. A. Ferenczi and A. Hall (2005). "Cdc42 and Par6-PKCzeta regulate the spatially localized association of Dlg1 and APC to control cell polarization." *J Cell Biol* **170**(6): 895-901.
- Faire, K., C. M. Waterman-Storer, D. Gruber, D. Masson, E. D. Salmon and J. C. Bulinski (1999). "E-MAP-115 (ensconsin) associates dynamically with microtubules in vivo and is not a physiological modulator of microtubule dynamics." *J Cell Sci* **112** (Pt 23): 4243-55.

- Faulkner, N. E., D. L. Dujardin, C. Y. Tai, K. T. Vaughan, C. B. O'Connell, Y. Wang and R. B. Vallee (2000). "A role for the lissencephaly gene LIS1 in mitosis and cytoplasmic dynein function." Nat Cell Biol **2**(11): 784-91.
- Fuchs, E. and D. W. Cleveland (1998). "A structural scaffolding of intermediate filaments in health and disease." Science **279**(5350): 514-9.
- Fuchs, E. and Y. Yang (1999). "Crossroads on cytoskeletal highways." Cell **98**(5): 547-50.
- Fukata, M., T. Watanabe, J. Noritake, M. Nakagawa, M. Yamaga, S. Kuroda, Y. Matsuura, A. Iwamatsu, F. Perez and K. Kaibuchi (2002). "Rac1 and Cdc42 capture microtubules through IQGAP1 and CLIP-170." Cell **109**(7): 873-85.
- Furukawa, R. and M. Feuchner (1997). "The structure, function, and assembly of actin filament bundles." Int Rev Cytol **175**: 29-90.
- Gadde, S. and R. Heald (2004). "Mechanisms and molecules of the mitotic spindle." Curr Biol **14**(18): R797-805.
- Galjart, N. (2005). "CLIPs and CLASPs and cellular dynamics." Nat Rev Mol Cell Biol **6**(6): 487-98.
- Galjart, N. and F. Perez (2003). "A plus-end raft to control microtubule dynamics and function." Curr Opin Cell Biol **15**(1): 48-53.
- Gamblin, T. C., F. Chen, A. Zambrano, A. Abrahama, S. Lagalwar, A. L. Guillozet, M. Lu, Y. Fu, F. Garcia-Sierra, N. LaPointe, R. Miller, R. W. Berry, L. I. Binder and V. L. Cryns (2003). "Caspase cleavage of tau: linking amyloid and neurofibrillary tangles in Alzheimer's disease." Proc Natl Acad Sci U S A **100**(17): 10032-7.
- Ganem, N. J. and D. A. Compton (2004). "The KinI kinesin Kif2a is required for bipolar spindle assembly through a functional relationship with MCAK." J Cell Biol **166**(4): 473-8.
- Ganem, N. J., K. Upton and D. A. Compton (2005). "Efficient mitosis in human cells lacking poleward microtubule flux." Curr Biol **15**(20): 1827-32.
- Gard, D. L., B. E. Becker and S. Josh Romney (2004). "MAPping the eukaryotic tree of life: structure, function, and evolution of the MAP215/Dis1 family of microtubule-associated proteins." Int Rev Cytol **239**: 179-272.
- Garner, C. C., A. Garner, G. Huber, C. Kozak and A. Matus (1990). "Molecular cloning of microtubule-associated protein 1 (MAP1A) and microtubule-associated protein 5 (MAP1B): identification of distinct genes and their differential expression in developing brain." J Neurochem **55**(1): 146-54.
- Graf, R., C. Daunderer and M. Schliwa (2000). "Dictyostelium DdCP224 is a microtubule-associated protein and a permanent centrosomal resident involved in centrosome duplication." J Cell Sci **113** (Pt 10): 1747-58.
- Han, G., B. Liu, J. Zhang, W. Zuo, N. R. Morris and X. Xiang (2001). "The Aspergillus cytoplasmic dynein heavy chain and NUDF localize to microtubule ends and affect microtubule dynamics." Curr Biol **11**(9): 719-24.
- Hartwig, J. H. and D. J. Kwiatkowski (1991). "Actin-binding proteins." Curr Opin Cell Biol **3**(1): 87-97.
- Helfand, B. T., L. Chang and R. D. Goldman (2004). "Intermediate filaments are dynamic and motile elements of cellular architecture." J Cell Sci **117**(Pt 2): 133-41.
- Herrmann, H. and U. Aebi (2004). "Intermediate filaments: molecular structure, assembly mechanism, and integration into functionally distinct intracellular Scaffolds." Annu Rev Biochem **73**: 749-89.
- Heutink, P. (2000). "Untangling tau-related dementia." Hum Mol Genet **9**(6): 979-86.

- Hirokawa, N. (1994). "Microtubule organization and dynamics dependent on microtubule-associated proteins." *Curr Opin Cell Biol* **6**(1): 74-81.
- Hodge, T. and M. J. Cope (2000). "A myosin family tree." *J Cell Sci* **113 Pt 19**: 3353-4.
- Holmfeldt, P., S. Stenmark and M. Gullberg (2004). "Differential functional interplay of TOGp/XMAP215 and the KinI kinesin MCAK during interphase and mitosis." *Embo J* **23**(3): 627-37.
- Hoogenraad, C. C., A. Akhmanova, N. Galjart and C. I. De Zeeuw (2004). "LIMK1 and CLIP-115: linking cytoskeletal defects to Williams syndrome." *Bioessays* **26**(2): 141-50.
- Hoogenraad, C. C., B. Koekkoek, A. Akhmanova, H. Krugers, B. Dortland, M. Miedema, A. van Alphen, W. M. Kistler, M. Jaegle, M. Koutsourakis, N. Van Camp, M. Verhoye, A. van der Linden, I. Kaverina, F. Grosveld, C. I. De Zeeuw and N. Galjart (2002). "Targeted mutation of Cyln2 in the Williams syndrome critical region links CLIP-115 haploinsufficiency to neurodevelopmental abnormalities in mice." *Nat Genet* **32**(1): 116-27.
- Howard, J. (1997). "Molecular motors: structural adaptations to cellular functions." *Nature* **389**(6651): 561-7.
- Howard, J. and A. A. Hyman (2003). "Dynamics and mechanics of the microtubule plus end." *Nature* **422**(6933): 753-8.
- Inoue, Y. H., M. do Carmo Avides, M. Shiraki, P. Deak, M. Yamaguchi, Y. Nishimoto, A. Matsukage and D. M. Glover (2000). "Orbit, a novel microtubule-associated protein essential for mitosis in *Drosophila melanogaster*." *J Cell Biol* **149**(1): 153-66.
- Janmey, P. A. (1991). "Mechanical properties of cytoskeletal polymers." *Curr Opin Cell Biol* **3**(1): 4-11.
- Jimbo, T., Y. Kawasaki, R. Koyama, R. Sato, S. Takada, K. Haraguchi and T. Akiyama (2002). "Identification of a link between the tumour suppressor APC and the kinesin superfamily." *Nat Cell Biol* **4**(4): 323-7.
- Job, D., O. Valiron and B. Oakley (2003). "Microtubule nucleation." *Curr Opin Cell Biol* **15**(1): 111-7.
- Karki, S. and E. L. Holzbaur (1999). "Cytoplasmic dynein and dynactin in cell division and intracellular transport." *Curr Opin Cell Biol* **11**(1): 45-53.
- King, S. M. (2000). "AAA domains and organization of the dynein motor unit." *J Cell Sci* **113 (Pt 14)**: 2521-6.
- Kline-Smith, S. L. and C. E. Walczak (2004). "Mitotic spindle assembly and chromosome segregation: refocusing on microtubule dynamics." *Mol Cell* **15**(3): 317-27.
- Kodama, A., I. Karakesisoglou, E. Wong, A. Vaezi and E. Fuchs (2003). "ACF7: an essential integrator of microtubule dynamics." *Cell* **115**(3): 343-54.
- Komarova, Y. A., A. S. Akhmanova, S. Kojima, N. Galjart and G. G. Borisy (2002). "Cytoplasmic linker proteins promote microtubule rescue in vivo." *J Cell Biol* **159**(4): 589-99.
- Krendel, M. and M. S. Mooseker (2005). "Myosins: Tails (and Heads) of Functional Diversity." *Physiology (Bethesda)* **20**(4): 239-51.
- Kull, F. J. (2000). "Motor proteins of the kinesin superfamily: structure and mechanism." *Essays Biochem* **35**: 61-73.

- Kural, C., H. Kim, S. Syed, G. Goshima, V. I. Gelfand and P. R. Selvin (2005). "Kinesin and dynein move a peroxisome in vivo: a tug-of-war or coordinated movement?" Science **308**(5727): 1469-72.
- Lacey, M. L. and L. T. Haimo (1994). "Cytoplasmic dynein binds to phospholipid vesicles." Cell Motil Cytoskeleton **28**(3): 205-12.
- Lariviere, R. C. and J. P. Julien (2004). "Functions of intermediate filaments in neuronal development and disease." J Neurobiol **58**(1): 131-48.
- Lemos, C. L., P. Sampaio, H. Maiato, M. Costa, L. V. Omel'yanchuk, V. Liberal and C. E. Sunkel (2000). "Mast, a conserved microtubule-associated protein required for bipolar mitotic spindle organization." Embo J **19**(14): 3668-82.
- Liang, Y., W. Yu, Y. Li, Z. Yang, X. Yan, Q. Huang and X. Zhu (2004). "Nudel functions in membrane traffic mainly through association with Lis1 and cytoplasmic dynein." J Cell Biol **164**(4): 557-66.
- Ligon, L. A., S. S. Shelly, M. Tokito and E. L. Holzbaur (2003). "The microtubule plus-end proteins EB1 and dynactin have differential effects on microtubule polymerization." Mol Biol Cell **14**(4): 1405-17.
- Ligon, L. A., M. Tokito, J. M. Finklestein, F. E. Grossman and E. L. Holzbaur (2004). "A direct interaction between cytoplasmic dynein and kinesin I may coordinate motor activity." J Biol Chem **279**(18): 19201-8.
- Lin, C. M., H. J. Chen, C. L. Leung, D. A. Parry and R. K. Liem (2005). "Microtubule actin crosslinking factor 1b: a novel plakin that localizes to the Golgi complex." J Cell Sci.
- Luna, E. J. and A. L. Hitt (1992). "Cytoskeleton--plasma membrane interactions." Science **258**(5084): 955-64.
- Maes, T., A. Barcelo and C. Buesa (2002). "Neuron navigator: a human gene family with homology to unc-53, a cell guidance gene from *Caenorhabditis elegans*." Genomics **80**(1): 21-30.
- Maiato, H., A. Khodjakov and C. L. Rieder (2005). "Drosophila CLASP is required for the incorporation of microtubule subunits into fluxing kinetochore fibres." Nat Cell Biol **7**(1): 42-7.
- Maiato, H., C. L. Rieder, W. C. Earnshaw and C. E. Sunkel (2003). "How do kinetochores CLASP dynamic microtubules?" Cell Cycle **2**(6): 511-4.
- Mallik, R. and S. P. Gross (2004). "Molecular motors: strategies to get along." Curr Biol **14**(22): R971-82.
- Maney, T., M. Wagenbach and L. Wordeman (2001). "Molecular dissection of the microtubule depolymerizing activity of mitotic centromere-associated kinesin." J Biol Chem **276**(37): 34753-8.
- Martinez-Lopez, M. J., S. Alcantara, C. Mascaro, F. Perez-Branguli, P. Ruiz-Lozano, T. Maes, E. Soriano and C. Buesa (2005). "Mouse Neuron navigator 1, a novel microtubule-associated protein involved in neuronal migration." Mol Cell Neurosci **28**(4): 599-612.
- Mathe, E., Y. H. Inoue, W. Palframan, G. Brown and D. M. Glover (2003). "Orbit/Mast, the CLASP orthologue of *Drosophila*, is required for asymmetric stem cell and cystocyte divisions and development of the polarised microtubule network that interconnects oocyte and nurse cells during oogenesis." Development **130**(5): 901-15.

- Matthews, L. R., P. Carter, D. Thierry-Mieg and K. Kemphues (1998). "ZYG-9, a *Caenorhabditis elegans* protein required for microtubule organization and function, is a component of meiotic and mitotic spindle poles." *J Cell Biol* **141**(5): 1159-68.
- Mennella, V., G. C. Rogers, S. L. Rogers, D. W. Buster, R. D. Vale and D. J. Sharp (2005). "Functionally distinct kinesin-13 family members cooperate to regulate microtubule dynamics during interphase." *Nat Cell Biol* **7**(3): 235-45.
- Mermall, V., P. L. Post and M. S. Mooseker (1998). "Unconventional myosins in cell movement, membrane traffic, and signal transduction." *Science* **279**(5350): 527-33.
- Miki, H., Y. Okada and N. Hirokawa (2005). "Analysis of the kinesin superfamily: insights into structure and function." *Trends Cell Biol*.
- Miki, H., M. Setou, K. Kaneshiro and N. Hirokawa (2001). "All kinesin superfamily protein, KIF, genes in mouse and human." *Proc Natl Acad Sci U S A* **98**(13): 7004-11.
- Miller, R. K., S. C. Cheng and M. D. Rose (2000). "Bim1p/Yeb1p mediates the Kar9p-dependent cortical attachment of cytoplasmic microtubules." *Mol Biol Cell* **11**(9): 2949-59.
- Mimori-Kiyosue, Y., N. Shiina and S. Tsukita (2000). "Adenomatous polyposis coli (APC) protein moves along microtubules and concentrates at their growing ends in epithelial cells." *J Cell Biol* **148**(3): 505-18.
- Mimori-Kiyosue, Y. and S. Tsukita (2003). "'Search-and-capture' of microtubules through plus-end-binding proteins (+TIPs)." *J Biochem (Tokyo)* **134**(3): 321-6.
- Moore, A. T., K. E. Rankin, G. von Dassow, L. Peris, M. Wagenbach, Y. Ovechkina, A. Andrieux, D. Job and L. Wordeman (2005). "MCAK associates with the tips of polymerizing microtubules." *J Cell Biol* **169**(3): 391-7.
- Moores, C. A., M. Perderiset, F. Francis, J. Chelly, A. Houdusse and R. A. Milligan (2004). "Mechanism of microtubule stabilization by doublecortin." *Mol Cell* **14**(6): 833-9.
- Moores, C. A., M. Yu, J. Guo, C. Beraud, R. Sakowicz and R. A. Milligan (2002). "A mechanism for microtubule depolymerization by KinI kinesins." *Mol Cell* **9**(4): 903-9.
- Morrison, E. E., B. N. Wardleworth, J. M. Askham, A. F. Markham and D. M. Meredith (1998). "EB1, a protein which interacts with the APC tumour suppressor, is associated with the microtubule cytoskeleton throughout the cell cycle." *Oncogene* **17**(26): 3471-7.
- Munemitsu, S., B. Souza, O. Muller, I. Albert, B. Rubinfeld and P. Polakis (1994). "The APC gene product associates with microtubules in vivo and promotes their assembly in vitro." *Cancer Res* **54**(14): 3676-81.
- Muresan, V. (2000). "One axon, many kinesins: What's the logic?" *J Neurocytol* **29**(11-12): 799-818.
- Nakamura, M., X. Z. Zhou and K. P. Lu (2001). "Critical role for the EB1 and APC interaction in the regulation of microtubule polymerization." *Curr Biol* **11**(13): 1062-7.
- Nathke, I. (2005). "Relationship between the role of the adenomatous polyposis coli protein in colon cancer and its contribution to cytoskeletal regulation." *Biochem Soc Trans* **33**(Pt 4): 694-7.
- Neuwald, A. F., L. Aravind, J. L. Spouge and E. V. Koonin (1999). "AAA+: A class of chaperone-like ATPases associated with the assembly, operation, and disassembly of protein complexes." *Genome Res* **9**(1): 27-43.

- Noetzel, T. L., D. N. Drechsel, A. A. Hyman and K. Kinoshita (2005). "A comparison of the ability of XMAP215 and tau to inhibit the microtubule destabilizing activity of XKCM1." *Philos Trans R Soc Lond B Biol Sci* **360**(1455): 591-4.
- Noiges, R., R. Eichinger, W. Kutschera, I. Fischer, Z. Nemeth, G. Wiche and F. Propst (2002). "Microtubule-associated protein 1A (MAP1A) and MAP1B: light chains determine distinct functional properties." *J Neurosci* **22**(6): 2106-14.
- Nolasco, S., J. Bellido, J. Goncalves, J. C. Zabala and H. Soares (2005). "Tubulin cofactor A gene silencing in mammalian cells induces changes in microtubule cytoskeleton, cell cycle arrest and cell death." *FEBS Lett.*
- Oiwa, K. and H. Sakakibara (2005). "Recent progress in dynein structure and mechanism." *Curr Opin Cell Biol* **17**(1): 98-103.
- Ono, S. (2003). "Regulation of actin filament dynamics by actin depolymerizing factor/cofilin and actin-interacting protein 1: new blades for twisted filaments." *Biochemistry* **42**(46): 13363-70.
- Ovechkina, Y. and L. Wordeman (2003). "Unconventional motoring: an overview of the Kin C and Kin I kinesins." *Traffic* **4**(6): 367-75.
- Pedrotti, B., M. Francolini, F. Cotelli and K. Islam (1996). "Modulation of microtubule shape in vitro by high molecular weight microtubule associated proteins MAP1A, MAP1B, and MAP2." *FEBS Lett* **384**(2): 147-50.
- Peeters, P. J., A. Baker, I. Goris, G. Daneels, P. Verhasselt, W. H. Luyten, J. J. Geysen, S. U. Kass and D. W. Moechars (2004). "Sensory deficits in mice hypomorphic for a mammalian homologue of unc-53." *Brain Res Dev Brain Res* **150**(2): 89-101.
- Perez, F., G. S. Diamantopoulos, R. Stalder and T. E. Kreis (1999). "CLIP-170 highlights growing microtubule ends in vivo." *Cell* **96**(4): 517-27.
- Pollard, T. D. and C. C. Beltzner (2002). "Structure and function of the Arp2/3 complex." *Curr Opin Struct Biol* **12**(6): 768-74.
- Popov, A. V. and E. Karsenti (2003). "Stu2p and XMAP215: turncoat microtubule-associated proteins?" *Trends Cell Biol* **13**(11): 547-50.
- Pring, M., M. Evangelista, C. Boone, C. Yang and S. H. Zigmond (2003). "Mechanism of formin-induced nucleation of actin filaments." *Biochemistry* **42**(2): 486-96.
- Pryer, N. K., R. A. Walker, V. P. Skeen, B. D. Bourns, M. F. Soboeiro and E. D. Salmon (1992). "Brain microtubule-associated proteins modulate microtubule dynamic instability in vitro. Real-time observations using video microscopy." *J Cell Sci* **103** (Pt 4): 965-76.
- Ramaekers, F. C. and F. T. Bosman (2004). "The cytoskeleton and disease." *J Pathol* **204**(4): 351-4.
- Rayment, I., H. M. Holden, M. Whittaker, C. B. Yohn, M. Lorenz, K. C. Holmes and R. A. Milligan (1993). "Structure of the actin-myosin complex and its implications for muscle contraction." *Science* **261**(5117): 58-65.
- Reisler, E. (1993). "Actin molecular structure and function." *Curr Opin Cell Biol* **5**(1): 41-7.
- Rickard, J. E. and T. E. Kreis (1991). "Binding of pp170 to microtubules is regulated by phosphorylation." *J Biol Chem* **266**(26): 17597-605.
- Rissman, R. A., W. W. Poon, M. Blurton-Jones, S. Oddo, R. Torp, M. P. Vitek, F. M. LaFerla, T. T. Rohn and C. W. Cotman (2004). "Caspase-cleavage of tau is an early event in Alzheimer disease tangle pathology." *J Clin Invest* **114**(1): 121-30.

- Roger, B., J. Al-Bassam, L. Dehmelt, R. A. Milligan and S. Halpain (2004). "MAP2c, but not tau, binds and bundles F-actin via its microtubule binding domain." Curr Biol **14**(5): 363-71.
- Rogers, S. L., G. C. Rogers, D. J. Sharp and R. D. Vale (2002). "Drosophila EB1 is important for proper assembly, dynamics, and positioning of the mitotic spindle." J Cell Biol **158**(5): 873-84.
- Rogers, S. L., U. Wiedemann, U. Hacker, C. Turck and R. D. Vale (2004). "Drosophila RhoGEF2 associates with microtubule plus ends in an EB1-dependent manner." Curr Biol **14**(20): 1827-33.
- Rowinsky, E. K. (1997). "The development and clinical utility of the taxane class of antimicrotubule chemotherapy agents." Annu Rev Med **48**: 353-74.
- Saffin, J. M., M. Venoux, C. Prigent, J. Espeut, F. Poulat, D. Giorgi, A. Abrieu and S. Rouquier (2005). "ASAP, a human microtubule-associated protein required for bipolar spindle assembly and cytokinesis." Proc Natl Acad Sci U S A.
- Sapir, T., M. Elbaum and O. Reiner (1997). "Reduction of microtubule catastrophe events by LIS1, platelet-activating factor acetylhydrolase subunit." Embo J **16**(23): 6977-84.
- Sawin, K. E. (2000). "Microtubule dynamics: the view from the tip." Curr Biol **10**(23): R860-2.
- Schroer, T. A. (2000). "Motors, clutches and brakes for membrane traffic: a commemorative review in honor of Thomas Kreis." Traffic **1**(1): 3-10.
- Schroer, T. A. (2001). "Microtubules don and doff their caps: dynamic attachments at plus and minus ends." Curr Opin Cell Biol **13**(1): 92-6.
- Schroer, T. A. (2004). "Dynactin." Annu Rev Cell Dev Biol **20**: 759-79.
- Schuyler, S. C. and D. Pellman (2001). "Microtubule "plus-end-tracking proteins": The end is just the beginning." Cell **105**(4): 421-4.
- Sellers, J. R. (2000). "Myosins: a diverse superfamily." Biochim Biophys Acta **1496**(1): 3-22.
- Shirasu-Hiza, M., P. Coughlin and T. Mitchison (2003). "Identification of XMAP215 as a microtubule-destabilizing factor in Xenopus egg extract by biochemical purification." J Cell Biol **161**(2): 349-58.
- Sproul, L. R., D. J. Anderson, A. T. Mackey, W. S. Saunders and S. P. Gilbert (2005). "Cik1 targets the minus-end Kinesin depolymerase kar3 to microtubule plus ends." Curr Biol **15**(15): 1420-7.
- Stewart, M. (1993). "Intermediate filament structure and assembly." Curr Opin Cell Biol **5**(1): 3-11.
- Suprenant, K. A., J. A. Tuxhorn, M. A. Daggett, D. P. Ahrens, A. Hostetler, J. M. Palange, C. E. VanWinkle and B. T. Livingston (2000). "Conservation of the WD-repeat, microtubule-binding protein, EMAP, in sea urchins, humans, and the nematode *C. elegans*." Dev Genes Evol **210**(1): 2-10.
- Tai, C. Y., D. L. Dujardin, N. E. Faulkner and R. B. Vallee (2002). "Role of dynein, dynactin, and CLIP-170 interactions in LIS1 kinetochore function." J Cell Biol **156**(6): 959-68.
- Tanaka, T., F. F. Serneo, C. Higgins, M. J. Gambello, A. Wynshaw-Boris and J. G. Gleeson (2004). "Lis1 and doublecortin function with dynein to mediate coupling of the nucleus to the centrosome in neuronal migration." J Cell Biol **165**(5): 709-21.

- Tian, G., S. A. Lewis, B. Feierbach, T. Stearns, H. Rommelaere, C. Ampe and N. J. Cowan (1997). "Tubulin subunits exist in an activated conformational state generated and maintained by protein cofactors." *J Cell Biol* **138**(4): 821-32.
- Tirnauer, J. S., S. Grego, E. D. Salmon and T. J. Mitchison (2002). "EB1-microtubule interactions in *Xenopus* egg extracts: role of EB1 in microtubule stabilization and mechanisms of targeting to microtubules." *Mol Biol Cell* **13**(10): 3614-26.
- Tirnauer, J. S., E. O'Toole, L. Berrueta, B. E. Bierer and D. Pellman (1999). "Yeast Bim1p promotes the G1-specific dynamics of microtubules." *J Cell Biol* **145**(5): 993-1007.
- Tsukada, M., A. Prokscha, E. Ungewickell and G. Eichele (2005). "Doublecortin association with actin filaments is regulated by neurabin II." *J Biol Chem* **280**(12): 11361-8.
- Vale, R. D. and R. A. Milligan (2000). "The way things move: looking under the hood of molecular motor proteins." *Science* **288**(5463): 88-95.
- Vallee, R. B. and M. P. Sheetz (1996). "Targeting of motor proteins." *Science* **271**(5255): 1539-44.
- Vallee, R. B., C. Tai and N. E. Faulkner (2001). "LIS1: cellular function of a disease-causing gene." *Trends Cell Biol* **11**(4): 155-60.
- van Breugel, M., D. Drechsel and A. Hyman (2003). "Stu2p, the budding yeast member of the conserved Dis1/XMAP215 family of microtubule-associated proteins is a plus end-binding microtubule destabilizer." *J Cell Biol* **161**(2): 359-69.
- Vaughan, K. T. and R. B. Vallee (1995). "Cytoplasmic dynein binds dynactin through a direct interaction between the intermediate chains and p150Glued." *J Cell Biol* **131**(6 Pt 1): 1507-16.
- Verhey, K. J., D. L. Lizotte, T. Abramson, L. Barenboim, B. J. Schnapp and T. A. Rapoport (1998). "Light chain-dependent regulation of Kinesin's interaction with microtubules." *J Cell Biol* **143**(4): 1053-66.
- Wade, R. H. and A. A. Hyman (1997). "Microtubule structure and dynamics." *Curr Opin Cell Biol* **9**(1): 12-7.
- Watanabe, T., S. Wang, J. Noritake, K. Sato, M. Fukata, M. Takefuji, M. Nakagawa, N. Izumi, T. Akiyama and K. Kaibuchi (2004). "Interaction with IQGAP1 links APC to Rac1, Cdc42, and actin filaments during cell polarization and migration." *Dev Cell* **7**(6): 871-83.
- Winder, S. J. and K. R. Ayscough (2005). "Actin-binding proteins." *J Cell Sci* **118**(Pt 4): 651-4.
- Wittmann, T. and C. M. Waterman-Storer (2005). "Spatial regulation of CLASP affinity for microtubules by Rac1 and GSK3{beta} in migrating epithelial cells." *J Cell Biol* **169**(6): 929-39.
- Woods, D. F., C. Hough, D. Peel, G. Callaini and P. J. Bryant (1996). "Dlg protein is required for junction structure, cell polarity, and proliferation control in *Drosophila* epithelia." *J Cell Biol* **134**(6): 1469-82.
- Wu, H., M. W. Maciejewski, S. Takebe and S. M. King (2005). "Solution structure of the Tctex1 dimer reveals a mechanism for dynein-cargo interactions." *Structure (Camb)* **13**(2): 213-23.
- Xiang, X. (2003). "LIS1 at the microtubule plus end and its role in dynein-mediated nuclear migration." *J Cell Biol* **160**(3): 289-90.
- Zigmond, S. H. (2004). "Formin-induced nucleation of actin filaments." *Curr Opin Cell Biol* **16**(1): 99-105.

Zumbrunn, J., K. Kinoshita, A. A. Hyman and I. S. Nathke (2001). "Binding of the adenomatous polyposis coli protein to microtubules increases microtubule stability and is regulated by GSK3 beta phosphorylation." Curr Biol **11**(1): 44-9.

The background of the page is a grayscale photograph of a city waterfront. In the foreground, a large body of water reflects the sky. A prominent crane with a long boom extends from the left side towards the center. In the background, a tall, modern building with many windows stands out against a cloudy sky. Several cars are parked along the waterfront promenade.

Chapter 2

Conformational changes in CLIP-170 regulate its binding to microtubules and dynactin localization.

J Cell Biol. 2004 Sep 27;166(7):1003-14.

Conformational changes in CLIP-170 regulate its binding to microtubules and dynactin localization

Gideon Lansbergen,¹ Yulia Komarova,^{3,4} Mauro Modesti,¹ Claire Wyman,^{1,2} Casper C. Hoogenraad,¹ Holly V. Goodson,⁵ Régis P. Lemaître,⁶ David N. Drechsel,⁶ Erik van Munster,⁷ Theodorus W.J. Gadella Jr.,⁷ Frank Grosveld,¹ Niels Galjart,¹ Gary G. Borisy,³ and Anna Akhmanova¹

¹MGC Department of Cell Biology and Genetics and ²Department of Radiation Oncology, Erasmus Medical Center, 3000 DR Rotterdam, Netherlands

³Department of Cell and Molecular Biology, Northwestern University Medical School, Chicago, IL 60611

⁴Laboratory of Cell Motility, A.N. Belozersky Institute, Moscow State University, Moscow, 119992, Russia

⁵Department of Chemistry and Biochemistry, University of Notre Dame, Notre Dame, IN 46556

⁶Max Planck Institute of Molecular Cell Biology and Genetics, 01307 Dresden, Germany

⁷Section of Molecular Cytology and Centre for Advanced Microscopy, Swammerdam Institute for Life Science, University of Amsterdam, 1098 SM Amsterdam, Netherlands

Cytoplasmic linker protein (CLIP)-170, CLIP-115, and the dynactin subunit p150^{Glued} are structurally related proteins, which associate specifically with the ends of growing microtubules (MTs). Here, we show that down-regulation of CLIP-170 by RNA interference results in a strongly reduced accumulation of dynactin at the MT tips. The NH₂ terminus of p150^{Glued} binds directly to the COOH terminus of CLIP-170 through its second metal-binding motif. p150^{Glued} and LIS1, a dynein-associating protein, compete for the interaction with the CLIP-170 COOH terminus, suggesting that LIS1 can act to release dynactin

from the MT tips. We also show that the NH₂-terminal part of CLIP-170 itself associates with the CLIP-170 COOH terminus through its first metal-binding motif. By using scanning force microscopy and fluorescence resonance energy transfer-based experiments we provide evidence for an intramolecular interaction between the NH₂ and COOH termini of CLIP-170. This interaction interferes with the binding of the CLIP-170 to MTs. We propose that conformational changes in CLIP-170 are important for binding to dynactin, LIS1, and the MT tips.

Introduction

Microtubules (MTs) are highly dynamic cytoskeletal elements, which undergo alternating phases of growth and shrinkage (Desai and Mitchison, 1997). This dynamic behavior allows MTs to search the cellular space and to establish and remodel contacts with various cellular components. Therefore, interactions of MT tips with different structures play an important role in many cellular processes and are regulated by a large number of factors. Recently, a diverse group of

proteins has attracted general interest by its ability to bind specifically to the plus ends of growing MTs. These proteins have been designated plus end-tracking proteins (+TIPs; for reviews see Schuyler and Pellman, 2001; Carvalho et al., 2003; Galjart and Perez, 2003; Howard and Hyman, 2003).

The first identified +TIP was the cytoplasmic linker protein (CLIP)-170 (Pierre et al., 1992). CLIP-170 contains two CAP-Gly motifs, which are surrounded by serine-rich regions at its NH₂ terminus, followed by a long coiled-coil structure and two putative metal binding domains ("CCHC zinc fingers" or "zinc knuckles") at the COOH terminus (Fig. 1 A). The closest homologue of CLIP-170 in vertebrates is CLIP-115, which is similar to CLIP-170 in its

The online version of this article contains supplemental material.

Address correspondence to Anna Akhmanova, MGC Dept. of Cell Biology and of Genetics, Erasmus Medical Center, P.O. Box 1738, 3000 DR Rotterdam, Netherlands. Tel.: 31-10-4087166. Fax: 31-10-4089468. email: anna.akhmanova@chello.nl

C.C. Hoogenraad's present address is The Picower Center for Learning and Memory, Massachusetts Institute of Technology, Cambridge, MA 02139.

Key words: plus end-tracking proteins; motor protein; cytoplasmic dynein; LIS1; CLIP-115

Abbreviations used in this paper: CLIP, cytoplasmic linker protein; FRET, fluorescence resonance energy transfer; HIS, 6X histidine; IP, immunoprecipitation; MT, microtubule; RNAi, RNA interference; siRNA, small interfering RNA; SFM, scanning force microscopy; +TIP, plus end-tracking protein.

structure, but lacks the COOH-terminal metal binding motifs (De Zeeuw et al., 1997; Fig. 1 A).

Another, more distant CLIP-170 family member, is p150^{Glued}, which contains one CAP-Gly domain, followed by coiled-coil regions (Holzbaur et al., 1991; Fig. 1 A). p150^{Glued} is the MT-binding subunit of dynactin, a large protein complex, which functions as an accessory factor for cytoplasmic dynein (Karki and Holzbaur, 1999; Allan, 2000).

In many cultured cells CLIPs and dynactin are observed to form cometlike accumulations at the MT tips (Perez et al., 1999; Vaughan et al., 1999). The motifs necessary and sufficient for the MT plus end localization include the CAP-Gly domains and the surrounding serine-rich regions of CLIPs and p150^{Glued} (Diamantopoulos et al., 1999; Hoogenraad et al., 2000; Vaughan et al., 2002).

A large body of data links CLIP-170 to the function of the dynein–dynactin complexes. In budding yeast, genetic analysis of spindle positioning placed Bik1p, the CLIP-170 homologue, in the dynein pathway and has shown that Bik1p contributes to the targeting of dynein to the astral MTs (Sheeman et al., 2003). In mammalian cells, overexpression of CLIP-170 enhances the accumulation of dynactin at the MT ends (Valetti et al., 1999; Hoogenraad et al., 2002; Goodson et al., 2003). This effect depends on the second metal binding motif of CLIP-170 (Goodson et al., 2003). In a separate line of investigation, it was shown that CLIP-170 binds to kinetochores of unattached chromosomes in a dynein–dynactin-mediated manner (Dujardin et al., 1998).

The only direct binding partner of the CLIP-170 COOH terminus, identified so far, is LIS1 (Coquelle et al., 2002). LIS1 is a multifunctional protein, which plays an essential role in brain development and interacts with dynein–dynactin (for reviews see Vallee et al., 2001; Wynshaw-Boris and Gambello, 2001). The binding of LIS1 to CLIP-170 depends on the second zinc knuckle of CLIP-170, and therefore, it has been proposed that the interaction between dynein–dynactin and CLIP-170 is mediated by LIS1 (Coquelle et al., 2002). Although attractive, this proposal is contradicted by a number of observations. First, endogenous CLIP-170 and dynactin can be readily observed at the ends of MTs in interphase cells, whereas endogenous LIS1 is found in a dotlike pattern along the MTs (Smith et al., 2000). Second, overexpression of LIS1 displaces dynactin from the MT ends (Faulkner et al., 2000). Third, endogenous LIS1 can be displaced from kinetochores by overexpressing a LIS1 deletion mutant, without removing either dynactin or CLIP-170 (Tai et al., 2002).

A simple explanation for all these observations can be offered by proposing a direct link between CLIP-170 and dynactin. Here, we provide experimental support for this idea and show that normal dynactin accumulation at MT tips depends on CLIP-170. We also show that CLIP-170 can adopt a folded conformation through an association between its NH₂ and COOH termini. This conformation is likely to be inhibitory for the binding of CLIP-170 to its partners, including dynactin, LIS1, and MTs.

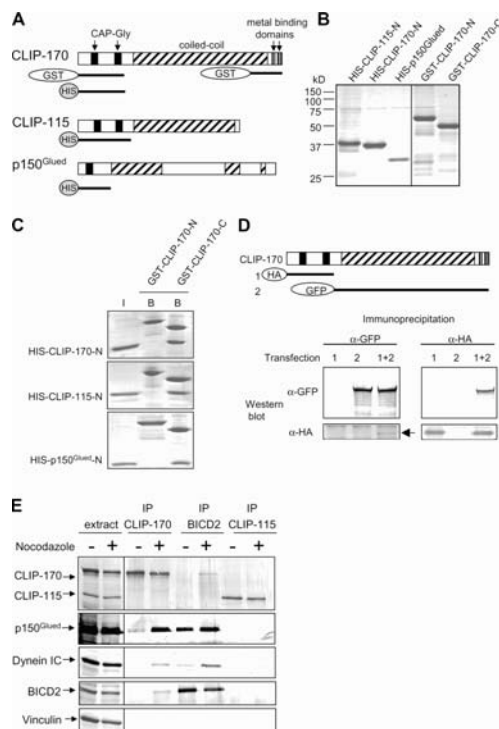


Figure 1. The COOH terminus of CLIP-170 interacts with the NH₂ termini of both CLIPs and p150^{Glued}. (A) Schematic representation of the protein fragments used in this work. (B) Purified fusion proteins shown on a Coomassie-stained gel. (C) GST pull-down assays in low salt conditions with the NH₂ termini of the two CLIPs and p150^{Glued}. Coomassie-stained gels are shown. I, 10% of the input; B, 25% of the protein retained on beads. (D) GST pull-down assays in low salt conditions with the NH₂ termini of the two CLIPs and p150^{Glued}. Anti-GFP or anti-HA antibodies were used for IP in low salt conditions. (E) IPs performed in low salt conditions from untransfected CHO cells that were either untreated or incubated for 1 h with 10 μM nocodazole. Antibody against vinculin served as a negative control.

Results

The COOH terminus of CLIP-170 interacts directly with the NH₂ termini of both CLIPs and p150^{Glued}

Our previous work showed that overexpression of the CLIP-170 COOH-terminal domain had a dominant negative effect: namely, it led to a highly decreased MT tip association of all three CAP-Gly-containing proteins (Komarova et al., 2002). We reasoned that the underlying mechanism might be the sequestration by the CLIP-170 COOH terminus of p150^{Glued} and the CLIPs by binding to their NH₂-terminal domains, which are necessary for their interaction with MTs. To test this possibility, we purified GST- and 6X histidine (HIS)-tagged fusions of the NH₂-terminal domains of CLIP-115, CLIP-170, p150^{Glued}, and the COOH terminus of CLIP-170 (Fig. 1, A and B). We

investigated by GST pull-down assays if these proteins could directly interact with each other and found that HIS-tagged NH₂ termini of both CLIPs and p150^{Glued} bound to the GST-tagged COOH terminus, but not the NH₂ terminus of CLIP-170 (Fig. 1 C).

In apparent contradiction with the *in vitro* data, endogenous CLIP-170 was never coprecipitated with the CLIP-170 COOH terminus (Komarova et al., 2002). This could be explained if the NH₂ and COOH termini of CLIP-170 interacted with each other within the same molecule. In this way, endogenous CLIP-170 could "titrate itself" out of the complex with the overexpressed CLIP-170 COOH terminus. This explanation predicts that the NH₂- and COOH-terminal domains of CLIP-170, expressed as separate proteins, should form a complex. Indeed, GFP-CLIP-170-N and HA-CLIP-170-C coexpressed in COS-1 cells, coprecipitated with each other (Fig. 1 D), supporting the data from the *in vitro* binding assays.

Endogenous CLIP-170 and dynactin interact *in vivo*

To investigate if the interaction between the COOH terminus of CLIP-170 and endogenous CAP-Gly proteins occurs *in vivo*, we used CLIP-170 antibodies to perform immunoprecipitations (IPs) on extracts from untransfected CHO cells. As a control, we used antibodies against CLIP-115, which is not expected to interact with dynactin, and Bicaudal D2 (BICD2), a dynein–dynactin binding protein, which does not coprecipitate with CLIP-170 under normal conditions (Hoogenraad et al., 2001). p150^{Glued}, but not CLIP-115, coprecipitated with both CLIP-170 and BICD2 (Fig. 1 E). As expected, CLIP-115 and p150^{Glued} did not coprecipitate with each other (Fig. 1 E). This experiment shows that CLIP-170 binds to dynactin under physiological conditions, whereas no association between CLIP-170 and CLIP-115 is detected. We cannot exclude, however, that CLIP-170 titrates itself out of the complex with CLIP-115, similar to what is likely to occur with the overexpressed CLIP-170 tail.

Interestingly, the coprecipitation between CLIP-170 and dynactin was enhanced by nocodazole treatment. After MT depolymerization, some coprecipitation was also observed between CLIP-170, cytoplasmic dynein, and BICD2, and the association of BICD2 with dynein was also increased (Fig. 1 E). This is in line with our previous observation that nocodazole treatment results in formation of dynein–dynactin–BICD2-containing aggregates (Hoogenraad et al., 2001). We observed that CLIP-170, but not CLIP-115, was also present in these structures, which apparently result from aggregation of dynein–dynactin with their binding partners after MT depolymerization (Fig. S1, available at <http://www.jcb.org/cgi/content/full/jcb.200402082/DC1>).

The CLIPs and p150^{Glued} preferentially bind to distinct zinc knuckles of CLIP-170

Next, we sought to determine the sites in the COOH-terminal domain of CLIP-170, important for the identified interactions. The deletion of metal-binding motifs abolished the dominant-negative action of the CLIP-170 COOH terminus (unpublished data), indicating that these motifs play a significant role in the association with CAP-Gly proteins. Therefore, we used mutated versions of the

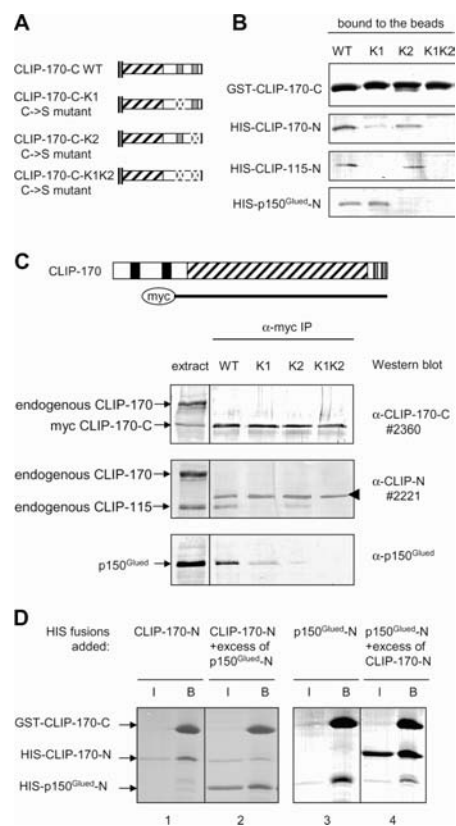
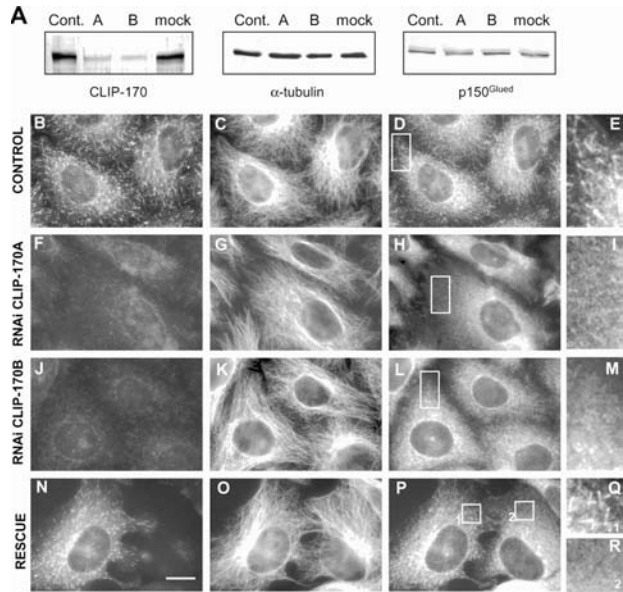


Figure 2. Distinct zinc knuckles of the CLIP-170 COOH terminus are responsible for its binding to the NH₂ termini of the two CLIPs and p150^{Glued}. (A) Schematic representation of the CLIP-170 zinc knuckle mutants. (B) Pull-down assays with the GST fusions of CLIP-170 zinc knuckle mutants and the NH₂ termini of the three CAP-Gly proteins, performed with purified proteins in high salt conditions. Coomassie staining is shown for the GST fusions, Western blots with anti-HIS antibodies for the HIS-tagged fusions. (C) IPs of CLIP-170 COOH-terminal constructs. Extracts were prepared from CHO cells transfected with the myc-tagged CLIP-170 COOH-terminal constructs, either wild type or with the zinc knuckle mutations, and IPs were performed with anti-myc antibodies in low salt conditions. Note that the "CLIP head" antibody 2221 cross-reacts with the CLIP-170-C proteins (arrowhead). (D) Competition assay between CLIP-170 and p150^{Glued} NH₂ termini for the binding to the CLIP-170 COOH terminus. The assay was performed in low salt with either a low amount of HIS-CLIP-170-N (1 and 2) and an 8× M excess of HIS-p150^{Glued}-N (2) or with a low amount of HIS-p150^{Glued}-N (3 and 4) and an 8× M excess of HIS-CLIP-170-N (4). I, 10% of the input, B, 25% of the proteins retained on the beads.

CLIP-170 COOH terminus, in which two cysteines of either the first, the second or both metal binding domains were exchanged for serines (CCHC to SSHC mutations [Goodson et al., 2003], designated K1, K2, and K1K2 mutants; Fig. 2 A). Using GST pull-down assays, we found that in low salt conditions (100 mM NaCl) the wild type

Figure 3. CLIP-170 recruits dynactin to the MT plus ends in HeLa cells. (A) Depletion of CLIP-170 by RNAi. Western blot analysis of the extracts of cells, treated with the RNAi duplex against luciferase (Cont.), CLIP-170A (lane "A"), CLIP-170B (lane "B"), or mock transfected. (B–M) Immunofluorescent staining of siRNA-treated cells. Cells were stained for CLIP-170 (B, F, and J), α -tubulin (C, G, and K), and p150^{Glued} (D, H, and L). Enlarged portions of the p150^{Glued}-stained cells, indicated by white rectangles, are shown in E, I and M. (N–R) Rescue of dynactin localization by CLIP-115(+tail) fusion. HeLa cells were transfected with the CLIP-170B duplex, and 60 h later were transfected with GFP-CLIP-115(+tail). (N) GFP signal. (O) Staining for α -tubulin. (P) Staining for p150^{Glued}. (Q and R) Enlarged portions of the two cells, either transfected or untransfected with the rescue construct, respectively. Bar, 10 μ m.



and all three mutants were still able to bind to the NH₂ termini of all three CAP-Gly proteins (not depicted). However, at 400 mM NaCl, the p150^{Glued} NH₂ terminus bound only to the CLIP-170 COOH-terminal fragments with an intact second metal binding domain (K1; Fig. 2 B). In contrast, an efficient interaction with the NH₂ termini of both CLIPs depended on the first zinc knuckle (Fig. 2 B). These data are consistent with the fact that the CLIP-170-mediated relocalization of dynactin depends on the second metal binding domain, whereas the self-association of CLIP-170, revealed as aggregate formation upon overexpression, relies on the first zinc knuckle (Coquelle et al., 2002; Goodson et al., 2003).

The selective binding of the CLIP NH₂ termini and dynactin to the two different zinc knuckles of CLIP-170 was further supported by IP of CLIP-170 COOH-terminal mutants from transfected CHO cells. Coprecipitation of CLIP-115 occurred only if the first zinc knuckle was intact (Fig. 2 C). p150^{Glued} displayed very little coprecipitation with the K2 and K1K2 mutants, underscoring the importance of the second metal binding domain of CLIP-170 for the association with dynactin. The binding between p150^{Glued} and the K1 mutant was reduced, compared with the nonmutated protein, suggesting that in cells the first zinc knuckle also contributes to the CLIP-170–dynactin interaction.

Although the NH₂ termini of CLIP-170 and p150^{Glued} associate with different zinc knuckles of CLIP-170, their binding sites are likely to overlap. Indeed, the addition of an excess of p150^{Glued} NH₂ terminus reduced the binding of CLIP-170 NH₂ terminus to CLIP-170 COOH terminus, and vice versa (Fig. 2 D). These data show that the two CAP-Gly proteins can interfere with each other's binding to the CLIP-170 COOH terminus.

CLIP-170 targets dynactin to the MT tips

We have demonstrated that CLIP-170 binds p150^{Glued} *in vivo* and *in vitro*. To address the role of CLIP-170 in the cytoplasmic distribution of dynactin, we knocked down CLIP-170 by RNA interference (RNAi) in HeLa cells, which express CLIP-170, but not CLIP-115 (unpublished data). We used two small interfering RNA (siRNA) duplexes (CLIP-170A and CLIP-170B), directed against different regions of CLIP-170 mRNA. Significant down-regulation of CLIP-170 was detected 3 d after treatment of cells with either duplex as evaluated by Western blotting and immunostaining of transfected cells (Fig. 3, A, F, and J). Densitometry analysis of Western blots indicated that the reduction in CLIP-170 level was >80% for the A duplex and >90% for the B duplex. Control treatment with a duplex directed against luciferase did not result in a decrease of CLIP-170 amount compared with mock-transfected cells. Down-regulation of CLIP-170 did not cause any change in the expression level of p150^{Glued} (Fig. 3 A).

Next, we examined the localization of p150^{Glued} in siRNA-treated cells. We detected prominent MT tip labeling by p150^{Glued} antibodies in cells treated with the control siRNA (Fig. 3, B–E). However, in cells treated with either CLIP-170A or CLIP-170B siRNA, a much more diffuse pattern of p150^{Glued} was observed (Fig. 3, F–M). We performed a rescue experiment by expressing a fusion construct, in which the COOH-terminal metal binding domain of CLIP-170 was attached to the end of CLIP-115 (GFP-CLIP-115(+tail)). This construct is not sensitive to the treatment with the CLIP-170A or CLIP-170B siRNA duplexes. Previously, we have shown that overexpression of GFP-CLIP-115(+tail) enhanced dynactin accumulation at the growing plus ends (Hoogenraad et al., 2002). Here, we observed that the expression of this fusion protein restored the normal

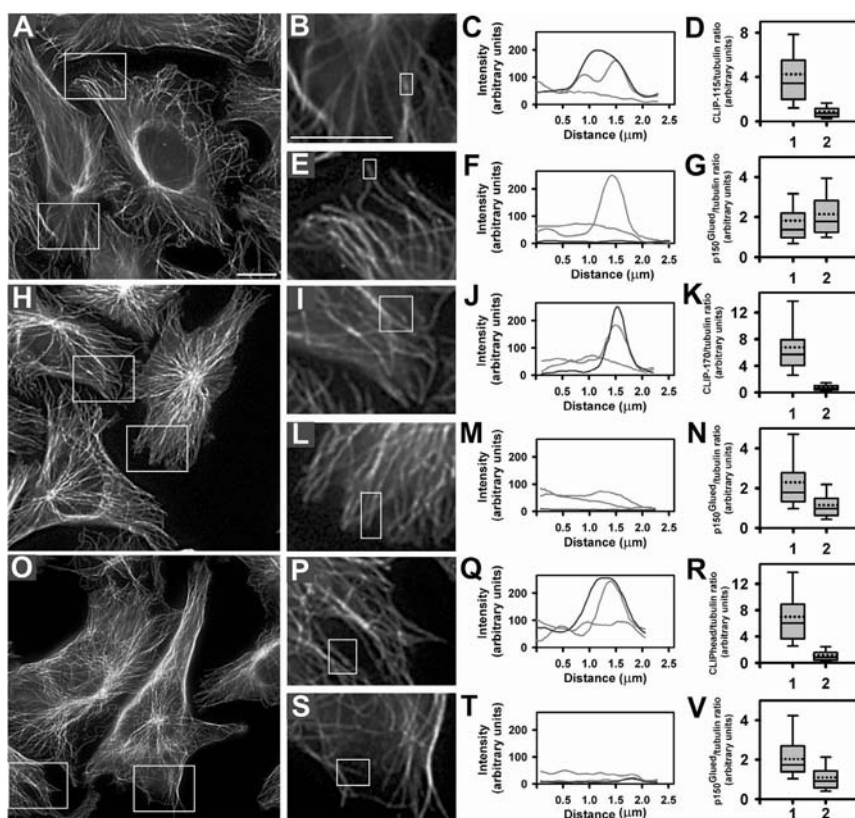


Figure 4. CLIP-170 recruits dynactin to the MT plus ends in CHO cells. RNAi experiments in CHO cells. In the fluorescent images (A, B, E, H, I, L, O, P, and S) and the line scans (C, F, J, M, Q, and T), the α -tubulin signals are shown in green, CLIP-specific signals in blue, and p150^{Glued} in red. Line scans correspond to individual MT plus ends, starting at $\sim 2 \mu\text{m}$ away from the MT end. The ratio of the signal of the plus end-tracking protein to tubulin in experimental cells was expressed as a percentage of the same ratio in control cells, which was taken for 100%. The box plot graphs (D, G, K, N, R, and V) are used to demonstrate statistical analysis of p150^{Glued}/tubulin or CLIP/tubulin ratio at the MT tip in control (1) and knockdown (2) cells. The boundaries of the box indicate the 25th and the 75th percentile, whiskers indicate the 90th and 10th percentiles. The median and mean are shown by a straight and a dotted line, respectively. The differences between the measured ratios are significant ($P < 0.0001$ for D, K, N, R, V; $P < 0.03$ for G, determined with the t test). In all cases 95% confidence intervals are nonoverlapping. (A–G) Knockdown of CLIP-115. (A, B, and E) Knockdown cells were identified by staining with CLIP-115-specific antibodies. (B and C) Control (untransfected) cells. (E and F) CLIP-115 knockdown cells. (H–N) Knockdown of CLIP-170. (H, I, and L) Knockdown cells were identified by staining with CLIP-170-specific antibodies. (I and J) Control (untransfected) cells. (L and M) CLIP-170 knockdown cells. (O–V) Knockdown of both CLIPs. (O, P, and S) Knockdown cells were identified by staining with the antibody against both CLIPs. (P and Q) Control (untransfected) cells. (S and T) CLIP-115 and CLIP-170 knockdown cells. Note that the centrosomal localization of dynactin is not affected by CLIP-170 knockdown. Bars, $10 \mu\text{m}$.

dynactin pattern when endogenous CLIP-170 was knocked down (Fig. 3, N–R). This experiment shows that the metal binding domains of CLIP-170 are involved in targeting of p150^{Glued} to the MT plus ends.

The large number of MT tips and other dynactin-positive granules made it difficult to quantify dynactin accumulation at MT tips in HeLa cells. Therefore, we switched to CHO cells, which have a sparser MT cytoskeleton. CHO cells co-express both CLIP-170 and CLIP-115; therefore, the effect of the knockdown of each single CLIP protein or both CLIPs simultaneously could be analyzed in this system.

Transfection of RNA duplexes did not work efficiently in CHO cells in our hands. Consequently, we used plasmid-based RNAi instead (Brummelkamp et al., 2002). The target sequences for CLIP-170 and CLIP-115 RNAi were chosen based on human-mouse homology. To confirm their identity with the hamster sequences, the corresponding portions of CLIP-170 and CLIP-115 cDNAs were obtained by RT-PCR from CHO cells and sequenced. To knock down both CLIPs, we combined two RNAi cassettes in the same vector. As a control, we used a GFP-expressing RNAi vector directed against luciferase.

CHO cells were transfected with different RNAi vectors and 4 d after transfection the cells were stained for CLIPs, p150^{Glued}, and tubulin (Fig. 4). The knockdown cells were identified by the strongly reduced CLIP staining, whereas the surrounding, nontransfected cells served as an internal control. CHO cells, transfected with the control vector, were detected by staining with anti-GFP antibody.

Line scan analysis (plots of intensity vs. distance), demonstrated that knockdown of CLIP-115 had no strong effect on the p150^{Glued} distribution (Fig. 4, A–G). RNAi-treated cells showed a reduction of CLIP-115-specific signal to $20 \pm 5.8\%$ (SEM) compared with control surrounding cells whereas the p150^{Glued} signal was slightly elevated to $117 \pm 3\%$ ($n = 197$ MT ends in 18 knockdown cells; 156 ends in 23 control cells). In contrast, knockdown of CLIP-170 ($12 \pm 5\%$ remaining) resulted in a significant reduction ($50 \pm 3.5\%$ remaining) of the p150^{Glued} signal at the MT tip (Fig. 4, H–N; $n = 271$ MT ends in 18 knockdown cells; 168 ends in 19 control cells). A similar result was obtained in cells where both CLIP species were knocked down simultaneously (Fig. 4, O–V). Quantification of the signals for the CLIPs (Fig. 4 R) and p150^{Glued} (Fig. 4 V) gave values of $16 \pm 6\%$ and $52 \pm 5\%$, respectively, compared with control levels ($n = 207$ MT plus ends in 19 knockdown cells; 157 ends in 20 control cells). No change in the distribution of either CLIPs or p150^{Glued} was observed in GFP-positive cells transfected with the control RNAi construct (unpublished data). All these data were confirmed by using an antibody against another dynactin subunit, dynamitin (unpublished data).

Furthermore, we observed no differences in the localization of endosomes, the Golgi apparatus, and mitochondria after CLIP-170 knockdown (Fig. S2, available at <http://www.jcb.org/cgi/content/full/jcb.200402082/DC1> and not depicted), indicating that a 50% reduction of dynactin association with MT tips had no significant consequences for the steady-state distribution of these organelles.

p150^{Glued} and LIS1 compete for the binding to the second metal binding domain of CLIP-170

Previous works have shown that LIS1 binds to the CLIP-170 COOH terminus through its second zinc knuckle (Coquelle et al., 2002). Using purified HIS-tagged mouse LIS1 protein (Fig. 5 A) and the GST fusions of CLIP-170 COOH terminus and its K1, K2, and K1K2 mutants, we confirmed this observation in an *in vitro* experiment with purified proteins (Fig. 5 B). Because both LIS1 and p150^{Glued} associate directly with the second metal binding motif of CLIP-170, we tested whether the addition of an excess of the NH₂-terminal fragments of CLIP-170 or p150^{Glued} could inhibit the interaction between CLIP-170 COOH terminus and LIS1. In the presence of the NH₂ terminus of CLIP-170, the association of LIS1 with CLIP-170 COOH terminus was somewhat reduced (Fig. 5 C). More strikingly, the addition of an excess of the p150^{Glued} NH₂ terminus completely abolished the interaction (Fig. 5 C). Because LIS1 and p150^{Glued} NH₂ terminus do not bind to each other (unpublished data), this result demonstrates that p150^{Glued} efficiently competes with LIS1 for binding to CLIP-170. We were not able to reduce the amount of p150^{Glued} bound to the COOH terminus of CLIP-170 by addition of an ex-

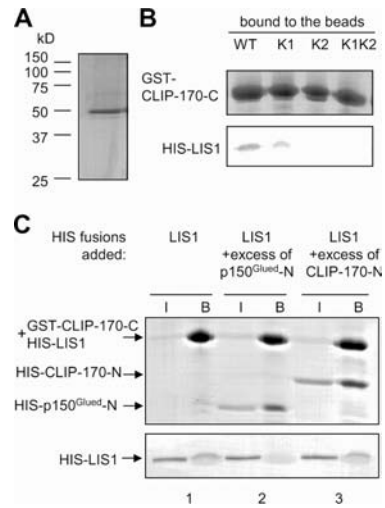


Figure 5. LIS1 and p150^{Glued} compete for binding to the COOH terminus of CLIP-170. (A) Coomassie-stained gel with purified HIS-LIS1 protein. (B) GST pull-down assay using purified HIS-LIS1 in low salt conditions with the wild type and the zinc knuckle mutants of the CLIP-170 COOH terminus. GST fusions are detected by Coomassie staining; HIS-tagged LIS1 detected by Western blotting with anti-HIS antibodies (note that HIS-LIS1 and GST-CLIP-170 have exactly the same size, 50 kD). (C) Competition between LIS1 and p150^{Glued} or CLIP-170 NH₂ termini for the binding to the CLIP-170 COOH terminus. GST pull-down assays were performed in low salt conditions with a low amount of HIS-LIS1 and an 8× M excess of either HIS-p150^{Glued}-N (2) or HIS-CLIP-170-N (3). The top panel shows a Coomassie-stained gel and the bottom panel shows a Western blot with anti-HIS antibodies. I, 10% of the input; B, 25% of the proteins bound to the beads.

cess of LIS1 (unpublished data). This indicates that at least *in vitro*, the CLIP-170 COOH terminus has a higher affinity for p150^{Glued} than for LIS1.

Evidence for intramolecular head-to-tail interaction in CLIP-170

The interaction between the NH₂ and COOH termini of CLIP-170 could be either intramolecular or intermolecular, leading to oligomerization of CLIP-170. To address these possibilities, we have analyzed the structure of the purified full-length CLIP-170 by scanning force microscopy (SFM; Fig. 6, A–F). The majority of the molecules (68.9% of the 536 identifiable molecules counted) resembled straight or bent rods (Fig. 6, B–D), supporting previous observations that CLIP-170 is a rod-shaped protein (Scheel et al., 1999). The length of CLIP-170 molecule, measured by us (95.3 ± 16.5 nm) was shorter, than the one previously observed by electron microscopy (~ 135 nm), because the rat brain isoform, used in our work, misses 115 aa of the central heptad repeat region, compared with the CLIP-170 from human placenta, analyzed by Scheel et al. (1999). In contrast to the latter work, we could frequently distinguish the two ends of the molecule. One of the ends of CLIP-170 often displayed two globular heads, which likely represent the NH₂-terminal

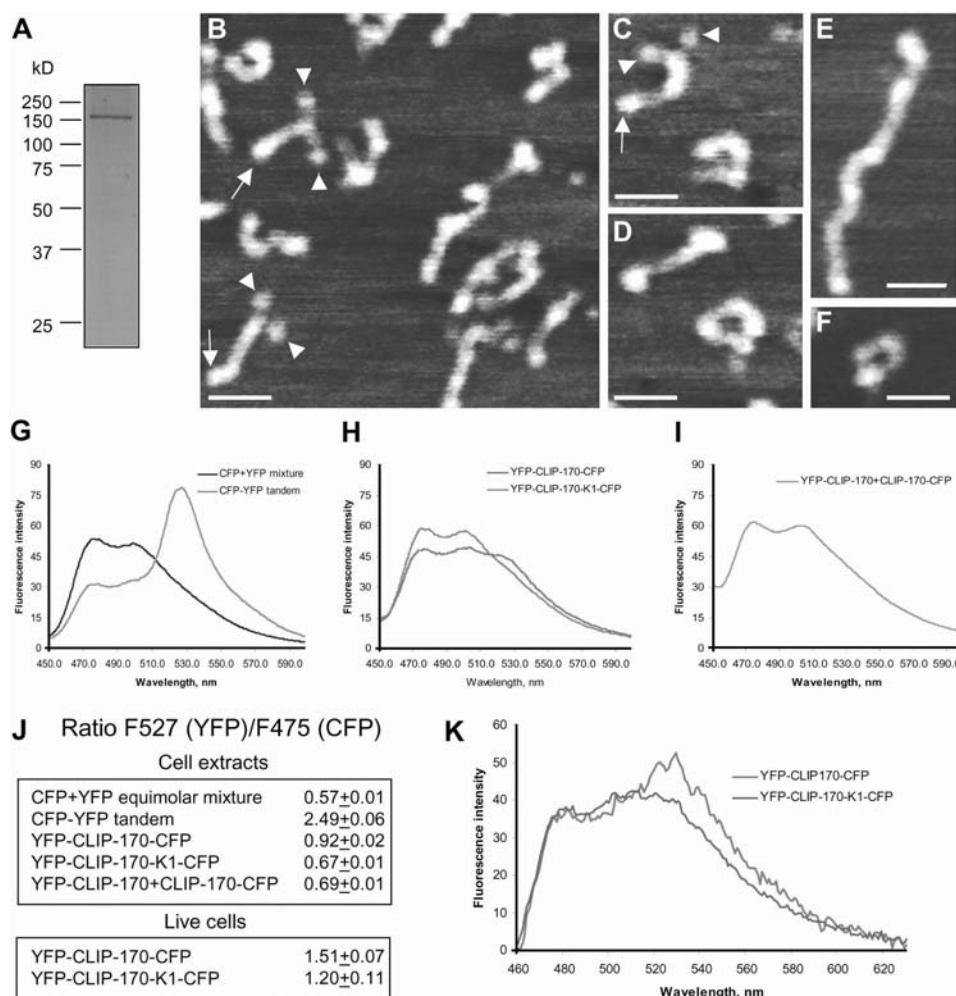


Figure 6. Evidence for intramolecular interaction between the terminal domains of CLIP-170. (A) Coomassie-stained gel with purified HIS-CLIP-170. (B–F) SFM images of the purified HIS-CLIP-170. Color represents height from 0 to 2 nm, blue to white. Bars, 50 nm. Globular head domains are indicated by arrowheads and the COOH-terminal domain is indicated by arrows. (G–I) Uncorrected emission spectra of the extracts of cells, transfected with the indicated constructs, measured with the excitation at 425 nm. Fluorescence intensity is shown in arbitrary units. (J) Ratios of emission at 527 nm (YFP acceptor) to 475 nm (CFP donor). Mean \pm SD was determined from three independent measurements (extracts) or seven different cells (live cells). (K) Uncorrected emission spectra of single live cells, transfected with the indicated constructs after background subtraction. Fluorescence intensity is shown in arbitrary units.

MT-binding domains (~ 350 aa), because they are larger than the COOH-terminal domains (~ 90 aa). These data strongly support the view that CLIP-170 forms parallel dimers.

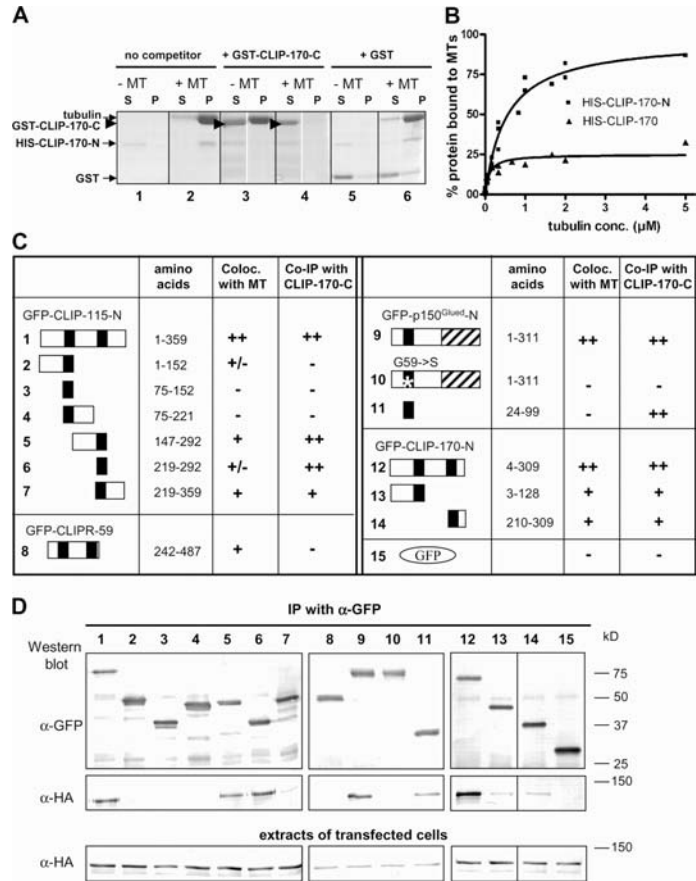
Furthermore, 10.6% of the molecules, classified as single dimers based on their length (average 100.2 ± 10.1 nm), displayed a donutlike shape (Fig. 6, B, C, D, and F). The presence of such molecules clearly demonstrates that the coiled-coiled tail of CLIP-170 is sufficiently flexible to allow the NH_2 and COOH termini to be brought into close proximity. In addition, we also observed CLIP-170 proteins

forming oligomers due to intermolecular end-to-end association (20.5% of the molecules counted; Fig. 6 E). Observation of both inter- and intramolecular association of CLIP-170 NH_2 and COOH termini might suggest that these interactions are transient and dynamic. Alternatively, our preparation might contain a mixture of molecules with different posttranslational modifications, which preferentially stabilize different CLIP-170 conformations.

Next, we reasoned that attaching fluorophores to the NH_2 and COOH termini of CLIP-170 (CFP donor and YFP ac-

Figure 7. The COOH terminus of CLIP-170 interferes with binding of the NH₂ terminus of CLIP-170 to MTs.

(A) MT pelleting assays. Coomassie-stained gels showing supernatants and pellets after incubation of MTs with the HIS-CLIP-170-N, either alone (1 and 2), preincubated with an 8× M excess of GST-CLIP-170-C (3 and 4) or with 15× M excess of GST (5 and 6). Note that GST-CLIP-170-C protein runs slightly below tubulin (arrowheads). S, supernatant; P, pellet. (B) MT pelleting assays with HIS-CLIP-170-N (~50 nM) or full-length CLIP-170 (~10 nM). The dissociation constant for HIS-CLIP-170-N binding to taxol-stabilized MTs, determined by best fit to the data, is $0.53 \pm 0.09 \mu\text{M}$ (\pm SEM). Not more than 30% of the full-length CLIP-170 could be pelleted with MTs. (C) Schematic representation of different fragments of CLIP-115, CLIP-59, p150^{Glued}, and CLIP-170 fused to GFP. Fusions were tested for colocalization with MTs in transfected COS-7 cells and their capacity to coprecipitate with the HA-CLIP-170 COOH terminus. (D) IPs with CLIP-170 COOH terminus. COS-1 cells were cotransfected with the HA-CLIP-170 COOH terminus together with the indicated GFP fusion proteins, and IP was performed with anti-GFP antibodies in a buffer with 150 mM NaCl. The expression of the HA-CLIP-170-C fusion was controlled by the Western blotting of the cell extracts with anti-HA antibodies (bottom).



ceptor) would allow us to detect fluorescence resonance energy transfer (FRET) if CLIP-170 indeed folds back and its NH₂ and COOH termini are brought within a 10-nm distance (Pollok and Heim, 1999). We generated a CLIP-170 fusion with YFP at the NH₂ terminus and a glycine linker, followed by CFP at the COOH terminus (YFP-CLIP-170-CFP). As a control, we used a mutated version of this CLIP-170 fusion protein, in which the first zinc knuckle, necessary for the interaction between the CLIP NH₂ and COOH termini, was disrupted (YFP-CLIP-170-K1-CFP).

COS-1 cells were transfected with plasmids, expressing either CFP or YFP, a CFP-YFP tandem fusion, YFP-CLIP-170-CFP or YFP-CLIP-170-K1-CFP and the fluorescence spectra of the resulting cell extracts were measured. A mixture of cell extracts, containing an equimolar amount of CFP and YFP, served as a negative FRET control, which displayed no significant emission of the YFP acceptor after the excitation of the CFP donor (Fig. 6 G). The CFP-YFP tandem, which served as a positive control, displayed marked sensitized YFP fluorescence after CFP excitation due to FRET (Fig. 6 G). A smaller, but significant YFP-sensitized

emission was displayed by the YFP-CLIP-170-CFP but not by the YFP-CLIP-170-K1-CFP-containing cell extract (Fig. 6 H). The occurrence of FRET in the extract, containing the YFP-CLIP170-CFP fusion, is indicated by the higher ratio of fluorescence at 527 nm (YFP emission) to fluorescence at 475 nm (CFP emission) upon excitation at 425 nm, as compared with CFP+YFP mixture or the YFP-CLIP-170-K1-CFP control (Fig. 6 J). The ratio of YFP to CFP fluorescence in the extract, containing YFP-CLIP-170-CFP protein, did not change after it was diluted, suggesting that the binding between the CLIP-170 head and tail was intra- and not intermolecular (unpublished data). This conclusion is further supported by the fact that the extracts prepared from cells, cotransfected with YFP-CLIP-170 and CLIP-170-CFP, display no significant FRET signal (Fig. 6 I).

We have also measured the emission spectra of live COS-7 cells, expressing the same constructs. We selected cells with low expression levels, in which fluorescent CLIP proteins localized to the plus ends, but formed no patches or MT bundles. Again, after CFP excitation, YFP-CLIP-170-CFP displayed higher YFP/CFP fluorescence ratios, than

the K1 mutant (Fig. 6, J and K), indicating that the interaction between NH₂ and COOH terminus of CLIP-170 occurs *in vivo*.

Inhibition of MT binding by head-to-tail interaction in CLIP-170

The proposed conformational change in CLIP-170 could regulate its association with MTs. We tested this idea by MT pelleting assay and found that the addition of an excess of the CLIP-170 COOH terminus abolished the pelleting of the CLIP-170 NH₂ terminus with MTs, whereas the addition of a control protein (GST) had no effect (Fig. 7 A). Similar results were obtained for MT pelleting of p150^{GluEd} NH₂ terminus (not depicted). We also observed that the full-length CLIP-170 pelleted with MTs much less efficiently than CLIP-170 NH₂ terminus (Fig. 7 B). This suggests that interaction of the COOH terminus of CLIP-170 either with its own NH₂ terminus or with p150^{GluEd} interferes with their binding to MTs, explaining the dominant negative effect of the CLIP-170 tail.

Next, we mapped the binding sites of the CAP-Gly proteins for the CLIP-170 COOH terminus. We initially used a collection of the CLIP-115 NH₂-terminal deletion mutants (Hoogenraad et al., 2000; Fig. 7 C and D) and found that only the fusions containing the second, but not the first CAP-Gly domain could coprecipitate CLIP-170 COOH terminus and associate with MTs in transfected cells (Hoogenraad et al., 2000; Fig. 7, C and D). Therefore, it appears that sites of interaction with MTs and with the COOH terminus of CLIP-170 are located in the second CAP-Gly domain of CLIP-115 and are in close proximity. Also in the case of p150^{GluEd}, the CAP-Gly domain is the portion of the protein interacting with CLIP-170 COOH terminus (Fig. 7, C and D). Interestingly, the G59S mutation of p150^{GluEd}, discovered in patients with neurodegenerative disease (Puls et al., 2003), abolishes the interaction of p150^{GluEd} with the CLIP-170 COOH terminus (Fig. 7, C and D), probably because it disrupts the folding of the CAP-Gly domain.

Mapping of the NH₂-terminal part of CLIP-170 uncovered differences between the two CLIPs: both CAP-Gly domains of CLIP-170 localized to MTs in transfected cells and coprecipitated, albeit weakly, with the CLIP-170 COOH terminus (Fig. 7, C and D). Interestingly, the YFP-CLIP-170-CFP molecule, containing only one (the second) CAP-Gly domain, could still produce a FRET signal (unpublished data). This indicates that the second CAP-Gly domain of CLIP-170 alone is sufficient for interaction with the COOH terminus.

We also tested if the MT-binding CAP-Gly domains of a more distant CLIP relative, CLIPR-59 (Perez et al., 2002), could bind to the CLIP-170 COOH terminus and found this not to be the case (Fig. 7, C and D). This result illustrates that the COOH terminus of CLIP-170 interacts only with a subset of the existing CAP-Gly proteins.

Discussion

Association of CLIP-170, dynactin, and LIS1 with MT tips

Here, we have shown that the COOH terminus of CLIP-170 interacts directly with the NH₂ terminus of p150^{GluEd}

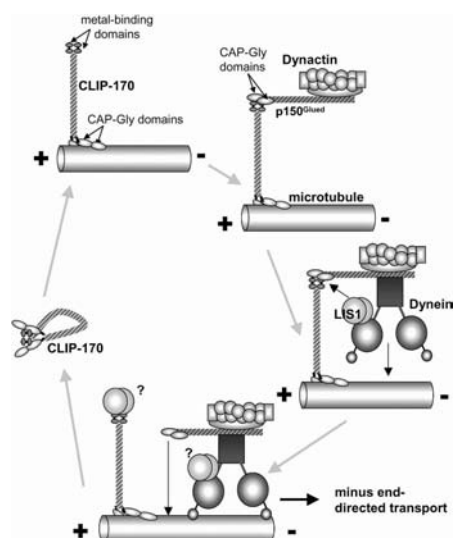


Figure 8. A model of the possible interactions between CLIP-170, dynactin, dynein, and LIS1 at the plus end of a growing MT. We propose that free, MT-unbound CLIP-170 can adopt a folded conformation through an intramolecular interaction of its terminal domains. Binding to MTs correlates with the unfolding of CLIP-170, which allows the interaction of the COOH-terminal domain with its binding partners, such as dynactin, resulting in their recruitment to the MT tip. Dynactin, in its turn, can subsequently recruit cytoplasmic dynein, together with LIS1. LIS1 might act to release dynactin from the complex with CLIP-170, facilitating MT minus end-directed transport. These interactions are probably coordinated with the association of dynein–dynactin complex with the cargo (omitted from the scheme). LIS1 may remain associated with dynein, or, alternatively, it may form a transient complex with CLIP-170. Other possible interactions not involving CLIP-170, such as direct binding of dynactin to the MT tips, are not depicted.

and is required for efficient recruitment of dynactin to the MT tips. Previously it has been observed that expression of CLIP-170 lacking a functional tail interferes with dynactin localization to MT tips (Goodson et al., 2003). CLIP-170 binds to the MT tips in a dynactin-independent manner, because dynactin, but not CLIP-170, is displaced from the tips by overexpression of LIS1 (Faulkner et al., 2000). Moreover, down-regulation of p150^{GluEd} does not change the distribution of CLIPs (unpublished data). Therefore, we propose that a large portion of dynactin accumulated at the MTs tips is “hitchhiking” on CLIP-170, using its capacity to recognize the growing MT plus ends (Fig. 8; the term hitchhiking was introduced by Carvalho et al., 2003).

This conclusion appears to contradict the observations that the NH₂ terminus of p150^{GluEd} binds directly to MTs and to EB1, another +TIP, which is not dependent on CLIP-170 for its MT plus end accumulation (Askham et al., 2002; Komarova et al., 2002; Vaughan et al., 2002; Ligon et al., 2003). We believe that p150^{GluEd} can indeed recognize the growing MT tips independently of CLIP-170, because the knockdown of CLIP-170 reduced, but did not abolish

dynactin accumulation at the MT tips. We propose that dynactin can interact with MT ends via three independent pathways: directly, via EB1 and through CLIP-170. In HeLa and CHO cells the third pathway contributes significantly to dynactin localization. It is possible that CLIP-170 serves as a transient facilitator of dynactin binding to MT ends.

We have found that LIS1 and p150^{Glued}, which show affinity for the same zinc knuckle of CLIP-170, cannot bind to this protein simultaneously. Although we were not able to compete p150^{Glued} binding to CLIP-170 with an excess of LIS1 *in vitro*, it is likely that in cells such competition can occur, because overexpression of LIS1 displaces dynactin from the MT tips (Faulkner et al., 2000). It was shown that a phosphorylated form of LIS1 colocalizes with CLIP-170 very efficiently (Coquelle et al., 2002); it is possible, therefore, that in cells phosphorylated LIS1 can displace dynactin from MT plus ends.

The function of the competitive relationship between p150^{Glued} and LIS1 is not yet clear. Although LIS1 was shown to interact with both dynein (through its heavy and intermediate chains) and dynactin (through dynamitin), most of the evidence suggests that LIS1 is primarily a partner of cytoplasmic dynein (Tai et al., 2002). We propose that a complex of dynein with LIS1 could bind to dynactin, which is targeted to the MT tip by CLIP-170. The dynein-associated LIS1 could then disrupt dynactin–CLIP-170 interaction, facilitating retrograde dynein transport (Fig. 8).

Alternatively, LIS1 could target dynein to MT tips through CLIP-170, but independently of dynactin. This sequence of interactions occurs in budding yeast, where Bik1p (CLIP-170 homologue) and Pac1p (LIS1 homologue) interact with each other and are both needed for efficient localization of dynein to the astral MTs (Lee et al., 2003; Sheeman et al., 2003). Removal of dynactin in this system enhances dynein localization to the astral MTs, because of a presumed decrease in dynein motor activity. However, it is possible that also in yeast, dynactin, and Pac1p compete with each other for binding to Bik1p, and in the absence of dynactin, the plus end localization of Pac1p and dynein is increased. It is likely that dynein interaction with the MT tips has essential functions, and it is not surprising that multiple, possibly redundant molecular links have evolved to ensure this interaction.

Function of dynactin accumulation at the MT tips

Our work has demonstrated that one of the functions of CLIP-170 is to concentrate dynactin at the tips of growing MTs. Several roles can be envisaged for this localization of dynactin. First, dynactin-bound MT ends can serve as sites for loading of cargos, such as cytoplasmic vesicles or endosomes (Vaughan et al., 1999). If this function were essential, knockdown of CLIP-170 would lead to mislocalization of membrane compartments. However, the steady-state organelle distribution appeared to be normal after CLIP-170 knockdown, as previously reported for other situations when p150^{Glued} localization to plus ends was abolished (Goodson et al., 2003). It is still possible, however, that the kinetics of some types of dynein-mediated transport is affected in the absence of CLIP-170.

Second, dynein–dynactin complexes interact with the cell cortex (Dujardin and Vallee, 2002; Dujardin et al., 2003). By associating with cortical sites, dynein motors are believed to pull at the MTs to reorient the MT network (Burakov et al., 2003). This process is important for the positioning of the mitotic spindle and for directional cell migration. Therefore, it is possible that CLIP-170 and dynactin, targeted to the MT plus ends, contribute to cell motility or spindle positioning.

Finally, CLIP-170, LIS1 and dynein–dynactin localize to kinetochores in prometaphase. A possible role for CLIP-170 in mitotic progression is suggested by overexpression of the CLIP-170 COOH terminus, which displaces endogenous CLIP-170 from the kinetochore and causes a prometaphase delay (Dujardin et al., 1998).

Regulatory role of the CLIP-170 head-to-tail conformation

We have found that CLIP-170 can fold back upon itself through an interaction between its NH₂ and COOH termini. We propose that CLIP-170 alternates between an active, extended conformation, in which it can interact with MTs and its COOH-terminal partners, p150^{Glued} and LIS1; and an inactive, folded conformation, in which it is not bound to other proteins (Fig. 8). The switching between the two conformations could be controlled by phosphorylation. This would explain the behavior of CLIP-170 in nocodazole-treated cells. MT depolymerization by nocodazole increases the rate of CLIP-170 dephosphorylation (Rickard and Kreis, 1991). Under these conditions CLIP-170 is probably in an “open” state, because it binds strongly to the few remaining nocodazole-resistant MTs and also to dynactin, accumulating in dynactin-positive aggregates.

The capacity of CLIP-170 to fold back is very reminiscent of conventional kinesin, the cargo-binding tail of which can associate with its MT-binding motor domain. This interaction prevents wasteful movement of motors not bound to cargo (for review see Verhey and Rapoport, 2001). Such autoinhibition appears to be a common theme in protein evolution with CLIP-170 providing an interesting example.

Materials and methods

Protein purification and *in vitro* binding assays

Protein fragments of CLIP-170, CLIP-115, and p150^{Glued} were produced in *E. coli*. To generate HIS-tagged fusions, the NH₂-terminal fragments of CLIP-170 (nt 183–1113 of the rat brain cDNA available from GenBank/EMBL/DBJ accession no. AJ237670) and p150^{Glued} (nt 270–890 of the rat cDNA available from GenBank/EMBL/DBJ accession no. X62160) were subcloned into pET-28a (Novagen), the NH₂-terminal fragment of CLIP-115 (nt 290–1336 of the rat cDNA available from GenBank/EMBL/DBJ accession no. AJ000485) was subcloned into pQE-9 (QIAGEN). HIS-tagged proteins were produced in Rosetta (DE3) pLysS *E. coli* (pET-28a) or BL21 *E. coli* (pQE-9) and purified using Ni-NTA agarose (QIAGEN) in nondenaturing conditions.

GST fusions of the CLIP-170 NH₂ terminus (nt 183–1046 of the rat cDNA available from GenBank/EMBL/DBJ accession no. AJ237670) and COOH terminus (nt 3555–4142 of the rat cDNA available from GenBank/EMBL/DBJ accession no. AJ237670) were generated in pGEX-2T and pGEX-3X, respectively. K1, K2, and K1K2 mutants of CLIP-170 COOH terminus (Goodson et al., 2003) were used to generate fusion proteins in pGEX-3X (the cDNA fragments corresponded to the nt 3832–4413 of the cDNA available from GenBank/EMBL/DBJ accession no. NM_002956). The GST fusion proteins were produced in BL21 *E. coli* and purified using glutathione-Sepharose 4B (Amersham Biosciences).

HIS-tagged LIS1 and CLIP-170 were purified using the Bac-to-Bac HT Baculovirus Expression System (Invitrogen) as described in the Online supplemental material.

All *in vitro* binding assays were performed in 20 mM Tris-HCl, pH 7.5, 100 mM (low salt) or 400 mM (high salt) NaCl, 1 mM β -mercaptoethanol and 1% Triton X-100 as described by Hoogenraad et al. (2000), using ~10 μ g of a GST fusion protein and 0.5–10 μ g of the HIS-tagged proteins. MT pelleting assays were performed using the MT-associated protein spin-down assay kit (Cytoskeleton, Inc.).

Antibodies

We used mouse mAbs against c-myc and vinculin (Sigma-Aldrich), penta-histidine tag (QIAGEN), p150^{Glued}, dynaminin, and GM130 (BD Biosciences), dynein intermediate chain (CHEMICON International, Inc.), GFP (Roche), HA tag (Babco), transferrin receptor (Boehringer), a rat mAb against α -tubulin (Abcam), rabbit antibody 2360 against CLIP-170 (Coquelle et al., 2002), antibody 2221, which recognizes both CLIPs, antibody 2238 against CLIP-115 (Hoogenraad et al., 2000) and antibody 2293 against BICD2 (Hoogenraad et al., 2001). The following secondary antibodies were used: alkaline phosphatase-labeled anti-rabbit and anti-mouse antibodies (Sigma-Aldrich); FITC-labeled goat anti-rabbit antibody (Nordic Laboratories); Alexa 594- and Alexa 350-labeled anti-rat and anti-mouse antibodies (Molecular Probes); TRITC- and FITC-conjugated donkey anti-mouse, anti-rabbit, and Cy5-coupled anti-rat antibodies (Jackson ImmunoResearch Laboratories).

Expression constructs, transfection, IP, and Western blotting

Human myc-tagged CLIP-170 COOH-terminal constructs were described by Goodson et al. (2003); HA-CLIP-170 NH₂ terminus, GFP-CLIP-170 COOH terminus and GFP-p150^{Glued}-N (Komarova et al., 2002); GFP-CLIP-115(+tail) (Hoogenraad et al., 2002); and the GFP-CLIP-115 NH₂-terminal deletion mutants (Hoogenraad et al., 2000). CFP-YFP tandem contained YFP, fused in frame downstream of CFP with a 20-amino acid linker. YFP-CLIP-170-CFP was derived from the GFP-CLIP-170 fusion, based on the rat brain CLIP-170 cDNA. To make this construct, the GFP was substituted for YFP, and the monomeric (A206K) CFP, preceded by a 7-amino acid linker, was fused to the end of the CLIP-170 ORF using a PCR-based strategy. PCR was also used to generate the YFP-CLIP-170-CFP mutants and C595 mutant of p150^{Glued}. GFP-CLIPR-59-MTB construct was provided by F. Perez (Institut Curie, Paris, France).

For IP, COS-1 cells were transfected by the DEAE-dextran method, as described by Hoogenraad et al. (2000). CHO cells were transfected with Lipofectamine 2000 (Invitrogen). Cells were lysed 24 h after transfection, and IPs and Western blotting were performed as described by Komarova et al. (2002).

Immunostaining, image acquisition, and analysis

Cell fixation and staining were performed as described by Komarova et al. (2002). Samples were analyzed either with a microscope (model DMRBE; Leica) with a PL Fluotar 100 \times , 1.3 NA objective, equipped with a CCD camera (C4880; Hamamatsu), or with an inverted microscope (model 200 Eclipse; Nikon) equipped with a Plan Fluor 100 \times , 1.3 NA objective, and a CH250 cooled CCD camera (Photometrics Ltd.). Images were prepared for presentation using Adobe Photoshop. Line scan analysis, measurements of fluorescence intensity, and densitometry analysis of Western blots were performed using MetaMorph. To estimate the accumulation of proteins at the MT end, the tip of MT was defined as a square box, four pixels on a side (0.36 μ m). Integrated fluorescence intensities within the box in each channel were measured after subtracting background. The ratio of the signals was computed using SigmaPlot.

RNAi

The following target sequences were used to design siRNAs: CLIP-170A, GGAGAAGCAGCAGCATT; CLIP-170B, TGAAGATGTCAGAGATAA; CLIP-115A, GGACACGATGAGCAGTAT; CLIP-115B, CTGGAATC-CAAGCTGGAC; and luciferase, CGTAGCGGGAATACCTCGA. siRNA duplexes were synthesized by QIAGEN and siRNA transfection was performed using Oligofectamine (Invitrogen).

RNAi vectors for CHO cells were designed based on the same target sequences, using the pSuper vector (Brummelkamp et al., 2002). The control vector was generated by inserting the luciferase RNAi cassette into the Asel site of pGFP-C1. Cells were transfected using FuGene 6 (Roche).

SFM imaging of the CLIP-170 protein

The topographic images of purified CLIP-170, deposited on freshly cleaved mica, were made with a Digital Instruments NanoScope IV operating in

tapping mode in air using NanoProbe silicone tips (Veeco/Digital Instruments). Images were collected as 1- μ m² fields (512 \times 512 pixels) and processed only by flattening to remove background slope using NanoScope software. The length of individual CLIP-170 proteins was determined by manually tracing the longest path from end to end.

FRET measurements in cell extracts and in cells

COS-1 cells were lysed 48 h after transfection in a buffer, containing 20 mM Tris-HCl, pH 7.5, 100 mM NaCl, protease inhibitors (Complete; Roche), 1% Triton X-100, and 10% glycerol; the lysates were precleared by centrifugation at 13,000 rpm for 20 min at 4°C. Emission spectra were measured using a fluorescence spectrophotometer (model F-4500; Hitachi) with the excitation at 425 nm (CFP) and 485 nm (YFP). Spectra were not corrected for PMT sensitivity. Background fluorescence of a crude extract prepared in the same way was negligible. The concentration of the CFP, YFP, or CFP-YFP fusion proteins in cell lysates was adjusted by Western blotting and by measuring the YFP fluorescence.

Emission spectra of live cells were recorded on a multimodal microscopy platform described elsewhere (Vermeer et al., 2004). Basically, a slit-spectrograph with a CCD camera was coupled to the exit port of an inverted wide-field fluorescence microscope. Resulting images yielded spectral information in the x axis and spatial information in the y axis, enabling the recording of spectra multiple objects within the field of view. Observations were done using 436 nm excitation, and a 460-nm long-pass emission filter. Due to the long-pass filtering and wavelength dependency of the detector sensitivity, the 460–500-nm spectral region is underestimated resulting in higher YFP/CFP detected ratios. During measurements, cells were kept at 37°C using a heated culture chamber and an objective heater.

Online supplemental material

Fig. S1 shows the colocalization of CLIP-170, but not CLIP-115 with dynactin in nocodazole-treated cells. Fig. S2 shows the distribution of endosomes and the Golgi after CLIP-170 knockdown. Online supplemental materials are available at <http://www.jcb.org/cgi/content/full/jcb.200402082/DC1>.

We thank Tony Hyman (Max Planck Institute of Molecular Cell Biology and Genetics, Dresden, Germany) and Franck Perez for providing materials.

This work was supported by the Netherlands Organization for Scientific Research grants to A. Akhmanova, N. Galjart, E. van Munster and T. Gadella, by an EU integrated project on Molecular Imaging (LSHG-CT-2003-503259), by a grant from the Association for International Cancer Research to M. Modesti, and by the National Institutes of Health grant GM25062 to G. Borisy.

Submitted: 17 February 2004

Accepted: 4 August 2004

References

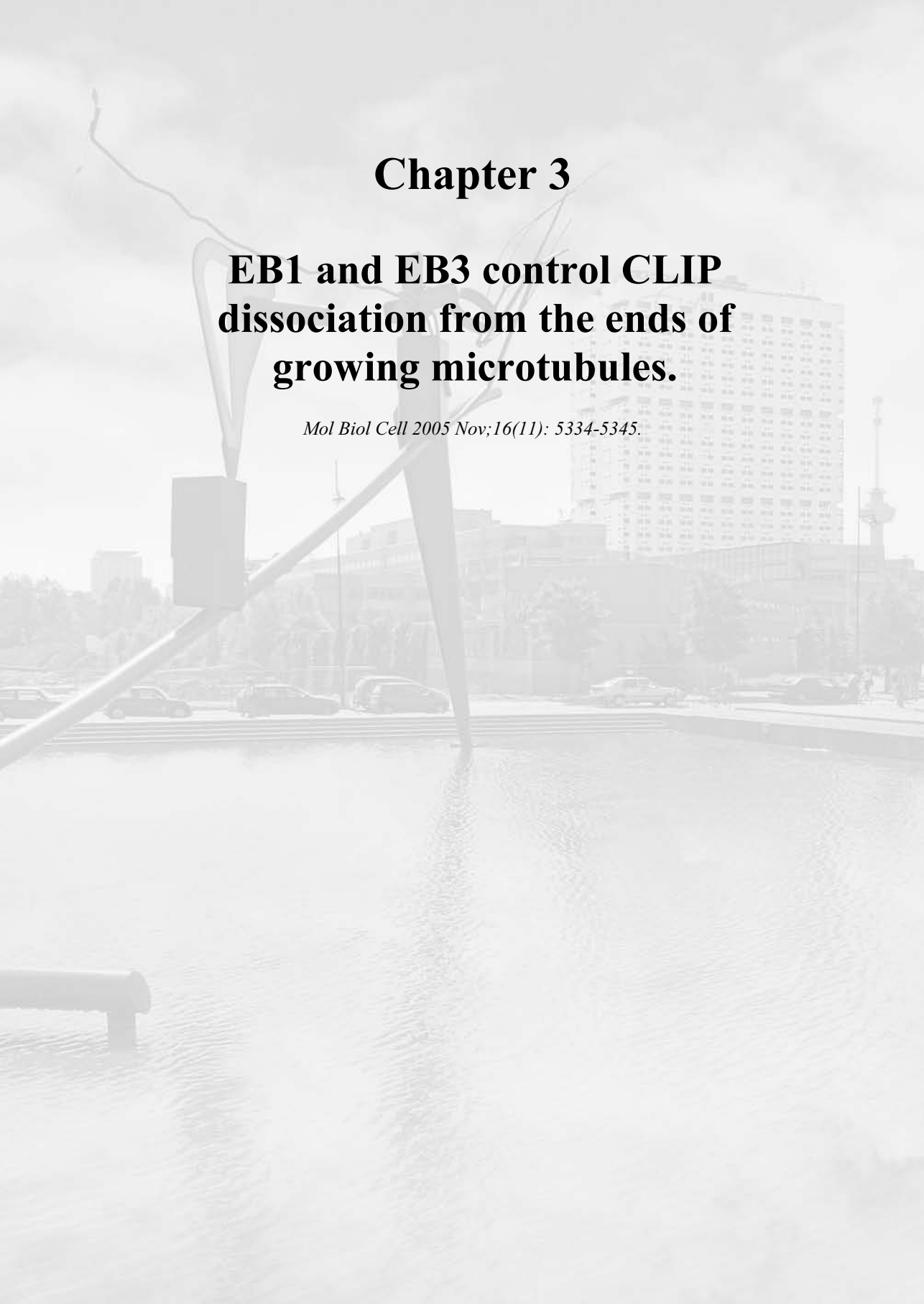
- Allan, V. 2000. Dynactin. *Curr. Biol.* 10:R432.
- Askham, J.M., K.T. Vaughan, H.V. Goodson, and E.E. Morrison. 2002. Evidence that an interaction between EB1 and p150(Glued) is required for the formation and maintenance of a radial microtubule array anchored at the centrosome. *Mol. Biol. Cell.* 13:3627–3645.
- Brummelkamp, T.R., R. Bernards, and R. Agami. 2002. A system for stable expression of short interfering RNAs in mammalian cells. *Science*. 296:550–553.
- Burakov, A., E. Nadezhkina, B. Slepchenko, and V. Rodionov. 2003. Centrosome positioning in interphase cells. *J. Cell Biol.* 162:963–969.
- Carvalho, P., J.S. Tirnauer, and D. Pellman. 2003. Surfing on microtubule ends. *Trends Cell Biol.* 13:229–237.
- Coquelle, F.M., M. Caspi, F.P. Cordelieres, J.P. Dompierre, D.L. Dujardin, C. Koifman, P. Martin, C.C. Hoogenraad, A. Akhmanova, N. Galjart, et al. 2002. LIS1, CLIP-170's key to the dynein/dynactin pathway. *Mol. Cell Biol.* 22:3089–3102.
- De Zeeuw, C.I., C.C. Hoogenraad, E. Goedknegt, E. Hertzberg, A. Neubauer, F. Grosveld, and N. Galjart. 1997. CLIP-115, a novel brain-specific cytoplasmic linker protein, mediates the localization of dendritic lamellar bodies. *Neuron*. 19:1187–1199.
- Desai, A., and T.J. Mitchison. 1997. Microtubule polymerization dynamics. *Annu. Rev. Cell Dev. Biol.* 13:83–117.
- Diamantopoulos, G.S., F. Perez, H.V. Goodson, G. Batelier, R. Melki, T.E. Kreis, and J.E. Rickard. 1999. Dynamic localization of CLIP-170 to microtubule plus ends is coupled to microtubule assembly. *J. Cell Biol.* 144:99–112.
- Dujardin, D., U.I. Wacker, A. Moreau, T.A. Schroer, J.E. Rickard, and J.R. De

- Mey. 1998. Evidence for a role of CLIP-170 in the establishment of metaphase chromosome alignment. *J. Cell Biol.* 141:849–862.
- Dujardin, D.L., and R.B. Vallee. 2002. Dynein at the cortex. *Curr. Opin. Cell Biol.* 14:44–49.
- Dujardin, D.L., L.E. Barnhart, S.A. Stehman, E.R. Gomes, G.G. Gundersen, and R.B. Vallee. 2003. A role for cytoplasmic dynein and LIS1 in directed cell movement. *J. Cell Biol.* 163:1205–1211.
- Faulkner, N.E., D.L. Dujardin, C.Y. Tai, K.T. Vaughan, C.B. O'Connell, Y. Wang, and R.B. Vallee. 2000. A role for the lissencephaly gene LIS1 in mitosis and cytoplasmic dynein function. *Nat. Cell Biol.* 2:784–791.
- Galjart, N., and F. Perez. 2003. A plus-end raft to control microtubule dynamics and function. *Curr. Opin. Cell Biol.* 15:48–53.
- Goodson, H.V., S.B. Skube, R. Stalder, C. Valetti, T.E. Kreis, E.E. Morrison, and T.A. Schroer. 2003. CLIP-170 interacts with dynactin complex and the APC-binding protein EB1 by different mechanisms. *Cell Motil. Cytoskeleton.* 55:156–173.
- Holzbaur, E.L., J.A. Hammarback, B.M. Paschal, N.G. Kravitz, K.K. Pfister, and R.B. Vallee. 1991. Homology of a 150K cytoplasmic dynein-associated polypeptide with the *Drosophila* gene Glued. *Nature.* 351:579–583.
- Hoogenraad, C.C., A. Akhmanova, F. Grosveld, C.I. De Zeeuw, and N. Galjart. 2000. Functional analysis of CLIP-115 and its binding to microtubules. *J. Cell Sci.* 113:2285–2297.
- Hoogenraad, C.C., A. Akhmanova, S.A. Howell, B.R. Dordland, C.I. De Zeeuw, R. Willemsen, P. Visser, F. Grosveld, and N. Galjart. 2001. Mammalian Golgi-associated Bicaudal-D2 functions in the dynein-dynactin pathway by interacting with these complexes. *EMBO J.* 20:4041–4054.
- Hoogenraad, C.C., B. Kockock, A. Akhmanova, H. Krugers, B. Dordland, M. Miedema, A. van Alphen, W.M. Kistler, M. Jaegle, M. Koutsourakis, et al. 2002. Targeted mutation of Cyln2 in the Williams syndrome critical region links CLIP-115 haploinsufficiency to neurodevelopmental abnormalities in mice. *Nat. Genet.* 32:116–127.
- Howard, J., and A.A. Hyman. 2003. Dynamics and mechanics of the microtubule plus end. *Nature.* 422:753–758.
- Karki, S., and E.L. Holzbaur. 1999. Cytoplasmic dynein and dynactin in cell division and intracellular transport. *Curr. Opin. Cell Biol.* 11:45–53.
- Komarova, Y.A., A.S. Akhmanova, S. Kojima, N. Galjart, and G.G. Borisov. 2002. Cytoplasmic linker proteins promote microtubule rescue in vivo. *J. Cell Biol.* 159:589–599.
- Lee, W.L., J.R. Oberle, and J.A. Cooper. 2003. The role of the lissencephaly protein Pac1 during nuclear migration in budding yeast. *J. Cell Biol.* 160:355–364.
- Ligon, L.A., S.S. Shelly, M. Tokito, and E.L. Holzbaur. 2003. The microtubule plus-end proteins EB1 and dynactin have differential effects on microtubule polymerization. *Mol. Biol. Cell.* 14:1405–1417.
- Perez, F., G.S. Diamantopoulos, R. Stalder, and T.E. Kreis. 1999. CLIP-170 highlights growing microtubule ends in vivo. *Cell.* 96:517–527.
- Perez, F., K. Pernet-Gallay, C. Nizak, H.V. Goodson, T.E. Kreis, and B. Goud. 2002. CLIPR-59, a new trans-Golgi/TGN cytoplasmic linker protein belonging to the CLIP-170 family. *J. Cell Biol.* 156:631–642.
- Pierre, P., J. Scheel, J.E. Rickard, and T.E. Kreis. 1992. CLIP-170 links endocytic vesicles to microtubules. *Cell.* 70:887–900.
- Pollok, B.A., and R. Heim. 1999. Using GFP in FRET-based applications. *Trends Cell Biol.* 9:57–60.
- Puls, I., C. Jonnakuty, B.H. LaMonte, E.L. Holzbaur, M. Tokito, E. Mann, M.K. Floeter, K. Bidus, D. Drayna, S.J. Oh, et al. 2003. Mutant dynactin in motor neuron disease. *Nat. Genet.* 33:455–456.
- Rickard, J.E., and T.E. Kreis. 1991. Binding of pp170 to microtubules is regulated by phosphorylation. *J. Biol. Chem.* 266:17597–17605.
- Scheel, J., P. Pierre, J.E. Rickard, G.S. Diamantopoulos, C. Valetti, F.G. van der Goot, M. Haner, U. Acbi, and T.E. Kreis. 1999. Purification and analysis of authentic CLIP-170 and recombinant fragments. *J. Biol. Chem.* 274:25883–25891.
- Schuyler, S.C., and D. Pellman. 2001. Microtubule “plus-end-tracking proteins”: the end is just the beginning. *Cell.* 105:421–424.
- Sheeman, B., P. Carvalho, I. Sagot, J. Geiser, D. Kho, M.A. Hoyt, and D. Pellman. 2003. Determinants of *S. cerevisiae* dynein localization and activation: implications for the mechanism of spindle positioning. *Curr. Biol.* 13:364–372.
- Smith, D.S., M. Niethammer, R. Ayala, Y. Zhou, M.J. Gambello, A. Wynshaw-Boris, and L.H. Tsai. 2000. Regulation of cytoplasmic dynein behaviour and microtubule organization by mammalian Lis1. *Nat. Cell Biol.* 2:767–775.
- Tai, C.Y., D.L. Dujardin, N.E. Faulkner, and R.B. Vallee. 2002. Role of dynein, dynactin, and CLIP-170 interactions in LIS1 kinetochore function. *J. Cell Biol.* 156:959–968.
- Valetti, C., D.M. Wetzel, M. Schrader, M.J. Hasbani, S.R. Gill, T.E. Kreis, and T.A. Schroer. 1999. Role of dynactin in endocytic traffic: effects of dynactin overexpression and colocalization with CLIP-170. *Mol. Biol. Cell.* 10:4107–4120.
- Vallee, R.B., C. Tai, and N.E. Faulkner. 2001. LIS1: cellular function of a disease-causing gene. *Trends Cell Biol.* 11:155–160.
- Vaughan, K.T., S.H. Tynan, N.E. Faulkner, C.J. Echeverri, and R.B. Vallee. 1999. Colocalization of cytoplasmic dynein with dynactin and CLIP-170 at microtubule distal ends. *J. Cell Sci.* 112:1437–1447.
- Vaughan, P.S., P. Miura, M. Henderson, B. Byrne, and K.T. Vaughan. 2002. A role for regulated binding of p150(Glued) to microtubule plus ends in organelle transport. *J. Cell Biol.* 158:305–319.
- Verhey, K.J., and T.A. Rapoport. 2001. Kinesin carries the signal. *Trends Biochem. Sci.* 26:545–550.
- Vermeer, J.E., E.B. Van Munster, N.O. Vischer, and T.W. Gadella Jr. 2004. Probing plasma membrane microdomains in cowpea protoplasts using lipidated GFP-fusion proteins and multimode FRET microscopy. *J. Microsc.* 214:190–200.
- Wynshaw-Boris, A., and M.J. Gambello. 2001. LIS1 and dynein motor function in neuronal migration and development. *Genes Dev.* 15:639–651.

Chapter 3

EB1 and EB3 control CLIP dissociation from the ends of growing microtubules.

Mol Biol Cell 2005 Nov;16(11): 5334-5345.



EB1 and EB3 Control CLIP Dissociation from the Ends of Growing Microtubules[□]

Yulia Komarova,* Gideon Lansbergen,[†] Niels Galjart,[†] Frank Grosveld,[†]
Gary G. Borisy,* and Anna Akhmanova[†]

*Department of Cell and Molecular Biology, Northwestern University Medical School, Chicago, IL 60611; and

[†]MGC Department of Cell Biology and Genetics, Erasmus Medical Center, 3000 DR Rotterdam, The Netherlands

Submitted July 11, 2005; Revised August 19, 2005; Accepted August 30, 2005
Monitoring Editor: Yixian Zheng

EBs and CLIPs are evolutionarily conserved proteins, which associate with the tips of growing microtubules, and regulate microtubule dynamics and their interactions with intracellular structures. In this study we investigated the functional relationship of CLIP-170 and CLIP-115 with the three EB family members, EB1, EB2(RP1), and EB3 in mammalian cells. We showed that both CLIPs bind to EB proteins directly. The C-terminal tyrosine residue of EB proteins is important for this interaction. When EB1 and EB3 or all three EBs were significantly depleted using RNA interference, CLIPs accumulated at the MT tips at a reduced level, because CLIP dissociation from the tips was accelerated. Normal CLIP localization was restored by expression of EB1 but not of EB2. An EB1 mutant lacking the C-terminal tail could also fully rescue CLIP dissociation kinetics, but could only partially restore CLIP accumulation at the tips, suggesting that the interaction of CLIPs with the EB tails contributes to CLIP localization. When EB1 was distributed evenly along the microtubules because of overexpression, it slowed down CLIP dissociation but did not abolish its preferential plus-end localization, indicating that CLIPs possess an intrinsic affinity for growing microtubule ends, which is enhanced by an interaction with the EBs.

INTRODUCTION

Microtubule (MT) plus end tracking proteins (+TIPs) are a group of MT binding factors, which associate predominantly with the ends of growing MTs and play a prominent role in regulating MT dynamics and in attachment of MTs to different cellular structures (Schuyler and Pellman, 2001; Carvalho *et al.*, 2003; Galjart and Perez, 2003; Howard and Hyman, 2003; Akhmanova and Hoogenraad, 2005). The dynamic accumulation of +TIPs at the ends of polymerizing MTs is an evolutionary conserved phenomenon, the mechanistic basis of which is poorly understood. MT plus end accumulation of proteins may depend on their motor-driven plus end-directed transport, specific association with the freshly polymerized MT tip coupled to quick dissociation from the older lattice (often called “treadmilling”) or preferential binding to other +TIPs (“hitchhiking”; Carvalho *et al.*, 2003; Akhmanova and Hoogenraad, 2005). Deciphering of the hierarchy of protein-protein interactions at the MT tip

is needed to understand the process of MT plus end tracking and the cellular functions that depend on it.

One of the most conserved families of +TIPs includes EB1 and its homologues present in mammals, plants, and fungi (for review, see Tirnauer and Bierer, 2000). In mammalian cells this family is represented by three members: EB1, EB2 (RP1), and EB3 (EBF3; Juwana *et al.*, 1999; Su and Qi, 2001). These proteins contain a calponin homology domain responsible for interactions with MTs (Hayashi and Ikura, 2003) and a coiled coil region, which determines their dimerization (Honnappa *et al.*, 2005; Slep *et al.*, 2005). In animal cells EB proteins may constitute the “core” of the plus end complex because they interact directly with most other known +TIPs including dynactin large subunit p150^{Glued}, APC, CLASPs, spectraplakins, RhoGEF2, and a catastrophe-inducing kinesin KLP10A (Askham *et al.*, 2002; Bu and Su, 2003; Ligon *et al.*, 2003; Rogers *et al.*, 2004; Honnappa *et al.*, 2005; Mennella *et al.*, 2005; Mimori-Kiyosue *et al.*, 2005; Slep *et al.*, 2005). Removal of these proteins from the MTs does not prevent specific accumulation of EBs at the distal ends of the MTs, making it unlikely that EBs “hitchhike” on any of the above-mentioned +TIPs (Berrueta *et al.*, 1998; Komarova *et al.*, 2002; Kodama *et al.*, 2003; Rogers *et al.*, 2004; Mimori-Kiyosue *et al.*, 2005). Studies in *Xenopus* extracts have shown that EB1 at the MT tip is immobile with respect to the MT lattice, suggesting that it binds to the freshly polymerized MT end and detaches from the older part of the MT (Tirnauer *et al.*, 2002).

Another +TIP conserved in animals and fungi is CLIP-170, a protein containing two MT-binding CAP-Gly domains at its N-terminus, a long coiled coil region responsible for dimerization, and two zinc finger-like domains at its C-terminus (Pierre *et al.*, 1992; Perez *et al.*, 1999). Similar to EB1,

This article was published online ahead of print in *MBC in Press* (<http://www.molbiolcell.org/cgi/doi/10.1091/mbc.E05-07-0614>) on September 7, 2005.

[□] The online version of this article contains supplemental material at *MBC Online* (<http://www.molbiolcell.org>).

Address correspondence to: Anna Akhmanova (anna.akhmanova@chello.nl).

Abbreviations used: GFP, green fluorescent protein; GST, glutathione S-transferase; HA, hemagglutinin; HIS, 6x histidine tag; co-IP, coimmunoprecipitation; mAb, monoclonal antibody; MT, microtubule; RNAi, RNA interference; siRNA, small interfering RNA; +TIPs, plus-end tracking proteins; YFP, yellow fluorescent protein.

mammalian CLIP-170 shows treadmilling behavior (Perez *et al.*, 1999), and recent *in vitro* studies have demonstrated that its localization to the growing MT ends may be due to copolymerization with tubulin oligomers (Arnal *et al.*, 2004). However, both in budding and fission yeast, MT plus end localization of CLIP-170 homologues Bik1p and Tip1p depends on kinesin-driven transport (Busch *et al.*, 2004; Carvalho *et al.*, 2004). In addition to being transported to the tip, Tip1p binds directly to the EB1 homologue, Mal3p, and requires Mal3p for accumulation at the MT tip (Busch and Brunner, 2004). In contrast, the budding yeast Bik1p does not require Bim1p, the EB1 homologue, for MT end accumulation (Carvalho *et al.*, 2004). These differences suggest that the mechanisms controlling plus end localization can vary between systems even although highly conserved proteins are involved.

The functional relationship between CLIP-170 and EB proteins in mammalian cells has not yet been fully elucidated. EB proteins do not require CLIP-170 or the other two CAP-Gly-containing +TIPs, CLIP-115 and p150^{Glued}, for MT plus end localization (Komarova *et al.*, 2002). On the other hand, the role of EB proteins in plus end tracking by CLIP family members has not yet been addressed. The possibility of interaction between CLIP-170 and EB proteins has been suggested by the binding of their fission yeast homologues, by the interaction between EB proteins and p150^{Glued}, and by the identification of the *Drosophila* homologue of CLIP-170, D-CLIP-190, in a pulldown assay with EB1 (Askham *et al.*, 2002; Bu and Su, 2003; Ligon *et al.*, 2003; Busch and Brunner, 2004; Rogers *et al.*, 2004). Further indications for EB1-CLIP-170 interaction were provided by the enhanced binding of EB1 to MTs caused by overexpression of the CLIP-170 N-terminus in cultured cells (Goodson *et al.*, 2003).

Here we show that CLIP-170 and a closely related protein CLIP-115 bind directly to EB1 and EB3 while displaying a lower affinity for EB2. This interaction depends on the C-terminal tails of the EB proteins, which are strikingly similar to those of α -tubulin. Further, we demonstrate that simultaneous depletion of EB1 and EB3 in cultured cells causes a reduced accumulation of CLIPs at the MT distal ends due to their diminished binding and quicker dissociation from the MT lattice. Overexpression of EB1 resulting in its even distribution along the MT lattice reduces the rate of CLIP dissociation from the growing ends but does not prevent CLIPs from tip-tracking. This observation rules out "hitchhiking" on EB1 as a simple mechanism for CLIP localization to the growing MT ends.

MATERIALS AND METHODS

Antibodies

Rat monoclonal antibodies against EB proteins were generated using GST fusions of EB1-C, EB2, and EB3 by Absea (Beijing, China). We used mouse mAbs against penta-histidine tag (Qiagen, Chatsworth, CA), EB1, EB3, and p150^{Glued} (BD Biosciences, Franklin Lakes, NY), green fluorescent protein (GFP; Roche, Indianapolis, IN), HA tag (BabCO, Richmond, CA), a rat mAb against α -tubulin (YL1/2 against EEY epitope, AbCam, Cambridge, United Kingdom), rabbit antibodies against GFP (AbCam), CLIP-170 (2360; Coquelle *et al.*, 2002), both CLIPs (2221; Hoogenraad *et al.*, 2000), and EB3 (02-1005-07; Stepanova *et al.*, 2003). The following secondary antibodies were used: alkaline phosphatase-conjugated anti-rabbit and anti-mouse antibodies (Sigma, St. Louis, MO), FITC-conjugated goat anti-rabbit antibody (Nordic Laboratories, Westbury, NY), Alexa 594- and Alexa 350-conjugated anti-rat and anti-mouse antibodies (Molecular Probes, Eugene, OR), TRITC- and FITC-conjugated donkey anti-mouse and anti-rabbit and Cy5-conjugated anti-rat antibodies (Jackson ImmunoResearch Laboratories, West Grove, PA).

Expression Constructs, Protein Purification, *In Vitro* Binding Assays, Coimmunoprecipitation, and Western Blotting

GST- and HIS-tagged N-terminal fragments of CLIP-170 and CLIP-115 were described previously (Lansbergen *et al.*, 2004). GST and HIS-tagged fusions of EB1, EB2, and EB3 were generated using mouse EB1 and EB2 cDNAs and a human EB3 cDNA, which were described elsewhere (Stepanova *et al.*, 2003). Both EB2 and EB3 cDNAs correspond to the "long" isoforms of these proteins. For GST fusions, the portions of the EB cDNAs encoding amino acids indicated in Figure 2A were obtained by PCR; the PCR primers included *Bam*HI and *Eco*RI sites directly up- and downstream of the coding sequences. These sites were used to subclone the PCR products in *Bam*HI/*Eco*RI-digested pGEX-3X vector; in the resulting fusion proteins the EB-encoding part was separated from the GST open reading frame by a linker composed of the Factor X cleavage site present in pGEX-3X. To generate HIS-tagged fusions, EB1 coding sequence or its portions were amplified with primers containing *Nde*I and *Eco*RI sites and subcloned into pET28a. Purification of the GST- and HIS-tagged proteins from *E. coli* and Western blotting were performed as described by Lansbergen *et al.* (2004).

For GST pulldown assays individual GST fusion proteins bound to glutathione Sepharose 4B beads (Amersham Biosciences, Piscataway, NJ) were combined with dissolved purified HIS-tagged proteins in a buffer containing 20 mM Tris HCl (pH 7.5), 100–300 mM NaCl, 1 mM β -mercaptoethanol, and 0.3–1% Triton X-100. After incubation for 1 h on a rotating wheel at 4°C, beads were separated from the supernatant by centrifugation and washed four times in the same buffer, and the proteins retained on the beads (including the GST fusion and the HIS-tagged protein bound to it) were analyzed on Coomassie-stained gels and by Western blotting.

The EB-GFP expression constructs used in this study were described by Stepanova *et al.* (2003). HA- and GFP-CLIP-170-N and -C by Komarova *et al.* (2002). GFP-EB1 and EB3 deletion mutants were generated by a PCR-based strategy and subcloned into *Bgl*II and *Eco*RI sites of pEGFP-C2 (Clontech, Palo Alto, CA). YFP-CLIP-170 was generated by subcloning an amplified fragment of a rat brain CLIP-170 cDNA (positions 192–4597 of the sequence with the accession number AJ237670) into *Xho*I and *Sal*I sites of pEYFP-C1 (Clontech). For coimmunoprecipitation (co-IP) experiments COS-1 cells were transfected by DEAE-dextran method and lysed 2 d after transfection and the lysates were used for co-IP with anti-GFP or anti-HA antibodies (diluted 1:30) as described by Hoogenraad *et al.* (2000).

RNAi and Rescue Constructs

RNAi vectors for Chinese hamster ovary (CHO)-K1 cells were based on the pSuper vector (Brummelkamp *et al.*, 2002). The used mouse target sequences for EB proteins are indicated in Figure 3B; the luciferase target sequence was CGTACCGCAATACITCGA. For simultaneous knockdown of EB1 and EB3, the two RNAi cassettes were combined in tandem in the same vector. To supply the RNAi cassettes with a selectable and a fluorescent marker, they were inserted into the *Ase*I site of pEGFP-C1 or pECPFP-C1. EB1 rescue constructs were prepared by a PCR-based strategy to introduce five silent substitutions in the target site of EB1 siRNA (resulting in a sequence TCTA-ACCAAGATCGAGCAA).

Cell Culture, Generation of the Stable Cell Line, and Introduction of RNAi Vectors

For Western blot analysis 80% confluent CHO-K1 cells were transfected using FuGene 6 (Roche) with different pECPFP-RNAi plasmids. Cells were replated 16 h after transfection into glucose and sodium pyruvate-free DMEM medium (Invitrogen, Carlsbad, CA) supplemented with 10% fetal bovine serum and 2 mg/ml G418 (Roche) and cultured for the next 72 h.

To produce a cell line stably expressing YFP-CLIP-170, cells were transfected and cultured as described above. For colony screening, cells were plated on coverslips and clones expressing low level of YFP-CLIP-170 were selected under a microscope using polystyrene cloning cylinders (Sigma).

For microinjection, cells were plated sparsely on coverslips with photoetched locator grids (Bellco Glass, Vineland, NJ) and 12–24 h later they were microinjected with different RNAi plasmids into nuclei. The needle concentration was 100 μ g/ml for RNAi plasmids and 70 μ g/ml for the rescue experiments with EB1, EB2, or EB1 Δ Ac. For detection of microinjected cells in live imaging experiments, cells were microinjected with a red fluorescent protein-expressing construct to produce a soluble marker. Cells were fixed or used for live observation 84–90 h after microinjection.

Immunostaining, Linescan Analysis, and Quantification of the Protein Amount at the MT Tips

Cell fixation and staining were performed as described by Komarova *et al.* (2002). Briefly, cells were fixed in cold methanol (–20°C), postfixed with 3% formaldehyde, and permeabilized with 0.15% Triton X-100. Fixed samples were analyzed by fluorescence deconvolution microscopy using a DeltaVision microscope system equipped with an Olympus IX70 inverted microscope (Lake Success, NY) and a PlanApo 60 \times 1.4 NA objective. We used 2 \times

Table 1. Rate of YFP-CLIP-170 dissociation from the growing MT plus ends

	k_{off} (s^{-1})	$\frac{1}{2}$ time of YFP-CLIP-170 dissociation (s)	No. of MT plus ends
Control cells	0.54 ± 0.12	1.4 ± 0.3	57
RNAi experiments			
RNAi to Luciferase	0.50 ± 0.10	1.5 ± 0.3	47
EB1 RNAi	0.52 ± 0.13	1.4 ± 0.4	95
EB1+EB3 RNAi	1.13 ± 0.80	0.7 ± 0.2	111
Rescue experiments after EB1+EB3 depletion			
EB1	0.42 ± 0.27	1.9 ± 0.5	59
EB1 Δ ACC	0.39 ± 0.16	2.0 ± 0.6	53
Expression of EB1 or EB1 mutants in control cells			
Untagged EB1	0.22 ± 0.08	3.7 ± 1.6	55
EB1 Δ ACC	0.44 ± 0.10	1.6 ± 0.3	39

The dissociation constants and half times of YFP-CLIP-170 dissociation were obtained for individual MT tips and the averaged values \pm SDs were computed for the analyzed population.

binning that gave a resolution of $0.22 \mu\text{m}$ per 1 pixel. Images were prepared for presentation using Adobe Photoshop (San Jose, CA). Linescan analysis and measurements of fluorescence intensity and densitometry analysis of Western blots were performed using MetaMorph software (Universal Imaging, West Chester, PA). For linescan analysis original images were converted to 300 dpi using Adobe Photoshop software and the analysis of intensity profiles along 1 pixel depth line at the MT tips was performed in MetaMorph. For estimation of the amount of the proteins bound to the outmost MT tips or to entire tips integrated fluorescence intensities within a box of four pixels on a side (outer tip) or a rectangle covering the entire positively stained tip (total bound) were measured for each channel after subtracting external background. The integrated intensities in RNAi depleted cells were expressed as a percentage of the integrated intensities in control cells, which were taken for 100%. About 200 MTs were analyzed in 10–20 control or depleted cells for each experimental condition. Data handling was performed using SigmaPlot software (Jandel Scientific, Corte Madera, CA).

Live Cell Imaging and Quantification of CLIP Dynamics

Cells stably expressing YFP-CLIP-170 were observed at 36°C on a Nikon Diaphot 300 inverted microscope (Melville, NY) equipped with a Plan 100 \times , 1.25 NA objective using YFP filter set. Images of 16-bit depth were collected with a CH350 slow scan, cooled CCD camera (Photometrics, Tucson, AZ) driven by Metamorph imaging software (Universal Imaging). The images were projected onto the CCD chip at a magnification of 250 \times , which corresponded to a resolution of $0.09 \mu\text{m}$ per 1 pixel. Time-lapse series of 30 images were acquired with a 0.5-s interval using stream acquisition mode. To achieve high temporal resolution, we had to limit the exposure time to 0.1–0.15 s. CLIP kinetics was analyzed on 16-bit depth images after subtraction of external background. We used a kymograph function to create a cross-sectional view of average intensity values within the line of 8 px along the YFP-CLIP-170 tracks over time. Using linescan analysis on the kymograph images, we determined the intensity decay of the fluorescence signal of a single pixel over time. We plotted the intensity decay over time for each YFP-CLIP-170 positive tip using SigmaPlot software and by applying exponential curve fitting we determined the dissociation constant (k_{off}). The half time of CLIP dissociation was calculated as $\ln 2/k_{\text{off}}$ for each CLIP-positive tip and averaged for the population. Photobleaching of the fluorescent signal due to sample illumination was not taken into account because it was negligible; the bleaching constant of YFP-CLIP-170 signal at the outer tips of growing MTs determined by exponential curve fitting to intensity decay was $0.01 \pm 0.004 \text{ s}^{-1}$. This value was insignificant compared with the constant of CLIP dissociation (Table 1); correction for photobleaching was therefore unnecessary.

RESULTS

CLIP-170 and CLIP-115 Bind Directly to EB Proteins

The CAP-Gly motif-containing domains of Tip1p (*Schizosaccharomyces pombe* homologue of CLIP-170) and p150^{Glued} bind directly to the C-terminal parts of Mal3p and the mammalian EB1 protein, respectively (Askham *et al.*, 2002; Bu and Su, 2003; Ligon *et al.*, 2003; Busch and Brunner, 2004). We therefore set out to test if the N-termini of CLIP-170 and CLIP-115 can also interact directly with EB family members. We used purified 6xhistidine (His)-tagged N-terminal frag-

ments of CLIP-170 and CLIP-115 (Figure 1A) in an *in vitro* pulldown assay with the purified glutathione *S*-transferase (GST) fusions of EB1, EB2, and EB3. In low-salt conditions (100 mM NaCl) both CLIP N-termini were efficiently retained by all three EB fusions but not by GST alone (Figure 1B). However, GST-EB2 could no longer bind to the CLIP N-terminal domains when the salt concentration was increased to 300 mM (Figure 1B).

To confirm this interaction we next performed co-IPs from transfected cells. We overexpressed the N- or the C-terminal part of CLIP-170 tagged with GFP in COS-1 cells and investigated if endogenous EB proteins could be coprecipitated with these CLIP-170 fragments. To detect all three endogenous EB family proteins, we used novel monoclonal antibodies (mAbs) specific for EB1, EB2, or EB3 (Supplementary Figure S1). We found that both EB1 and EB3 but not EB2 coprecipitated with the N-terminus of CLIP-170, whereas none of the EB proteins coprecipitated with the C-terminus of CLIP-170 (Figure 1C). It should be noted that previously in a similar experiment we failed to observe a co-IP of EB1 with the CLIP-170 N-terminus (Komarova *et al.*, 2002). This contradiction is explained by the fact that in the current study we used a new anti-EB1 mAb (mAb KT51), which is much more sensitive on Western blot than the anti-EB1 mAb from BD Biosciences used in our previous study. We conclude that CLIP-170 and CLIP-115 can bind directly to EB1 and EB3 and display a lower affinity for EB2.

To map further the CLIP interacting domains in EB1 and EB3, we used a series of EB1/EB3 deletion mutants (Figure 2A). Experiments with the N-terminus of p150^{Glued} have shown that it binds to the C-terminal part of EB1 and that the deletion of last two amino acids of EB1 is sufficient to abolish the interaction (Askham *et al.*, 2002; Bu and Su, 2003). The C-terminal tails of EB proteins are strikingly similar to the tail of α -tubulin because they contain several acidic residues and terminate with a tyrosine (Figure 2B). In *Saccharomyces cerevisiae* the CLIP-170 homologue Bik1p depends on the C-terminal aromatic residue of α -tubulin for the binding to MTs (Badin-Larcon *et al.*, 2004). The same is likely to be true for the mammalian CLIP-170 because it is mislocalized in mouse neurons, in which the pool of C-terminally tyrosinated α -tubulin is strongly reduced because of a deficiency in tubulin tyrosine ligase (Erck *et al.*, 2005). Taking into account all these observations, we hypothesized that the CLIP N-termini bind to the C-terminal regions of EB1 and EB3 in a manner dependent on the C-terminal

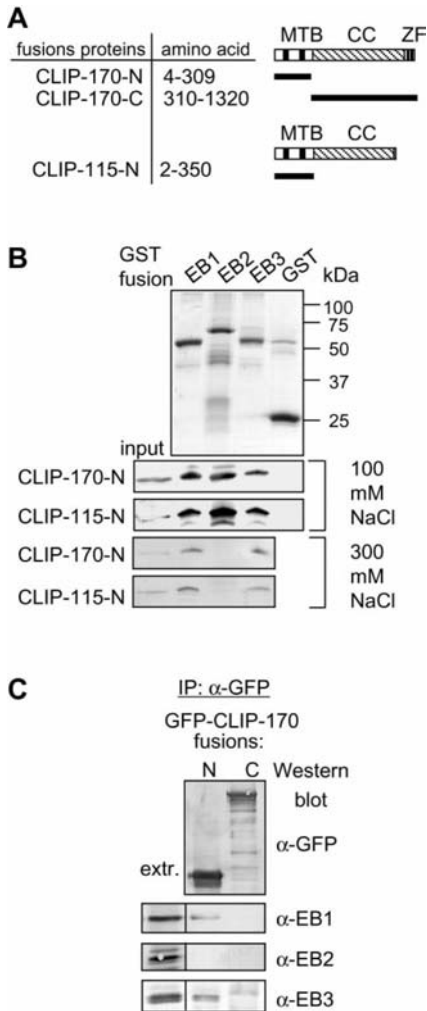


Figure 1. CLIP and EB proteins interact directly. (A) Schematic representation of the CLIP protein structure and the deletion mutants used in this study. MTB, microtubule-binding domain, CC, coiled coil, ZF, zinc finger-like domains. (B) GST pulldown assays with the indicated GST fusions. Coomassie-stained gel is shown for the GST fusions and Western blots with anti-HIS antibodies for the HIS-tagged CLIP N-termini. Ten percent of the input and 50% of the material bound to the beads were loaded on gel. (C) IP with anti-GFP antibodies from COS-1 cells transfected with the indicated GFP-CLIP-170 deletion mutants. Rat mAbs were used to detect EB1 and EB2 and rabbit polyclonal antibodies to detect EB3.

tyrosine. To test this idea, we performed GST pulldown assays with GST fusions of different EB1/EB3 deletion mutants and a HIS-tagged CLIP-170 N-terminus (Figure 2, C and D). We observed that the C-terminal half of EB1 was

sufficient for the interaction with the CLIP-170 N-terminus. Removal of the tails of EB1/EB3 or their C-terminal tyrosine alone prevented HIS-tagged CLIP-170 N-terminus from binding to GST-EB fusions, confirming our hypothesis (Figure 2, C and D).

We also performed a reverse assay where we tested the *in vitro* binding of HIS-tagged EB1 or its mutants to GST-tagged CLIP-170 N-terminus. Full-length HIS-tagged EB1 displayed a strong affinity for GST-CLIP-170 N-terminus but not to GST-EB1, which was used as a negative control (Figure 2E). EB1 is known to form stable dimers (Honnappa *et al.*, 2005; Slep *et al.*, 2005), but we did not observe association between differently tagged EB1 proteins purified from bacteria. HIS-tagged EB1 mutants lacking either the C-terminal tyrosine or the whole acidic tail did show weak binding to the GST-coupled CLIP-170 N-terminus but not to GST-EB1 (Figure 2E). This observation is in line with previously published data indicating that in addition to the EB1 tail, the EB1 coiled coil region may also be important for binding to p150^{Glued} N-terminus (Wen *et al.*, 2004). GST-fused CLIP-170 N-terminus might have a higher affinity for EB mutants than its HIS-tagged version because it is expected to be a dimer due to self-association of GST, whereas HIS-tagged CLIP N-termini are likely monomeric.

Next we investigated if the acidic tail of EB1 and in particular its C-terminal tyrosine are important for interaction between EB1 and CLIP-170 N-terminus in cell lysates. To address this question we performed co-IPs from COS-1 cells cotransfected with constructs expressing hemagglutinin (HA)-tagged CLIP-170 N-terminus and GFP-EB1 fusion or its deletion mutants. Although GFP-EB1 and GFP-EB1 C-terminus coprecipitated with HA-CLIP-170 N-terminus (Figure 2F, lanes 1 and 4) GFP-EB1 or GFP-EB1-C lacking the whole acidic tail or its C-terminal tyrosine did not copurify with CLIP-170 N-terminus (Figure 2F, lanes 2, 5, and 7). A similar result was obtained when we used longer CLIP-170 mutants, which contain a portion of the coiled coil region and can dimerize (unpublished data). Our data indicate that the absence of the C-terminal tyrosine of EB1 makes its affinity for CLIP-170 in the extract too low to allow a co-IP.

It should be noted that in mammalian cells α -tubulin undergoes repetitive cycles of dephosphorylation and tyrosination. Using an antibody, which specifically recognizes the EEY epitope, we observed no tyrosine addition to dephosphorylated EB1 in COS-1 cells, indicating that it is not a substrate for a tyrosine kinase in these cells (Figure 2F).

In line with the idea that the very C-terminus of EB1 is important for the interaction with CLIP-170 and p150^{Glued}, we observed that the attachment of the GFP tag to the C-terminus of EB1 abolished its interaction with these CAP-Gly proteins when they were expressed at endogenous levels (Figure 2G) or when HA-tagged CLIP-170 N-terminus was overexpressed (Figure 2F, lanes 3 and 6). The widely used EB1-GFP fusion should therefore be treated with some caution because it might have a dominant negative effect due to its inability to interact with the CLIPs and dynactin.

Our data indicate that CLIP-170 and CLIP-115 can bind to EB1 and EB3 directly. However, we were unable to co-IP these proteins when they were both present at endogenous levels (unpublished data). We propose that the interactions between these proteins are transient and/or occur normally only in the context of MT tip binding.

EB Depletion Decreases CLIP Accumulation at MT Tips Mainly through Influencing CLIP Dynamics

Direct interactions between CLIPs and EBs suggested that these proteins may bind to the MT ends cooperatively. Ex-

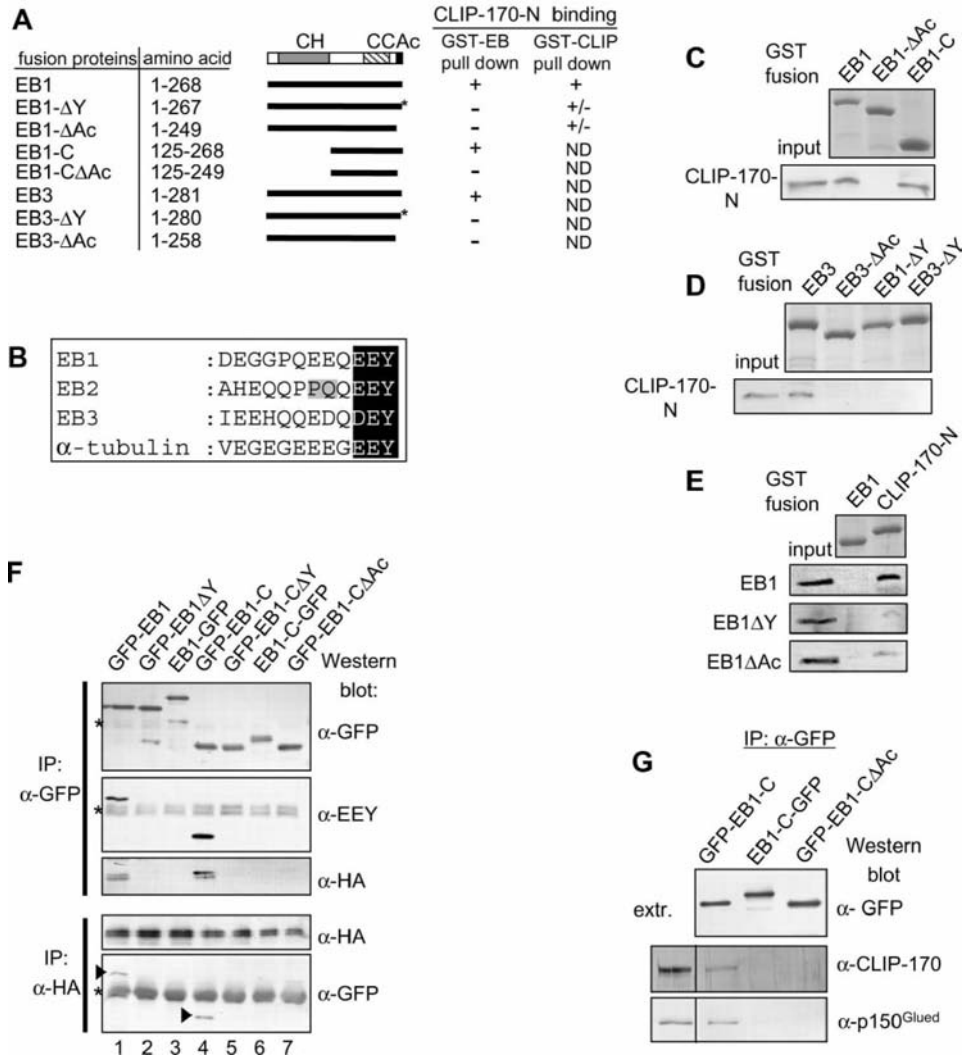


Figure 2. The C-terminal tails of EB1 and EB3 contribute to the association of these proteins with CLIP-170. (A) Schematic representation of the EB protein structure and the deletion mutants used in this study. CH, calponin homology domain; CC, coiled coil; Ac, acidic tail. Absence of the C-terminal tyrosine is indicated by asterisks. Binding to CLIP-170 N-terminus in GST-pull-down experiments is indicated: +, strong binding; +/-, weak binding; -, no binding detected; ND, not determined. In the left column the data for binding of HIS-tagged CLIP-170-N to GST-tagged EB1 mutants are indicated; in the right column the data for binding HIS-tagged EB1 mutants to GST-tagged CLIP-170-N are summarized. (B) Alignment of the C-terminal tails of the human EB1, EB2, and EB3 (Su and Qi, 2001) and α-tubulin (accession number P68363). In contrast to the other three proteins EB2 has uncharged amino acids at positions 5 and 6 counting from the C-terminus (indicated by a gray box). Similarity of the last three amino acids is emphasized by a black box. (C–E) GST pull-down assays with the indicated GST fusions. Coomassie-stained gel is shown for the GST fusions and Western blots with anti-HIS antibodies for the HIS-tagged CLIP-170 N-terminus and EB mutants. Ten percent of the input and 25% of the material bound to the beads were loaded on gel. (F) COS-1 cells were cotransfected with HA-CLIP-170 N-terminus and the indicated GFP-EB1 (or EB1-GFP) fusions. IPs were performed with anti-HA or anti-GFP antibodies and the resulting precipitates were analyzed with antibodies against HA, GFP, or the EEY epitope. The cross-reacting IgG heavy chain when present is indicated by an asterisk. Arrowheads in the lower panel indicate GFP-positive bands (GFP-EB1 and GFP-EB1-C, which coprecipitate with HA-CLIP-170 N-terminus). (G) IPs with anti-GFP antibodies from COS-1 cells transfected with the indicated GFP-EB1 (or EB1-GFP) expression constructs were analyzed by Western blotting with antibodies against GFP, CLIP-170 (2360), or p150^{Glued}.

pression of a dominant negative CLIP-170 mutant demonstrated that EB proteins do not require CLIPs or dynactin for the plus end binding (Komarova *et al.*, 2002), and examination of cells after depletion of both CLIPs by RNAi confirmed this conclusion (unpublished data). To test if the EB proteins are needed for the binding of CLIPs to MT ends in mammalian cells, we used plasmid-based RNA interference (RNAi; Brummelkamp *et al.*, 2002) in CHO-K1 cells. Target regions were selected from the open reading frames of the mouse EB1, EB2, and EB3 genes (Figure 3B), and their 100% identity with hamster sequences was confirmed by sequencing the corresponding portions of the EB cDNAs obtained by RT-PCR from CHO-K1 cells. Next we validated the effectiveness of different RNAi vectors to silence EB proteins in a population of CHO-K1 cells. Insertion of RNAi cassettes into pECFP-C1 vector, which contains a neomycin-resistance gene, permitted us to select RNAi plasmid-transfected cells for resistance to G418. As a control we used a CFP-expressing RNAi vector directed against luciferase. Starting at 16 h after transfection with RNAi vectors, cells were treated with G418 for 72 h and then collected for Western blot analysis. Using microscopic examination, we determined that after such treatment >95% of the cells in the population were CFP-positive. Immunoblotting and densitometry analysis demonstrated that each single EB species was down-regulated by ~90% both when a single EB protein or several proteins in combination were knocked down (Figure 3, A and C). Depletion of any particular EB protein had no effect on the protein levels of other family members or on the levels of actin, tubulin, CLIP-170 and CLIP-115 (Figure 3A).

Next we analyzed whether the depletion of EB proteins had any effect on the localization of endogenous CLIPs. The distribution of CLIP-170 and CLIP-115 in correlation to the depletion of EB family members was evaluated by triple immunostaining at 84–90 h after nuclear microinjection of RNAi vectors. Microinjection allowed us to obtain a reasonably homogeneous population of cells displaying a knockdown of one or several EB proteins. In untreated CHO-K1 cells CLIP-170 and CLIP-115 visualized with an antibody, which recognizes both proteins displayed “comet”-like structures with an average length of ~2 μ m at the MT distal ends. These ends were also positive for endogenous EB1 and EB3 (Figure 3, D, G, and I, rectangles marked with “1”). Linescan analysis (plots of intensity vs. distance along the MT distal end, Figure 3E) demonstrated that the distribution of CLIPs and EBs was identical and overlapping. Knockdown of EB1 alone caused no significant change either in accumulation or in distribution of the CLIPs at the MT tip (Figure 3, D, F, and L). However, simultaneous depletion of EB1 and EB3 led to a reduction of the CLIP signal at the MT tips to ~44%, whereas the level of remaining EB1 and EB3 proteins was only ~11% (Figure 3, G, H, and M). Similar results were obtained when all three EB proteins were knocked down simultaneously (Figure 3, I, K, and N), suggesting that EB2 had no strong effect on the CLIP distribution.

The diminished accumulation of CLIPs at the MT tips after the depletion of EB proteins could be either due to their reduced association with the outer MT plus ends or a result of a redistribution. To test these possibilities we quantified CLIP-positive signals at the outer tips of MTs (within a 0.36- μ m square box at the very end of the MT). We found that CLIP association measured in this way was slightly reduced (to ~77% of the normal level) after knock down of EB1 and EB3 (Figure 3M). However, the length of the CLIP-positive comet was reduced approximately by half as demonstrated by linescan plots (Figure 3, E, F, H, J, and K). This effect correlated with the distribution of the remaining EB1

and EB3, which were strongly concentrated as small dots at the distal tips of the MTs with an intensity of ~19% of their normal level at the outer tip (Figure 3M). Shortened CLIP-positive comets with a reduced intensity were also observed after knocking down EB1 and EB3 in HeLa cells with the aid of the human versions of the RNAi vectors (Figure 3B and unpublished data), indicating that the observed effects were not a peculiarity of the CHO-K1 cells.

The influence of EB proteins on CLIP distribution could possibly be explained by a change in CLIP dynamics. To analyze CLIP behavior in live cells, we generated a line of CHO-K1 cells stably expressing yellow fluorescent protein (YFP)-CLIP-170 at a level comparable to that of the endogenous CLIP-170 (Figure 4A). The average length of YFP-positive comets at the MT ends in this cell line was similar to that measured for the endogenous CLIP-170 in fixed cells, suggesting that YFP-CLIP-170 behavior reflects the dynamics of the endogenous protein. Using live imaging with a high temporal resolution, we were unable to find any evidence for transport of CLIP-170 to the MT tip in CHO-K1 cells (unpublished data). Kymograph analysis of individual growing MT plus ends (Figure 4, B and C) demonstrated very fast CLIP association with the freshly polymerized MT tip and slower dissociation from the older part of MT. Our data support previous observations on CLIP dynamics, suggesting that CLIP molecules remain stationary with respect to the MT lattice.

Analysis of the dissociation curve indicated that it could be fitted to an exponential decay (Figure 4D), which allowed us to calculate the dissociation constant and the half time of the CLIP dissociation. In control cells CLIP-170 dissociated with a half time of 1.4 ± 0.3 s (Table 1). Knockdown of EB1 alone had no effect on CLIP-170 dissociation rate (Figure 4, E–G, Table 1), while simultaneous depletion of EB1 and EB3 decreased the half time of YFP-CLIP-170 dissociation by a factor of 2 (Figure 4, H–J, Table 1). Depletion of EB proteins had no effect on the rate of MT growth as demonstrated by similar slopes of the kymographs (31.0 ± 6.6 , 31.7 ± 6.0 , and $32.0 \pm 4.2^\circ$ for control, EB1, and EB1+EB3 RNAi treatments, respectively; Figure 4, C, F, and I). Although we used only CLIP-170 in our kinetic studies, similar distribution of the endogenous CLIP-170 and CLIP-115 in fixed preparations suggested that both proteins had similar dynamics.

CLIP Accumulation at the MT Tips Is Fully Restored by EB1 and Partially Restored by EB1 Δ Ac

To exclude the possibility that enhanced dissociation of CLIP-170 is due to an off-target activity of our RNAi tools, we rescued the cells microinjected with EB1 and EB3 RNAi vectors with a plasmid expressing nontagged EB1. This rescue construct was resistant to the anti-EB1 small interfering (si) RNA because of five silent substitutions in the siRNA target region. EB1 expression could completely restore the normal YFP-CLIP-170 dissociation rate (Table 1).

We also performed a rescue of EB1/EB3 knockdown using EB1 Δ Ac mutant, which has a strongly reduced affinity to CLIP-170 (Figure 2, C–E). To detect endogenous EB1 in cells expressing EB1 Δ Ac we used the KT51 mAb, which does not react with EB1 Δ Ac (Supplementary Figure S1). The EB1 Δ Ac mutant was visualized with anti-EB1 mAb from BD Biosciences, which recognizes an epitope in the coiled coil domain (Askham *et al.*, 2002). For quantification of CLIP distribution we chose cells in which EB1 Δ Ac was localized exclusively at the tips and not along the MT lattice. The level of EB1 Δ Ac expression estimated by measuring of the signal

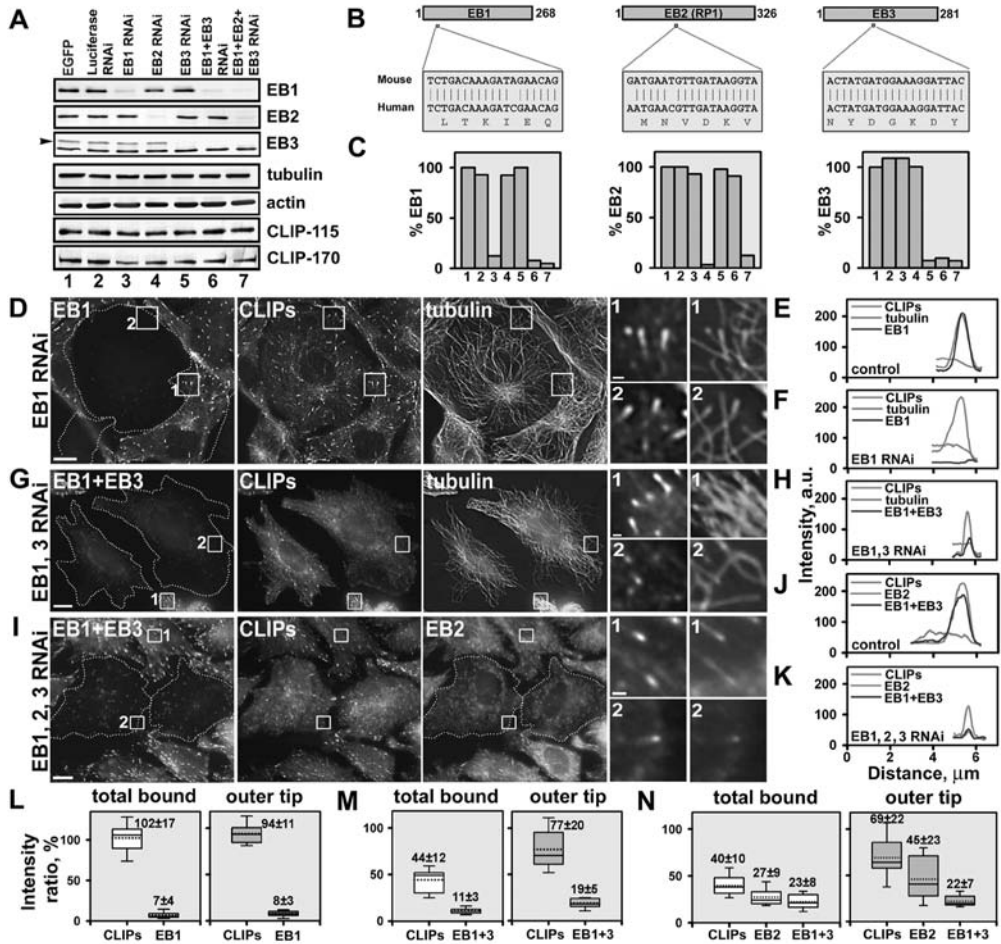


Figure 3. Simultaneous knockdown of EB1 and EB3 proteins results in the reduction of CLIP accumulation at the MT tips. (A) Western blot analysis of the cell extracts prepared from 1) cells transfected with pECFP-C1 or cells transfected with hairpin constructs encoding RNAi to 2) Luciferase; 3) EB1; 4) EB2; 5) EB3; 6) EB1+EB3; 7) EB1+EB2+EB3. EB proteins were detected by rat mAbs KT51 (anti-EB1), KT52 (anti-EB2), and KT53 (anti-EB3; see also Supplementary Figure S1). Note that anti-EB3 antibody also reacts with an unknown species of ~28 kDa that is insensitive to EB3 RNAi. The EB3-specific band is indicated by an arrowhead. CLIP-115 and CLIP-170 were detected with the 2221 antibody. Actin serves as a loading control. (B) Schematic representation of the relative positions and sequences of the mouse EB1, EB2, and EB3 RNAi target regions and their alignment to human sequences. Corresponding amino acid sequences are indicated below. (C) Densitometry analysis of EB protein levels from the blots shown in A. Bar plots represent relative protein levels after expression of different hairpin constructs indicated by numbers, which are the same as in A. Protein levels in the extracts of pECFP-expressing cells (1) were assigned for 100%. (D–K) Distribution of CLIPs at the MT tips after depletion of EB family members. CHO-K1 cells were stained for EB1, CLIPs, and tubulin (D); EB1+EB3, CLIPs, and tubulin (G); EB1+EB3, CLIPs, and EB2 (I) 84 h after microinjection with hairpin construct encoding RNAi to EB1 (D); EB1 and EB3 (G); EB1, EB2, and EB3 (I). Cells with depleted proteins are indicated by dotted lines. Bars, 10 μ m. Enlarged insets from the control (1) and treated cells (2) for CLIPs (grayscale) and for overlays (in color) are shown on the right; CLIPs, red; tubulin (D and G) or EB2 (I), green; EB1 (D) or EB1+EB3 (G and I); blue. Bars in the insets, 1 μ m. Line scan analysis illustrates the distribution of CLIPs and EB proteins bound the whole tip or to its outer part after depletion of EB1 (F), after simultaneous depletion of EB1 and EB3 (H), or all three EB members (K). Note that the length of CLIP-positive structures is twice as short compared with control cells. (L–N) Quantification of the amount of CLIPs and EB proteins bound the whole tip or to its outer part after depletion of EB1 (L), EB1 and EB3 (M), or all three EB proteins (N). The integrated intensity of CLIPs and EB proteins at the MT tips in depleted cells was expressed as a percentage of the intensity in control cells from the same image, which was taken for 100% and plotted as box graphs. The boundaries of the box and whiskers indicate the 25th and the 75th percentile, and the 90th and 10th percentiles respectively. The median and mean are shown by a straight and a dotted line. The numbers on the graphs indicate the average values and standard deviations. The values for CLIPs in L are statistically different from M and N (Student's test; $p < 0.0001$) with 95% confidence of nonoverlapping intervals. The values for CLIPs shown in M are statistically not different from those in N. Data are derived from measurements of 146–568 individual MT tips in 10–20 cells per treatment group.

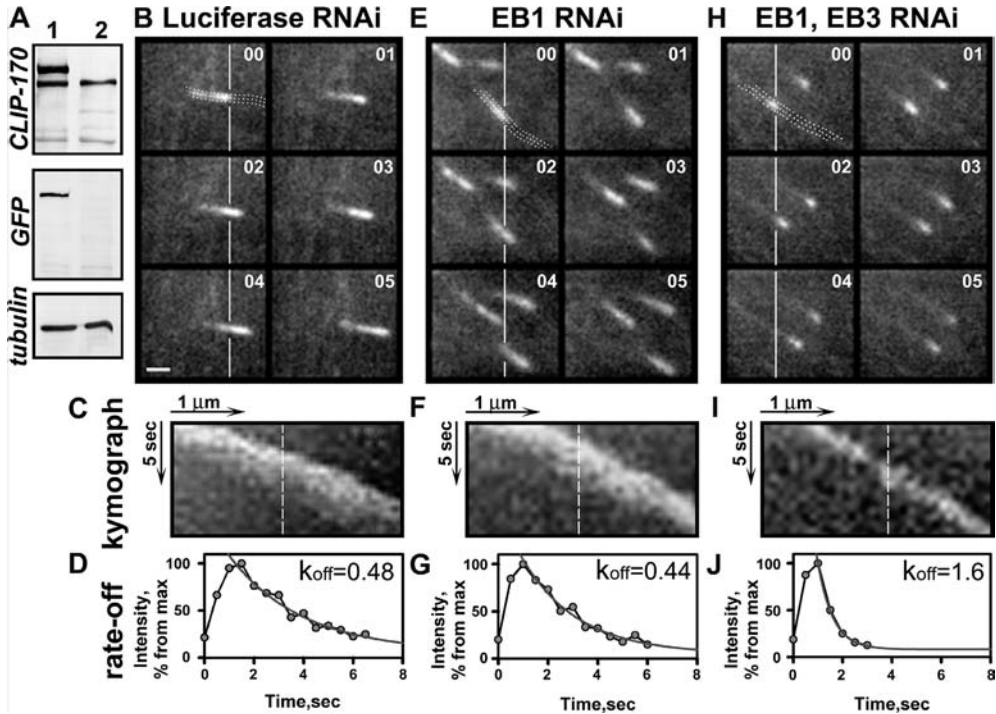


Figure 4. Depletion of EB proteins increases the rate of CLIP-170 dissociation from the MT tips. (A) Western blots of the cell extracts prepared from CHO-K1 cells stably expressing YFP-CLIP-170 (after fluorescence-activated cell sorting) probed with CLIP-170 specific antibody 2360, anti-GFP and anti-tubulin antibodies; parental CHO-K1 cell line was used as a control. (B–J) YFP-CLIP-170 kinetics in CHO-K1 cells. The time-lapse images of YFP-CLIP-170 in the cells expressing hairpin constructs containing target sequence either for Luciferase RNAi (B); EB1 RNAi (E); or EB1+EB3 RNAi (H). Images were acquired every 0.5 s. The vertical lines correspond to very tip of CLIP-170 comets on the first image. Time is shown in seconds in the top right corner. Bar, 1 μ m. A kymograph function was used to create a cross-sectional view of the YFP-CLIP-170 intensity over time (C, F, and I). The dotted lines in B, E, and H indicate the path of MT growth along which the cross-sectional views were obtained. The fluctuations of the fluorescent intensities along the dashed line represent association and dissociation of YFP-CLIP from the MT plus ends and are plotted on the graphs below (D, G, and J). The exponential curve fitting gives the dissociation constant (k_{off}).

at the MT tips was $230 \pm 90\%$ of endogenous EB1 in control cells. EB1 Δ Ac mutant localized efficiently to the MT tips of cells depleted for EB1 and EB3 and induced an almost complete loss of the residual EB1 from the MT ends, probably due to competition (Figure 5, A–C). Total accumulation of endogenous EB1 at the MT tips of such rescued cells constituted only $3.2 \pm 1.2\%$ of those in control cells (Figure 5D). Also endogenous EB3 was almost undetectable in such cells (unpublished data).

Surprisingly, EB1 Δ Ac could efficiently rescue CLIP distribution (Figure 5, A–D). It caused an increase of CLIP accumulation measured at the MT tip from $44.2 \pm 12.0\%$ in EB1/EB3 knockdown cells to $75.9 \pm 14.6\%$ of the level in control cells, suggesting that only $\sim 25\%$ of CLIP accumulation may be accounted for by the CLIP-EB interaction mediated by the EB1 tail. Even more strikingly, the rate of CLIP dissociation was completely restored by the expression of EB1 Δ Ac (Table 1), indicating that CLIP-EB binding via the tail of EB1 has no influence on CLIP dissociation.

EB2 Cannot Rescue CLIP-170 Accumulation at the Tips of EB1/EB3-depleted Cells

The depletion of either EB1/EB3 or all three EB species caused similar effects on CLIP accumulation at the MT tips. There are two possible explanations of this result: either EB2 has a function distinct from EB1 and EB3 or endogenous EB2 level in CHO-K1 cells is too low to support normal CLIP distribution, especially given the lower affinity of this protein for the CLIPs compared with EB1 and EB3. To distinguish between these possibilities, we attempted to rescue CLIP accumulation after the simultaneous EB1 and EB3 knockdown by overexpressing EB2. To our surprise, mild overexpression ($204 \pm 150\%$ compared with endogenous level) of EB2 in EB1/EB3 knockdown cells led to further loss of the CLIPs from the MT tips, reducing the level of the total MT tip-bound CLIPs to $\sim 27\%$ of that in control cells (Figure 6). Linescan analysis demonstrated that the length of CLIP-stained MT tips was $\sim 1 \mu$ m, similar to that observed in EB1/EB3-depleted cells. Higher levels of EB2 overexpres-

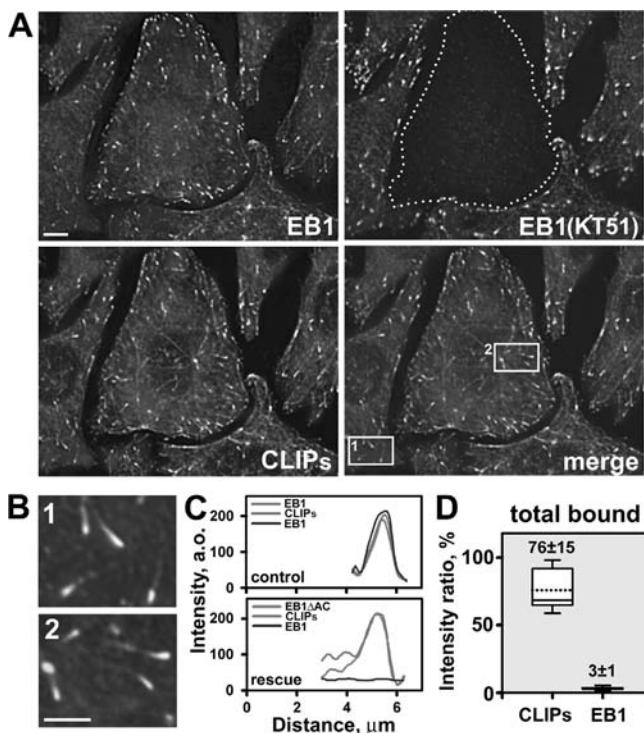


Figure 5. EB1 Δ Ac partially restores CLIP accumulation after simultaneous EB1/EB3 depletion. (A) CHO-K1 cells depleted of endogenous EB1 and EB3 proteins and rescued with EB1 Δ Ac were stained for EB1 with the BD Biosciences mAb (recognizes both the endogenous EB1 and the rescue construct, red), KT51 mAb (recognizes only the endogenous EB1, blue), and the CLIPs (green). Bar, 10 μ m. (B) Enlarged areas of a control (1) and a rescued cell (2). Bar, 5 μ m. (C) Linescan analysis demonstrates that the length of the CLIP positive structures was restored in the cells rescued with the EB1 Δ Ac mutant. (D) Quantification of the amount of CLIPs and EB1 bound the whole MT plus end in cells depleted of EB1 and EB3 and rescued with EB1 Δ Ac. The data are plotted in the same way as in Figure 3, L–N. The data are derived from 161 and 121 individual MT tips in 24 and 11 cells for control and rescue, respectively.

sion (to an extent when it was no longer bound to the tips but rather distributed evenly along the MTs) did not improve CLIP accumulation at the tips either (unpublished data). This suggests that overexpression of EB2 in EB1/EB3-depleted cells did not lead to a change in CLIP dissociation rate compared with EB1/EB3 depletion, although very low signal of YFP-CLIP-170 at the MT tips made live imaging with high temporal resolution impossible in this case. It appears therefore, that EB2 has fundamentally different properties from EB1 and EB3 with respect to its relationship with the CLIPs.

Overexpression of EB1 Decreases the Rate of CLIP-170 Dissociation

Because decreased levels of EB1 and EB3 caused quicker release of CLIP-170 from the MTs we expected an increased level of EB1/EB3 proteins to have the opposite effect. Indeed, moderate levels of EB1 overexpression, which resulted in redistribution of EB1 along the whole length of MTs without causing their stabilization or bundling, induced elongation of CLIP-positive comets at the MT ends (Figure 7, A–C). Such moderate increase in EB1 level caused no significant change in MT growth rate, whereas the half time of YFP-CLIP-170 dissociation was increased by a factor 2 compared with control cells (Figure 7D, Table 1). As a control, we used a HA-tagged EB1 mutant EB1 Δ CC (1–184), which lacks the C-terminal part including the coiled coil region. EB1 Δ CC decorates MTs but has no preferential affinity for

their growing ends (unpublished data). Overexpression of this mutant caused no significant change in CLIP-170 dissociation rate (Table 1), indicating that the observed effect correlates with the capacity of the EB proteins for plus end association. Importantly, overexpression of EB1 did not cause complete redistribution of the CLIPs along the MTs. Although EB1 decorated MTs along their length, CLIPs still concentrated at the MT tips but dissociated with a slower rate. This indicates that CLIPs do not simply “hitchhike” on the EBs to target the growing tips but recognize these sites through another mechanism.

DISCUSSION

Protein-protein interactions at the growing MT plus ends create a flexible and dynamic network, which contributes to the spatial accumulation of +TIPs (for recent review, see Akhmanova and Hoogenraad, 2005). The core element of this network is likely represented by EB1 and its family members. Here we show that similar to other +TIPs, CLIPs also require EB proteins for efficient plus end localization. Direct interaction between the CLIPs and EB1/EB3 proteins provides the most straightforward explanation of this observation. EB-dependent mechanism of CLIP accumulation at the MT tips may be evolutionary conserved because Mal3p, the *S. pombe* EB1 homologue interacts directly with Tip1p, the CLIP-170 homologue and is strictly required for Tip1p binding to the growing MT ends (Busch and Brunner, 2004).

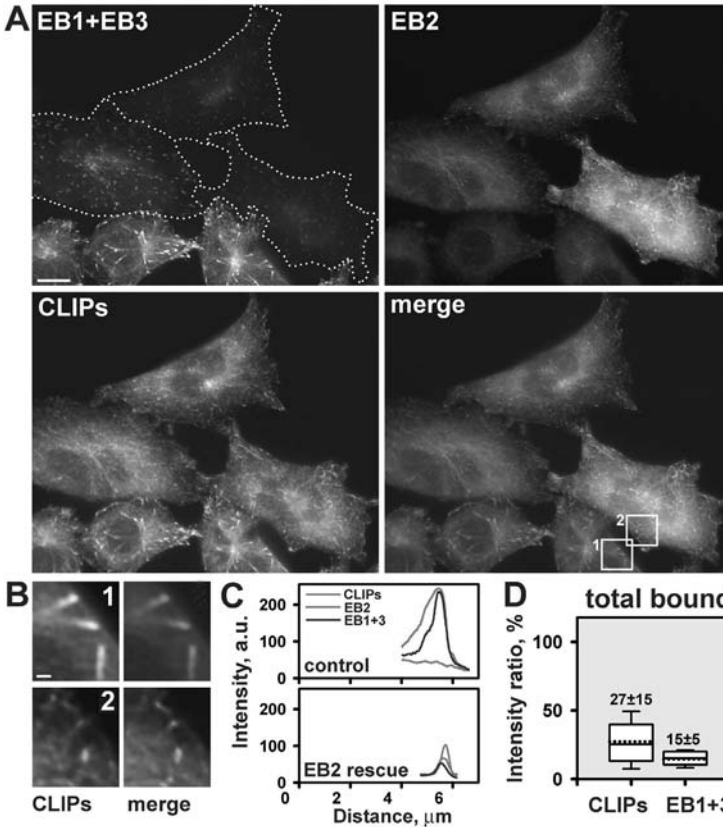


Figure 6. Overexpressed EB2 does not restore CLIP accumulation after depletion of EB1 and EB3. (A) CHO-K1 cells, depleted of endogenous EB1 and EB3 and expressing exogenous EB2 were stained for EB1+EB3 (blue), EB2 (green), and the CLIPs (red). Cells with depleted EB1 and EB3 proteins are indicated by dotted lines. Bar, 10 μ m. (B) Enlarged areas from a control (1) and an EB1+EB3-depleted cell expressing moderate levels of exogenous EB2 (2). Bar, 1 μ m. (C) Linescan analysis demonstrates the distribution of CLIPs, EB2, and EB1+EB3 at the individual MT plus ends in a control cell and in a cell rescued with EB2. (D) Quantification of the amount of CLIPs and EBs bound the whole MT plus end in cells with depleted EB1 and EB3 and overexpressing exogenous EB2. The data are plotted in the same way as in Figure 3, L-N. Data are derived from 152 and 229 individual MT tips in 17 and 13 cells for control and rescue, respectively.

We have demonstrated that the acidic tail of EB1/EB3 and specifically its C-terminal tyrosine contributes to CLIP binding. CLIP-EB interaction via the tail of EB proteins plays a significant role in vivo because CLIP accumulation at the MT plus ends was higher in control cells than in cells depleted for EB1/EB3 and rescued with the EB1 Δ Ac mutant. The tail of EB1 or EB3, however, is not the sole site of their interaction with the CLIPs because EB1 Δ Ac can still bind, albeit weakly, to the CLIP-170 N-terminus in vitro. In agreement with this observation p150^{Glued}, a CLIP family member, depends for its association with EB1 on additional more N-terminal sequences within the so-called EB1-like motif (Wen *et al.*, 2004). The crystal structure of the EB1-like motif has been recently solved and was shown to include a dimeric parallel coiled coil and a four-helix bundle (Honnappa *et al.*, 2005; Slep *et al.*, 2005). This structure revealed a highly conserved surface patch with a hydrophobic cavity and a polar rim, which play an essential role in the binding to APC and spectraplakins (Honnappa *et al.*, 2005; Slep *et al.*, 2005). It is possible that CLIP family members may also require the EB1-like motif for their interaction. The role of the EB1 acidic tail, which is expected to be highly flexible, might primarily involve recruitment and docking of CLIP at

the surface of the EB1-like motif or some other part of EB1 protein.

There are strong indications that CLIPs bind to acidic tail of tubulin (Badin-Larcon *et al.*, 2004; Erck *et al.*, 2005), suggesting that CLIPs may use the same sites for interaction with the EB proteins and tubulin. This does not necessarily contradict the idea that CLIPs and EBs bind to MTs cooperatively, because mammalian CLIPs contain two copies of CAP-Gly domain and are dimers, so that each CLIP molecule has four potential sites for tubulin/EB binding. Besides, in addition to the binding site accommodating tubulin/EB acidic tails with their C-terminal aromatic residue, other CLIP surfaces are likely to be involved in EB and/or tubulin binding. It is tempting to speculate that when CLIPs and EBs simultaneously bind to MTs, the highly flexible acidic tails of tubulin might substitute for the function of the EB tails. In this way, EB tails would not be essential for efficient interaction with CLIPs in a triple complex with tubulin. This might explain why EB1 Δ Ac can partially restore CLIP accumulation and fully restore the rate of CLIP dissociation in the absence of EB1 and EB3.

An intriguing question is why the EB2 protein, a close relative of EB1 and EB3, can only poorly interact with the

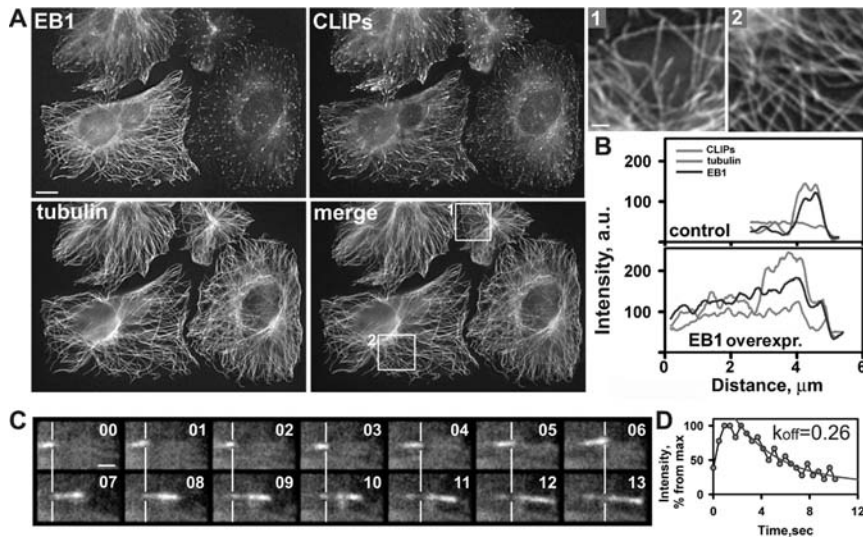


Figure 7. Moderate overexpression of EB1 reduces the rate of CLIP dissociation from the MT tips. (A) CHO-K1 cells expressing exogenous untagged EB1 were stained for EB1 (blue), CLIP (red), and tubulin (green). Bar, 5 μm . Enlarged insets are from the control (1) and EB1 expressing cells (2). Bar, 1 μm . (B) Linescan analysis of individual MT plus ends from a control cell and a cell expressing exogenous EB1 (where it is evenly distributed along the MT length); CLIP-positive labeling becomes twice as long ($\sim 4 \mu\text{m}$) in such EB1-overexpressing cells. (C) Time-lapse images of YFP-CLIP-170 in the cell expressing exogenous EB1. Images were acquired every 0.5 s. Time is shown in seconds in the top right corner. Lines correspond to outmost CLIP-170 tips on the first row images and demonstrate that in most cases YFP-CLIP-170 is still bound to the MT lattice 7 s after it appears at the outmost tips. Bar, 1 μm . (D) A graph of intensity decay of YFP signal over time and its fitting to an exponential decay curve.

CLIPs and cannot rescue their accumulation at the MT tips after depletion of EB1 and EB3. The surface residues within the EB1 motif are highly conserved between EB1, EB2, and EB3. However, the tail of EB2 differs considerably from those of EB1 and EB3. First, it contains two uncharged residues near its tip instead of acidic amino acids present in EB1, EB3, and α -tubulin (Figure 2B). Second, the tripeptide V254-I255-P256 present in the EB1 tail is substituted for GHT in human EB2 and GQT in the mouse EB2. The crystal structure of EB1 dimer showed that this tripeptide from one monomer can interact with the hydrophobic cavity of the other monomer (Honnappa et al., 2005; Slep et al., 2005). This interaction might be important for positioning of the acidic tail with respect to the rest of the molecule. Its hydrophilic character in EB2 might affect the tail conformation and, therefore, have an influence on the binding of protein partners.

Although direct interaction of CLIPs and EBs provides an attractive explanation for the observed dependence of CLIPs on EB1 and EB3 for their MT end accumulation, we cannot rule out possible indirect mechanisms. First, EB1 and EB3 may recruit additional proteins, which in turn may increase binding of the MT tip for CLIPs. Such candidate +TIPs, which can associate with both CLIPs and EBs include p150^{Glued} and CLASPs (Askham et al., 2002; Bu and Su, 2003; Ligon et al., 2003; Lansbergen et al., 2004; Mimori-Kiyosue et al., 2005). Second, presence of EB proteins may cause displacement of certain factors, which help CLIPs to dissociate. However, our data on EB1 overexpression do not support these possibilities because in these conditions CLIP dissociates from the MTs two times slower but, unlike EB1, it does not redistribute along the MT length.

Finally, EB1 and EB3 may be influencing the MT structure itself. The polymerizing MT tip is believed to have a structure different from the rest of the MT lattice because of the presence of tubulin sheets, protruding protofilaments or a GTP cap (Carvalho et al., 2003; Howard and Hyman, 2003). It is possible that both EBs and CLIPs recognize this structure and remain at the plus ends as long as the structure is retained. If EB proteins would help to maintain this structure slowing down its conversion to the regular MT lattice, this would explain how they influence the release of CLIPs from the tips. Interesting in this respect is an observation of EB1-associated curved filamentous extensions at the MT plus ends in *Xenopus* extracts (Tirnauer et al., 2002).

Both direct and indirect interactions with EB proteins may contribute to the proper CLIP distribution. Nevertheless, the loss of CLIPs from the MT tips after EB knockdown is not proportional to the extent of the EB depletion. Because we were unable to achieve a complete knockdown of EB proteins, we cannot exclude that in the absence of these proteins CLIPs would fail to bind to MT tips altogether. However, because the CLIPs could still bind to the outer MT tips at a slightly reduced level when the depletion of EB proteins was quite profound, we propose that the primary mechanism of CLIP accumulation at the MT tips is EB-independent. This conclusion is further supported by the fact that CLIP-170 still tip-tracks when EB1 is distributed along the whole MT lattice because of overexpression. Several in vitro studies provided evidence for copolymerization with tubulin as the model of CLIP targeting to the MT plus ends (Diamantopoulos et al., 1999; Arnal et al., 2004). Our in vivo data are in agreement with this model. Depletion of EB family members did not cause major changes in the rate of CLIP association

with the growing plus ends, which appears almost instantaneous.

EB-independent mechanism of CLIP binding to the MT plus ends is also essential in budding and fission yeast. However, unlike the mammalian system, it involves an MT plus end-directed motor, kinesin, which transports the CLIP-170 homologues to the MT ends (Busch *et al.*, 2004; Carvalho *et al.*, 2004). This ancient mechanism may have been replaced later in evolution as insufficient for ensuring CLIP accumulation at the fast growing MT ends in mammals. Taken together, our study emphasizes that the interactions between different +TIPs are an important contributing factor for their specific localization.

ACKNOWLEDGMENTS

We thank Dr. J. M. Schober for the comments on the manuscript. This work was supported by the Netherlands Organisation for Scientific Research grants to A.A. and N.G., and by the National Institutes of Health Grant GM25062 to G.B.

REFERENCES

- Akhmanova, A., and Hoogenraad, C. C. (2005). Microtubule plus-end-tracking proteins: mechanisms and functions. *Curr. Opin. Cell Biol.* 17, 47–54.
- Arnal, I., Heichette, C., Diamantopoulos, G. S., and Chretien, D. (2004). CLIP-170/tubulin-curved oligomers coassemble at microtubule ends and promote rescues. *Curr. Biol.* 14, 2086–2095.
- Askham, J. M., Vaughan, K. T., Goodson, H. V., and Morrison, E. E. (2002). Evidence that an interaction between EB1 and p150(Glued) is required for the formation and maintenance of a radial microtubule array anchored at the centrosome. *Mol. Biol. Cell.* 13, 3627–3645.
- Badin-Larcon, A. C., Boscheron, C., Soleilhac, J. M., Piel, M., Mann, C., Denarier, E., Fournest-Lieuvain, A., Lafanechere, L., Bornens, M., and Job, D. (2004). Suppression of nuclear oscillations in *Saccharomyces cerevisiae* expressing Glu tubulin. *Proc. Natl. Acad. Sci. USA* 101, 5577–5582.
- Berrueta, L., Kraeft, S. K., Tirnauer, J. S., Schuyler, S. C., Chen, L. B., Hill, D. E., Pellman, D., and Bierer, B. E. (1998). The adenomatous polyposis coli-binding protein EB1 is associated with cytoplasmic and spindle microtubules. *Proc. Natl. Acad. Sci. USA* 95, 10596–10601.
- Brummelkamp, T. R., Bernards, R., and Agami, R. (2002). A system for stable expression of short interfering RNAs in mammalian cells. *Science* 296, 550–553.
- Bu, W., and Su, L. K. (2003). Characterization of functional domains of human EB1 family proteins. *J. Biol. Chem.* 278, 49721–49731.
- Busch, K. E., and Brunner, D. (2004). The microtubule plus end-tracking proteins mal3p and tip1p cooperate for cell-end targeting of interphase microtubules. *Curr. Biol.* 14, 548–559.
- Busch, K. E., Hayles, J., Nurse, P., and Brunner, D. (2004). Tea2p kinesin is involved in spatial microtubule organization by transporting tip1p on microtubules. *Dev. Cell* 6, 831–843.
- Carvalho, P., Gupta, M. L., Jr., Hoyt, M. A., and Pellman, D. (2004). Cell cycle control of kinesin-mediated transport of Bik1 (CLIP-170) regulates microtubule stability and dynein activation. *Dev. Cell* 6, 815–829.
- Carvalho, P., Tirnauer, J. S., and Pellman, D. (2003). Surfing on microtubule ends. *Trends Cell Biol.* 13, 229–237.
- Coquelle, F. M. *et al.* (2002). LIS1, CLIP-170's key to the dynein/dynactin pathway. *Mol. Cell Biol.* 22, 3089–3102.
- Diamantopoulos, G. S., Perez, F., Goodson, H. V., Batelier, G., Melki, R., Kreis, T. E., and Rickard, J. E. (1999). Dynamic localization of CLIP-170 to microtubule plus ends is coupled to microtubule assembly. *J. Cell Biol.* 144, 99–112.
- Erck, C. *et al.* (2005). A vital role of tubulin-tyrosine-ligase for neuronal organization. *Proc. Natl. Acad. Sci. USA* 102, 7853–7858.
- Galjart, N., and Perez, F. (2003). A plus-end raft to control microtubule dynamics and function. *Curr. Opin. Cell Biol.* 15, 48–53.
- Goodson, H. V., Skube, S. B., Stalder, R., Valetti, C., Kreis, T. E., Morrison, E. E., and Schroer, T. A. (2003). CLIP-170 interacts with dynactin complex and the APC-binding protein EB1 by different mechanisms. *Cell Motil. Cytoskelet.* 55, 156–173.
- Hayashi, I., and Ikura, M. (2003). Crystal structure of the amino-terminal microtubule-binding domain of end-binding protein 1 (EB1). *J. Biol. Chem.* 278, 36430–36434.
- Honnappa, S., John, C. M., Kostrewa, D., Winkler, F. K., and Steinmetz, M. O. (2005). Structural insights into the EB1-APC interaction. *EMBO J.* 24, 261–269.
- Hoogenraad, C. C., Akhmanova, A., Grosveld, F., De Zeeuw, C. I., and Galjart, N. (2000). Functional analysis of CLIP-115 and its binding to microtubules. *J. Cell Sci.* 113, 2285–2297.
- Howard, J., and Hyman, A. A. (2003). Dynamics and mechanics of the microtubule plus end. *Nature* 422, 753–758.
- Juwana, J. P., Henderikx, P., Mischo, A., Wadle, A., Fadle, N., Gerlach, K., Arends, J. W., Hoogenboom, H., Pfreundschuh, M., and Renner, C. (1999). EB/RP gene family encodes tubulin binding proteins. *Int. J. Cancer* 81, 275–284.
- Kodama, A., Karakesisoglou, I., Wong, E., Vaezi, A., and Fuchs, E. (2003). ACF7: an essential integrator of microtubule dynamics. *Cell* 115, 343–354.
- Komarova, Y. A., Akhmanova, A. S., Kojima, S., Galjart, N., and Borisov, G. G. (2002). Cytoplasmic linker proteins promote microtubule rescue in vivo. *J. Cell Biol.* 159, 589–599.
- Lansbergen, G. *et al.* (2004). Conformational changes in CLIP-170 regulate its binding to microtubules and dynactin localisation. *J. Cell Biol.* 166, 1003–1014.
- Ligon, L. A., Shelly, S. S., Tokito, M., and Holzbaur, E. L. (2003). The microtubule plus-end proteins EB1 and dynactin have differential effects on microtubule polymerization. *Mol. Biol. Cell* 14, 1405–1417.
- Mennella, V., Rogers, G. C., Rogers, S. L., Buster, D. W., Vale, R. D., and Sharp, D. J. (2005). Functionally distinct kinesin-13 family members cooperate to regulate microtubule dynamics during interphase. *Nat. Cell Biol.* 7, 235–245.
- Mimori-Kiyosue, Y. *et al.* (2005). CLASP1 and CLASP2 bind to EB1 and regulate microtubule plus-end dynamics at the cell cortex. *J. Cell Biol.* 168, 141–153.
- Perez, F., Diamantopoulos, G. S., Stalder, R., and Kreis, T. E. (1999). CLIP-170 highlights growing microtubule ends in vivo. *Cell* 96, 517–527.
- Pierre, P., Scheel, J., Rickard, J. E., and Kreis, T. E. (1992). CLIP-170 links endocytic vesicles to microtubules. *Cell* 70, 887–900.
- Rogers, S. L., Wiedemann, U., Hacker, U., Turck, C., and Vale, R. D. (2004). *Drosophila* RhoGEF2 associates with microtubule plus ends in an EB1-dependent manner. *Curr. Biol.* 14, 1827–1833.
- Schuyler, S. C., and Pellman, D. (2001). Microtubule “plus-end-tracking proteins”: the end is just the beginning. *Cell* 105, 421–424.
- Slep, K. C., Rogers, S. L., Elliott, S. L., Ohkura, H., Kolodziej, P. A., and Vale, R. D. (2005). Structural determinants for EB1-mediated recruitment of APC and spectraplakins to the microtubule plus end. *J. Cell Biol.* 168, 587–598.
- Stepanova, T., Slemmer, J., Hoogenraad, C. C., Lansbergen, G., Dortland, B., De Zeeuw, C. I., Grosveld, F., van Cappellen, G., Akhmanova, A., and Galjart, N. (2003). Visualization of microtubule growth in cultured neurons via the use of EB3-GFP (end-binding protein 3-green fluorescent protein). *J. Neurosci.* 23, 2655–2664.
- Su, L. K., and Qi, Y. (2001). Characterization of human MAPRE genes and their proteins. *Genomics* 71, 142–149.
- Tirnauer, J. S., and Bierer, B. E. (2000). EB1 proteins regulate microtubule dynamics, cell polarity, and chromosome stability. *J. Cell Biol.* 149, 761–766.
- Tirnauer, J. S., Grego, S., Salmon, E. D., and Mitchison, T. J. (2002). EB1-microtubule interactions in *Xenopus* egg extracts: role of EB1 in microtubule stabilization and mechanisms of targeting to microtubules. *Mol. Biol. Cell* 13, 3614–3626.
- Wen, Y., Eng, C. H., Schmoranzler, J., Cabrera-Poch, N., Morris, E. J., Chen, M., Wallar, B. J., Alberts, A. S., and Gundersen, G. G. (2004). EB1 and APC bind to mDia to stabilize microtubules downstream of Rho and promote cell migration. *Nat. Cell Biol.* 6, 820–830.



Chapter 4

CLASP1 and CLASP2 bind to EB1 and regulate microtubule plus-end dynamics at the cell cortex.

J Cell Biol. 2005 Jan 3;168(1):141-53.

CLASP1 and CLASP2 bind to EB1 and regulate microtubule plus-end dynamics at the cell cortex

Yuko Mimori-Kiyosue,¹ Ilya Grigoriev,^{2,3} Gideon Lansbergen,⁴ Hiroyuki Sasaki,^{1,5} Chiyuki Matsui,¹ Fedor Severin,⁶ Niels Galjart,⁴ Frank Grosveld,⁴ Ivan Vorobjev,³ Shoichiro Tsukita,^{7,8} and Anna Akhmanova⁴

¹KAN Research Institute, Kyoto Research Park, Shimogyo-ku, Kyoto 600-8815, Japan

²Department of Cell Biology and Histology and ³Laboratory of Cell Motility, A.N. Belozersky Institute, Moscow State University, Vorobjevi Gory, Moscow, 119992, Russia

⁴MGC Department of Cell Biology and Genetics, Erasmus Medical Center, 3000 DR Rotterdam, Netherlands

⁵Institute of DNA Medicine, Jikei University School of Medicine, Minato-ku, Tokyo 105-8461, Japan

⁶BIOTEC, TU Dresden, Proteomics and Cellular Machines, Tatzberg 47-51, 01307 Dresden, Germany

⁷Department of Cell Biology, Faculty of Medicine, Kyoto University, Sakyo-ku, Kyoto 606-8315, Japan

⁸Solution Oriented Research for Science and Technology, Japan Science and Technology Corporation, Sakyo-ku, Kyoto 606-8501, Japan

CLIP-associating protein (CLASP) 1 and CLASP2 are mammalian microtubule (MT) plus-end binding proteins, which associate with CLIP-170 and CLIP-115. Using RNA interference in HeLa cells, we show that the two CLASPs play redundant roles in regulating the density, length distribution and stability of interphase MTs. In HeLa cells, both CLASPs concentrate on the distal MT ends in a narrow region at the cell margin. CLASPs stabilize MTs by promoting pauses and restricting MT growth and shortening episodes to this peripheral cell

region. We demonstrate that the middle part of CLASPs binds directly to EB1 and to MTs. Furthermore, we show that the association of CLASP2 with the cell cortex is MT independent and relies on its COOH-terminal domain. Both EB1- and cortex-binding domains of CLASP are required to promote MT stability. We propose that CLASPs can mediate interactions between MT plus ends and the cell cortex and act as local rescue factors, possibly through forming a complex with EB1 at MT tips.

Introduction

Microtubules (MTs) are polar filaments, which can undergo alternating phases of growth and shortening, a behavior termed dynamic instability (Desai and Mitchison, 1997). In living cells, a large number of protein factors regulate dynamic instability, thus determining the shape of the MT network in different phases of the cell cycle and in different cell regions. An interesting group of MT-associated factors, involved in regulation of MT dynamics, binds specifically to the ends of growing MTs. These factors, named +TIPs (plus-end tracking proteins), include members of structurally unrelated protein families, such as end binding proteins EB1, EB2 (RP1), and EB3, cytoplasmic linker proteins CLIP-170 and CLIP-115, dynactin large subunit p150^{Glued}, adenomatous polyposis coli (APC), and CLIP-associating proteins (CLASPs; for reviews see Schuyler and Pellman, 2001; Carvalho et al., 2003; Howard and Hyman, 2003; Mimori-Kiyosue and Tsukita, 2003).

CLASPs are a family of MT-associated proteins, conserved in animals and fungi (Inoue et al., 2000; Lemos et al., 2000). A distant member of this family, the budding yeast Stu1p, was isolated as a suppressor of a cold-sensitive tubulin mutation and an essential component of the mitotic spindle (Pasqualone and Huffaker, 1994; Yin et al., 2002). The first member of this family from higher organisms to be characterized in detail, the *Drosophila* Orbit/MAST, was also shown to be essential for mitosis (Inoue et al., 2000; Lemos et al., 2000), and the same holds true for one of the three *C. elegans* homologues, cls-2 (R106.7; Gonczy et al., 2000). Mammalian homologues, CLASP1 and 2, were initially characterized through their ability to bind to CLIP-170 and CLIP-115 (Akhmanova et al., 2001). The interaction between the CLASP and CLIP counterparts was also observed in flies (Mathe et al., 2003).

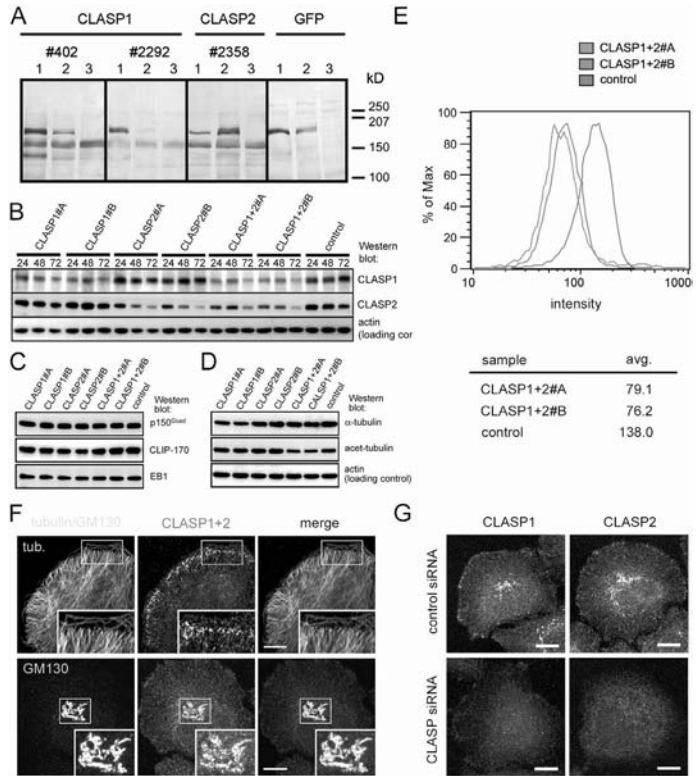
CLASP family members participate in generating polarized MT networks: in migrating fibroblasts, CLASP2 is involved in stabilizing MTs specifically at the leading edge (Akhmanova et al., 2001), whereas during fly oogenesis, Orbit/MAST organizes MTs, which interconnect the oocyte and the nurse cells (Mathe et al., 2003). During mitosis, Orbit/MAST plays a role in maintaining the bipolarity of the mitotic spindle, in the MT-

The online version of this article contains supplemental material.

Correspondence to Anna Akhmanova: anna.akhmanova@chello.nl

Abbreviations used in this paper: APC, adenomatous polyposis coli; CLASP, CLIP-associating protein; HIS, 6x histidine; mRFP, monomeric RFP; MT, microtubule; siRNA, small interfering RNA; +TIPs, plus-end tracking proteins; TIRF, total internal reflection fluorescence.

Figure 1. Characterization of CLASP-specific antibodies and RNAi tools. (A) Lysates of HeLa cells, transfected with GFP-CLASP1 α (lane 1), GFP-CLASP2 α (lane 2), or mock transfected (lane 3), were analyzed by Western blotting with the indicated antibodies. (B) Lysates of HeLa cells, transfected with the indicated siRNAs, were prepared 24, 48, or 72 h after transfection and analyzed by Western blotting with the indicated antibodies. (C and D) Lysates of HeLa cells, transfected with the indicated siRNAs, were prepared 72 h after transfection and analyzed by Western blotting with the indicated antibodies. (E) HeLa cells, transfected either with the control siRNA, CLASP1+2#A or #B siRNAs, were stained with the mixture of antibodies #402 or #2358 72 h after transfection and analyzed by FACS. (F) HeLa cells were stained with a mixture of antibodies #402 (CLASP1) and #2358 (CLASP2) and either α -tubulin or the Golgi marker GM130. Bars, 10 μ m. (G) HeLa cells, transfected either with the control siRNA or the CLASP1+2#B siRNAs, were stained with antibodies #402 or #2358 72 h after transfection. Bars, 10 μ m.



kinetochore attachment and chromosome congression (Maiato et al., 2002). Similar functions were ascribed to the human CLASP1 (Maiato et al., 2003a,b). In addition, Orbit/MAST is needed for cytokinesis, because it stabilizes the interior MTs of the central spindle, necessary for the progression of the cleavage furrow (Inoue et al., 2004). Although the MT-stabilizing role of CLASP homologues has been established, the effect of CLASPs on the parameters of MT dynamic instability has not been analyzed, and the functional redundancy of the two mammalian CLASPs has not been addressed.

In this study, we show that CLASP1 and 2 have similar and redundant roles in organizing the interphase MTs in HeLa cells. CLASPs stabilize MTs, by retaining their plus ends in the peripheral cortical region, where they are pausing or undergo short polymerization–depolymerization excursions. To get insight into the mechanism of CLASP action, we have analyzed the targeting domains of the CLASP proteins. We show that a short repetitive region in the middle part of CLASP1 and 2 can bind to EB1 and EB3 and recognize growing MT tips, whereas the COOH-terminal domain of CLASP2 associates with the Golgi apparatus and cell cortex. We propose that the MT-stabilizing activity of CLASPs depends on the interaction with the EB proteins.

Results

Characterization of siRNAs, specific for CLASP1 and CLASP2

To detect CLASP1 protein, we have raised two new antibodies against CLASP1, #402 and #2292, which strongly react with GFP-CLASP1 α , and display some cross-reactivity with GFP-CLASP2 α (Fig. 1 A). To detect CLASP2 we have used the previously described antibody #2358 (Akhmanova et al., 2001), which strongly reacts with GFP-CLASP2 α and cross-reacts to some extent with GFP-CLASP1 α (Fig. 1 A). All three antibodies recognized endogenous HeLa cell proteins of \sim 160 kD, in agreement with the predicted molecular weight of CLASP1/2 α isoforms.

To knock down CLASP1 and 2, we have selected two different small interfering RNAs (siRNAs), specific for CLASP1 (these will be referred to as CLASP1#A and CLASP1#B) and two siRNAs, specific for CLASP2 (CLASP2#A and CLASP2#B). The siRNAs were transfected into HeLa cells separately, or as combinations of the two “A” siRNAs (CLASP1+2#A) or the two “B” siRNAs (CLASP1+2#B). Three days after transfection, the levels of both CLASP1 and CLASP2, estimated by Western blotting,

were reduced by $\sim 70\%$, which can be regarded as a hypomorphic state (Fig. 1 B). Control siRNAs had no effect on CLASP levels (Fig. 1 B and not depicted).

The partial down-regulation of CLASPs, separately or together, had no effect on the levels of tubulin or other +TIPs (Fig. 1, C and D). However, when CLASP1 and CLASP2 were knocked down simultaneously, the amount of acetylated tubulin (a marker of stable MTs; Bulinski and Gundersen, 1991) was diminished by $\sim 40\%$, suggesting that MT stability was reduced (Fig. 1 D), confirming our previous findings in 3T3 fibroblasts (Akhmanova et al., 2001).

CLASP1- and CLASP2-directed antibodies #402 and #2358 produced similar staining patterns in interphase HeLa cells: in line with previous observations (Akhmanova et al., 2001; Maiato et al., 2003a), they decorated the Golgi apparatus, the centrosome, and MT plus ends (Fig. 1 F and not depicted). The MT tip staining, which nicely colocalized with other +TIPs (EB1, CLIP-170, and p150^{Glued}), was especially prominent in the $\sim 1\text{-}\mu\text{m}$ region at the cell edges, which were not in contact with other cells (Fig. 1 F; Fig. S1, available at <http://www.jcb.org/cgi/content/full/jcb.200405094/DC1>). Specific accumulation of CLASPs at the cell edge was confirmed by expressing GFP-tagged CLASPs in HeLa cells (Video 1, available at <http://www.jcb.org/cgi/content/full/jcb.200405094/DC1>).

After CLASP1+2 siRNA treatment, all CLASP-specific signals were strongly reduced (Fig. 1, E and G). Analysis of the CLASP1+2 knockdown cells by FACS after staining with CLASP1 and 2 antibodies showed that they represent a reasonably homogeneous population (Fig. 1 E). These cells displayed a dim diffuse pattern, which was likely in part due to background staining with anti-CLASP antibodies, whereas the specific signals at the MT tips, Golgi, and the centrosome were greatly diminished (Fig. 1 G).

Organization of the MT network after CLASP knockdown

Simultaneous knockdown of the two CLASPs caused mitotic defects, which were similar to those observed in the Orbit/MAST mutants (Maiato et al., 2002; Inoue et al., 2004) and will be described elsewhere (unpublished data). In interphase cells, a significant decrease in density of the MT network was observed (Fig. 2, A and B). This effect was particularly obvious in cells, which had no contacts with their neighbors and, therefore, we confined our analysis to such isolated cells.

To get a measure of MT density, we have determined integrated intensity of α -tubulin staining after methanol fixation, which preserves MT polymer, while soluble tubulin is extracted. This analysis indicated that MT density was significantly decreased, only when combinations of CLASP1 and CLASP2-specific siRNAs were used, whereas partial knockdown of either CLASP separately had no visible effect (Fig. 2 C). The fact that integrated intensity was a valid measure of MT density was confirmed by counting the number of MTs in a cell sector, which was decreased by $\sim 30\%$ after both CLASPs were knocked down (Fig. 2 D). A decrease in integrated intensity of tubulin staining after partial CLASP1/2 knockdown was especially obvious in the central part of the cell, around the

Golgi apparatus (Fig. 2 E). It should be noted that the morphology of the Golgi complex was not significantly affected by CLASP knockdown (unpublished data).

Because our siRNA treatment resulted only in a partial depletion of the two CLASP proteins, we analyzed the dependence of the severity of the observed phenotype on the CLASP1/2 levels. The density of MTs was proportional to the level of CLASP1/2 proteins (Fig. 2 F), indicating that CLASPs regulate MT number in a concentration-dependent manner.

Because the amount of total tubulin was not affected by CLASP1+2 siRNA treatment (Fig. 1 D), the diminished number of MTs should have resulted in increased levels of nonpolymerized tubulin. This was confirmed by the analysis of confocal microscope images of tubulin staining in formaldehyde-fixed cells, in which soluble tubulin is maintained during the staining procedure (Fig. 2, I and J).

Most strikingly, the distribution of MT plus ends near the cell margin was changed after CLASP depletion. In control cells, most MTs terminated at $\sim 1\text{-}\mu\text{m}$ distance from the cell edge. This population of MTs was selectively lost after CLASP knockdown, whereas a small peak of plus ends was observed at $\sim 2\text{-}\mu\text{m}$ distance from the edge (Fig. 2 G). This change in MT plus-end distribution was also apparent in cells, stained for EB1, CLIP-170, and p150^{Glued} (Fig. S1). The distribution of MT ends in the internal cytoplasm was almost identical in control and CLASP1+2#B siRNA-treated cells (Fig. 2 G).

We have also noticed that after CLASP knockdown, MTs were often oriented along the cell margin, whereas in control cells most MTs were perpendicular to the cell edge (Fig. 2 H). Analysis of the angles between the MTs and the cell margin indicated that the number of MTs, deviating by $>45^\circ$ from the cell radius, was increased by a factor of 2.6, when both CLASPs were partially depleted.

HeLa cells do not migrate, but their membranes exhibit protrusion activity and retrograde flow. The rate of the retrograde flow was reduced almost by half in CLASP1+2#B siRNA-treated cells, compared with control (Fig. S2, available at <http://www.jcb.org/cgi/content/full/jcb.200405094/DC1>). It is possible that CLASPs directly affect the membrane flow, by influencing the process of secretion or the dynamics of the actin cytoskeleton; the observed effect, however, may also be a consequence of the altered MT organization.

MT dynamics after CLASP knockdown

To confirm that the observed effects on the MT network result from the knockdown of CLASP proteins, rather than unspecific effects of the used RNA duplexes, we transfected cells, treated with CLASP1+2 siRNA combinations, with rescue constructs, encoding GFP or monomeric RFP (mRFP) fusions of CLASP1 α or CLASP2 α , resistant to the siRNAs due to silent substitutions in the siRNA target regions. Both CLASP1 α and 2 α fusions could restore MT density and the alignment of MT tips along the cell cortex (Fig. 3 A; Video 2, available at <http://www.jcb.org/cgi/content/full/jcb.200405094/DC1>). After the rescue with mRFP-CLASP2 α the number of MT ends in a sector increased from 14.0 ± 4.3 in surrounding CLASP knockdown cells to 27.9 ± 2.6 in cells, expressing the rescue con-

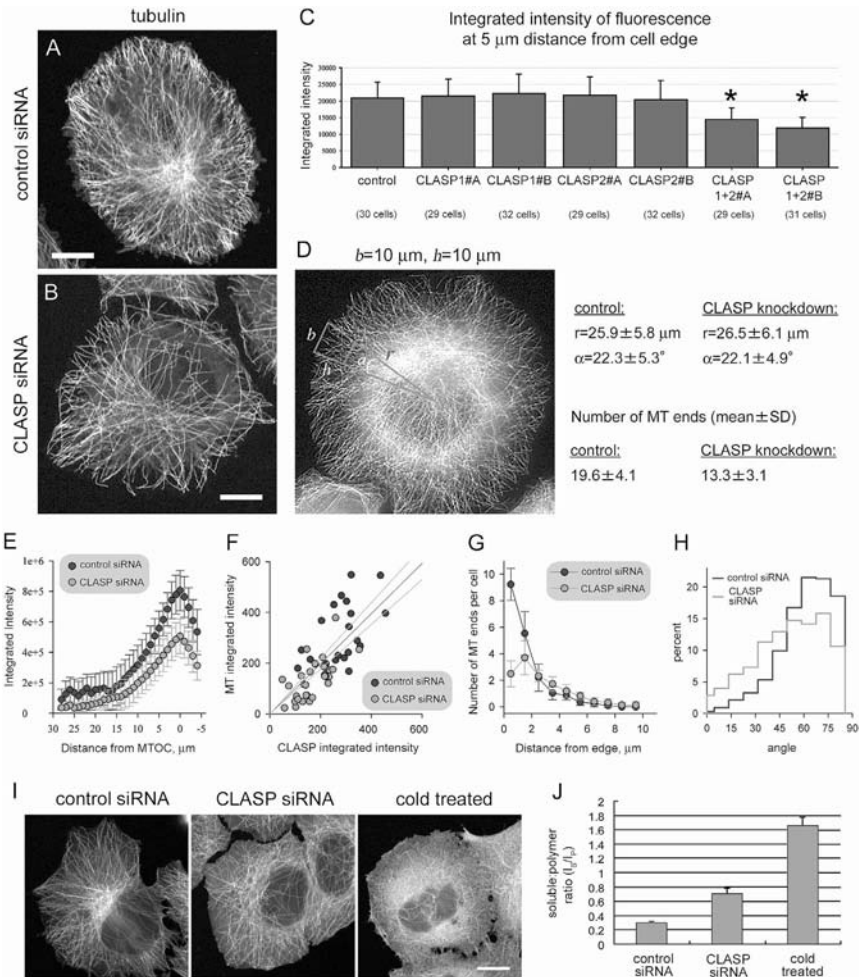


Figure 2. Effect of CLASP knockdown on the interphase MT network. (A and B) HeLa cells 72 h after transfection with the control siRNA (A) or CLASP1+2#B siRNAs (B), fixed with methanol, and stained for α -tubulin. Bars, 10 μm . (C) Plots of integrated intensity of fluorescence of α -tubulin staining, which was performed as in A and B, in HeLa cells 72 h after transfection with the indicated siRNAs. The integrated intensity was measured within a $5\text{-}\mu\text{m}^2$ box at 5 μm distance from the cell edge, with subtracting the background. Measurements were performed in ~ 30 cells per siRNA in three different cell regions. Values significantly different from the control ($P < 0.001$) are indicated by asterisks. (D) Number of MT ends in a trapezoid part of the cell sector (with a base b and side h) in HeLa cells 72 h after transfection with the control siRNA (30 cells, $n = 587$) or CLASP1+2#B siRNAs (30 cells, $n = 401$). (E) Integrated intensity within a $5\text{-}\mu\text{m}^2$ box was measured along the cell radius in the same cells as described in D. MTOC, the MT organizing center, was determined as the site of radial gathering of MTs. (F) HeLa cells, transfected either with the control siRNA or the CLASP1+2#B siRNAs, were methanol fixed and stained for CLASPs (using with the mixture of antibodies #402 or #2358) and for tubulin 72 h after transfection. Representative cells were selected to include examples with both high and low levels of CLASP staining. Integrated intensity of CLASP staining was plotted versus integrated intensity of tubulin staining. Each dot represents an average of five independent measurements in different areas at the periphery of one cell. The regression line is shown in red and the 95% confidence interval is indicated by gray lines. (G) Distribution of distances from MT ends to the cell edge within the trapezoid part of the cell sector shown in D. Analyzed images were the same as in D. (H) Distribution of angles of distal segments of MTs to the cell radius. Analyzed images were the same as in D. (I) Confocal microscope images (1- μm optical sections) of HeLa cells, fixed with formaldehyde 72 h after transfection with the control or CLASP1+2#B siRNAs and stained for α -tubulin. Control cells were also incubated for 1 h at 4°C before fixation, to depolymerize MTs ("cold treated"). Bar, 10 μm . (J) Plots of the ratio of the intensity of soluble tubulin staining I_s (after subtracting background) to the intensity of polymer staining I_p (after subtracting background and I_s), obtained from the images as shown in H. Measurements were performed in 20 control cells ($n = 158$), 35 CLASP-knockdown cells ($n = 225$), and 18 cold-treated cells ($n = 130$). Error bars represent the SD.

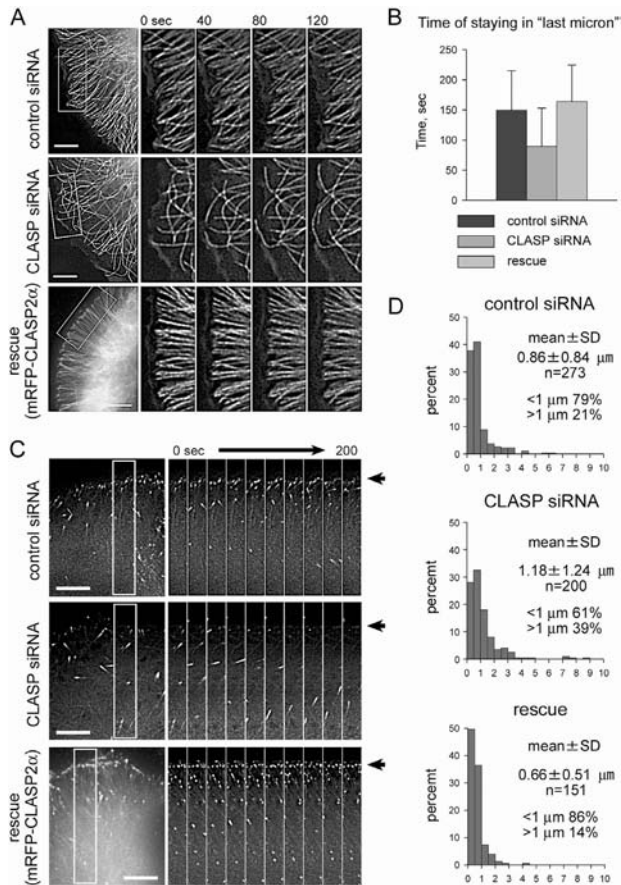


Figure 3. Effect of CLASP knockdown on MT dynamics. (A) Time-lapse images of HeLa cells, stably expressing GFP- α -tubulin, 72 h after transfection with the control or CLASP1+2#A siRNAs. For rescue, CLASP1+2#A siRNA-treated cells were transfected with mRFP-CLASP2 α 48 h after the siRNA transfection and observed 24 h later. In the "rescue" panel mRFP-CLASP2 α is shown in red and GFP- α -tubulin is shown in green. Bars, 5 μ m. (B) Time of staying of MT ends within 1 μ m distance from the cell edge, determined from the time-lapse image series as shown in A (cells were imaged with 2-s interval). The difference between the control and CLASP knockdown is statistically significant ($P < 0.001$), the difference between control and rescue is not significant. (C) Time-lapse images of HeLa cells, stably expressing EB1-GFP, 72 h after transfection with the control or CLASP1+2#A siRNAs. Rescue was performed as described in A. In the "rescue" panel mRFP-CLASP2 α is shown in red and EB1-GFP is shown in green. Cell margin is indicated by an arrow. Bars, 5 μ m. (D) Length of the shortening excursions from the cell edge, measured from the same dataset as in A and B. Error bars represent the SD.

struct. This increase was above the levels in control cells (19.6 ± 4.1), probably due to overexpression of the rescue construct by a factor of 3–4 compared with endogenous CLASPs (unpublished data). Remarkably, the time the MT plus ends stayed in the vicinity (1 μ m distance) from the cell edge was significantly reduced after both CLASPs were knocked down and restored after the rescue with mRFP-CLASP2 α (Fig. 3 B).

We have also analyzed HeLa cells stably expressing a GFP fusion of EB1, which binds predominantly to the ends of growing MTs (Mimori-Kiyosue et al., 2000). In control cells a large number of MT ends at the cell periphery was strongly positive for EB1, suggesting that these MTs were growing (Fig. 3 C). This accumulation of EB1-positive ends was clearly reduced after the partial CLASP depletion and restored after the knockdown cells were rescued with mRFP-CLASP2 α (Fig. 3 C; Video 3, available at <http://www.jcb.org/cgi/content/full/jcb.200405094/DC1>). In many cases, EB1 signals at the periphery of control cells appeared rather static, while their intensity varied greatly. This could be explained if pausing MTs or

MTs, which started to depolymerize, retained small amounts of EB1, whereas the enhancement of EB1 signal would correlate with MT growth.

We conclude that when CLASP levels are normal, MT ends are maintained in the proximity of cell margin, but remain dynamic. This can be most easily accounted for by very short alternating bursts of MT growth and shrinkage. Indeed, the number of MTs, displaying longer (>1 μ m) depolymerization episodes, was increased after the partial CLASP knockdown (Fig. 3 D). This effect was reversed by introducing the mRFP-CLASP2 α rescue construct.

The analysis of parameters of MT dynamic instability (Table I) revealed that in the cortical 1- μ m-wide region MTs spent more time pausing and exhibited less frequent transitions to growth or shortening in control cells, than in cells with partially depleted CLASPs. In addition, shortening and growing MTs underwent more frequent reverse transitions (rescues or catastrophes, respectively); as a result, dynamic MT ends were maintained in the vicinity of the cell margin, accounting for the

Table 1. Parameters of dynamic instability

	Control		CLASP knockdown	
	1- μ m region at the cell edge	Cell interior	1- μ m region at the cell edge	Cell interior
Rate of growth, μm/min				
Direct MT observation	9.9 \pm 3.5	11.7 \pm 4.8	11.1 \pm 1.4	12.6 \pm 5.1
Subtraction analysis		14.4 \pm 3.9		18.2 \pm 5.8
EB1 tracks		15.9 \pm 6.0		22.8 \pm 7.3
Rate of shortening, μm/min				
Direct MT observation	-12.0 \pm 6.2	-20.7 \pm 11.6	-12.6 \pm 6.5	-17.8 \pm 11.3
Subtraction analysis		-35.6 \pm 11.2		-28.2 \pm 9.8
Transition frequencies				
Growth-Shortening, s ⁻¹	0.078	0.035	0.030	0.045
Growth-Pause, s ⁻¹	0.402	0.238	0.360	0.250
Shortening-Growth, s ⁻¹	0.066	0.085	0.019	0.072
Shortening-Pause, s ⁻¹	0.275	0.213	0.217	0.210
Pause-Growth, s ⁻¹	0.016	0.053	0.032	0.046
Pause-Shortening, s ⁻¹	0.026	0.038	0.038	0.040
Time in growth, %	6.0	16.7	13.3	14.5
Time in pauses, %	88.9	69.3	80.1	70.7
Time in shortening, %	5.1	14.0	6.6	14.8

HeLa cells, stably expressing GFP- α -tubulin or EB1-GFP, were imaged with a 2-s interval 72 h after transfection with the control or CLASP1+2#B siRNAs. Life history plots of 65 MTs in five control cells and 75 MTs in five CLASP knockdown cells were analyzed as described by Shelden and Wadsworth (1993). In addition, to obtain more accurate values of growth and shortening rates in the internal cytoplasm, subtraction analysis (Vorobjev et al., 1999) and measurements of displacements of EB1-GFP comets were used. The differences in rates, obtained by different methods, can be explained by a higher contribution of the pausing state to the growth/shortening episodes at the cell periphery, which can be detected by direct observation, as compared with those inside the cells, which can be identified by subtraction analysis. EB1 associates predominantly with growing MTs (Mimori-Kiyosue et al., 2000) and, therefore, MT pauses hardly contribute to the growth episodes, which are detected by this method. The data are presented in format: mean \pm SD. Rates are instantaneous (measured within one interval between successive frames).

observed longer time of staying of MT ends at the cell periphery in control cells, compared with CLASP knockdown cells. Treatment with CLASP1+2 siRNAs had no significant effect on transition frequencies in the internal cytoplasm, proving that CLASPs are truly local regulators of MT dynamics. However, MT growth rate was higher, and the MT shrinkage rate lower in CLASP knockdown cells, compared with control cells (Table 1). This can be explained by the increased level of soluble tubulin after the partial CLASP depletion (Fig. 2, I and J). It should be noted that the large contribution of the pausing to growth and shortening episodes at the cell margin makes the differences in growth and shrinkage rates at the cell periphery much less apparent, than those in the internal cytoplasm.

CLASP1 and 2 bind to EB1 and EB3

To get a better insight into the mechanism of CLASP action at the MT tip, we have determined domains of CLASP1 and 2, responsible for their plus-end accumulation. Our previous study has shown that the COOH-terminal domains of CLASP1 and 2 bind to CLIP-170 and CLIP-115, but are not essential for MT tip targeting by CLASPs (Akhmanova et al., 2001). Deletion mapping of CLASP2 γ (the shortest splice form of CLASP2, which associates efficiently with the MT tips; Akhmanova et al., 2001) identified a region of \sim 140 aa in the middle of CLASP2, CLASP2-M, which was sufficient to target GFP to the ends of growing MTs (Fig. 4, A-E). The corresponding region of CLASP1 (CLASP1-M) could also direct GFP to the MT tips (Fig. 4, F and G). This region is extremely rich in serines, arginines, and lysines, and contains a number of short direct repeats of several types, which are conserved between

CLASP1, CLASP2, and their *Drosophila* homologue, Orbit/MAST (Fig. 4 H).

To understand how the CLASP2-M fragment targets MT plus ends, we have purified 6x histidine (HIS)-tagged GFP-CLASP2-M and GFP from bacteria (Fig. 4 I). In vitro pelleting assays demonstrated that GFP-CLASP2-M, but not GFP alone, could bind to taxol-stabilized MTs in vitro (Fig. 4 J). It is possible that the interaction between the MTs and CLASP2-M is at least partly due to the positively charged character of this fragment and the presence of highly acidic COOH termini in α - and β -tubulin. Interestingly, +TIPs, which belong to the EB family, such as EB1 and EB3, also possess highly acidic COOH termini, similar to those of tubulins. Therefore, we tested if CLASP2-M could associate with EB1 and EB3, and found that it was indeed the case. Among the CLASP2 fragments, only CLASP2-M could coprecipitate EB1 and EB3 (Fig. 4 K). The corresponding region of CLASP1 could also coprecipitate EB1 and EB3 (Fig. 4 K), suggesting that this property is conserved between the two CLASPs. In vitro, purified GFP-CLASP2-M bound to purified EB1 and EB3, fused to GST. It associated with the COOH-, but not the NH₂-terminal half of the EB1 protein (Fig. 4, L and M). This binding was highly specific, because a number of other basic proteins tested, such as histone H1, did not bind to EB1 COOH terminus (unpublished data).

Also the full-length CLASP1 α and CLASP2 γ , expressed in COS-1 cells, associated with the GST fusions of EB1, EB3 and EB1 COOH terminus (Fig. 4 M). In contrast, the CLASP2- Δ M mutant, which contains an in-frame deletion removing the EB1-binding fragment, was no longer pulled down by GST-

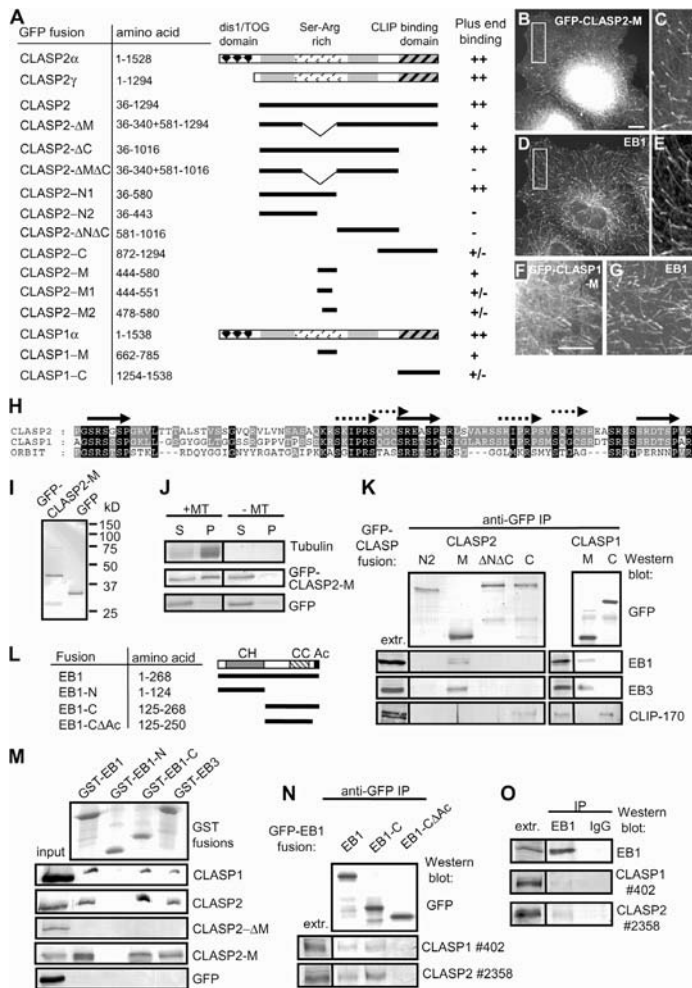


Figure 4. Identification of the MT plus-end binding and EB1-binding domains in CLASP1 and 2. (A–G) GFP fusions of CLASP2 α , CLASP2 γ , different CLASP2 γ deletion mutants, CLASP1 α and its deletion mutants were transfected in COS-1 or COS-7 cells, fixed and counterstained for EB1, and the MT plus-end accumulation was assessed as: ++, strong +, clearly visible; +/-, weakly detectable -, undetectable. B, C, and F, GFP signal; D, E, and G, EB1 staining. Bars, 10 μ m. (H) Alignment of the repetitive part of the CLASP2-M fragment with the corresponding regions of CLASP1 and *D. melanogaster* Orbit/MAST. Repeats of different types are indicated by different arrows. (I) Coomassie-stained gel, showing purified His-tagged GFP-CLASP2-M and GFP. (J) MT pelleting assay with purified GFP-CLASP2-M and GFP. Coomassie-stained gel is shown for tubulin and Western blots with anti-GFP antibodies for the GFP fusions. S, supernatant; P, pellet. (K) Immunoprecipitation with anti-GFP antibodies from COS-1 cells, transfected with the indicated GFP-CLASP1 and 2 deletion mutants. (L) Schematic representation of EB1 structure and the deletion mutants used in this study. CH, calponin homology domain; CS, coiled coil; Ac, acidic tail domain. (M) GST pull-down assays with the indicated GST fusions. Purified GFP-CLASP2-M and GFP or extracts of COS-1 cells, overexpressing GFP-CLASP1 α , GFP-CLASP2, and GFP-CLASP2- Δ M were used. Coomassie-stained gel is shown for the GST fusions and Western blots with anti-GFP antibodies for the GFP fusions. 10% of the input and 25% of the material, bound to the beads, were loaded on gel. (N) Immunoprecipitation with anti-GFP antibodies from COS-1 cells, transfected with the indicated GFP-EB1 fusions. (O) Immunoprecipitation with a rabbit polyclonal antibody against EB1 or a control rabbit IgG from untransfected COS-1 cells.

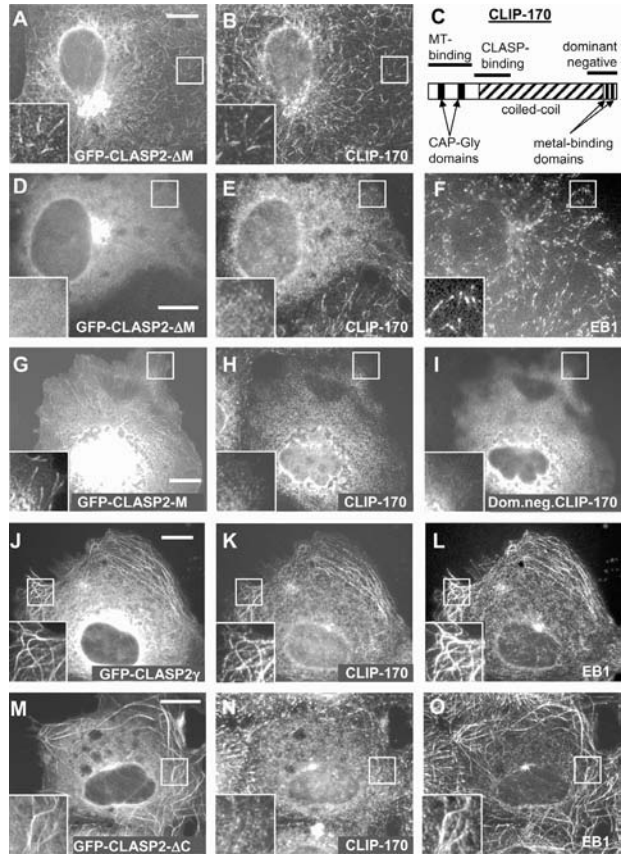
EB1 or EB3 fusions (Fig. 4 M). Endogenous CLASP1 and CLASP2 coprecipitated with EB1-GFP fusion, as well as with the GFP-EB1 COOH terminus, but only when the acidic tail of this protein (the last 18 aa) was intact (Fig. 4 N). The validity of interaction CLASP1/2-EB1 was further confirmed by coprecipitation, albeit a weak one, of endogenous CLASP1 and 2 proteins with endogenous EB1 (Fig. 4 O). Together, these data establish that CLASP1 and 2 bind to EB1 and EB3. This interaction is likely to be transient and regulated, and may occur preferentially in the context of MT tip binding, which would account for the weak coprecipitation of endogenous proteins.

Although GFP-CLASP2-M associated with MT ends (Fig. 4, B–E), unexpectedly, the in-frame deletion of this fragment did not preclude the binding of the rest of the CLASP2 γ protein (CLASP2- Δ M mutant) to the MT tips (Fig. 5, A and B). In fact,

the COOH-terminal region of CLASP2, containing the CLIP-binding domain, could also weakly target MT tips, suggesting that CLIPs can recruit CLASP to the growing MT ends. We have used a dominant negative CLIP-170 mutant, overexpression of which removes endogenous CLIPs, but not EB1 and EB3 from the MT tips (Fig. 5 C; Komarova et al., 2002), to determine if the binding of different CLASP mutants to MT ends is CLIP dependent. We found that GFP-CLASP2-ΔM mutant depended on the presence of CLIPs for the association with MT ends, whereas GFP-CLASP2-M did not (Fig. 5, D–I). It is possible that the interaction with EB1/EB3, which occurs in addition to binding directly to MTs, increases the affinity of CLASPs for the growing MT ends and contributes to the specific CLASP accumulation at these sites.

Next, we examined if CLASPs can recruit EB1 to MTs and found, that indeed, overexpressed CLASP1 α and

Figure 5. Dependence of CLASP2 deletion mutants on CLIP-170 for their localization to the MT tips and EB1 recruitment to the MTs. (A and B) COS-7 cells were transfected with GFP-CLASP2- Δ M and stained for CLIP-170. (C) Schematic representation of the structure of CLIP-170 and the dominant negative construct, used in this study. (D–F) COS-7 cells were cotransfected with GFP-CLASP2- Δ M and the dominant negative CLIP-170, and stained for EB1 and the endogenous CLIP-170, using the antibody against its NH₂ terminus. The cells, expressing the dominant negative CLIP-170 construct, can be recognized by the diffuse pattern of endogenous CLIP-170 staining. (G–I) COS-7 cells were cotransfected with GFP-CLASP2-M and the dominant negative CLIP-170, and stained for EB1, the endogenous CLIP-170 (using the antibody against its NH₂ terminus) and the dominant negative CLIP-170 (using the antibody against its COOH terminus). (J–L) COS-7 cells were transfected with GFP-CLASP2 γ (J) and stained for CLIP-170 (K) and EB1 (L). (M–O) COS-7 cells were transfected with GFP-CLASP2- Δ C (M) and stained for CLIP-170 (N) and EB1 (O). Enlarged portions of the boxed areas are shown in the insets. Bars, 10 μ m.



CLASP2 γ induced strong accumulation of EB1 along the MTs (Fig. 5, J and L; not depicted). In these conditions, CLIP-170 was also accumulated on the MT bundles (Akhmanova et al., 2001; Fig. 5 K and not depicted). However, EB1 recruitment was CLIP independent, because it was also observed with the CLASP2- Δ C mutant, which cannot bind to CLIPs and, when present at high levels, actually displaced CLIP-170 from the MTs (Fig. 5, M–O). CLASP2- Δ M mutant did not accumulate efficiently along the MTs and did not influence EB1 localization (unpublished data). Although we cannot exclude that CLASPs cause accumulation of EB1 at MT bundles by modifying the structure of the MT lattice, the EB1 recruitment is most likely due to direct CLASP–EB1 interaction.

CLASP2 COOH-terminal domain is responsible for targeting to the cell cortex and the Golgi complex

The observation that MT ends of control HeLa cells localized in the close proximity of the cell margin raised a possibility that they come in contact with the cell cortex. To sup-

port this idea, we used total internal reflection fluorescence (TIRF) microscopy, which visualizes only a very narrow region (~ 200 nm) at the bottom of the cell. Indeed, in live cells, transfected with either GFP-CLASP1 α or GFP-CLASP2 γ , the accumulation of these proteins at the distal MT ends at the cell periphery was readily observed by TIRF, indicating that they are very close to the substrate (Fig. 6, A and B). In control cells, expressing GFP- α -tubulin or EB3-GFP (a plus-end marker, similar to EB1-GFP; Stepanova et al., 2003), a large proportion of the MT ends at the cell margin was visualized by TIRF (Fig. 6, C and E; Video 4, available at <http://www.jcb.org/cgi/content/full/jcb.200405094/DC1>), again suggesting their proximity to the cortical region under the cell. In striking contrast, CLASP1+2 siRNA-treated cells displayed only a few peripheral MT ends, visible by TIRF microscopy (Fig. 6, D and F; Video 4), indicating that most of the MT tips at the cell margin are not touching the underlying cortex. Therefore, we conclude that CLASPs bring peripheral MT segments in close contact with the cortex underneath the cell.

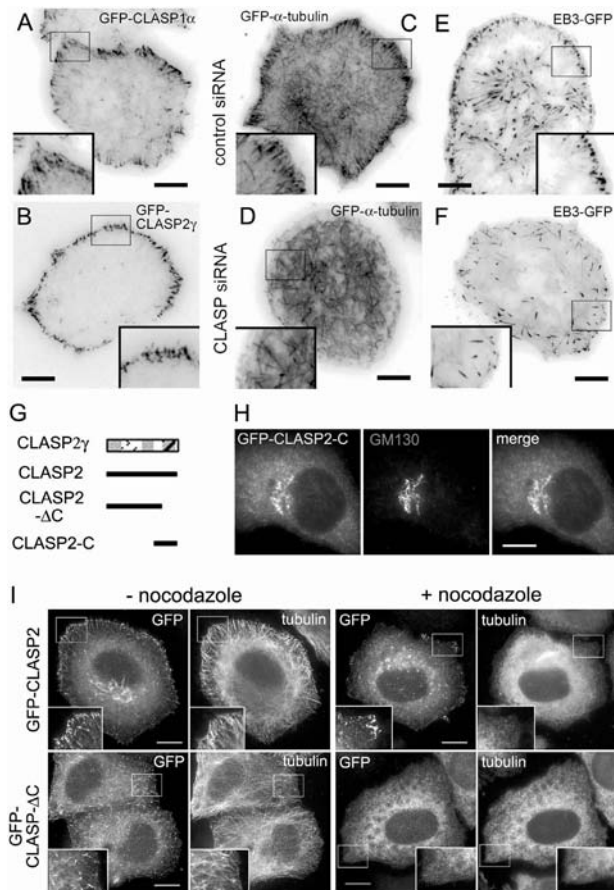


Figure 6. The COOH-terminal domain of CLASP2 is responsible for association with the cell cortex and Golgi complex. (A–F) TIRF microscopy images of live HeLa cells, expressing GFP-CLASP1 α (A), GFP-CLASP2 γ (B), GFP- α -tubulin (C and D), or EB3-GFP (E and F). Cells were either not treated with siRNAs (A and B), or treated for 72 h with control (C and E) or CLASP1+2#B siRNAs (D and F). The contrast is inverted. Bars, 10 μ m. (G) Schematic representation of CLASP2 γ and the relevant deletion mutants. (H) HeLa cells were transfected with GFP-CLASP2-C and stained for the Golgi marker GM130. Bar, 10 μ m. (I) HeLa cells were transfected with GFP-CLASP2 or GFP-CLASP2- Δ C and were either fixed directly or treated with 10 μ M nocodazole for 1 h before fixation and stained for α -tubulin. Bars, 10 μ m.

These observations prompted us to investigate which CLASP2 domains are responsible for cortical and/or membrane targeting. Deletion analysis demonstrated that the COOH-terminal portion of CLASP2 alone was sufficient to target GFP to the Golgi, whereas the GFP-CLASP2- Δ C mutant, lacking the COOH-terminal 278 aa, was unable to accumulate at the Golgi (Fig. 6, G and H; not depicted). To investigate the cortical localization of CLASP2 deletion mutants, we made use of the fact that the peripheral accumulation of the full-length CLASP1 and 2 was partially maintained after the MTs were depolymerized with nocodazole (Fig. 6 I and not depicted). This MT-independent localization was not observed with GFP-CLASP2- Δ C mutant, indicating, that, similar to the Golgi localization, it depends on the COOH-terminal domain of CLASP2. It should be noted that our previous studies identified the COOH-terminal \sim 280 aa of CLASP2 as the CLIP-binding region (Akhmanova et al., 2001). However, CLIPs are not present at the Golgi and do not accumulate at the cell cortex in MT-independent manner (unpublished data), suggesting that

association of CLASP2 with these structures is not dependent on CLIPs.

Both the EB1-binding and the COOH-terminal domains of CLASP2 are required to rescue the organization of the MT network after CLASP knockdown

We have established that the middle (EB1-binding) and COOH-terminal domains of CLASP2 target the protein to the MT plus ends and the cell cortex, respectively. To clarify, which CLASP domains are critical to stabilize MTs at the cell edge, we have performed rescue experiments using GFP fusions of the full-length CLASP1 and 2 or CLASP2 deletion mutants (Fig. 7, A–D, G, and H). We have examined the ratio between the MT and GFP signal, to determine, which proteins can restore MT density at low expression levels (Fig. 7 H). From these experiments, it became clear that both full-length CLASPs could restore MT density more efficiently than the CLASP2 deletion mutants CLASP2- Δ C or - Δ M, which lack ei-

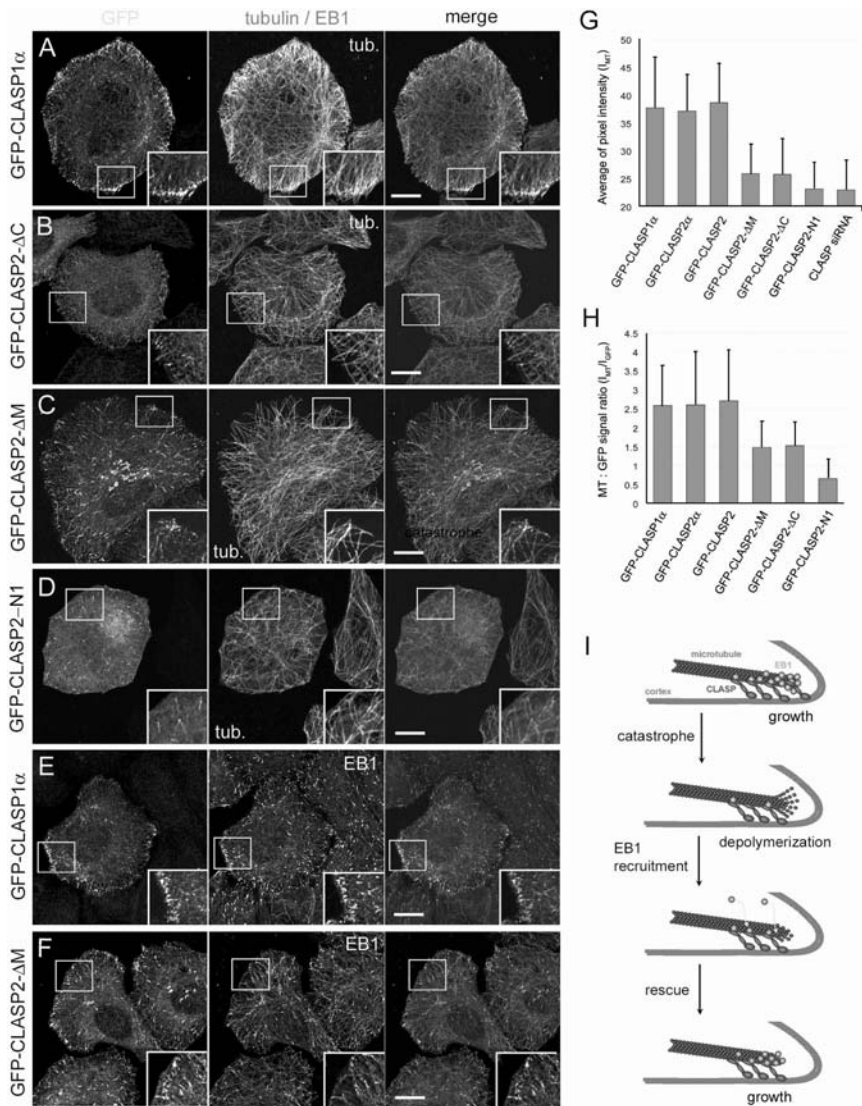


Figure 7. Rescue of CLASP knockdown with CLASP2 deletion mutants and a model for CLASP action at the cell cortex. (A–F) HeLa cells, depleted for CLASPs as described in Fig. 3 A, were transfected with different rescue constructs (indicated on the left), fixed with methanol and stained for α -tubulin (A–D) or EB1 (E and F). Cell images were collected with the confocal microscope (1- μ m-thick optical sections). GFP (green) and tubulin/EB1 (red) signals are superimposed on the right. Enlarged portions of the boxed areas are shown in the insets. Bars, 10 μ m. (G) Average of pixel intensity of α -tubulin staining (\sim 10 cells per construct). (H) Ratio of the average pixel intensity of MT fluorescence (I_{MT}) to the integrated intensity of GFP fluorescence (I_{GFP} ; \sim 10 cells per construct). (I) Proposed model of CLASP rescue activity at the cell cortex. CLASPs can interact with the plus end of a growing MT directly and/or through the association with EB1 and the same time make contact with the cell cortex. After the MT undergoes a catastrophe, most of the EB1 proteins are lost from the tip, but CLASPs remain associated with the cortex and the peripheral stretches of the depolymerizing MT. By enhancing the affinity of EB1–MT interaction at these sites, CLASPs help to retain and/or recruit EB1 to such MTs, leading to their rescue. The oscillations of EB1 signals at the cortical MT tips in control cells support this idea [with strong EB1 accumulation corresponding to growth episodes, and weak EB1 accumulation observed during pausing/depolymerization events]. Error bars represent the SD.

ther the COOH-terminal or the EB1-binding motif. A shorter deletion mutant, CLASP2-N1, displayed no rescue activity in this assay (Fig. 7 G), and was used as a negative control in this experiment. It should be noted that these deletion mutants associated with MT tips in CLASP1 + 2 siRNA-treated cells as efficiently as in control cells, suggesting that they do not depend on heterodimerization with endogenous CLASPs for their plus-end localization (although due to the partial character of the knockdown, we cannot fully rule out this possibility). In addition, full-length CLASPs, but not the CLASP2- Δ C or - Δ M deletion mutants were able to rescue the characteristic enrichment of the EB1-positive tips at the cell margin (Fig. 7, E and F; not depicted). These results indicate that both the EB1-binding and the cortex-binding COOH-terminal domains of CLASP2 are needed to stabilize MT ends at the cell periphery.

Discussion

In this study, we have used an RNAi approach to reduce the levels of CLASP1 and CLASP2 in HeLa cells. The specificity of the used siRNAs is supported by the fact that two different oligonucleotides for each CLASP produced similar effects on the MT network, which were not observed with control siRNAs. Moreover, significant defects in MT density and stability were only observed when combinations of siRNAs, specific for the two CLASPs, were transfected into cells simultaneously. The phenotype, caused by CLASP1/2-specific siRNAs could be rescued by introducing into cells CLASP1 or 2 expression constructs, insensitive to the used siRNA duplexes. These data indicate that the observed defects were due to reduction of the CLASP1/2 expression, rather than the off target activities of the used siRNAs.

HeLa cells express CLASP1 α and CLASP2 α isoforms, which are \sim 77% similar in their protein sequence. Our data, based on the antibody staining, expression of GFP fusion proteins, RNAi-mediated phenotypes and their rescues, indicate that these two CLASPs display very similar localizations and functions in interphase cells. These observations do not rule out, however, that in the context of the whole organism these proteins may have some unique and specific functions. The depletion of CLASPs in our system was only partial, and it is likely that additional and more severe phenotypes would be observed after a complete loss of both CLASPs. Also, we cannot exclude that a complete inactivation of one of the two CLASPs would have different effects compared with the \sim 70% inactivation of both, although our results have provided no indication for such a possibility.

Our previous study, based on the analysis of tubulin modifications, has shown that CLASPs are involved in locally stabilizing MTs at the leading edge of motile fibroblasts (Akmanova et al., 2001). Our new findings fully support the role of CLASPs in stabilizing MTs, by showing that the MT density and the amount of acetylated tubulin are reduced after CLASP knockdown. Detailed analysis of MT behavior shows that CLASPs strongly affect MT plus-end dynamics locally, in the 1- μ m-broad region at the cell margin. This is in line with the accumulation of CLASP proteins at the distal segments of MTs

specifically in this region of the cell cortex. In the presence of CLASPs, MTs at the cell edge remain dynamic, but keep undergoing alternating frequent rescues and catastrophes. MT pausing, apparently stimulated by CLASPs, might in fact be not a truly nondynamic state, but rather very short alternating growth and shrinking episodes, with amplitudes below the resolution of the fluorescent microscope. We propose that the main activity of CLASPs is MT rescue at the cell edge, which reduces the number of long depolymerization episodes and increases MT longevity. It is possible, that interaction with EB1 is mechanistically important for the CLASP rescue activity by stimulating a switch to the growth phase, because EB proteins promote MT growth (Tirnauer et al., 2002; Busch and Brunner, 2004). The capacity of CLASPs to enhance EB1 accumulation at the MTs is fully in line with this idea, which is also supported by the recent findings showing the essential role of EB1 for generation of stable interphase MTs (Wen et al., 2004). The importance of CLASP-EB interaction is underscored by a recently published report, showing that the *Drosophila* CLASP homologue, Orbit/MAST is present among the proteins, pulled down by GST-EB1 (Rogers et al., 2004). We propose that CLASPs, associated with the distal segments of MTs at the cell cortex, are partially retained on MTs when they start shrinking and can rescue MTs by enhancing their affinity for EB1 (Fig. 7 I).

CLASP-dependent rescues are quickly followed by catastrophes, which we believe to be caused by the cell edge acting as an impermeable boundary (Janson et al., 2003). If our assumption is correct, how can we explain that the MTs, rescued by CLASP, do not make a turn and start to grow along the cell edge, as observed after the CLASP1/2 knockdown? We propose that CLASPs, bound to the growing MT tip and at the same time associated with the cell cortex, bring the MT end in very close proximity to the cell edge. An abrupt MT turning at this point would require a considerable distortion of the MT lattice, which would be energetically unfavorable; therefore, a catastrophe occurs instead. Catastrophes at the cell edge may also be caused by MT-destabilizing factors, such as depolymerizing kinesins or stathmin, and we cannot rule out that there is a functional interplay between CLASPs and such MT-destabilizing proteins.

The effect of CLASPs on MT rescue is local, whereas the transition frequencies in the internal cytoplasm are not significantly affected. Therefore, CLASP function is different from that of CLIPs, which affect MT rescue frequency throughout the cell (Komarova et al., 2002). It is possible that CLIP-CLASP interaction can contribute for the CLASP rescue activity. However, we cannot exclude that the interaction with CLIPs regulates CLASP accumulation at the MT tips, as opposed to other cellular structures, such as the cortex or the Golgi apparatus, whereas the effect of CLASPs on MT dynamics is CLIP independent.

The rescue activity of CLASPs is likely to be relevant to the mitotic function of these proteins. CLASPs/Orbit/MAST are present at the kinetochores, and their inactivation results in monopolar spindles with chromosomes buried in the interior of the aster (Maiato et al., 2002, 2003a). If CLASPs exhibit a local MT rescue activity at the kinetochore, similar to that shown

by us at the cell cortex, this would explain why in the absence of CLASPs/Orbit/MAST the kinetochore fibers are unable to regrow, once they start shortening, causing the chromosomes to be "reeled in" to the pole (Maiato et al., 2002, 2003a).

We have observed very few depolymerizing minus ends either in control or in CLASP knockdown cells (unpublished data), indicating, that in HeLa cells MT renewal is accounted for by plus-end dynamics and that CLASPs do not play a significant role in stabilizing MT minus ends. However, the striking effect of CLASP depletion on MT density indicates, that in addition to regulating plus-end dynamics, CLASPs might play a role in MT nucleation.

Recent studies have identified two other large +TIPs, spectraplakins ACF7 and APC, as MT-stabilizing proteins, which, similar to CLASPs, act the leading edge of motile cells (Kodama et al., 2003; Wen et al., 2004). Similar to CLASPs, APC also binds to EB1 and is negatively regulated by GSK3 β (Su et al., 1995; Zumbunn et al., 2001). ACF7 might be an EB1-binding protein, too, because its *Drosophila* homologue, Short stop, interacts with the fly homologue of EB1 (Subramanian et al., 2003). CLASPs and APC can bind the cell cortex (this study; Mimori-Kiyosue and Tsukita, 2001), and ACF7 can directly associate with actin filaments (Kodama et al., 2003), suggesting that these proteins can link MTs to these structures. Studies of MT organization at the muscle-tendon junction in fly larvae indicate that Short stop and APC are acting together (Subramanian et al., 2003). No similar data are available for their mammalian counterparts, so the analysis of a potential functional synergism or redundancy between CLASPs, APC, and the spectraplakins presents an important challenge for future studies.

Materials and methods

Cell lines and transfection of plasmids and siRNAs

HeLa, COS-1, and COS-7 cells were grown as described previously (Akhmanova et al., 2001). Effectene or Superfect transfection reagents (QIAGEN) were used for plasmid transfection. Mass transfection of COS-1 cells was performed by DEAE-dextran method (Akhmanova et al., 2001). Stable clones were selected in the presence of 0.3–0.4 mg/ml G418 (Calbiochem). Synthetic siRNAs (Prologis) were transfected, using Oligofectamine (Invitrogen). siRNAs were directed against the following target sites: CLASP1#A, GCCATTATGCCAATCTATCT; CLASP1#B, GGATGATTACAAGACTGG; CLASP2#A, GTTCAGAAAGCCCTGTATG; CLASP2#B, GACATACATGGGCTCTTAGA; control (scrambled CLASP1#A), GCACTCATTATGACTCCAT. 7–10% confluent HeLa cells were transfected, using Oligofectamine (Invitrogen) with siRNAs at the minimal effective concentration (10 nM for CLASP1#A and CLASP1#B, 200 nM for CLASP2#A and CLASP2#B), whereas the control siRNA was used at 200 nM concentration.

Expression constructs

We used the previously described expression vectors for GFP-CLASP1 α , GFP-CLASP2 γ , GFP-CLASP2 (Akhmanova et al., 2001), EB1-GFP, EB3-GFP (Stepanova et al., 2003), and GFP- α -tubulin (CLONTECH Laboratories, Inc.). GFP-CLASP2 α was constructed in pEGFP-C1 by linking the 5' portion of the human truncated EST clone 7k43h10.x1 (IMAGE:3478506) to the nucleotides 194–5614 of the KIAA0627 cDNA. All CLASP2 deletion mutants were derived from the GFP-CLASP2 construct, using restriction sites (Fig. 4 A), with the exception of CLASP2-C, M1 and M2, which were generated by PCR, as well as CLASP1 deletion mutants. Dominant negative CLIP-170 construct, used in this study, contained nucleotides 2871–4597 of the rat brain CLIP-170 cDNA (GenBank/EMBL/DBL accession no. AJ237670). CLASP1/2 rescue constructs were prepared by a PCR-based strategy, by introducing five silent substitutions in the target site of CLASP1#A siRNA (resulting in a sequence GCTATCATGCCTACCATT)

and six silent substitutions in the target site of CLASP2#A siRNA (resulting in a sequence GTCCAAAGGCTCTCGAC). GFP was substituted for mRFP (gift of R. Tsien, University of California, San Diego, La Jolla, CA; Campbell et al., 2002) to generate red fluorescent fusions.

Protein purification, in vitro binding assays, immunoprecipitation, and Western blotting

To produce HIS-tagged proteins, GFP (derived from pEGFP-C1; CLONTECH Laboratories, Inc.) or GFP-CLASP2-M fragment of CLASP2 were subcloned into pET-28a, expressed in Rosetta (DE3) plys *E. coli* and purified using Ni-NTA agarose (QIAGEN). GST-tagged fusions of mouse EB1 (GenBank/EMBL/DBL accession no. NM_007896) and human EB3 (Stepanova et al., 2003) were produced in BL21 *E. coli* and purified using glutathione-Sepharose 4B (Amersham Biosciences). GST pull-down assays, immunoprecipitations and Western blotting were performed as described previously (Akhmanova et al., 2001). To estimate the degree of protein knockdown after RNAi, the signals in experimental lanes were compared with serial dilutions of the control extract, present on the same Western blot. MT pelleting assays were performed using the MT-associated protein spin-down assay kit (Cytoskeleton, Inc.).

Antibodies and immunofluorescent staining

Rabbit antibodies against CLASP1 (#402 and #2292) and EB1 were raised as described previously (Akhmanova et al., 2001), using GST fusions of the mouse CLASP1 COOH terminus (GenBank/EMBL/DBL accession no. AJ288061) and the mouse full-length EB1. We used mouse mAbs against EB1 and p150^{Glued} (Transduction Laboratories), α - and β -tubulin and acetylated tubulin (Sigma-Aldrich), actin (CHEMICON International, Inc.); rat mAb against α -tubulin (YL1/2; Abcam), rabbit pAbs against GFP (MBL; CHEMICON International Inc., and Abcam), CLASP2 (Akhmanova et al., 2001) and CLIP-170 (Coquelle et al., 2002), EB3 (Stepanova et al., 2003) and chicken pAb against GFP (CHEMICON International, Inc.). For secondary antibodies, Cy2-conjugated anti-mouse IgG and anti-rabbit IgG pAbs, Texas red-conjugated anti-mouse IgG, anti-rat IgG, and anti-rabbit IgG pAb, Cy5-conjugated anti-mouse IgG, anti-rat IgG, and anti-rabbit IgG pAbs were purchased from Jackson ImmunoResearch Laboratories. Fresh medium was added to cells ~2 h before fixation. Cell fixation and staining were performed as described previously (Mimori-Kiyosue et al., 2000).

Fluorescence microscopy and image analysis

Images of cells were collected with a DeltaVision optical sectioning system using PlanApo 100 \times /1.40 NA oil, PlanApo 60 \times /1.40 NA oil ph3 or UPlanApo 20 \times /0.70 NA dry objectives (Olympus), using a cooled CCD camera (Series300 CH350; Photometrics). Fluorescence signals were visualized using a quad filter set (86000; Chroma Technology Corp.) for multiple color imaging, or Endow GFP bandpass emission filter set (41017; Chroma Technology Corp.) for GFP imaging. The out-of-focus signals were removed using the deconvolution technique with the DeltaVision system. Confocal imaging was performed using LSM510 confocal laser scanning microscope (v. 2.3; Carl Zeiss Microimaging, Inc.). TIRF microscopy was performed on an Olympus IX70 (PlanApo 100 \times /1.45 NA, oil TIRFM objective), equipped with a 488-nm argon laser line (MELLES GRIOU), an objective-type TIRF illuminator (Olympus), and an OrcaER cooled CCD camera (Hamamatsu Photonics). The system was controlled by Aquacosmos software (Hamamatsu Photonics). The quantification and analysis of fluorescent signals was performed using MetaMorph software (Universal Imaging Corp.). Images were prepared for publication using Photoshop (Adobe). Statistical analysis was performed using with a SigmaPlot (SPSS Inc.) and Statistica for Windows (StatSoft Inc.). Unless stated differently, the statistical significance of the observed differences was evaluated using Kolmogorov-Smirnov two-sample test and in all plots SD is indicated. For FACS analysis, suspended cells were fixed in cold ethanol, labeled with anti-CLASP1/2 antibodies and Cy5-conjugated secondary antibody, and analyzed using FACSCalibur (Becton Dickinson).

Online supplemental material

Fig. S1 demonstrates the changes in distribution of +TIPs after CLASP knockdown. Fig. S2 illustrates the effect of CLASP knockdown on the retrograde flow. The videos show (Video 1) the behavior of GFP-CLASP1 in interphase cells; (Videos 2 and 3) time-lapse series of control, CLASP1+2 siRNA-treated and mRFP-CLASP2-rescued cells, depicting the dynamics of MTs and EB1-GFP, and (Video 4) the behavior of EB3-GFP in the control or CLASP1+2 siRNA cells observed with TIRF microscopy. Online supplemental material is available at <http://www.jcb.org/cgi/content/full/jcb.200405094/DC1>.

We are grateful to Dr. H. Yamauchi for continuous encouragement, to M. Nihimura for excellent assistance with FACS analysis, to S. Dekker for preparing purified GFP protein, to Y. Komarova for fruitful discussions, and to Dr. R. Tsien for providing mRFP.

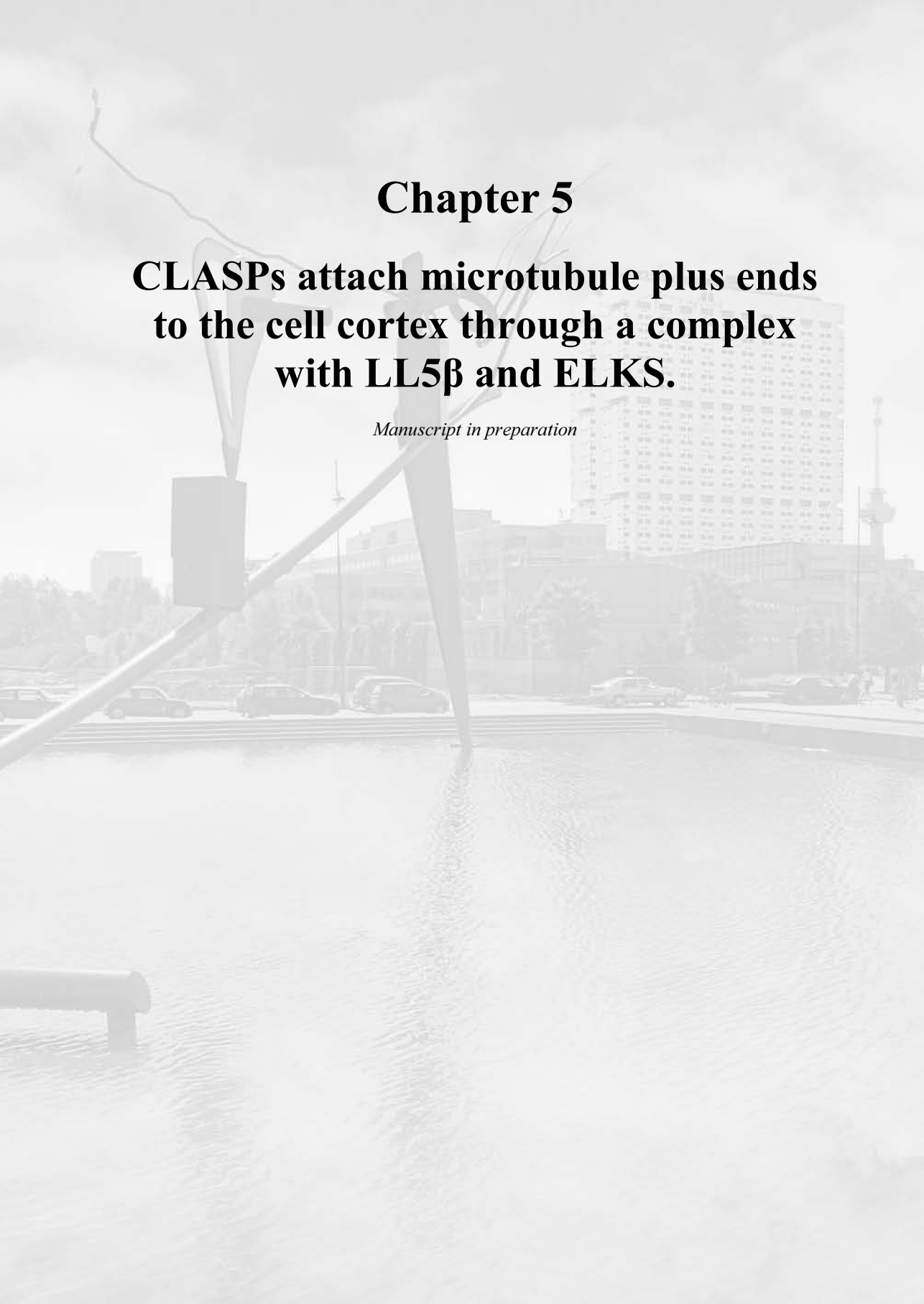
This study was supported by Russian Foundation for Basic Research, grant 02-04-48839 to I. Vorobiev, and by the Netherlands Organization for Scientific Research and Dutch Cancer Society grants to A. Akhmanova and N. Galjart.

Submitted: 20 May 2004

Accepted: 10 November 2004

References

- Akhmanova, A., C.C. Hoogenraad, K. Drabek, T. Stepanova, B. Dortland, T. Verkerk, W. Vermeulen, B.M. Burgering, C.I. De Zeeuw, F. Grosveld, and N. Galjart. 2001. Clasps are CLIP-115 and -170 associating proteins involved in the regional regulation of microtubule dynamics in motile fibroblasts. *Cell*. 104:923–935.
- Bulinski, J.C., and G.G. Gundersen. 1991. Stabilization of post-translational modification of microtubules during cellular morphogenesis. *Bioessays*. 13:285–293.
- Busch, K.E., and D. Brunner. 2004. The microtubule plus end-tracking proteins mal3p and tip1p cooperate for cell-end targeting of interphase microtubules. *Curr. Biol.* 14:548–559.
- Campbell, R.E., O. Tour, A.E. Palmer, P.A. Steinbach, G.S. Baird, D.A. Zacharias, and R.Y. Tsien. 2002. A monomeric red fluorescent protein. *Proc. Natl. Acad. Sci. USA*. 99:7877–7882.
- Carvalho, P., J.S. Tirnauer, and D. Pellman. 2003. Surfing on microtubule ends. *Trends Cell Biol.* 13:229–237.
- Coquelle, F.M., M. Caspi, F.P. Cordelieres, J.P. Dompierre, D.L. Dujardin, C. Koifman, P. Martin, C.C. Hoogenraad, A. Akhmanova, N. Galjart, et al. 2002. LIS1, CLIP-170's key to the dynein/dynactin pathway. *Mol. Cell Biol.* 22:3089–3102.
- Desai, A., and T.J. Mitchison. 1997. Microtubule polymerization dynamics. *Annu. Rev. Cell Dev. Biol.* 13:83–117.
- Gonczy, P., C. Echeverri, K. Oegema, A. Coulson, S.J. Jones, R.R. Copley, J. Duperon, J. Oegema, M. Brehm, E. Cassin, et al. 2000. Functional genomic analysis of cell division in *C. elegans* using RNAi of genes on chromosome III. *Nature*. 408:331–336.
- Howard, J., and A.A. Hyman. 2003. Dynamics and mechanics of the microtubule plus end. *Nature*. 422:753–758.
- Inoue, Y.H., M. do Carmo Avides, M. Shiraki, P. Deak, M. Yamaguchi, Y. Nishimoto, A. Matsukage, and D.M. Glover. 2000. Orbit, a novel microtubule-associated protein essential for mitosis in *Drosophila melanogaster*. *J. Cell Biol.* 149:153–166.
- Inoue, Y.H., M.S. Savoian, T. Suzuki, E. Mathe, M.T. Yamamoto, and D.M. Glover. 2004. Mutations in *orbit/mast* reveal that the central spindle is comprised of two microtubule populations, those that initiate cleavage and those that propagate furrow ingression. *J. Cell Biol.* 166:49–60.
- Janson, M.E., M.E. de Dood, and M. Dogterom. 2003. Dynamic instability of microtubules is regulated by force. *J. Cell Biol.* 161:1029–1034.
- Kodama, A., I. Karakesisoglou, E. Wong, A. Vaezi, and E. Fuchs. 2003. ACF7: an essential integrator of microtubule dynamics. *Cell*. 115:343–354.
- Komarova, Y.A., A.S. Akhmanova, S. Kojima, N. Galjart, and G.G. Borisov. 2002. Cytoplasmic linker proteins promote microtubule rescue in vivo. *J. Cell Biol.* 159:589–599.
- Lemos, C.L., P. Sampaio, H. Maiato, M. Costa, L.V. Omel'yanchuk, V. Liberal, and C.E. Sunkel. 2000. Mast, a conserved microtubule-associated protein required for bipolar mitotic spindle organization. *EMBO J.* 19:3668–3682.
- Maiato, H., P. Sampaio, C.L. Lemos, J. Findlay, M. Carmena, W.C. Earnshaw, and C.E. Sunkel. 2002. MAST/Orbit has a role in microtubule-kinetochore attachment and is essential for chromosome alignment and maintenance of spindle bipolarity. *J. Cell Biol.* 157:749–760.
- Maiato, H., E.A. Fairley, C.L. Rieder, J.R. Swedlow, C.E. Sunkel, and W.C. Earnshaw. 2003a. Human CLASP1 is an outer kinetochore component that regulates spindle microtubule dynamics. *Cell*. 113:891–904.
- Maiato, H., C.L. Rieder, W.C. Earnshaw, and C.E. Sunkel. 2003b. How do kinetochores CLASP dynamic microtubules? *Cell Cycle*. 2:511–514.
- Mathe, E., Y.H. Inoue, W. Palframan, G. Brown, and D.M. Glover. 2003. Orbit/Mast, the CLASP orthologue of *Drosophila*, is required for asymmetric stem cell and cystocyte divisions and development of the polarised microtubule network that interconnects oocyte and nurse cells during oogenesis. *Development*. 130:901–915.
- Mimori-Kiyosue, Y., and S. Tsukita. 2001. Where is APC going? *J. Cell Biol.* 154:1105–1109.
- Mimori-Kiyosue, Y., and S. Tsukita. 2003. "Search-and-capture" of microtubules through plus-end-binding proteins (+TIPs). *J. Biochem. (Tokyo)*. 134:321–326.
- Mimori-Kiyosue, Y., N. Shiina, and S. Tsukita. 2000. The dynamic behavior of the APC-binding protein EB1 on the distal ends of microtubules. *Curr. Biol.* 10:865–868.
- Pasqualone, D., and T.C. Huffaker. 1994. STU1, a suppressor of a β -tubulin mutation, encodes a novel and essential component of the yeast mitotic spindle. *J. Cell Biol.* 127:1973–1984.
- Rogers, S.L., U. Wiedemann, U. Hacker, C. Turck, and R.D. Vale. 2004. *Drosophila* RhoGEF2 associates with microtubule plus ends in an EB1-dependent manner. *Curr. Biol.* 14:1827–1833.
- Schuyler, S.C., and D. Pellman. 2001. Microtubule "plus-end-tracking proteins": the end is just the beginning. *Cell*. 105:421–424.
- Shelden, E., and P. Wadsworth. 1993. Observation and quantification of individual microtubule behavior in vivo: microtubule dynamics are cell-type specific. *J. Cell Biol.* 120:935–945.
- Stepanova, T., J. Slemmer, C.C. Hoogenraad, G. Lansbergen, B. Dortland, C.I. De Zeeuw, F. Grosveld, G. van Cappellen, A. Akhmanova, and N. Galjart. 2003. Visualization of microtubule growth in cultured neurons via the use of EB3-GFP (end-binding protein 3-green fluorescent protein). *J. Neurosci.* 23:2655–2664.
- Su, L.K., M. Burrell, D.E. Hill, J. Gyuris, R. Brent, R. Wiltshire, J. Trent, B. Vogelstein, and K.W. Kinzler. 1995. APC binds to the novel protein EB1. *Cancer Res.* 55:2972–2977.
- Subramanian, A., A. Prokop, M. Yamamoto, K. Sugimura, T. Uemura, J. Betschinger, J.A. Knoblich, and T. Volk. 2003. Shortstop recruits EB1/APC1 and promotes microtubule assembly at the muscle-tendon junction. *Curr. Biol.* 13:1086–1095.
- Tirnauer, J.S., S. Grego, E.D. Salmon, and T.J. Mitchison. 2002. EB1-microtubule interactions in *Xenopus* egg extracts: role of EB1 in microtubule stabilization and mechanisms of targeting to microtubules. *Mol. Biol. Cell*. 13:3614–3626.
- Vorobjev, I.A., V.I. Rodionov, I.V. Maly, and G.G. Borisov. 1999. Contribution of plus and minus end pathways to microtubule turnover. *J. Cell Sci.* 112:2277–2289.
- Wen, Y., C.H. Eng, J. Schmoranz, N. Cabrera-Poch, E.J. Morris, M. Chen, B.J. Wallar, A.S. Alberts, and G.G. Gundersen. 2004. EB1 and APC bind to mDia to stabilize microtubules downstream of Rho and promote cell migration. *Nat. Cell Biol.* 6:820–830.
- Yin, H., L. You, D. Pasqualone, K.M. Kopski, and T.C. Huffaker. 2002. Stu1p is physically associated with beta-tubulin and is required for structural integrity of the mitotic spindle. *Mol. Biol. Cell*. 13:1881–1892.
- Zumbrunn, J., K. Kinoshita, A.A. Hyman, and I.S. Nathke. 2001. Binding of the adenomatous polyposis coli protein to microtubules increases microtubule stability and is regulated by GSK3 beta phosphorylation. *Curr. Biol.* 11:44–49.



Chapter 5

CLASPs attach microtubule plus ends to the cell cortex through a complex with LL5 β and ELKS.

Manuscript in preparation

CLASPs attach microtubule plus ends to the cell cortex through a complex with LL5 β and ELKS.

**Gideon Lansbergen^{1*}, Ilya Grigoriev^{1*}, Yuko Mimori-Kiyosue²,
Jeroen Demmers³, Toshihisa Ohtsuka^{2,4}, Niels Galjart¹, Frank Grosveld¹
and Anna Akhmanova^{1#}.**

¹MGC Department of Cell Biology and Genetics, Erasmus Medical Center, 3000 DR Rotterdam, The Netherlands.

²KAN Research Institute, Kyoto Research Park, Shimogyo-ku, Kyoto 600-8815, Japan.

³MGC Department of Biochemistry, Erasmus Medical Center, 3000 DR Rotterdam, The Netherlands.

⁴Department of Clinical and Molecular Pathology, Toyama Medical and Pharmaceutical University, Sugitani 2630 Toyama, Japan.

* These authors contributed equally to this paper.

Abstract

CLASP1 and CLASP2 are mammalian microtubule-stabilising proteins, which can mediate the interaction between distal microtubule ends and the cell cortex. Using pull down assays coupled to mass spectrometry, we have identified two novel partners of CLASP1 and CLASP2, LL5 β and ELKS. LL5 β and ELKS form a cortical complex, which is often adjacent to, but does not overlap with focal adhesions. This complex colocalises with CLASPs at the cortical regions of HeLa cells, as well as at the leading edge of motile 3T3 fibroblasts. Both LL5 β and ELKS are required for cortical CLASP accumulation and normal microtubule organisation in HeLa cells. LL5 β is a phosphatidylinositol-3,4,5-triphosphate (PIP3)-binding protein, and the recruitment of LL5 β to the cell cortex is influenced by PI3 kinase activity, but does not require intact microtubules. We propose that LL5 β and ELKS can form a PIP3-regulated cortical platform, to which CLASPs attach distal microtubule ends.

Introduction

Microtubule networks are highly dynamic structures, which can rapidly alter their shape during cell motility and morphogenesis. Microtubule organisation strongly depends on the interaction of the microtubule plus ends with the actin cytoskeleton and cortical cell regions. In mammalian interphase cells microtubule plus ends usually face the cell periphery and can be linked to the cortex by different plus end tracking proteins (+TIPs), including dynein and dynactin, CLIP-170 in a complex with IQGAP1 and Rac1/Cdc42, APC acting in concert with a number of cortical factors, spectraplakins, or CLASPs (Akhmanova and Hoogenraad, 2005; Carvalho et al., 2003; Galjart and Perez, 2003; Howard and Hyman, 2003; Schuyler and Pellman, 2001).

CLASPs are evolutionary conserved proteins, which play an essential role in cell division in fungi, insects and mammals (for review, see Galjart, 2005; Maiato et al., 2003). In addition, in interphase cells CLASPs are involved in forming polarised microtubule arrays (Akhmanova et al., 2001; Mathe et al., 2003; Wittmann and Waterman-Storer, 2005). CLASPs can bind directly to microtubules, as well as to the members of two other +TIP families, the CLIPs and the EB proteins (Akhmanova et al., 2001; Mathe et al., 2003; Mimori-Kiyosue et al., 2005). Although the mechanism of plus end tracking by CLASPs is still obscure, these interactions are likely to contribute to CLASP localisation to the plus ends. Unlike many other +TIPs, which bind to all growing microtubule ends throughout the cell, CLASPs associate with microtubules in a spatially regulated manner. In migrating fibroblasts, CLASPs specifically bind to the microtubule tips of at the leading, but not at the trailing edge, and contribute to microtubule stabilisation (Akhmanova et al., 2001). In motile epithelial cells, CLASPs also preferentially bind to microtubules at the leading edges; however, in this case they decorate not only the tips, but also long stretches of the microtubule lattice (Wittmann and Waterman-Storer, 2005). In both systems GSK3 β appears to be a key regulator of the CLASP affinity for microtubules (Akhmanova et al., 2001; Wittmann and Waterman-Storer, 2005). In fibroblasts PI3 kinase activity is also important for the polarised CLASP distribution (Akhmanova et al., 2001), in agreement with the fact that PI3 kinase acts upstream of GSK3 β in different systems (Doble and Woodgett, 2003).

Studies in HeLa cells have demonstrated that CLASPs can attach dynamic microtubule plus ends to certain cortical regions, and stabilise them by repeatedly rescuing them from depolymerisation (Mimori-Kiyosue et al., 2005). In this way the density of the microtubule arrays linked to particular areas of the cell cortex can be increased. Here we identified LL5 β (Paranavitane et al., 2003) and ELKS (also known as CAST2, Rab6IP2 or ERC1; (Deguchi-Tawarada et al., 2004; Monier et al., 2002; Nakata et al., 1999; Wang et al., 2002)) as the components of the molecular link between CLASP-bound microtubule tips and the cell cortex. LL5 β is a phosphatidylinositol-3,4,5-triphosphate-binding protein

(PIP3)-binding protein (Paranavitane et al., 2003). Our study, therefore, provides a new connection between PI3 kinase activity and microtubule stabilisation by CLASPs.

Results

Identification of LL5 β and ELKS as CLASP binding partners

To identify novel binding partners of CLASP2 in HeLa cells we have used pull down assays combined with mass spectrometry. We generated a construct, encoding biotinylation- and green fluorescent protein (GFP)-tagged CLASP2 α (bio-GFP-CLASP2 α) and transiently co-expressed it in HeLa cells together with the protein-biotin ligase BirA. In these conditions, subcellular localisation of bio-GFP-CLASP2 α was very similar to that of GFP-CLASP2 α and of endogenous CLASP2 (data not shown). Bio-GFP-CLASP2 α was efficiently biotinylated by BirA, as confirmed by Western blots probed with labelled streptavidin (data not shown).

Next, biotinylated proteins from cells expressing bio-GFP-CLASP2 α together with BirA or BirA alone were isolated using streptavidin beads and analysed on a Coomassie-stained gel (Fig.1a), by Western blotting (Fig.1b) and by mass spectrometry. In addition to background proteins, which were present in both lanes, we observed in the bio-GFP-CLASP2 α pull down lane a strong band at ~190 kDa, which was identified as GFP-CLASP2 α (Fig.1b and data not shown). It should be noted that endogenous CLASP2 and CLASP1 were not co-purified with the tagged CLASP2 α (Fig.1b), suggesting that these proteins do not homo- or heteromultimerise or occur as very stable multimers, formed co-translationally. A band of ~170 kDa, present specifically in the bio-GFP-CLASP2 α lane was identified as CLIP-170, a known CLASP binding partner (Akhmanova et al., 2001) (Fig.1b). In addition, mass spectrometry analysis of the whole bio-GFP-CLASP2 α lane revealed two proteins, which were not present in BirA-only control – LL5 β (Paranavitane et al., 2003) and ELKS (Deguchi-Tawarada et al., 2004; Monier et al., 2002; Nakata et al., 1999; Wang et al., 2002) (Table 1). The validity of mass spectrometry results was confirmed by Western blotting with LL5 β - and ELKS-specific antibodies (Fig.1b). We also generated bio-GFP fusions of LL5 β and ELKS and used them for streptavidin pull down assays. Bio-GFP-tagged overexpressed LL5 β and ELKS efficiently pulled down endogenous ELKS and LL5 β , respectively; they also precipitated CLASP1 and 2, but not CLIP-170 or α -tubulin (Fig.1c). It should be noted that ELKS has several splice isoforms, including the neuronal ELKS α and the ubiquitously expressed ELKS ϵ , which differ in their C-terminal regions (Nakata et al., 2002). LL5 β and CLASPs were co-precipitated with both isoforms (Fig.1c and data not shown), indicating that the interaction with LL5 β and CLASPs does not depend on the ELKS C-terminal tail.

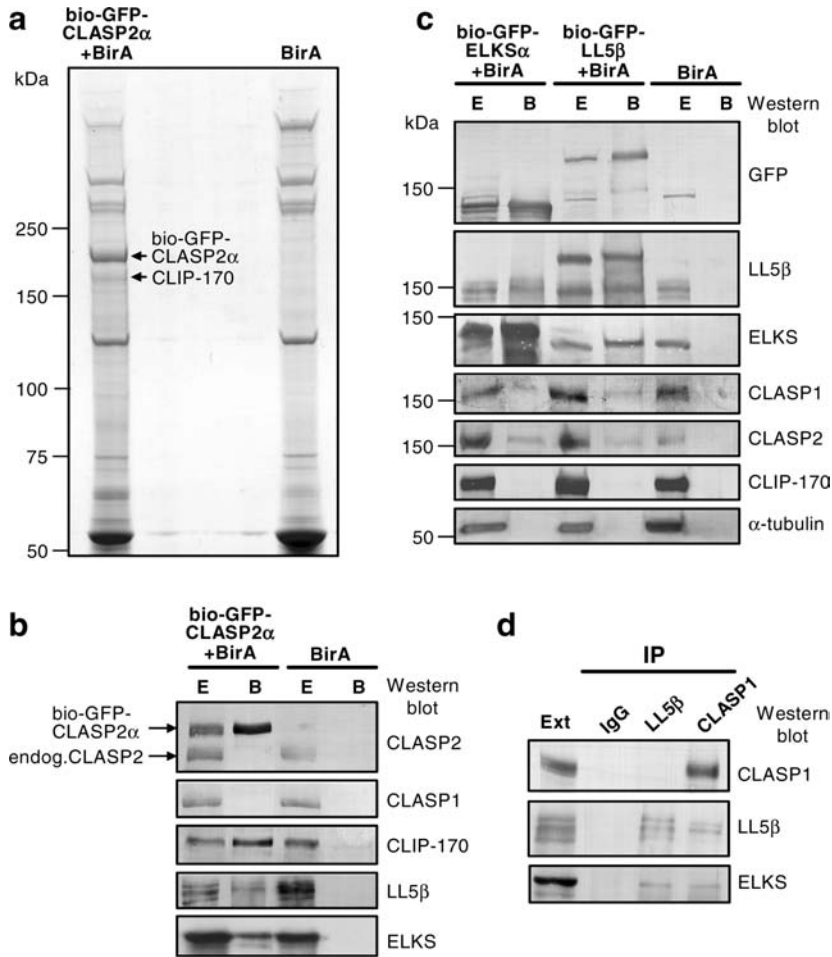


Figure 1. Identification of LL5β and ELKS as CLASP binding partners.

a-c. Streptavidin pull down assays were performed with lysates of HeLa cells, co-expressing bio-GFP-CLASP2α together with BirA, bio-GFP-ELKSα together with BirA, bio-GFP-LL5β together with BirA or BirA alone. Proteins, bound to streptavidin beads were analysed on a Coomassie-stained gel (a) or by Western blotting with the indicated antibodies. In panel (a) only the fraction, bound to the beads, was loaded. In panels (b) and (c) the extract before the pull down (lanes marked “E”) and proteins, bound to the beads (lanes marked “B”) are shown. Lanes marked “E” correspond to 25% of the extract, used to obtain lanes marked “B”.

d. Immunoprecipitations from extracts of untransfected HeLa cells with the indicated antibodies. Lane marked “Ext” shows 5% of the input. In the experiments shown in this figure, rabbit antibodies against LL5β and ELKS were used.

Endogenous ELKS (corresponding to the “long” ELKS isoforms δ and/or ϵ , (Nakata et al., 2002; Ohara-Imaizumi et al., 2005)) and LL5 β co-precipitated with the endogenous CLASP1 from HeLa cell extracts (Fig.1d). ELKS was also present in LL5 β immunoprecipitates; however, CLASPs did not co-purify with endogenous LL5 β (Fig.1d), probably because the LL5 β antibody, used in this experiment, was directed against the CLASP-interacting region of LL5 β , M2 (see below), and hindered the LL5 β -CLASP interaction. Taken together, CLASPs, LL5 β and ELKS appear to form a complex in HeLa cells. CLIP-170, another known CLASP partner, is not present in this complex.

Table 1. Mass Spectrometry results for Bio-GFP-CLASP2 α

Identified proteins	Molecular weight (D)	NCBI GI number	Mascot Score	Identified Peptides
CLIP-associating protein 2, CLASP2	145046	7513045	1115	20
Restin, microtubule-vesicle linker CLIP-170	161632	420071	580	12
LL5 beta protein	142071	27650425	267	5
ELKS (Rab6 interacting protein 2, ERC1, CAST2)	128236	51827892	142	3

The table shows proteins identified in a pull down with streptavidin beads from an extract of HeLa cells co-expressing Bio-GFP-CLASP2 α and biotin ligase BirA. The list is corrected for background proteins, which were identified in a control pull-down from HeLa cells expressing BirA only. For each identified protein, the list is filtered for duplicates and shows only the hits with the highest Mascot score and most identified peptides.

CLASPs and ELKS colocalise with LL5 β and depend on it for their cortical localisation.

We next examined the relative distribution of endogenous CLASPs, LL5 β and ELKS in HeLa cells. Our previous study has shown that in HeLa cells CLASPs are present at the Golgi complex and microtubule plus ends, and are especially abundant at the distal microtubule ends located close to the cell margin (Mimori-Kiyosue et al., 2005). Both LL5 β and ELKS displayed significant overlap with CLASPs at the cell periphery (Fig.2a,b). The accumulation and colocalisation of all these proteins was particularly apparent at the “free” cell edges, where cells did not make contact with other cells. LL5 β and ELKS showed an almost complete colocalisation at the cell edges (Fig.2c). For these immunolocalisation

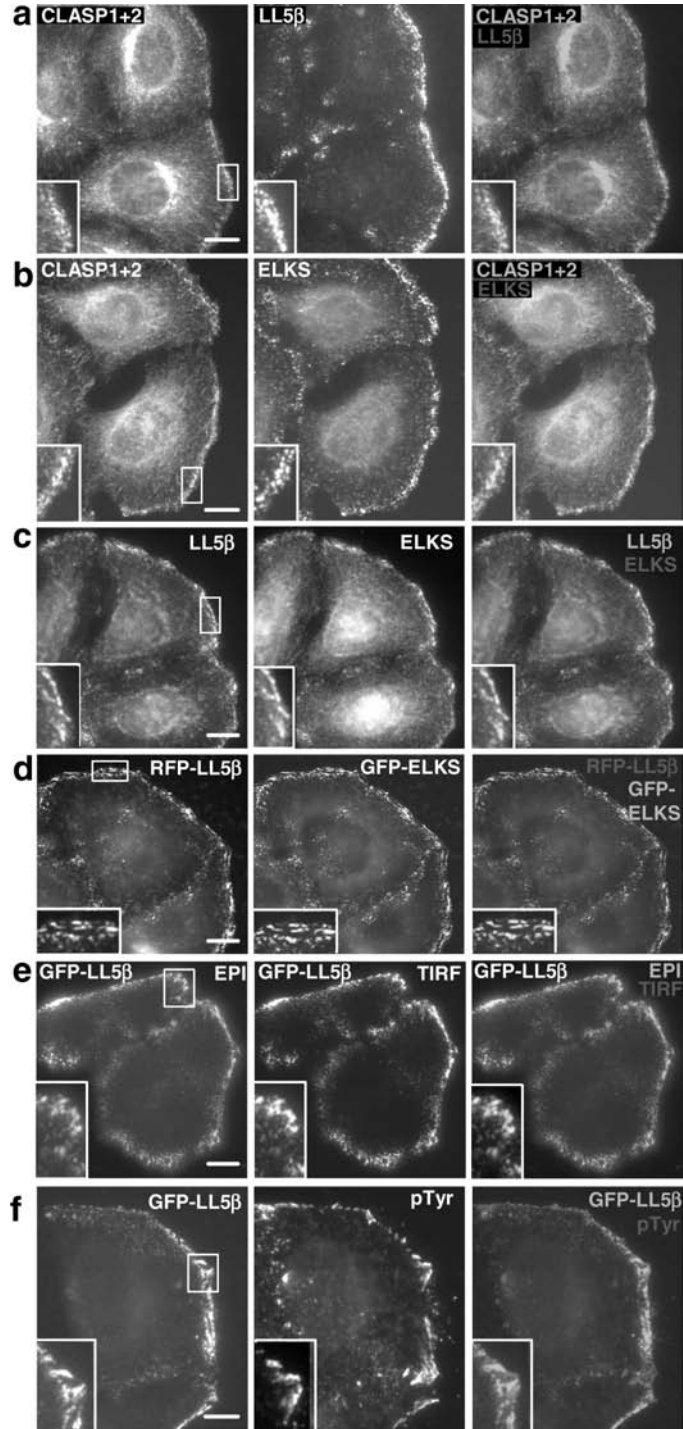
Figure 2. Colocalisation of CLASPs, LL5 β and ELKS at peripheral cortical sites of HeLa cells.

a-c. HeLa cells were fixed with methanol and stained with a mixture of antibodies against CLASP1 and CLASP2 (a, b, green in the overlay), mouse anti-LL5 β antibody (a, red in the overlay); rabbit anti-LL5 β antibody (c, green in the overlay) and mouse anti-ELKS antibody (b,c, red in the overlay).

d. HeLa cells were transfected with RFP-LL5 β (red in the overlay) and GFP-ELKS ϵ (green in the overlay), fixed with PFA and imaged directly.

e. Epifluorescence (EPI, green in the overlay) and TIRF microscopy (red in the overlay) images of live HeLa cells, expressing GFP-LL5 β . Bar, 10 μ m.

f. HeLa cells were transfected with GFP-LL5 β (green in the overlay), fixed with PFA and stained with antibodies against a focal adhesion marker phosphotyrosine (red in the overlay). White rectangles indicate the portion of the figure shown enlarged in the left corner of each panel. Bars, 10 μ m.



experiments we used methanol fixation, which allows an optimal staining with the antibodies against CLASPs, LL5 β and ELKS but may not preserve all cellular components, such as soluble cytosolic proteins. We therefore confirmed the colocalisation of LL5 β and ELKS in paraformaldehyde (PFA)-fixed cells, co-expressing the red fluorescent protein (RFP) and GFP-tagged versions of the two proteins (Fig.2d). The correspondence of the staining pattern and the *in vivo* distribution of CLASPs was established previously (Mimori-Kiyosue et al., 2005).

Live cell imaging of GFP-LL5 β in HeLa cells further confirmed its preferential accumulation at the edges (Fig.2e). Epifluorescence and TIRF microscopy produced very similar pictures (Fig.2e). Since TIRF microscopy visualises ~200 nm at the bottom of the cell, this result indicates that most of the LL5 β -positive structures are confined to the ventral plasma membrane, in agreement with the localisation of CLASP-decorated peripheral microtubule tips near the cortex underneath the cell (Mimori-Kiyosue et al., 2005). LL5 β -ELKS signals never overlapped with focal adhesions but often formed a complementary pattern (Fig.2f), further supporting cortical localisation of LL5 β -ELKS complexes.

To address the hierarchy of interactions between CLASPs, LL5 β and ELKS at the cortex we next knocked down CLASP1, CLASP2, LL5 β and ELKS by RNA interference (RNAi). Western blot analysis showed that we could achieve a ~90% knockdown of CLASP1, LL5 β and ELKS and a ~70% knockdown of CLASP2 (Fig.3a). After partial depletion of the two CLASPs, LL5 β and ELKS still displayed a punctate distribution in the periphery of HeLa cells (Fig.3b,c) and colocalised with each other (data not shown), indicating that LL5 β and ELKS are not dependent on CLASPs for cortical targeting. On the other hand, depletion of LL5 β abolished cortical accumulation of both CLASPs and ELKS. In these conditions, CLASPs were still present at the microtubule plus ends and the Golgi apparatus, but displayed no bright rim of peripheral accumulation (Fig.3d), while ELKS was distributed diffusely in the cytoplasm (Fig.3e). The latter observation was confirmed by transfecting GFP-ELKSe into LL5 β -depleted cells (Fig.3f).

ELKS knockdown also affected the distribution of its partners, albeit less dramatically: CLASP accumulation at the cell edge was reduced (compare Fig.3g with Fig.2b), while LL5 β , still present at the cortex, showed a more diffuse localisation than in control cells (compare Fig.3h with Fig.2c). Some colocalisation of CLASP-positive microtubule tips with the LL5 β puncta was still observed at the periphery of ELKS-depleted cells (Fig.3i), suggesting that ELKS may not be essential for the CLASP-LL5 β interaction. To explore this possibility, we next investigated in more detail which domains of CLASPs and LL5 β interact with each other. Our previous study indicated that CLASPs could bind to the cortex via their C-terminal domain even in the absence of microtubules. Indeed, RFP-CLASP2, but not its deletion mutant RFP-CLASP2- Δ C lacking the 278 C-terminal amino

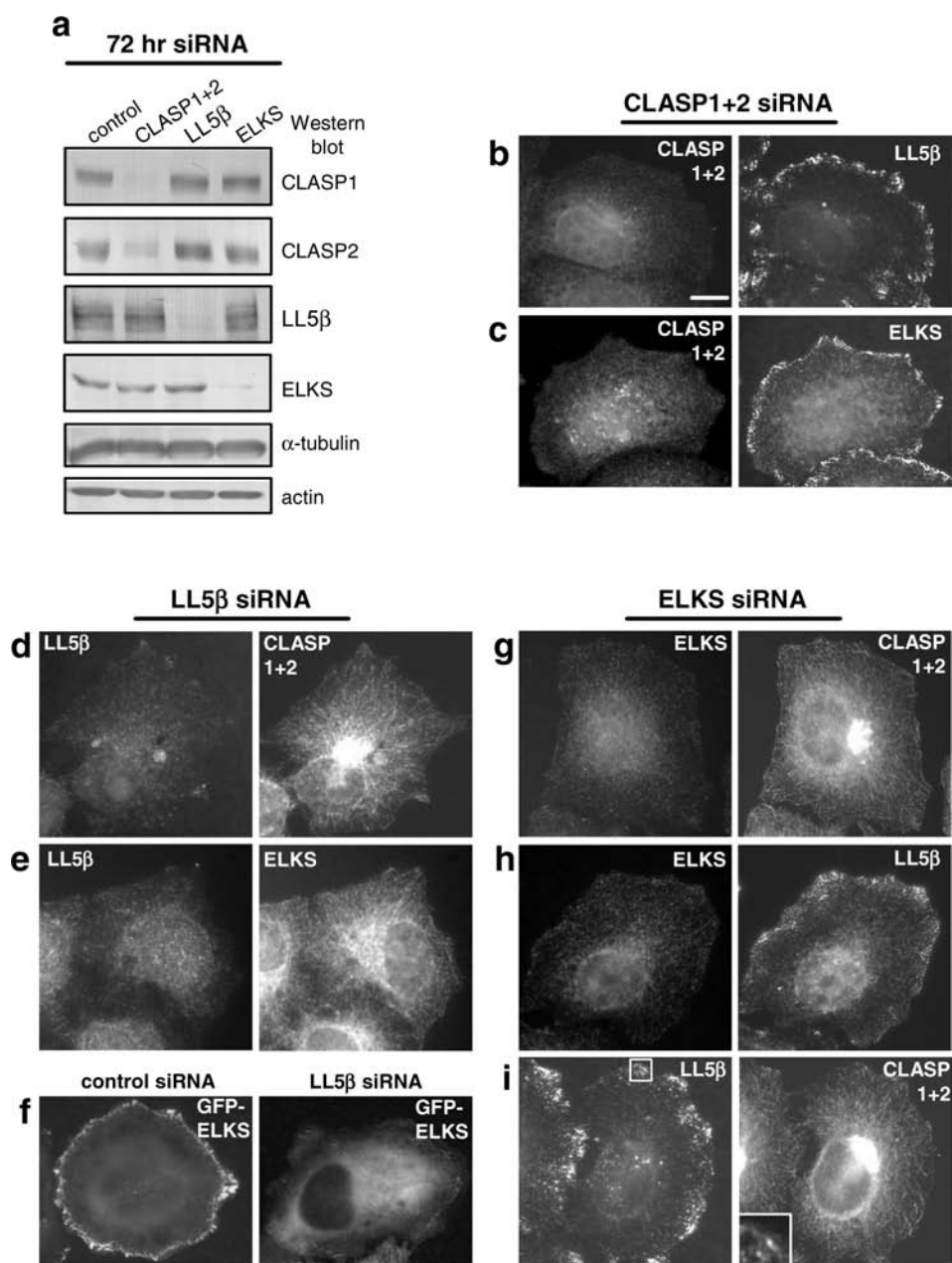


Figure 3. LL5 β and ELKS are required for efficient cortical accumulation of CLASPs in HeLa cells.

a. Western blot analysis of the extracts of HeLa cells cultured for 72 hrs after transfection with the indicated siRNAs.

b-i. HeLa cells were cultured for 72 hrs after transfection with the indicated siRNAs. Cells were fixed with methanol (panels b-e, g-i) and stained with a mixture of antibodies against CLASP1 and CLASP2 (b,c,d,g,i), mouse anti-LL5 β antibodies (b,d,i), rabbit anti-LL5 β antibodies (e,h) and mouse anti-ELKS antibodies (c,e,g,h). In the panel (i) the part of the image, indicated by the white square, is enlarged and shown as an overlay, with CLASP staining in green and LL5 β staining in red. In the panel (f) cells were transfected with GFP-ELKS ϵ 48 hrs after siRNA transfection, fixed with PFA 24 hrs later and imaged directly. Bar, 10 μ m.

acids (Fig.4c), extensively colocalised with GFP-LL5 β at the periphery of HeLa cells, in which microtubules were disassembled by nocodazole (Fig.4a,b). Next, we performed GST pull down assays with LL5 β fragments, purified from bacteria (Fig.4d,e). CLIP-170 N-terminus served as a negative control in this experiment. GFP-CLASP1 α and GFP-CLASP2 α as well as the bacterially purified CLASP1 C-terminus bound specifically to the LL5 β -M2 fragment (Fig.4e), indicating that CLASPs and LL5 β can interact directly through the coiled coil M2 region of LL5 β and the CLASP C-terminus.

Using immunoprecipitation from extracts of cells transfected with GFP-tagged LL5 β deletion mutants, we next investigated which part of LL5 β interacts with ELKS. Since potential multimerisation of LL5 β fragments with the endogenous full length LL5 β could obscure the results of this experiment, we used COS-1 cells, which express very little LL5 β but contain endogenous ELKS and CLASPs (data not shown). While both CLASP1 and CLASP2 co-precipitated with GFP-LL5 β -M2, confirming the results of the GST pull down assays, ELKS co-precipitated with a different, non-overlapping LL5 β fragment M1 (Fig.4f). Therefore, LL5 β interacts with CLASPs and ELKS through different domains. CLASPs and ELKS can probably bind to LL5 β independently of each other, since the depletion of either of these proteins does not prevent the interaction of LL5 β with the other. So far, we have found no evidence for direct interaction between CLASPs and ELKS; however, we cannot exclude that these proteins do make contact in a triple complex with LL5 β .

LL5 β -ELKS complex participates in organising microtubules in HeLa cells

Our previous study demonstrated that CLASPs decorate distal microtubule ends at the cell edge (Mimori-Kiyosue et al., 2005). Since the peripheral CLASP signals overlapped extensively with those of LL5 β and ELKS, it seemed likely that the two latter proteins would colocalise with microtubule ends as well. Indeed, in control cells microtubules or small microtubule bundles often terminated at LL5 β -positive patches (Fig.5a).

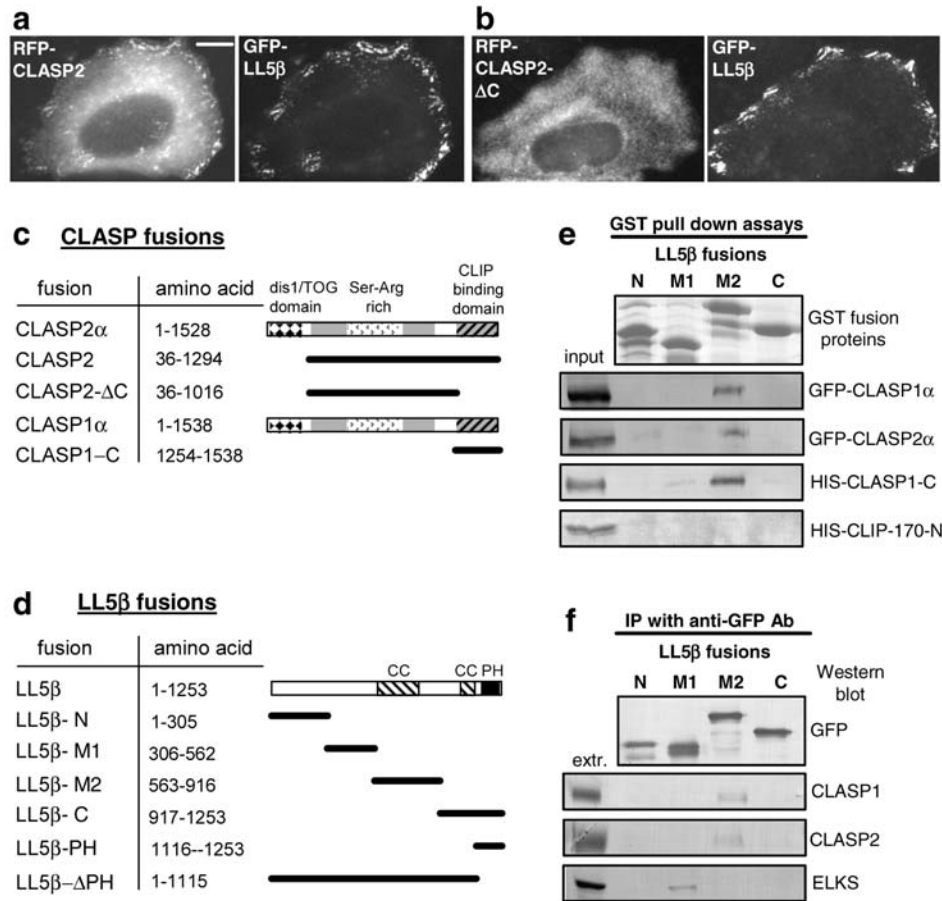


Figure 4. LL5 β binds to CLASPs and ELKS through different domains.

a,b. HeLa cells were co-transfected with GFP-LL5 β together with either RFP-CLASP2 or RFP-CLASP2- Δ C. 24 hrs later cells were treated with 10 μ M nocodazole for 1 hr, PFA-fixed and imaged directly. Bar, 10 μ m. c,d. Schematic representation of the structure of CLASP1, CLASP2, LL5 β and their deletion mutants used in this study. CC- region with heptad repeats (potential coiled coil), PH- pleckstrin homology domain. e. GST pull down assays with the indicated GST fusions. Extracts of COS-1 cells, overexpressing GFP-CLASP1 α or GFP-CLASP2 α or purified HIS-CLASP1-C and HIS-CLIP-170-N were used for binding. Coomassie-stained gel is shown for the GST fusions and Western blots with anti-HIS antibodies for the HIS fusions. 10% of the input and 25% of the material, bound to the beads, were loaded on gel. d. Immunoprecipitations from the extracts of COS-1 cells, transiently expressing the indicated GFP-LL5 β fusions. The precipitates were analysed on Western blots with the indicated antibodies. Extr., 5% of the input.

Simultaneous depletion of the two CLASPs in interphase HeLa cells caused a decrease in microtubule density and a loss of cortically associated microtubule tips at the cell margin, due decreased microtubule rescues at the cell periphery (Mimori-Kiyosue et al., 2005). Since LL5 β and ELKS are required for cortical CLASP accumulation, it seemed likely that their depletion, and concomitant loss of CLASPs from the cell edge would cause an effect, similar to that of CLASP depletion. To quantify the effect of different siRNAs on the microtubule network, we used the intensity of anti-tubulin staining in methanol-fixed cells, which was previously shown to be a reliable measure of microtubule density, since methanol fixation preserves the microtubules, but not the soluble tubulin pool (Mimori-Kiyosue et al., 2005). Microtubule density was diminished in both ELKS and LL5 β knockdown cells (Fig.5b,c). This decrease was less pronounced in the case of ELKS depletion, probably because CLASP-positive tips could still make some contacts with the LL5 β at the cell cortex (Fig.3i). Also the accumulation of microtubule tips at the peripheral ventral cortex, observed by TIRF microscopy in live HeLa cells, expressing GFP- α -tubulin (Mimori-Kiyosue et al., 2005), was clearly reduced in ELKS-depleted cells and often undetectable in LL5 β -depleted cells (Fig.5d). In conclusion, LL5 β and ELKS act in concert with CLASPs to organise microtubule tips at the cortex of HeLa cells.

While LL5 β -ELKS-CLASP complexes are needed for the normal microtubule organisation, microtubules are not strictly required for the cortical accumulation of these proteins (Fig.4a, Fig.5e). Interestingly, microtubule disassembly by nocodazole often caused some redistribution of LL5 β -ELKS puncta to the regions directly surrounding focal adhesions (Fig.5e). This relocation might be attributable to some signalling cascades, associated with the activation of Rho GTPase and enhanced formation of focal adhesions and stress fibres caused by microtubule depolymerisation (Bershadsky et al., 1996; Liu et al., 1998).

Regulation of LL5 β localisation in HeLa cells and Swiss 3T3 fibroblasts by PI3 kinase

Our results demonstrated that LL5 β is essential for recruitment of CLASPs and ELKS to the cell cortex. Previous investigations showed that LL5 β contains a pleckstrin homology (PH) domain which can bind to PIP3 (Paranavitane et al., 2003), raising the possibility that the presence of PIP3 and hence PI3 kinase activity might regulate the distribution of LL5 β and its partners. The deletion of the PH domain of LL5 β abolished its localisation to cortical clusters (Fig.6a); in agreement with previously published data, LL5 β - Δ PH localised to small vesicle-like structures, and not to the cell edge, indicating that the PH domain is important for cortical localisation of LL5 β (Paranavitane et al., 2003). The LL5 β PH domain itself, tagged with GFP, did localise to the plasma membrane of HeLa cells (Fig.6b). However,

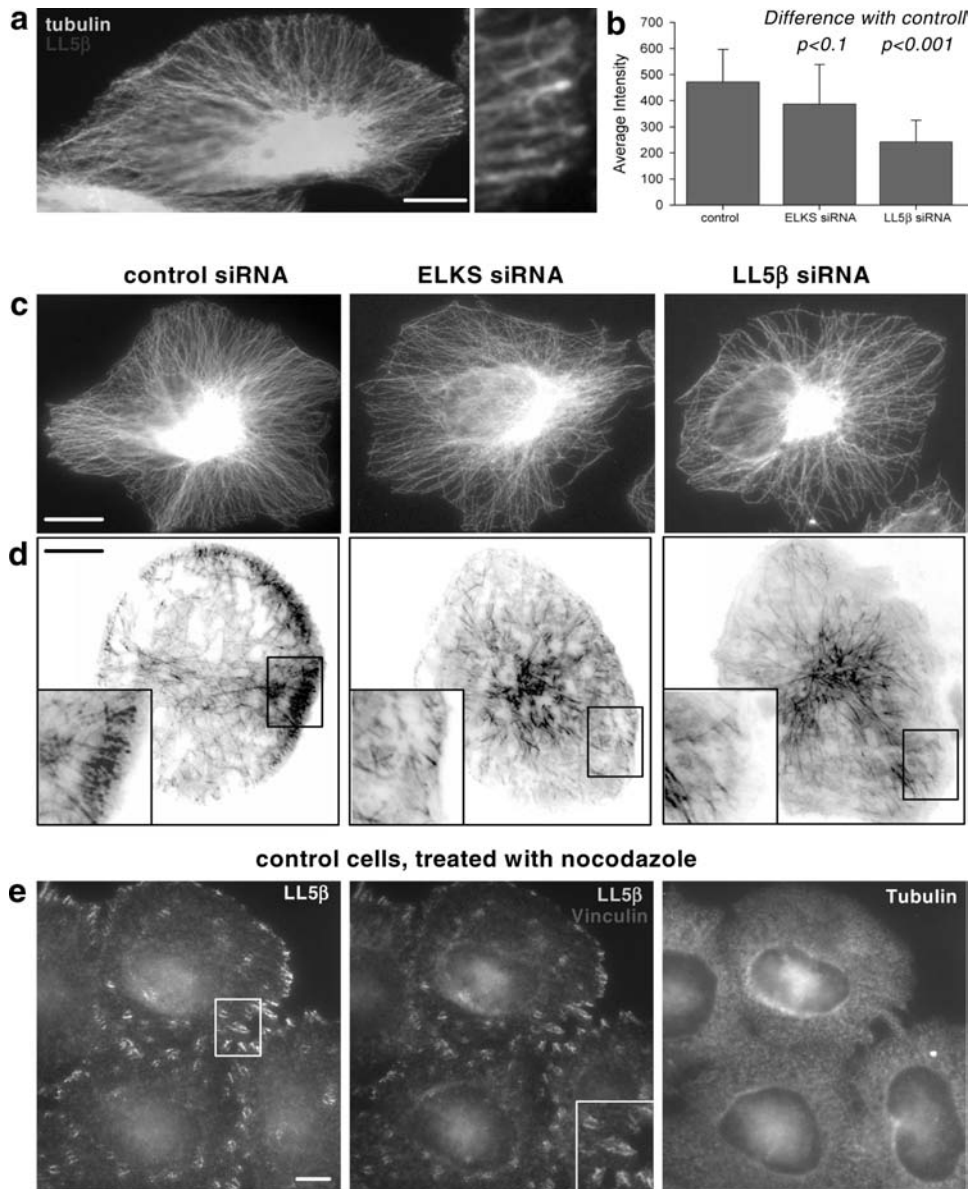


Figure 5. Relationship between LL5 β -ELKS complexes and microtubules in HeLa cells.

- a. HeLa cells, fixed with methanol, were stained with antibodies against α -tubulin and LL5 β . An enlargement of the rightmost cell margin is shown on the right.
- b, c. HeLa cells were cultured for 72 hrs after transfection with the indicated siRNAs, fixed with methanol and stained for α -tubulin. b. Plots of average intensity of the staining within a 5 μm^2 box at 5 μm distance from the cell edge, with subtracting the background. Measurements were performed in 20 cells per siRNA in 3 different cell regions. Standard deviation is shown by whiskers. Statistical analysis was performed using Komogorov-Smirnov two sample test.
- c. Images of individual HeLa cells, treated with the indicated siRNAs.
- d. HeLa cells, stably expressing GFP- α -tubulin, were imaged by TIRF microscopy 72 hrs after transfection with the indicated siRNAs.
- e. HeLa cells were treated with 10 μM nocodazole for 1 hr, fixed with methanol and stained with antibodies against LL5 β (green in the overlay), focal adhesion marker vinculin (red in the overlay) and α -tubulin. Bars, 10 μm .

this fusion protein was not restricted to the ventral cortex, but was abundantly present at all filopodia and sites of intercellular contacts. This distribution was affected by inhibiting PI3 kinase with wortmannin (Fig.6c) or LY294002 (not shown), which caused its redistribution to the nucleus.

We next investigated the distribution of PIP3 using the yellow fluorescent protein (YFP) fusion of the PH domain of Akt as a sensor (Haugh et al., 2000). Also this protein was not restricted to the basal plasma membrane and had a tendency to localise to filopodia (not shown). Ratiometric imaging using CFP as a reference demonstrated that in the ventral membrane PIP3 was most abundant in filopodia and was somewhat enriched in the peripheral cell regions harbouring the CLASP-LL5 β -ELKS complexes (visualised with RFP-CLASP2) (Fig.6d).

The peripheral accumulation of LL5 β -ELKS-CLASP signals was very strongly reduced in serum-starved HeLa cells and could be restored within ~60 min after serum addition (Fig.6e,f). Interestingly, PI3 kinase inhibition with wortmannin during serum addition to serum-starved cells markedly reduced, albeit not abolished LL5 β recruitment to the cell edges (Fig.6e,f,h). LY294002 addition had a milder effect on the serum-induced LL5 β relocalisation to the cell margin, but resulted in a more irregular, patchy pattern of LL5 β distribution (Fig.6e,f). Treatment of serum-grown HeLa cells with PI3 kinase inhibitors diminished, but did not eliminate the cortical band of LL5 β -positive signals (Fig.6g). This conclusion was confirmed by the quantification of the ratio between the LL5 β signals at the cell margin and in the internal cytoplasm (Fig.6i). Taken together, these results suggest that PIP3 is likely to contribute to the proper cortical localisation of LL5 β , but

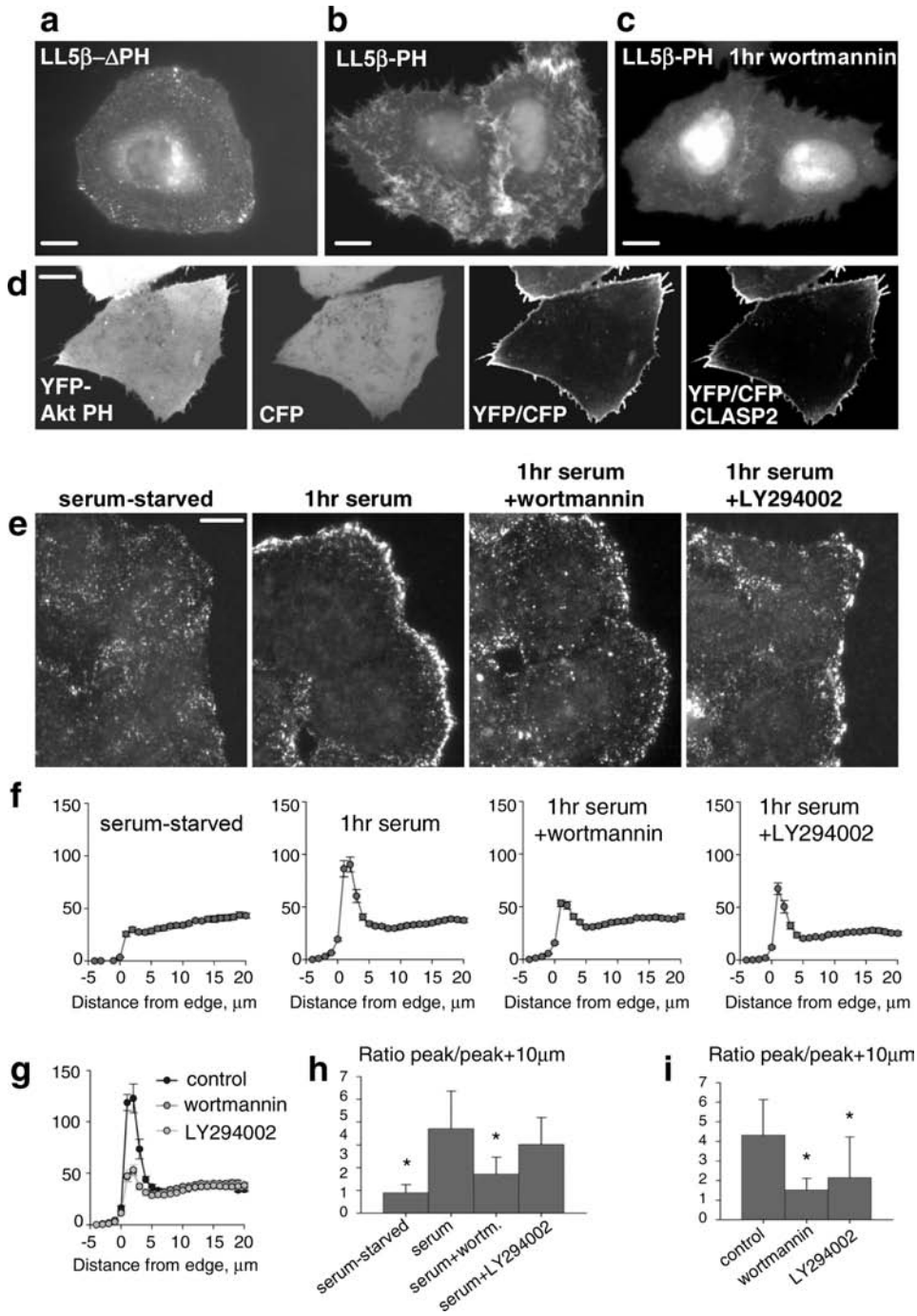


Figure 6. Inhibition of PI3 kinase activity affects the recruitment and maintenance of cortical LL5 β clusters.

a-c. HeLa cells transiently expressing GFP-LL5 β - Δ PH (a) or GFP-LL5 β -PH (b,c) were fixed with PFA and imaged directly. In panel (c) cells were incubated for 1 hr with 100 nM wortmannin before fixation.

d. Confocal images of the basal plasma membrane of HeLa cells, transiently expressing YFP-AktPH, CFP and RFP-CLASP2. In the right two panels the YFP/CFP ratio is shown by shades of grey. RFP-CLASP2 signals are shown in red.

e. HeLa cells were serum-starved for 3 days, and either fixed directly or incubated for 1 hr in medium containing serum and 0.1%DMSO, serum and 100 nM wortmannin or serum and 100 μ M LY294002. Cells were fixed with methanol and stained with the mouse anti-LL5 β antibody.

f. Plots of average intensity of fluorescence of LL5 β staining, performed as described in (e). The average intensity was measured within a 1 μ m² box along the cell radius, with subtracting the background. Measurements were performed in 5 different cell regions in 20 cells per treatment. Whiskers show the standard error of mean.

g. Plots of average intensity of fluorescence of LL5 β staining in control serum-grown cells and in serum-grown cells treated with 100 nM wortmannin or 100 μ M LY294002 for 1 hr. Quantification was performed as in (f).

h,i. Ratio of the peak value of average intensity of LL5 β staining to the average intensity in the internal cytoplasm at a 10 μ m distance from the peak along the same radius. Values, significantly different from those for the serum-stimulated cells (h) or for the control serum-grown cells (i) are indicated by asterisks ($p < 0.001$, Kolmogorov-Smirnov two sample test). Bars, 10 μ m.

additional factors are involved in it. It is possible that the PH domain of LL5 β binds to some other lipids. Alternatively, additional proteins might be involved in the membrane recruitment of LL5 β .

We next investigated if the cortical accumulation of LL5 β -ELKS-CLASP complexes was a peculiarity of HeLa cells. We detected no significant expression of LL5 β or peripheral accumulation of CLASPs in COS-1 or COS-7 cells (data not shown). However, both LL5 β and ELKS were strongly accumulated at the leading edges of Swiss 3T3 fibroblasts, migrating into a monolayer wound (Fig.7a,b). LL5 β and ELKS-positive signals colocalised with each other (Fig.7b) and partially overlapped with CLASP-decorated microtubule ends at the leading edge (Fig.7a). Also in low density cultures LL5 β was strongly enriched at the leading edges of fibroblasts with a characteristic motile shape (Fig.7c). Similar to HeLa cells, the focal adhesions were free of LL5 β label (Fig.7c).

Our previously published data on CLASP2 showed that it bound only weakly to microtubule tips in serum-starved cells, but acquired a highly polarised distribution in response to serum (Akhmanova et al., 2001). In agreement with these data, as well as

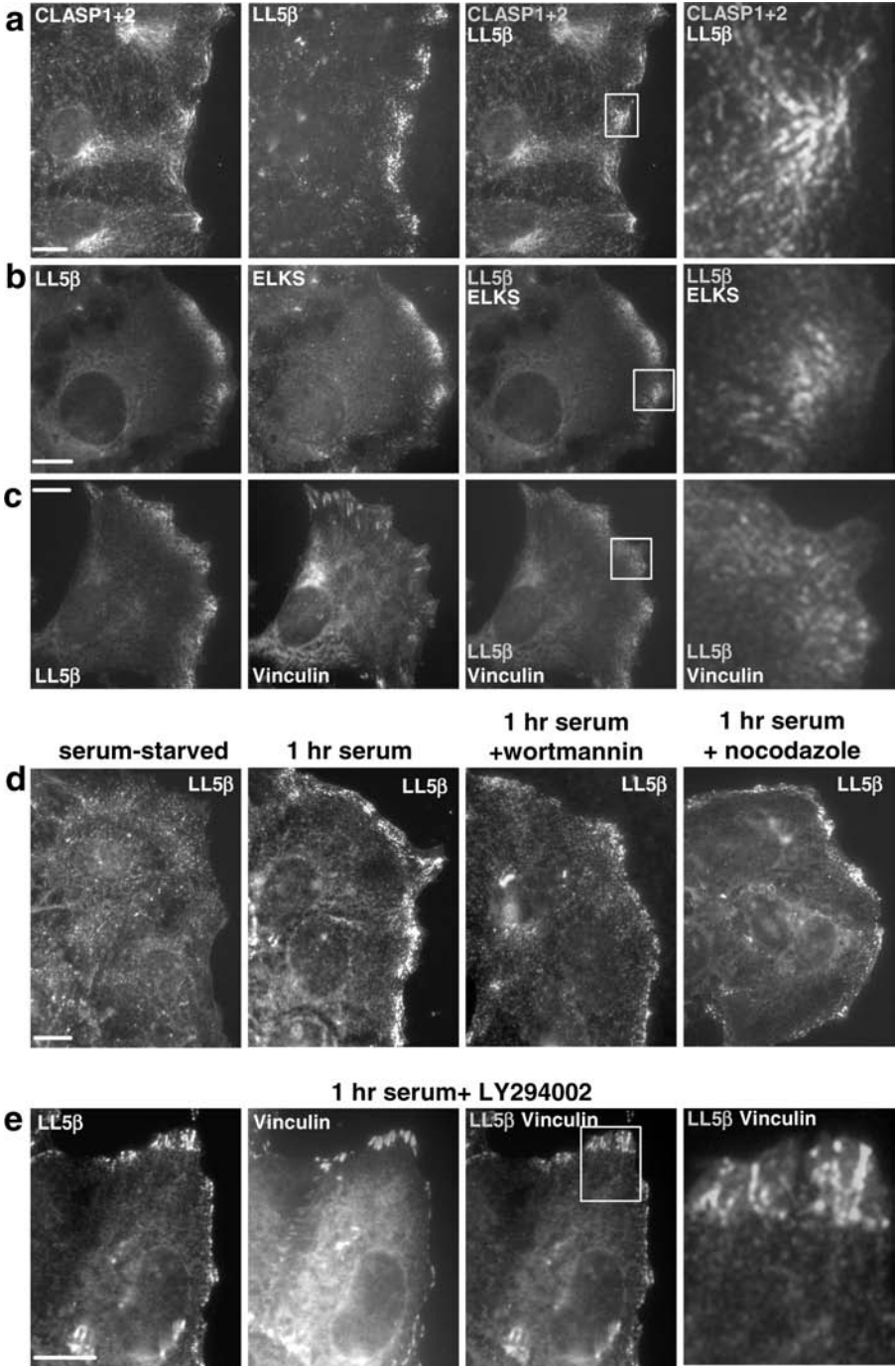


Figure 7. CLASP-LL5 β -ELKS complexes localise to the leading edge in migrating Swiss 3T3 fibroblasts.

- a,b. Swiss 3T3 cells were grown to a monolayer, serum-starved for 2 days and serum stimulated for 1 hour after scratching the monolayer. Cells were fixed with methanol and stained with a mixture of antibodies against CLASP1 and CLASP2 (a, green in the overlay), mouse anti-LL5 β antibody (a, red in the overlay); rabbit anti-LL5 β antibody (b, green in the overlay) and mouse anti-ELKS antibody (b, red in the overlay).
- c. Swiss 3T3 were grown at low density in serum-containing medium, fixed with methanol and stained with a rabbit anti-LL5 β antibody (b, green in the overlay) and mouse anti-vinculin antibody (b, red in the overlay).
- d,e. Swiss 3T3 were grown to a monolayer, serum-starved for 2 days and after scratching the monolayer, were incubated for 1 hour in serum-free medium (serum-starved), in serum-containing medium supplemented with either 0.1%DMSO (1hr serum) or with one of the indicated inhibitors (100 nM wortmannin, 10 μ M nocodazole or 100 μ M LY294002). Cells were fixed with methanol and stained with a rabbit anti-LL5 β antibody (green in the overlay in panel (e)) and mouse anti-vinculin antibody (red in the overlay in panel (e)). White rectangles indicate the portion of the overlay shown enlarged on the right. Bars, 10 μ m.

the LL5 β behaviour in HeLa cells, LL5 β cortical signals were almost undetectable in serum-starved 3T3 fibroblasts (Fig.7d), but were strongly recruited to the leading edge within ~20 minutes after serum addition (Fig.7d). Similar to HeLa cells, this recruitment was partially inhibited by the addition of PI3K inhibitor wortmannin (Fig.7d), and to a lesser extent by LY294002 (Fig.7d,e). The latter reagent induced patches of LL5 β , which often correlated with focal adhesions (Fig.7e). Recruitment of LL5 β to the leading cell edges also occurred in the presence of microtubule-depolymerising drug nocodazole, indicating that intact microtubules are not strictly required for the polarised distribution of LL5 β . Given the fact that CLASPs are needed for microtubule stabilisation at the leading edge of Swiss 3T3 cells (Akhmanova et al., 2001) and that the behaviour of LL5 β -ELKS-CLASP complexes is similar in HeLa and 3T3 cells, it seems likely that these complexes contribute the polarisation of the microtubule network in 3T3 fibroblasts.

Discussion

In this study we have identified a novel link between interphase microtubules and the cell cortex. This link includes CLASPs, well-characterised +TIPs, and LL5 β and ELKS, which have no similarities to microtubule-binding proteins and appear to form a microtubule-independent membrane-bound complex. The data from this paper combined with our previous study (Mimori-Kiyosue et al., 2005) suggest that CLASPs laterally attach distal microtubule ends to LL5 β -ELKS puncta (see model in Fig.8), allowing the microtubule ends to polymerise and depolymerise freely, but restricting their dynamic behaviour to the peripheral cell region. This attachment increases the stability and density of the parts of microtubule network directed to the LL5 β -ELKS-enriched cortical sites.

CLASPs bind directly to LL5 β (and the cell cortex) through their C-terminus, the same domain, which we have previously shown to interact with CLIP-170 (Akhmanova et al., 2001). Although CLIP-170 was the most abundant partner, co-purified with CLASP2, it was not co-precipitated together with LL5 β and ELKS, suggesting that CLASPs participate in the cortical complexes independently of CLIP-170. Similarly, CLASPs bind to the Golgi complex through their C-terminal domain, while CLIP-170 is not present at the Golgi (Mimori-Kiyosue et al., 2005). It seems that the binding partners of the C-terminal domain of CLASPs determine the subcellular site of CLASP activity. Binding to the CLIPs is probably needed to enhance CLASP localisation to the microtubule plus ends and may serve as an attenuator of CLASP interaction with the Golgi and/or the cell cortex.

Membrane targeting of the CLASP-LL5 β -ELKS complex is dependent on LL5 β , since the depletion of this protein leads to the loss of its partners from the cortex. A previous study demonstrated that LL5 β binds to PIP3 (Paranavitan et al., 2003). Our data with PI3K inhibitors support the idea that PIP3 is important for the proper recruitment of LL5 β to the cortex. However, whereas the PIP3-binding PH domain of LL5 β is necessary for its cortical localisation, this domain alone, as well as the PH domain of Akt, an established PIP3 sensor (Haugh et al., 2000), show a much broader membrane localisation in HeLa cells. Therefore, the spatial distribution of LL5 β must be determined by other binding partners or regulatory factors, which are probably dependent on the cell interaction with extracellular matrix, since LL5 β complexes are strongly enriched at the ventral cortex. Interesting in this respect is the frequent clustering of LL5 β around focal adhesions, which is particularly apparent in nocodazole-treated cells. It indicates that focal adhesion-derived signals might play a role in regulating LL5 β recruitment. Existence of a connection with the actin cytoskeleton is also suggested by the binding of LL5 β to γ -filamin, an actin-cross-linking protein (Paranavitan et al., 2003).

LL5 β has two homologues, LL5 α and a more distantly related LL5 γ , which have not been characterised yet (Katoh, 2003; Kishi et al., 2005). Our preliminary data indicate

that LL5 α is expressed in HeLa cells only at a very low level, which might explain the essential role of LL5 β for targeting ELKS and CLASPs to the cortex in this cell type. However, in other cell types the LL5 β homologues may share its functions to organise microtubule arrays.

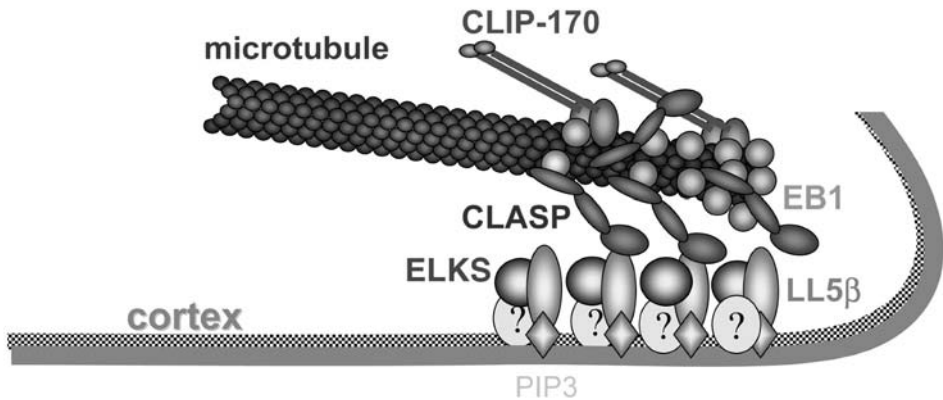


Figure 8. A model for cortical microtubule attachment through CLASPs, LL5 β and ELKS.

CLASPs can interact with the plus end of a growing microtubule directly and/or through the association with EB1 and the same time make contact with the cell cortex through the association with LL5 β . LL5 β clusters at the membrane are formed with the participation of ELKS and are recruited to the membrane by PIP3, as well as other lipid and/or protein partners. As an alternative, CLASPs can form a microtubule tip-bound complex with CLIP-170, which is not involved in LL5 β -mediated membrane attachment.

ELKS, the second component of the identified complex, has no membrane-binding motifs; its structure is composed of domains of heptad repeats (Nakata et al., 1999). ELKS, as well as its brain-specific homologue CAST were identified in numerous studies on protein-protein interactions (Deguchi-Tawarada et al., 2004; Ko et al., 2003; Lu et al., 2005; Monier et al., 2002; Nakata et al., 1999; Ohtsuka et al., 2002; Takao-Rikitsu et al., 2004; Wang et al., 2002), and are likely to play a scaffolding role. In agreement with this idea, depletion of ELKS did not abolish the targeting of LL5 β to the cortex, but prevented it from forming tight peripheral clusters. ELKS depletion also failed to prevent CLASP-LL5 β interaction, and therefore had a milder effect on microtubule density. Since RNAi-mediated depletion is never complete, we cannot exclude that the LL5 β cortical puncta, observed after ELKS knockdown were due to remaining low levels of ELKS. Still, we favour the idea that the role of ELKS in the complex is an accessory one. Such an interpretation is in line with absence of essential function of the only ELKS homologue in worms (Deken et al., 2005).

The potential functions of the microtubule-cortex link described here extend beyond the regulation of microtubule density and stability. Microtubule attachment to certain peripheral sites may be important for organising endo- and exocytosis. Remarkable

in this respect is the recent demonstration of the frequent coincidence of the docking sites of insulin granules with the ELKS clusters at the membrane of insulin-secreting pancreatic β cells (Ohara-Imaizumi et al., 2005). Another potential function is suggested by the enrichment of LL5 β around focal adhesions after microtubule disassembly. This localisation is reminiscent of the enrichment of dynamin, a large GTPase necessary for endocytosis, around focal adhesions after nocodazole washout (Ezratty et al., 2005). Dynamin, as well as targeting by microtubules are required for focal adhesion disassembly (Ezratty et al., 2005; Kaverina et al., 1999), and the capacity of the LL5 β -containing complexes to accumulate around focal adhesions and connect microtubules to the cortex raises the question about the involvement of LL5 β and its partners in focal adhesion dynamics.

A promising avenue of investigation is the potential function of the CLASP- LL5 β -ELKS complex in neurons. CLASPs are present in growth cones and are required for axon guidance (Lee et al., 2004). ELKS and its homologue CAST1 are also enriched in axons, where they constitute an important component of the presynaptic sites, cytomatrix at the active zone (Deguchi-Tawarada et al., 2004; Ohtsuka et al., 2002). LL5 β was so far only identified at post-synaptic sites at the neuromuscular junction, while its neuronal localisation still remains to be elucidated (Kishi et al., 2005). CLASP-LL5 β -ELKS complexes seem to be attractive candidates to mediate microtubule-membrane attachment during neurite morphogenesis and synaptogenesis in developing neurons. Taken together, our data describe a novel component of cytoarchitecture, which could be employed in different cellular and tissue settings.

Materials and Methods

Cell lines and transfection of plasmids and siRNAs

HeLa, COS-1, COS-7 and Swiss 3T3 cells were grown as described previously (Akhmanova et al., 2001). Nocodazole, wortmannin and LY294002 were purchased from Sigma. PolyFect (Qiagen), Lipofectamine 2000 (Invitrogen) or FuGENE 6 (Roche) transfection reagents were used for plasmid transfection. Mass transfection of COS-1 cells was performed by DEAE-dextran method (Akhmanova et al., 2001). The stable HeLa clone, expressing GFP- α -tubulin was cultured in the presence of 0.4 mg/ml G418 (Roche). Synthetic siRNAs were transfected, using Oligofectamine (Invitrogen) at a concentration 100 nM or with HiPerFect (Qiagen) at a concentration 5 nM. Both methods yielded very similar results. SiRNAs against CLASP1 and CLASP2 (CLASP1#B and CLASP2#B), as well as the control oligonucleotide were described previously (Mimori-Kiyosue et al., 2005). siRNA against LL5 β (siRNA 38298, Ambion) was directed against the sequence

GGAGATTTTGGATCATCTA, siRNA against ELKS (siRNA 43397, Ambion) was directed against the sequence GTGGGAAAACCCTTTCAAT.

Expression constructs

The expression vectors for GFP-CLASP1/2 and their deletion mutants were described previously (Akhmanova et al., 2001; Mimori-Kiyosue et al., 2005). GFP- α -tubulin, pECFP and pEGFP vectors were purchased from Clontech. GFP-LL5 β (Paranavitan et al., 2003) was a gift from Dr. L.Stephens (The Babraham Institute, Cambridge, UK). To generate RFP-LL5 β , GFP was substituted for mRFP (a gift of Dr. R.Tsien (UCSD, La Jolla, USA)). GFP-LL5 β deletion mutants were produced by a PCR-based strategy in pEGFP-C2. GFP-ELKS α was described by Deguchi-Tawarada et al., 2004. To generate GFP-ELKS ϵ , mouse ELKS ϵ cDNA was obtained from the total mouse brain RNA by RT-PCR with RNA PCR kit (TAKARA, Japan) and cloned into pCAEGFP vector (Niwa et al., 1991), which was a gift from Dr. M. Takeichi (RIKEN, Kobe, Japan). Biotinylation tags were inserted in GFP-CLASP2 α , GFP-LL5 β , GFP-ELKS α and GFP-ELKS ϵ by cloning at the NheI and AgeI sites in front of the GFP a linker, encoding the amino acid sequence MASGLNDIFEAQKIEWHEGGG. BirA expression construct (pSCT-HA-BirA, (Driegen et al., 2005)) was a gift from Dr. D.Meijer (Erasmus MC, Rotterdam, The Netherlands). YFP-AktPH was a gift from Dr. T.Balla (NICHD, Bethesda, USA). YFP-AktPH and CFP were inserted into the pSV40_Zeo2 (Invitrogen), to express the two genes in the same cell at equal expression levels.

Streptavidin pull down assays, mass spectrometry and analysis of mass spectrometry data

HeLa cells were transiently transfected using Lipofectamine 2000 (Invitrogen) and used for extract preparation ~16 hours later. Cells were washed with PBS and lysed in ice cold buffer containing 100 mM NaCl, 20 mM Tris-HCl, pH 7.5, 1% Triton X-100 and protease inhibitors (Complete; Roche). Cell lysates were centrifuged at 13,000 rpm for 15 minutes at 4°C, and the supernatant was incubated for 45 minutes with Dynabeads M-280 Streptavidin (Dyna). After magnetic separation, the beads were washed three times in a buffer containing 150 mM NaCl, 20 mM Tris-HCl, pH 7.5, 0.1% Triton X-100 and protease inhibitors. Subsequently, the beads were resuspended and boiled in NuPAGE LDS Sample Buffer, containing NuPAGE Reducing Agent (Invitrogen). After magnetic separation, the supernatants were run on a 3-8% NuPAGE Tris-Acetate Gel and stained with the Colloidal Blue Staining Kit (Invitrogen), or analysed on Western blot.

For mass spectrometry, each gel lane was cut into ~30 slices using an automatic gel slicer and subjected to in-gel reduction with dithiothreitol, alkylation with iodoacetamide and digestion with trypsin (Promega, sequencing grade), essentially as described by (Wilm

et al., 1996). NanoLC-MS/MS was performed on a CapLC system (Waters, Manchester, UK) coupled to a Q-ToF Ultima mass spectrometer (Waters, Manchester, UK), operating in positive mode and equipped with a Z-spray source. Peptide mixtures were trapped on a Jupiter™ C18 reversed phase column (Phenomenex; column dimensions 1.5 cm × 100 μm, packed in-house) at a flow rate of 7 μl/min. Peptide separation was performed on Jupiter™ C18 reversed phase column (Phenomenex; column dimensions 15 cm × 50 μm, packed in-house) using a linear gradient from 0 to 80% B (A = 0.1 M acetic acid; B = 80% (v/v) acetonitrile, 0.1 M acetic acid) in 70 min and at a constant flow rate of 200 nl/min using a splitter. The column eluent was directly sprayed into the ESI source of the mass spectrometer. Mass spectra were acquired in continuum mode; fragmentation of the peptides was performed in a data-dependent mode (1 survey scan and three MS/MS channels, MS/MS spectra < 5 sec).

Peak lists were automatically created from raw data files using the ProteinLynx Global Server software (version 2.0). The background subtraction threshold for noise reduction was set to 35% (background polynomial 5). Smoothing (Savitzky-Golay) was performed (number of iterations: 1, smoothing window: 2 channels). Deisotoping and centroiding settings were: minimum peak width: 4 channels, centroid top: 80%, TOF resolution: 5000, NP multiplier: 1. The Mascot search algorithm (version 2.0, MatrixScience, London, UK) was used for searching against the NCBI nr database (release data: 20th April 2005; taxonomy: *H. sapiens*) that was available on the MatrixScience server. The peptide tolerance was typically set to 150 ppm and MS/MS tolerance to 0.2 Da. Only doubly and triply charged peptides were searched for. A maximum number of 1 missed cleavage by trypsin was allowed and carbamidomethylated cysteine and oxidised methionine were set as fixed and variable modifications, respectively. Individual Mascot score cut-off values for each peptide MS/MS spectrum were >35. Peptide MS/MS spectra with individual Mowse scores below 40 were checked manually and either interpreted as valid identifications or discarded.

Protein purification, in vitro binding assays, immunoprecipitation and Western blotting

To produce HIS-tagged CLASP1-C, a mouse CLASP1 cDNA fragment (nucleotides 1-810 of the sequence AJ288061) was cloned into pET-28a, expressed in Rosetta (DE3) pLysS *E. coli* and purified using Ni-NTA agarose (Qiagen). GST-tagged fusions of LL5β fragments were generated using pGEX-3X, produced in BL21 *E. coli* and purified using glutathione-Sepharose 4B (Amersham Biosciences). GST pull-down assays, immunoprecipitations, Western blotting and signal quantifications were performed as described previously (Mimori-Kiyosue et al., 2005).

Antibodies and immunofluorescent staining

Rabbit antibodies against LL5 β were raised as described before (Akhmanova et al., 2001) using purified GST-LL5 β -M2 fusion. We used rabbit polyclonal antibodies against GFP (Abcam), CLASP1 (Mimori-Kiyosue et al., 2005), CLASP2 (Akhmanova et al., 2001), CLIP-170 (Coquelle et al., 2002), ELKS (Deguchi-Tawarada et al., 2004), mouse monoclonal antibodies against LL5 β (a gift from Dr. J. Sanes, Washington University, St. Louis, USA, (Kishi et al., 2005)), actin (Chemicon); phosphotyrosine and vinculin (Sigma) and a rat monoclonal antibody against α -tubulin (YL1/2, Abcam). For secondary antibodies, Alexa 350 and Alexa 594-conjugated goat antibodies against rabbit, rat and mouse IgG were purchased from Molecular probes, and FITC-conjugated goat anti-rabbit antibody from Nordic Laboratories. Fresh medium was added to cells ~1-2 hrs before fixation. Cells were fixed for 20 min in 100% methanol at -20°C or in 4% PFA in phosphate-buffered saline (PBS) at room temperature, permeabilised in 0.15% Triton X-100 in PBS, blocked in 1% bovine serum albumin in PBS and incubated with antibodies as described previously (Akhmanova et al., 2001).

Fluorescence microscopy and image analysis

Unless indicated differently, images of cells were collected with a Leica DMRBE microscope with a PL Fluotar 100x, 1.3 NA objective, equipped with a Hamamatsu CCD camera (C4880). Confocal imaging was performed using LSM510 confocal laser scanning microscope (Ver. 2.3, Carl Zeiss). TIRF microscopy was performed on an Olympus IX70 (PlanApo 100x/1.45 NA, oil TIRFM objective), equipped with an argon laser (488 nm line) and an OrcaER cooled CCD camera (Hamamatsu photonics), controlled by Aquacosmos software (Hamamatsu photonics) or on a Nikon TE2000U (PlanApo 60x/1.45 NA, oil TIRFM objective), equipped with an argon laser (488 nm line) and a Cascade 512B CCD camera (Photometrics), controlled by MetaMorph software (Universal Imaging Corp.). The quantification and analysis of fluorescent signals was performed using MetaMorph software. Images were prepared for publication using Photoshop (Adobe). Statistical analysis was performed using with a SigmaPlot (SPSS Inc) and Statistica for Windows (StatSoft Inc.).

Acknowledgements

We are grateful to Dr. D. Meijer, Dr. L. Stephens, Dr. J. Sanes, Dr. R. Tsien, Dr. T. Balla and Dr. M. Takeichi for sharing reagents and K. Bezstarosti for the technical assistance. This study was supported by the Netherlands Organisation for Scientific Research grant to A. Akhmanova.

References

- Akhmanova, A., and C.C. Hoogenraad. 2005. Microtubule plus-end-tracking proteins: mechanisms and functions. *Curr Opin Cell Biol.* 17:47-54.
- Akhmanova, A., C.C. Hoogenraad, K. Drabek, T. Stepanova, B. Dortland, T. Verkerk, W. Vermeulen, B.M. Burgering, C.I. De Zeeuw, F. Grosveld, and N. Galjart. 2001. Clasps are CLIP-115 and -170 associating proteins involved in the regional regulation of microtubule dynamics in motile fibroblasts. *Cell.* 104:923-35.
- Bershadsky, A., A. Chausovsky, E. Becker, A. Lyubimova, and B. Geiger. 1996. Involvement of microtubules in the control of adhesion-dependent signal transduction. *Curr Biol.* 6:1279-89.
- Carvalho, P., J.S. Tirnauer, and D. Pellman. 2003. Surfing on microtubule ends. *Trends Cell Biol.* 13:229-37.
- Coquelle, F.M., M. Caspi, F.P. Cordelieres, J.P. Dompierre, D.L. Dujardin, C. Koifman, P. Martin, C.C. Hoogenraad, A. Akhmanova, N. Galjart, J.R. De Mey, and O. Reiner. 2002. LIS1, CLIP-170's key to the dynein/dynactin pathway. *Mol Cell Biol.* 22:3089-102.
- Deguchi-Tawarada, M., E. Inoue, E. Takao-Rikitsu, M. Inoue, T. Ohtsuka, and Y. Takai. 2004. CAST2: identification and characterization of a protein structurally related to the presynaptic cytomatrix protein CAST. *Genes Cells.* 9:15-23.
- Deken, S.L., R. Vincent, G. Hadwiger, Q. Liu, Z.W. Wang, and M.L. Nonet. 2005. Redundant localization mechanisms of RIM and ELKS in *Caenorhabditis elegans*. *J Neurosci.* 25:5975-83.
- Doble, B.W., and J.R. Woodgett. 2003. GSK-3: tricks of the trade for a multi-tasking kinase. *J Cell Sci.* 116:1175-86.
- Driegen, S., R. Ferreira, A. van Zon, J. Strouboulis, M. Jaegle, F. Grosveld, S. Philipsen, and D. Meijer. 2005. A generic tool for biotinylation of tagged proteins in transgenic mice. *Transgenic Res.* 14:477-482.
- Ezratty, E.J., M.A. Partridge, and G.G. Gundersen. 2005. Microtubule-induced focal adhesion disassembly is mediated by dynamin and focal adhesion kinase. *Nat Cell Biol.* 7:581-90.
- Galjart, N. 2005. CLIPs and CLASPs and cellular dynamics. *Nat Rev Mol Cell Biol.* 6:487-98.
- Galjart, N., and F. Perez. 2003. A plus-end raft to control microtubule dynamics and function. *Curr Opin Cell Biol.* 15:48-53.
- Haugh, J.M., F. Codazzi, M. Teruel, and T. Meyer. 2000. Spatial sensing in fibroblasts mediated by 3' phosphoinositides. *J Cell Biol.* 151:1269-80.
- Howard, J., and A.A. Hyman. 2003. Dynamics and mechanics of the microtubule plus end. *Nature.* 422:753-8.

- Katoh, M. 2003. Identification and characterization of human LL5A gene and mouse L15a gene in silico. *Int J Oncol.* 23:1477-83.
- Kaverina, I., O. Krylyshkina, and J.V. Small. 1999. Microtubule targeting of substrate contacts promotes their relaxation and dissociation. *J Cell Biol.* 146:1033-44.
- Kishi, M., T.T. Kummer, S.J. Eglén, and J.R. Sanes. 2005. LL5 β : a regulator of postsynaptic differentiation identified in a screen for synaptically enriched transcripts at the neuromuscular junction. *J Cell Biol.* 169:355-66.
- Ko, J., M. Na, S. Kim, J.R. Lee, and E. Kim. 2003. Interaction of the ERC family of RIM-binding proteins with the liprin- α family of multidomain proteins. *J Biol Chem.* 278:42377-85.
- Lee, H., U. Engel, J. Rusch, S. Scherrer, K. Sheard, and D. Van Vactor. 2004. The microtubule plus end tracking protein Orbit/MAST/CLASP acts downstream of the tyrosine kinase Abl in mediating axon guidance. *Neuron.* 42:913-26.
- Liu, B.P., M. Chrzanowska-Wodnicka, and K. Burridge. 1998. Microtubule depolymerization induces stress fibers, focal adhesions, and DNA synthesis via the GTP-binding protein Rho. *Cell Adhes Commun.* 5:249-55.
- Lu, J., H. Li, Y. Wang, T.C. Sudhof, and J. Rizo. 2005. Solution structure of the RIM1 α PDZ domain in complex with an ELKS1b C-terminal peptide. *J Mol Biol.* 352:455-66.
- Maiato, H., C.L. Rieder, W.C. Earnshaw, and C.E. Sunkel. 2003. How do kinetochores CLASP dynamic microtubules? *Cell Cycle.* 2:511-4.
- Mathe, E., Y.H. Inoue, W. Palframan, G. Brown, and D.M. Glover. 2003. Orbit/Mast, the CLASP orthologue of *Drosophila*, is required for asymmetric stem cell and cystocyte divisions and development of the polarised microtubule network that interconnects oocyte and nurse cells during oogenesis. *Development.* 130:901-15.
- Mimori-Kiyosue, Y., I. Grigoriev, G. Lansbergen, H. Sasaki, C. Matsui, F. Severin, N. Galjart, F. Grosveld, I. Vorobjev, S. Tsukita, and A. Akhmanova. 2005. CLASP1 and CLASP2 bind to EB1 and regulate microtubule plus-end dynamics at the cell cortex. *J Cell Biol.* 168:141-53.
- Monier, S., F. Jollivet, I. Janoueix-Lerosey, L. Johannes, and B. Goud. 2002. Characterization of novel Rab6-interacting proteins involved in endosome-to-TGN transport. *Traffic.* 3:289-97.
- Nakata, T., Y. Kitamura, K. Shimizu, S. Tanaka, M. Fujimori, S. Yokoyama, K. Ito, and M. Emi. 1999. Fusion of a novel gene, ELKS, to RET due to translocation t(10;12)(q11;p13) in a papillary thyroid carcinoma. *Genes Chromosomes Cancer.* 25:97-103.

- Nakata, T., T. Yokota, M. Emi, and S. Minami. 2002. Differential expression of multiple isoforms of the ELKS mRNAs involved in a papillary thyroid carcinoma. *Genes Chromosomes Cancer*. 35:30-7.
- Niwa, H., K. Yamamura, and J. Miyazaki. 1991. Efficient selection for high-expression transfectants with a novel eukaryotic vector. *Gene*. 108:193-9.
- Ohara-Imaizumi, M., T. Ohtsuka, S. Matsushima, Y. Akimoto, C. Nishiwaki, Y. Nakamichi, T. Kikuta, S. Nagai, H. Kawakami, T. Watanabe, and S. Nagamatsu. 2005. ELKS, a protein structurally related to the active zone-associated protein CAST, is expressed in pancreatic beta cells and functions in insulin exocytosis: interaction of ELKS with exocytotic machinery analyzed by total internal reflection fluorescence microscopy. *Mol Biol Cell*. 16:3289-300.
- Ohtsuka, T., E. Takao-Rikitsu, E. Inoue, M. Inoue, M. Takeuchi, K. Matsubara, M. Deguchi-Tawarada, K. Satoh, K. Morimoto, H. Nakanishi, and Y. Takai. 2002. Cast: a novel protein of the cytomatrix at the active zone of synapses that forms a ternary complex with RIM1 and munc13-1. *J Cell Biol*. 158:577-90.
- Paranavitane, V., W.J. Coadwell, A. Eguinoa, P.T. Hawkins, and L. Stephens. 2003. LL5beta is a phosphatidylinositol (3,4,5)-trisphosphate sensor that can bind the cytoskeletal adaptor, gamma-filamin. *J Biol Chem*. 278:1328-35.
- Schuyler, S.C., and D. Pellman. 2001. Microtubule "plus-end-tracking proteins": The end is just the beginning. *Cell*. 105:421-4.
- Takao-Rikitsu, E., S. Mochida, E. Inoue, M. Deguchi-Tawarada, M. Inoue, T. Ohtsuka, and Y. Takai. 2004. Physical and functional interaction of the active zone proteins, CAST, RIM1, and Bassoon, in neurotransmitter release. *J Cell Biol*. 164:301-11.
- Wang, Y., X. Liu, T. Biederer, and T.C. Sudhof. 2002. A family of RIM-binding proteins regulated by alternative splicing: Implications for the genesis of synaptic active zones. *Proc Natl Acad Sci U S A*. 99:14464-9.
- Wilm, M., A. Shevchenko, T. Houthaeve, S. Breit, L. Schweigerer, T. Fotsis, and M. Mann. 1996. Femtomole sequencing of proteins from polyacrylamide gels by nano-electrospray mass spectrometry. *Nature*. 379:466-9.
- Wittmann, T., and C.M. Waterman-Storer. 2005. Spatial regulation of CLASP affinity for microtubules by Rac1 and GSK3beta in migrating epithelial cells. *J Cell Biol*. 169:929-39.

Chapter 6

**Mass spectrometry analysis of
membrane-bound protein complexes
cross-linked with formaldehyde:
identification of liprin- α 1 as a
component of LL5 β -containing cortical
clusters in HeLa cells**

Mass spectrometry analysis of membrane-bound protein complexes cross-linked with formaldehyde: identification of liprin- α 1 as a component of LL5 β -containing cortical clusters in HeLa cells

**Gideon Lansbergen¹, Casper Hoogenraad², Karel Bezstarosti³,
Jeroen Demmers³, Frank Grosveld¹ and Anna Akhmanova¹.**

¹ MGC Department of Cell Biology and Genetics, Erasmus Medical Center, 3000 DR Rotterdam, The Netherlands.

² Department of Neuroscience, Erasmus Medical Center, 3000 DR Rotterdam, The Netherlands.

³ MGC Department of Biochemistry, Erasmus Medical Center, 3000 DR Rotterdam, The Netherlands.

Summary

In this chapter we describe an optimised procedure for using mass spectrometry to identify components of membrane-bound protein complexes. This procedure is based on formaldehyde cross-linking, followed by one-step protein purification. Cultured cells, expressing biotinylation-tagged protein of interest are fixed with formaldehyde, membrane proteins are solubilised with an anionic detergent and used for streptavidin pull down assay. Purified protein complexes are de-cross-linked and subjected to mass spectrometry. We applied this procedure to a membrane-bound fragment of LL5 β , a cortical protein involved in attaching microtubules to the membrane. We show that at least one of the isolated potential partners of LL5 β , liprin- α 1, is indeed a component of the LL5 β clusters at the margin of HeLa cells.

Results and discussion

In our previous study (Chapter 5) we showed that CLASPs, LL5 β and ELKS form a complex, which is responsible for the attachment of microtubules to the cortex of HeLa cells. We found that LL5 β is likely to be the core component of the complex, because its depletion by RNA interference caused loss of its partners, CLASPs and ELKS, from the peripheral cortical sites. LL5 β is a phosphatidylinositol-3,4,5-triphosphate (PIP3)-binding

protein and its recruitment to the plasma membrane is regulated by PI3 kinase activity (Paranavitan et al., 2003, Chapter 5). However, inhibition of PI3 kinase resulted only in a partial loss of LL5 β from the cell cortex, suggesting that additional partners may be involved in anchoring LL5 β at the membrane.

To identify such partners, we have first searched for LL5 β -binding proteins in the Triton-X100 soluble fraction of HeLa cells. Biotinylation- and green fluorescent protein (GFP)-tagged LL5 β (bio-GFP-LL5 β ; Chapter 5) was transiently co-expressed in HeLa cells together with the protein-biotin ligase BirA. Biotinylated proteins and their binding partners were isolated by streptavidin pull down and subjected to mass spectrometry (Appendix A). The most abundant proteins, co-purified with LL5 β , were ELKS (already described in Chapter 5) and plectin. Plectin is a large cytoskeletal linker, which can bind to intermediate filaments as well as actin and microtubules; it participates in plasma membrane-cytoskeleton junctions (Wiche, 1998). Unfortunately, in immunofluorescent staining of HeLa cells we were unable to find significant colocalisation of LL5 β and plectin, because the first was mainly restricted to cortical clusters while the latter was mostly present along intermediate filaments (data not shown). It is still possible that LL5 β -plectin interaction is functionally important; however, we were unable to find cytological evidence supporting the idea that plectin contributes to the cortical targeting of LL5 β . Taken together, this analysis of LL5 β partners suggested some links to cytoskeletal components, but provided no clear clues on the specific targeting of LL5 β to the ventral plasma membrane.

The disadvantage of using non-ionic detergents, such as Triton X-100, to solubilise cell proteins prior to pull down assays is that many membrane proteins are lost in the insoluble fraction. One notorious example are lipid raft proteins, which can be isolated based on their insolubility in Triton-containing buffers (Rajendran and Simons, 2005). To dissolve most cellular proteins, one can use anionic detergents, such as sodium dodecylsulfate (SDS). Unfortunately SDS also denatures proteins and thereby dissociates protein complexes. To overcome this problem, one can cross-link the interacting proteins before extracting them in an SDS-containing buffer, to preserve the association between the protein partners. We chose formaldehyde cross-linking, because formaldehyde is a cell-permeable fixation reagent. Its other big advantage is that it induces cross-links that can be fully reversed by heating. As a result protein peptides do not retain chemical modifications, which would alter their mass and complicate their identification by mass spectrometry. Formaldehyde cross-linking has been widely used to study chromatin architecture (Orlando, 2000; Orlando et al., 1997). It has been also applied in combination with mass spectrometry to search for novel components of protein complexes (see Vasilescu et al., 2004, and references therein). We combined formaldehyde cross-linking with the highly efficient and rapid streptavidin-based purification of biotinylated proteins (de Boer et al., 2003; Chapter 5).

We have initially applied this procedure to the full-length bio-GFP-LL5 β , but were unable to recover significant amounts of this fusion protein after cross-linking (data not shown). Instead, we used bio-GFP-LL5 β -C deletion mutant (Fig.1a), because it is the smallest LL5 β fragment which localises to the ventral membrane and colocalises with the endogenous LL5 β (Fig.1b) After some optimisation, we developed a protocol which allowed us to dissolve the cross-linked proteins from the Triton-X100-insoluble fraction and perform an efficient streptavidin pull down (Fig.2; see also Materials and Methods). The proteins co-purified with bio-GFP-LL5 β -C after formaldehyde cross-linking were identified by mass spectrometry (Appendix B).

Analysis of the mass spectrometry results indicated that the endogenous full-length LL5 β co-purified with LL5 β -C, because the sample contained N-terminal LL5 β peptides, which were not present in LL5 β -C. ELKS, an abundant component of LL5 β clusters (Chapter 5), was also present among the isolated proteins. In addition, we identified several actin-binding proteins, including calponin-2, IQGAP1 and filamin. Filamin was already identified as a partner of LL5 β (Paranavitane et al., 2003). In HeLa cells, filamin displayed a broad distribution, which mostly correlated with the actin fibres but showed no specific enrichment at the LL5 β patches (data not shown). Binding to filamin may play a role in linking LL5 β -based microtubule attachment sites to the actin network. We also identified two focal adhesion components, zyxin and talin (Zaidel-Bar et al., 2004). Given the fact that LL5 β patches are often clustered around focal adhesions (Chapter 5), this potential link is interesting and deserves further investigation.

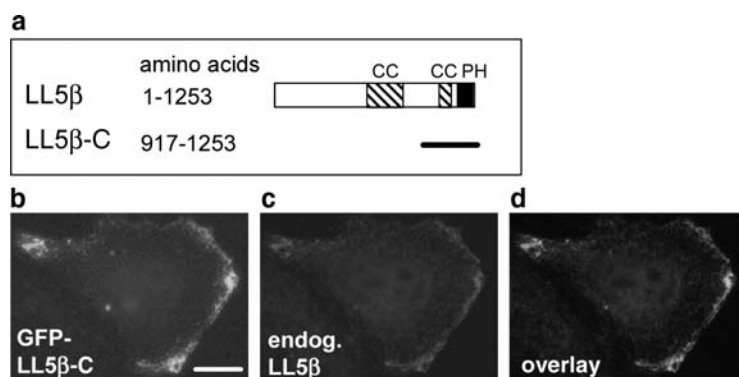


Figure 1. a. Schematic representation of LL5 β structure and the LL5 β -C deletion mutant, used in this study. CC-coiled coil domain, PH – pleckstrin homology domain.

b-d. HeLa cells were transfected with GFP- expression construct. One day later cells were fixed and stained with a rabbit polyclonal antibody against LL5 β (this antibody is raised against the middle part of LL5 β and does not cross-react with GFP-LL5 β -C. (b) GFP signal; (c) endogenous LL5 β ; (d) overlay with GFP shown in green and endogenous LL5 β in red. Bar, 10 μ m.

The list of proteins cross-linked to bio-GFP-LL5 β -C also included liprin- α 1 and liprin- β 1. Liprins comprise an evolutionary conserved protein family, present in worms, flies and vertebrates (Serra-Pages et al., 1998). In humans this family includes four liprin- α (α 1- α 4) and two liprin- β (β 1 and β 2) genes (Serra-Pages et al., 1998). They contain N-terminal coiled coil domains and C-terminal SAM domains (Katoh, 2003; Serra-Pages et al., 1998). α - and β - liprins interact with each other through their C-terminal parts; they can also homodimerise via the N-terminal domains (Serra-Pages et al., 1998). Liprin- α 1 was initially identified as the binding partner of receptor protein tyrosine phosphatase LAR (Pulido et al., 1995; Serra-Pages et al., 1995). Subsequent studies demonstrated that liprins have multiple protein partners, suggesting that they are scaffolding proteins acting at the plasma membrane or on vesicles (Ko et al., 2003a; Ko et al., 2003b; Schoch et al., 2002; Shin et al., 2003; Wyszynski et al., 2002). We decided to focus our attention on these proteins, because liprin- α 1 was already identified as a binding partner of ELKS (Ko et al., 2003b), a prominent component of LL5 β patches (Chapter 5). In agreement with these data, liprin- β 1 was present among the proteins identified in the bio-GFP-ELKS α pull down assay (Appendix A).

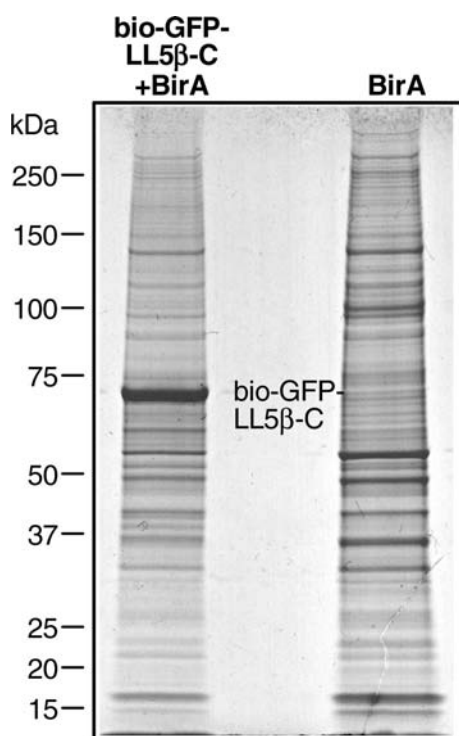


Figure 2.

Streptavidin pull down assays were performed with the extracts of HeLa cells, co-expressing bio-GFP-LL5 β -C together with BirA or BirA alone. The cells were cross-linked with formaldehyde and extracted with Triton X-100. Triton-insoluble material was dissolved in an SDS-containing buffer and used for the pull down assay. Proteins, bound to streptavidin beads were analysed on a Coomassie-stained 4-12% acrylamide gel.

To investigate the subcellular localization of liprin- α 1, we transfected HeLa cells with a hemagglutinin (HA)-tagged liprin- α 1 expression construct and co-stained the cells with antibodies against the HA tag and LL5 β (Fig.3a). HA-liprin- α 1 was present in the cytoplasm and displayed prominent colocalisation with the endogenous LL5 β . Also the endogenous liprin- α 1 colocalised with LL5 β in HeLa cells (Fig.3b). Surprisingly, the depletion of ELKS, the common binding partner of LL5 β and liprin- α 1, did not abolish their colocalisation (Fig.3c), although LL5 β and liprin- α 1-positive puncta acquired a more diffuse distribution, in agreement with the data shown in Chapter 5. Since the RNAi-based depletion is always incomplete, we cannot exclude that the colocalisation of LL5 β and liprin- α 1 is caused by the residual small amounts of ELKS. Alternatively, LL5 β and liprin- α 1 may be binding to each other directly or through another common partner.

Depletion of LL5 β abolished cortical accumulation of liprin- α 1 (Fig. 3d), similar to its effect on ELKS distribution (Chapter 5). After LL5 β knockdown, very little liprin- α 1 was detectable in methanol-fixed cells, probably because it became soluble and was extracted during the staining procedure. This result is in agreement with our previous conclusion that LL5 β forms the core of cortical clusters responsible for microtubule attachment (Chapter 5). Still, it is possible that liprins contribute to the cortical localization of LL5 β . Liprin- α 1 binds to LAR, a transmembrane tyrosine phosphatase (Pulido et al., 1995; Serra-Pages et al., 1995), which may provide an additional membrane anchor to LL5 β and its partners. In agreement with this notion, we did identify LAR among the proteins cross-linked to bio-GFP-LL5 β -C (Appendix B). Interestingly, LAR partially colocalises with focal adhesions (Serra-Pages et al., 1995) and may be in some way responsible for clustering of LL5 β patches around focal adhesions after certain drug treatments (Chapter 5).

Cytological data presented above support the existence of a physical and functional link between LL5 β and liprins. Therefore, we can conclude that the simple and rapid method of purification of cross-linked protein complexes described here is valid and can be applied to searching for partners of membrane-associated proteins. The identified connection between LL5 β and liprins requires further biochemical and functional analysis. Future studies will likely focus on the role of these protein complexes in neuronal tissue, since similar to CLASPs and ELKS, liprins and LAR are involved in the control of synapse formation and axon guidance (for review, see Johnson and Van Vactor, 2003; Zarnescu and Moses, 2004). It would be interesting to investigate whether complexes of CLASPs, LL5 β , ELKS and liprins are formed in neurons and whether they are involved in microtubule organisation in developing or mature neuronal cells.

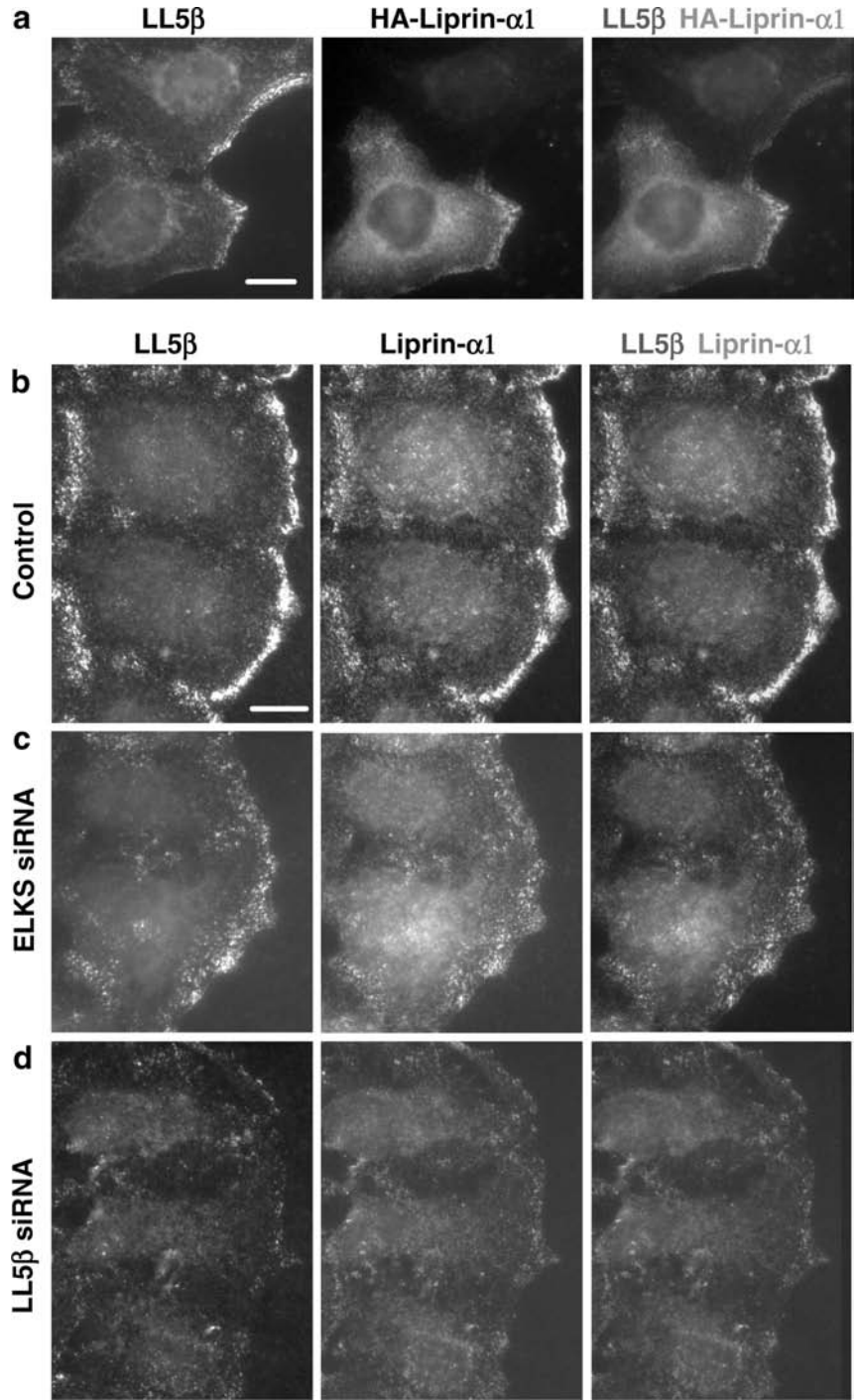


Figure 3.

a. HeLa cells were transfected with a construct expressing HA-liprin- α 1, fixed and co-stained with antibodies against the HA tag and LL5 β . Bar, 10 μ m.

b-d. HeLa cells were cultured for 72 hrs after transfection with the indicated siRNAs. Cells were fixed with methanol and stained with the indicated antibodies. Bar, 10 μ m.

Materials and methods***Cell lines, transfection of plasmids and siRNAs, expression constructs, antibodies and immunofluorescent staining***

HeLa cells were grown as described previously (Akhmanova et al., 2001). Lipofectamine 2000 (Invitrogen) or FuGENE 6 (Roche) transfection reagents were used for plasmid transfection. Synthetic siRNAs were transfected, using HiPerFect (Qiagen) at a concentration 5 nM. The control oligonucleotide were described previously (Mimori-Kiyosue et al., 2005). siRNA against LL5 β (siRNA 38298, Ambion) was directed against the sequence GGAGATTTTGGATCATCTA, siRNA against ELKS (siRNA 43397, Ambion) was directed against the sequence GTGGGAAAACCCTTTCAAT.

GFP-LL5 β -C expression construct was generated by PCR as described in Chapter 5. Bio-GFP-LL5 β -C was produced by cloning at the NheI and AgeI sites in front of the GFP a linker, encoding the amino acid sequence MASGLNDIFEAQKIEWHEGGG. BirA expression construct (pSCT-HA-BirA, Driegen et al., 2005) was a gift from Dr. D.Meijer (Erasmus MC, Rotterdam, The Netherlands). HA-tagged liprin- α 1 construct was generated in the mammalian expression vector GW1 (CMV promoter).

Rabbit antibodies against liprin- α 1 were raised against the peptide SFRRAPSWRKKFRPKDIR; the antibody was affinity purified against its own peptide before use. We used rabbit antibodies against LL5 β (Chapter 5) and mouse monoclonal antibodies against the HA tag (Babco) and LL5 β (a gift from Dr. J.Sanes, Washington University, St.Louis, USA, Kishi et al., 2005). For secondary antibodies, we used Alexa 594-conjugated goat anti-mouse antibodies (Molecular probes) and FITC-conjugated goat anti-rabbit antibodies (Nordic Laboratories).

For immunofluorescent staining, fresh medium was added to cells ~1-2 hrs before fixation. Cells were fixed for 20 min in 100% methanol at -20°C , permeabilised in 0,15% Triton X-100 in PBS, blocked in 1% bovine serum albumin in PBS and incubated with primary antibodies (all diluted 1:300) for 1 hr at room temperature. Slides were washed 3 times with PBS/0,15% Tween-20, incubated with the secondary antibodies, washed again 3 times with the same buffer, incubated briefly with 70% and 100% ethanol, air-dried and mounted in Vectashield.

Streptavidin pull down and mass spectrometry analysis of protein complexes cross-linked with formaldehyde

16 hrs after transfection with Lipofectamine 2000, HeLa cells co-expressing protein-biotin ligase BirA and bio-GFP-LL5 β -C were washed with PBS and cross-linked with 0.5% formaldehyde PBS for 10 minutes at room temperature. Cells were washed with PBS containing 125 mM glycine and lysed in ice cold buffer containing 100 mM NaCl, 20 mM Tris-HCl, pH 7.5, 0.5% Triton X-100 and protease inhibitors (Complete; Roche). Cell lysates were centrifuged at 13,000 rpm for 15 minutes at 4°C, and the pellet was resuspended in a buffer containing 100 mM NaCl, 50 mM Tris-HCl, pH 7.5, 0.5% SDS, protease inhibitors (Complete; Boehringer), followed by sonication and centrifugation at 13,000 rpm for 15 minutes. The supernatant was incubated for 45 minutes with Dynabeads M-280 Streptavidin (Dyna). After magnetic separation, the beads were washed three times in a buffer containing 250 mM NaCl, 20 mM Tris-HCl, pH 7.5, 0.1% Triton X-100 and protease inhibitors (Complete; Roche). Thereafter, the beads were resuspended in NuPAGE LDS Sample Buffer and NuPAGE Reducing Agent (Invitrogen) and boiled for at least 20 minutes to de-cross-link. After magnetic separation, the supernatant was loaded and run on a 4-12% NuPAGE Bis-Tris Gel, followed by staining with the Colloidal Blue Staining Kit (Invitrogen). Mass spectrometry and analysis of mass spectrometry results were performed as described in Chapter 5.

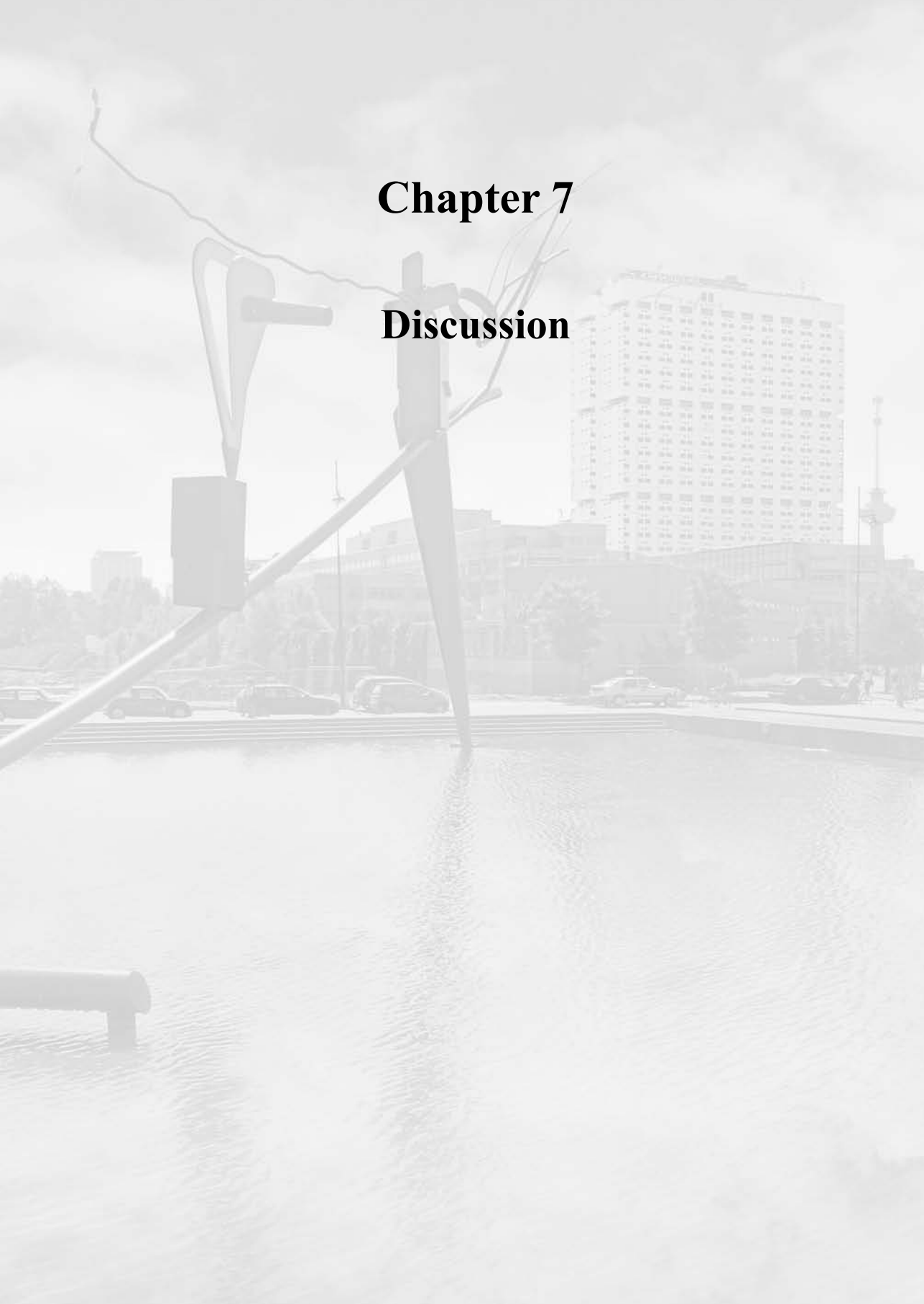
References

- Akhmanova, A., C.C. Hoogenraad, K. Drabek, T. Stepanova, B. Dortland, T. Verkerk, W. Vermeulen, B.M. Burgering, C.I. De Zeeuw, F. Grosveld, and N. Galjart. 2001. Clasps are CLIP-115 and -170 associating proteins involved in the regional regulation of microtubule dynamics in motile fibroblasts. *Cell*. 104:923-35.
- de Boer, E., P. Rodriguez, E. Bonte, J. Krijgsveld, E. Katsantoni, A. Heck, F. Grosveld, and J. Strouboulis. 2003. Efficient biotinylation and single-step purification of tagged transcription factors in mammalian cells and transgenic mice. *Proc Natl Acad Sci U S A*. 100:7480-5.
- Driegen, S., R. Ferreira, A. van Zon, J. Strouboulis, M. Jaegle, F. Grosveld, S. Philipsen, and D. Meijer. 2005. A generic tool for biotinylation of tagged proteins in transgenic mice. *Transgenic Res*. 14:477-482.
- Johnson, K.G., and D. Van Vactor. 2003. Receptor protein tyrosine phosphatases in nervous system development. *Physiol Rev*. 83:1-24.
- Katoh, M. 2003. Identification and characterization of human PPFIA4 gene in silico. *Int J Mol Med*. 12:1009-14.
- Kishi, M., T.T. Kummer, S.J. Eglen, and J.R. Sanes. 2005. LL5beta: a regulator of postsynaptic differentiation identified in a screen for synaptically enriched transcripts at the neuromuscular junction. *J Cell Biol*. 169:355-66.
- Ko, J., S. Kim, J.G. Valtchanoff, H. Shin, J.R. Lee, M. Sheng, R.T. Premont, R.J. Weinberg, and E. Kim. 2003a. Interaction between liprin-alpha and GIT1 is required for AMPA receptor targeting. *J Neurosci*. 23:1667-77.
- Ko, J., M. Na, S. Kim, J.R. Lee, and E. Kim. 2003b. Interaction of the ERC family of RIM-binding proteins with the liprin-alpha family of multidomain proteins. *J Biol Chem*. 278:42377-85.
- Mimori-Kiyosue, Y., I. Grigoriev, G. Lansbergen, H. Sasaki, C. Matsui, F. Severin, N. Galjart, F. Grosveld, I. Vorobjev, S. Tsukita, and A. Akhmanova. 2005. CLASP1 and CLASP2 bind to EB1 and regulate microtubule plus-end dynamics at the cell cortex. *J Cell Biol*. 168:141-53.
- Orlando, V. 2000. Mapping chromosomal proteins in vivo by formaldehyde-crosslinked-chromatin immunoprecipitation. *Trends Biochem Sci*. 25:99-104.
- Orlando, V., H. Strutt, and R. Paro. 1997. Analysis of chromatin structure by in vivo formaldehyde cross-linking. *Methods*. 11:205-14.
- Paranavitane, V., W.J. Coadwell, A. Eguinoa, P.T. Hawkins, and L. Stephens. 2003. LL5beta is a phosphatidylinositol (3,4,5)-trisphosphate sensor that can bind the cytoskeletal adaptor, gamma-filamin. *J Biol Chem*. 278:1328-35.

- Pulido, R., C. Serra-Pages, M. Tang, and M. Streuli. 1995. The LAR/PTP delta/PTP sigma subfamily of transmembrane protein-tyrosine-phosphatases: multiple human LAR, PTP delta, and PTP sigma isoforms are expressed in a tissue-specific manner and associate with the LAR-interacting protein LIP.1. *Proc Natl Acad Sci U S A*. 92:11686-90.
- Rajendran, L., and K. Simons. 2005. Lipid rafts and membrane dynamics. *J Cell Sci*. 118:1099-102.
- Schoch, S., P.E. Castillo, T. Jo, K. Mukherjee, M. Geppert, Y. Wang, F. Schmitz, R.C. Malenka, and T.C. Sudhof. 2002. RIM1alpha forms a protein scaffold for regulating neurotransmitter release at the active zone. *Nature*. 415:321-6.
- Serra-Pages, C., N.L. Kedersha, L. Fazikas, Q. Medley, A. Debant, and M. Streuli. 1995. The LAR transmembrane protein tyrosine phosphatase and a coiled-coil LAR-interacting protein co-localize at focal adhesions. *Embo J*. 14:2827-38.
- Serra-Pages, C., Q.G. Medley, M. Tang, A. Hart, and M. Streuli. 1998. Liprins, a family of LAR transmembrane protein-tyrosine phosphatase-interacting proteins. *J Biol Chem*. 273:15611-20.
- Shin, H., M. Wyszynski, K.H. Huh, J.G. Valtschanoff, J.R. Lee, J. Ko, M. Streuli, R.J. Weinberg, M. Sheng, and E. Kim. 2003. Association of the kinesin motor KIF1A with the multimodular protein liprin-alpha. *J Biol Chem*. 278:11393-401.
- Vasilescu, J., X. Guo, and J. Kast. 2004. Identification of protein-protein interactions using in vivo cross-linking and mass spectrometry. *Proteomics*. 4:3845-54.
- Wiche, G. 1998. Role of plectin in cytoskeleton organization and dynamics. *J Cell Sci*. 111 (Pt 17):2477-86.
- Wyszynski, M., E. Kim, A.W. Dunah, M. Passafaro, J.G. Valtschanoff, C. Serra-Pages, M. Streuli, R.J. Weinberg, and M. Sheng. 2002. Interaction between GRIP and liprin-alpha/SYD2 is required for AMPA receptor targeting. *Neuron*. 34:39-52.
- Zaidel-Bar, R., M. Cohen, L. Addadi, and B. Geiger. 2004. Hierarchical assembly of cell-matrix adhesion complexes. *Biochem Soc Trans*. 32:416-20.
- Zarnescu, D.C., and K. Moses. 2004. Born again at the synapse: a new function for the anaphase promoting complex/cyclosome. *Dev Cell*. 7:777-8.

Chapter 7

Discussion



7.1 Introduction

Microtubules (MTs) constitute one of the main structural components of the eukaryotic cytoskeleton. They are made up of tubulin heterodimers that polymerize into protofilaments. Laterally attached protofilaments form hollow tubes with a diameter of about 25 nm. MTs are dynamic: they have a fast growing (plus) end and a slow growing (minus) end, which switch between phases of growth, pause and shrinkage, a phenomenon called dynamic instability. The dynamic properties of MTs enable them to function in many processes, such as cell division, vesicle transport, cell polarization and migration. In general, MT minus ends are often stable, while the plus-ends undergo growth and depolymerization excursions. They explore the cellular space and can be captured by certain cellular targets such as kinetochores or the cell cortex. This so-called "search-and-capture" mechanism (1, 2) is highly regulated by MT plus-end-tracking proteins (+TIPs), which associate specifically with the plus-ends of growing MTs and regulate their dynamics (3-6). The mechanism of the specific +TIP localization still remains largely enigmatic. Its unravelling is complicated by the fact that many +TIPs interact with each other as well as with other MT associated proteins (MAPs), forming highly dynamic protein-protein complexes at the growing MT ends. Many of these complexes are conserved from yeasts to mammals and are essential for normal cell functioning. In this thesis we have mainly focussed on deciphering the hierarchy of interactions between mammalian +TIPs, as well as their role in cortical MT stabilization. In this chapter we will discuss how our findings fit with the knowledge on the organization and functioning of the +TIP complexes in different model systems.

7.2 EB1: a spider in the web

EB1 family members are well-characterized +TIPs, which are conserved in plants, yeasts and mammals (7). In general, all EB-like proteins share a common role in preventing microtubules from pausing and total depolymerization. In all species EB homologues promote MT polymerization by increasing MT rescue frequencies, and decreasing the rate of depolymerization and the time MTs spend pausing (8-10). However, *Drosophila* EB1 and budding yeast Bim1p increase the catastrophe frequencies, in contrast to the fission yeast Mal3p and vertebrate EB1, which decrease the catastrophe frequencies (9-12).

The important role of EB proteins is underscored by the fact that virtually all +TIPs shown to interact with MTs directly are also able to bind to the EBs (Fig. 1). EB1 was initially identified as a binding partner of the tumour suppressor APC (13). The budding yeast homologue of EB1, Bim1p, interacts with Kar9p, which is often regarded as a

counterpart of APC (14, 15). EB1 interacts with the COOH-terminus of APC, the part that is lost due to mutations in many malignant colorectal cancers (13, 16-18). EB1 contributes to the accumulation of APC at the MT ends, where EB1-APC complexes can promote MT polymerization and stability (19, 20). The mammalian formin mDia, acting downstream of RhoA, associates directly with both EB1 and APC, and may form a triple complex with these proteins, regulating their MT-stabilizing activity (21).

Two other groups of large MT-stabilizing +TIPs – MT-actin cross-linking factor (MACF) family of spectraplakins and CLASPs – can also associate with EB1. Spectraplakins bind to both actin and MTs through their opposite ends and may coordinate the interaction between the two cytoskeletal networks. Both mammalian MACF2 and the *Drosophila* homologue Shot accumulate at MT tips through a direct interaction with EB1 and contribute to the control of cell polarity and migration (18, 22, 23).

In this thesis, we have shown that CLASPs also interact with EB1 (and EB3) directly (24). Similar to spectraplakins, CLASPs may also need EB proteins for their plus-end targeting. In addition to a direct effect, EBs might contribute to the plus-end accumulation of CLASPs indirectly, through binding to the CLIPs (see below), since CLIPs are also CLASP binding partners (25). CLASP-EB interactions may be also important for the MT rescue function of CLASPs. When MTs start shrinking, CLASPs are partially retained on the distal segments of MTs and rescue MTs by enhancing their affinity for EB1. Since EBs promote MT growth, it is possible that EBs stimulate a switch to the growth phase, causing a rescue. The *Drosophila* CLASP homologue, Orbit/Mast, was co-purified in an EB1-pull down assay, suggesting that the interaction is conserved in evolution (22). However, a recent study suggests that at least in mitosis Orbit/Mast acts independently of EB1 (26), though it should be noted that the authors analysed only one of the several *Drosophila* EB1 homologues.

The structure of EB1 has been extensively characterized. It contains an NH₂-terminal calponin homology domain, which binds to MTs (27), a coiled coil domain (“EB1 motif”), which dimerizes and at the same time forms a surface for binding of various partners (17, 18) and a negatively charged COOH-terminal tail. The region of APC that binds to EB1 contains a conserved Ile-Pro sequence, which binds to a hydrophobic cavity of the EB1 motif (17). Interestingly, the Ile-Pro sequence within a similar conserved context is also found in the EB1-binding regions of spectraplakins as well as in the EB1-interacting repeat motifs present in CLASPs (18, 24, 28). This suggests that APC, spectraplakins and CLASPs bind to EB1 in a similar way. It should be noted that in addition to the EB1 motif, the highly negatively charged tails of EB1 also play a significant role in the interactions with EB partners, at least in the case of CLASPs (24).

The acidic tails of EB1 are also essential in the association with another group of +TIPs - the CAP-Gly (cytoskeleton associated protein with a conserved glycine) domain

containing proteins, which include the CLIPs and p150^{Glued}, the large subunit of the dynein accessory complex dynactin. p150^{Glued} contains a single NH₂-terminal CAP-Gly domain per monomeric subunit, which is essential for the binding to MTs as well as EB1 (16, 29-31). The MT plus-end accumulation of p150^{Glued} may partly result from the direct MT binding; however, it probably mostly occurs via hitchhiking on CLIP-170 and EB1 (29, 31-33).

A number of recent studies, including our own, produced evidence of a direct interaction between EB proteins and the CLIP family members, including *S. pombe* Tip1p, *Drosophila* CLIP-190 and mammalian CLIP-170 and CLIP-115 (12, 34-36). *Drosophila* CLIP-190 interacts directly with EB1 via its MT-binding CAP-Gly domain and requires EB1 for plus-end binding (35). Also Mal3p, the fission yeast EB1 homologue, binds to Tip1p, the CLIP homologue, and is needed for its plus-end localization (12). In this thesis we have shown that CLIP-170 and CLIP-115 interact directly with EB1 via their CAP-Gly-containing NH₂-terminal domains, and that this interaction plays a role in CLIP accumulation at the MT tips (36). This accumulation is governed by two kinetic parameters – association and dissociation rates. Our data suggest that CLIPs can recognize and bind the growing MT tips independently of EB proteins, while the latter mainly control CLIP dissociation from the MTs (36). A very rapid dissociation of CLIPs from the MTs caused by the lack of EB proteins may strongly reduce their MT tip accumulation and might appear in immunofluorescent staining as an absence of binding, especially if the sensitivity of CLIP staining were not very high. Therefore, the mechanism described by us for the mammalian cells might also hold true for flies and fission yeast. The EB-dependent dissociation control might have been lost by the budding yeast CLIP homologue, Bik1p, explaining why it does not require Bim1p, the EB1 homologue, for MT plus-end targeting (37).

A recent structural study has shown that p150^{Glued} makes contact predominantly with the tail of EB1 (31). This result is in complete agreement with other studies, including our own, on the critical binding region of EB1 for both CLIPs and p150^{Glued}. All CAP-Gly family members interact with the acidic COOH-terminus of EB1 in a manner dependent on the last tyrosine (Tyr268) of EB1 (16, 31, 36). The acidic tail of EB1 contains a sequence that is strikingly similar to the tail of α -tubulin. It is therefore interesting to note that MT binding of the budding yeast CLIP-170 homologue Bik1p depends on the COOH-terminal aromatic residue of α -tubulin (38). Moreover, mouse neurons deficient in tubulin tyrosine ligase (TTL) show a perturbed distribution of mammalian CLIP-170 due to a strongly reduced pool of COOH-terminally tyrosinated α -tubulin (39). The binding of CAP-Gly family members to α -tubulin as well as to EB1-like proteins thus depends on their last tyrosine. Taken together, the results obtained in different studies and species display significant similarities and demonstrate that the interaction of various +TIPs with EB1 is highly conserved in evolution.

Interestingly, p150^{Glued} was found to act as an allosteric activator for the auto-inhibited head-to-tail conformation of EB1. By binding the COOH-terminal tail of EB1, p150^{Glued} releases the NH₂-terminus of EB1 to stimulate MT assembly (31). An EB1-APC complex was also shown to promote MT growth (19), suggesting that other partners, which bind to the EB1 COOH-terminus, may serve as EB1 activators by inducing a conformational change. Existence of self-inhibitory closed conformations may represent a common theme in regulating rapidly recycling +TIPs, since we have shown that this principle also applies to CLIP-170 (32).

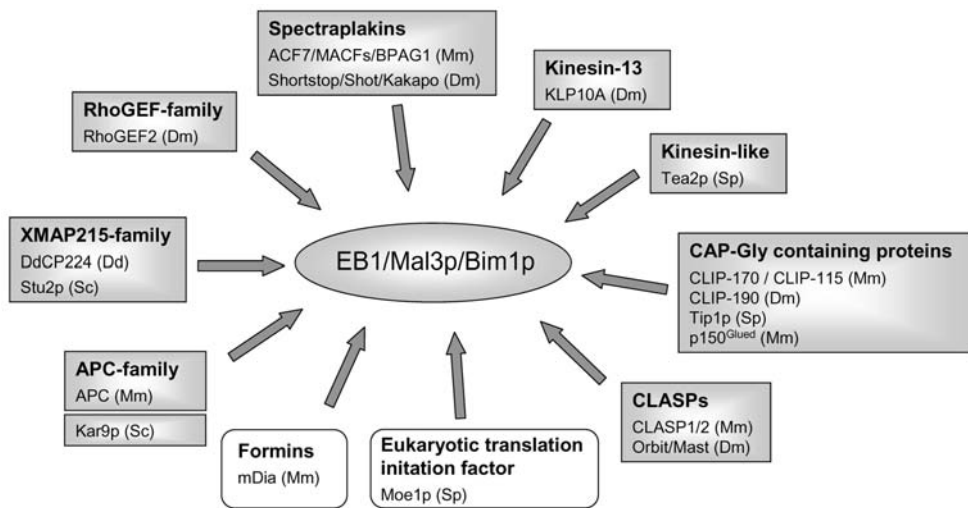


Figure 1: EB1 interacting proteins. The figure illustrates the binding partners of EB1, Bim1p and Mal3p of different species, with MT plus-end binding proteins (+TIPs) shown in blue boxes. *S. cerevisiae* (Sc), *S. Pombe* (Sp), *D. Melanogaster* (DM), mammals (Mm) (16, 17, 21, 22, 24, 29-31, 34-36, 40-43).

All above-mentioned EB1 partners stimulate MT rescue and/or promote MT growth and stability. Strikingly, MT destabilizing factors such as the *Drosophila* kinesin-13 family member KLP10A also accumulate on MT plus-ends through hitchhiking on EB1 (40). In addition, the XMAP215 family members in *Dictiostelium* (DdCP224) and budding yeast (Stu2p) interact with EB1 and regulate MT dynamics (42, 44). In different studies, XMAP215 family members have been shown to function as MT stabilizers as well as destabilizers, and so may aid or oppose the activity of the catastrophe-inducing kinesin-13 family members (45-49). The interaction of EBs with MT stabilizing and destabilizing factors at the MT tips might help to create a balance of activities, necessary for rapid regulation of MT dynamic properties. These functionally diverse interactions may also

account for the partly controversial effects of EB depletion on the MT dynamics in different systems.

Interaction with EB1 might also be needed to transiently concentrate certain regulatory molecules at the MT tips. This mechanism may apply to the *Drosophila* Rho-type DRhoGEF2, which regulates actomyosin contraction in epithelial cells during gastrulation (22). DRhoGEF2 associates with MT plus-ends via EB1, and may use MT dynamics to contact certain cortical subdomains (22). Microtubule-cortex interactions, regulated by different +TIPs, are therefore important not only for organizing the MT network, but also for regulating cortical dynamics, shape and contractility. These interactions, based on similar building blocks in systems as divergent as yeasts and humans, will be the focus of the remaining part of this chapter.

7.3 MT-cortex interactions in yeasts.

MT networks are able to associate with or be in close proximity to membrane structures. Although MTs seem to form self-assembled complexes with cationic liposomes, it is more plausible that interactions with cellular membranes, like the plasma membrane, depend on particular proteins (50). To date, a large number of proteins have been characterized, which contain specific domains to interact with MTs or membranes. Some of these proteins belong to the group of MAPs or +TIPs and cross-bridge MTs and membranes, either directly or indirectly, and cause MT stabilization. MT-cortex interactions are important for diverse cellular processes, including mitosis, migration, vesicle transport and polarization. For instance, secretory vesicles often move to the plasma membrane along the MTs and MT anchoring at the plasma may thus define the sites of secretion.

In budding yeast (*Saccharomyces cerevisiae*) temporal and spatial MT-cortex interactions regulate correct spindle positioning in the bud during mitosis. The capture of astral MTs by the cell cortex is closely linked to the progression of mitosis. MTs grow from the spindle pole body (SPB) in the mother cell towards the tip of the bud and are captured at the bud cortex. Subsequently, the SPB is pulled into the bud whereas a newly formed SPB remains in the mother cell, resulting in chromosomal separation along the mother-bud axis (for review see (51)). One of the mechanisms of MT delivery to the bud cortex comprises the Kar9p-mediated transport of MTs along actin cables (Fig. 2a). Kar9p forms a complex with Bim1p and is transported along MTs from the SPB to the bud neck by the motor activity of kinesins. There, the Kar9p-Bim1p complexes, bound to MT tips, are further pulled by myosin along actin filaments towards the bud tip (51-54). This MT movement causes reorientation of the spindle. The formin Bni1p and an actin interactor Bud6p participate in this process by organizing actin cables (55). Kar9p also has a function in

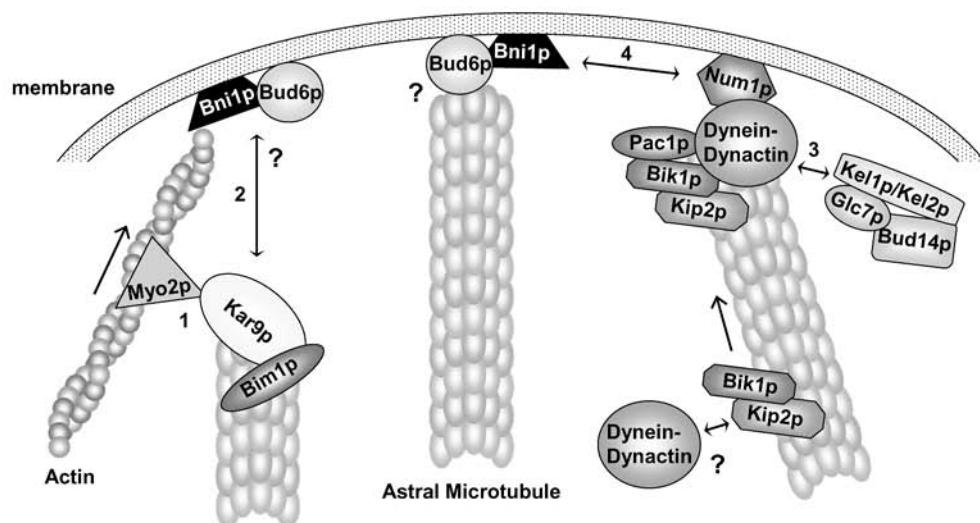
preventing the MTs inside the bud from depolymerization (56, 57). It is clear that Kar9-mediated MT capture is regulated by Cdk1 (51-54), but the details of this regulation are complicated and require further elucidation. Bud6p can probably also capture MTs at the bud cortex in a separate pathway, independent of Kar9p (51, 56).

During anaphase, cytoplasmic dynein exerts pulling forces on the astral MTs, causing the insertion of the mitotic spindle into the bud neck. Targeting of cytoplasmic dynein to MT tips depends on Bik1p (CLIP-170), Pac1p (LIS1) and possibly Kip2p (37, 58, 59) (Fig.2a). Dynein is the central minus-end directed motor that generates pulling forces on MTs involved in spindle positioning at mitosis, as well as the movement of the nucleus and the centrosome during cell migration in different systems (60). In budding yeast, the connection of cytoplasmic dynein with the cell cortex is mediated by the cortical protein Num1p. Num1p contains a COOH-terminal pleckstrin homology (PH) domain, which can specifically bind phosphoinositides. Num1p binds to Bni1p and requires Bni1p for its bud tip localization (61). Although the dynein-mediated spindle positioning pathway is actin-independent (51), the dynein-dynactin complex is regulated by Bud14p-Glc7p phosphatase, which requires intact actin cytoskeleton and kelch domain-containing proteins Kell1p/Kel2p for the accumulation at the bud tip (62).

In shmooing budding yeast, MT plus-ends are anchored to the cortex through two different mechanisms depending on their dynamics. During MT polymerization Bim1p links MT plus-ends to the cortex in a Kar9-dependent manner, while during depolymerization the minus-end directed kinesin Kar3 anchors MTs with the cortex via a certain membrane factor (63, 64).

In fission yeast (*Schizosaccharomyces pombe*) MTs regulate cell growth and polarization by recruiting essential polarity factors to the cell ends that modulate the actin cytoskeleton. After cell division, the rod-shaped yeast cells grow in a monopolar manner, but then change to a bipolar growth during the G2 phase of the cell cycle. The switch of polarization, in which the new cell end starts to grow, is called “new end take off” (NETO) and is induced by MTs (65). Interphase MTs are arranged in anti-parallel bundles with overlapping minus-ends near the nucleus and the plus-ends extending towards the cell periphery. To induce NETO, the CLIP-170 homologue Tip1p is transported to MT plus-ends by Tea2p kinesin and accumulates there in a Mal3p (EB1 homologue) dependent manner (Fig. 2b) (43, 66, 67). Tip1p recruits the kelch repeat protein Tea1p, which is essential for polarized cell growth (68). When MTs depolymerize at the cell end, Tea1p remains targeted to the cell cortex through an interaction with the prenylated membrane anchor protein Mod5p; in its turn, Tea1p restricts Mod5p distribution to the cell ends (69). In addition, Tea1p directly interacts with Tea4p (homologue of the *S.cerevisiae* Bud14p), which in its turn recruits the actin-nucleating formin For3p to the cell tip (70). With the aid of Bud6p, For3p nucleates actin cables from the new end to initiate polarized cell growth

A. Bud-cortex in budding yeast



B. End-tip fission yeast (during NETO)

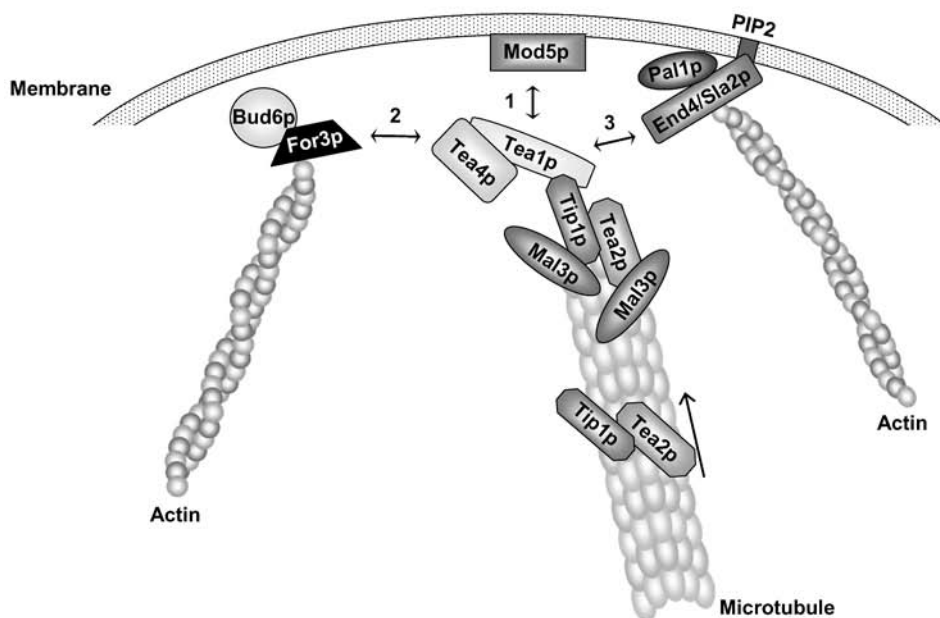


Figure 2: MT-cortex interactions in yeasts: A. The bud cortex in *S. cerevisiae* (budding yeast). Astral MTs interact with the cortex through different mechanisms. 1. Upon phosphorylation by Cdk1, Kar9p can be transported in complex with Bim1p towards the bud neck in a Kip2p/Kip3p-dependent manner. Subsequently, the Kar9p/Bim1p-complex is transported along actin filaments towards the bud tip by the type V myosin Myo2p (51-54). 2. The Kar9p/Bim1p-complex anchors astral MTs at the bud cortex with proposed support of the actin-interacting protein 3 (Aip3/Bud6p) and the Rho-family activated formin Bni1p. This notion is based on the fact that cortical localization of Kar9p is affected by inactivation of Bud6p or Bni1p, as well as treatment of the actin-depolymerizing agent latrunculin A (55, 72). In addition, Bud6p is able to (directly) link astral MTs at the bud-cortex in a Kar9p-independent manner (56, 57). The dynein/dynactin-complex plays a role in the organization of the mitotic spindle. It binds to Bik1p and may be delivered to MT plus-ends together with it by the action of a kinesin-7, Kip2p (37, 58). The pleckstrin homology domain protein Num1p attaches dynein-dynactin to the membrane and may also activate the dynein motor (58, 61). 3. This mechanism of dynein activation is supported, possibly via Num1p, by the Bud14p-Glc7 phosphatase complex together with the cortical kelch-domain proteins Kel1p/Kel2p (62). 4. Additionally, Num1p can associate with the Bni1p/Kar9p-complex, although its localization at the bud tip is only dependent on Bni1p (61).

B. The cell end in *S. pombe* (fission yeast). MT tips are targeted to the cell end and promote actin nucleation, which is involved in polarized growth. Tip1p is transported along MTs by the kinesin-7 family member Tea2p, and accumulates at the plus-ends in a Mal3p-dependent manner (43, 66, 67). 1. Tip1p can recruit the Tea1p/Tea4p-complex. Tea1p can be linked to the cell end by associating with the membrane-binding protein Mod5p (68-70). 2. The polarized deposition of Tea1p-Tea4p recruits the For3p/Bud6p-complex to the cell end by binding directly to Tea4p (70). Subsequently, actin is nucleated and polymerized to promote polarized cell growth and thereby NETO (65, 68, 71). 3. Tea1p is also necessary for the recruitment of the actin-binding protein End4/Sla2p, which is able to bind PIP2 through a specific AP180 N-terminal homology domain (73, 74). Together with a novel partner Pal1p, End4/Sla2p is thought to be involved in the establishment of a new growth zone (75).

and thereby NETO (65, 68, 71). End4/Sla2, a phosphatidylinositol-4,5-diphosphate (PIP2)- and actin-binding protein, also participates in the organization of the actin cytoskeleton at the membrane and localizes to the new cell ends in a Tea1p-dependent manner (73, 74). In conclusion, fission yeast MTs play an essential function in recruiting polarity factors to the cell end to promote actin nucleation, which is required for NETO. In general, the cross-talk between +TIPs and actin organizing proteins is well conserved from yeasts to mammals.

7.4 +TIPs at the mammalian cell cortex

Similar to yeasts, mammals utilize multiple overlapping systems for organizing their cortical microtubules. A large part of this thesis focuses on CLASPs, +TIPs involved in MT stabilization and attachment at the periphery of interphase cells. CLASPs are conserved from fungi and plants to animals, with well-studied homologues in *D. melanogaster* (Orbit/Mast), *C. elegans* (CLS-2/R106.7) and *S. cerevisiae* (Stu1p) (Table 1). Several studies have shown that CLASPs are essential for mitosis and participate in the generation of polarized MT networks (28, 76-79). Mammalian CLASP2 acts as a MT stabilizer at the

leading edge of motile cells, where its activity is negatively regulated by GSK3 β , a downstream target of PI3 kinase, and Rac1 (25, 80). In this thesis we show that CLASP1 and CLASP2 play redundant roles in the organization of interphase MTs in HeLa cells. CLASPs stabilize MT plus-ends at the cell periphery by inducing pauses and/or short polymerization-depolymerization transitions. As already mentioned, CLASPs act as local rescue factors, possibly with the aid of EB proteins. Moreover, CLASPs can localize to the cell cortex in a MT-independent manner (24). This property is shared by CLASP isoforms, which lack membrane-binding domains, indicating that the cortical localization of CLASPs is effected by additional membrane-bound proteins. Using mass spectrometry, we identified new binding partners of CLASP2 α , LL5 β and ELKS, which cross-bridge CLASP-bound MTs with the cell cortex (Chapter 5) (Fig. 3a). LL5 β can be linked to the plasma membrane through its COOH-terminal pleckstrin homology (PH) domain, which binds membrane-bound phosphatidylinositol-3,4,5-triphosphate (PIP3) (81). In addition, ELKS, and probably also LL5 β interact with liprin, which might be linked to the plasma membrane through a receptor protein tyrosine phosphatase LAR (Chapter 6) (Fig.3a). In addition to this indirect membrane link, the brain-specific CLASP2 β isoform may anchor MTs at the membranes directly, since it has a dual palmitoylation motif at the NH₂-terminus (25).

Other pathways of MT capture at the cell cortex are dependent on the +TIP APC. Similar to CLASPs, APC is also negatively regulated by GSK3 β and binds directly to EB1 (13, 20). APC accumulates at MT plus-ends through different mechanisms, where it can stabilize MTs, stimulate their polymerization and anchor them to the cell cortex (19-21, 82). Like CLASPs (except CLASP2 β), APC has no membrane-binding domain and appears to make use of actin-binding proteins, such as mDia (a RhoA effector) and IQGAP1 (a Rac1/Cdc42 effector), to attach MTs to the cell cortex (21, 83-85). In an alternative pathway, APC interacts with Dlg1 to link MTs to the plasma membrane and generate polarized MT arrays (86). Similar to APC, also CLIP-170 is shown to interact with IQGAP1 to target MT plus-ends to the cell cortex (87). As discussed above, EB1 is involved in all MT-related activities of APC; it also binds to mDia and may form a tripartite complex together with mDia and APC at MT plus-ends (21). Moreover, EB1 was shown to interact with the spectraplakins (18), which can link MTs to the actin filaments, organize the directional growth of MTs along actin fibers and stabilize MTs in mDia-dependent fashion (88). CLASP-, APC- and spectraplakin-based pathways show clear similarities, as they all depend on EB1, are regulated by an overlapping set of signaling molecules (GSK3 β , mDia) and stabilize MTs, thereby connecting them to the plasma membrane. It is unclear so far whether these MT stabilizers can act on the same MT simultaneously or sequentially, or whether they compete with each other. The only study where two of these +TIPs, CLASP2

Mammalian cortex (interphase)

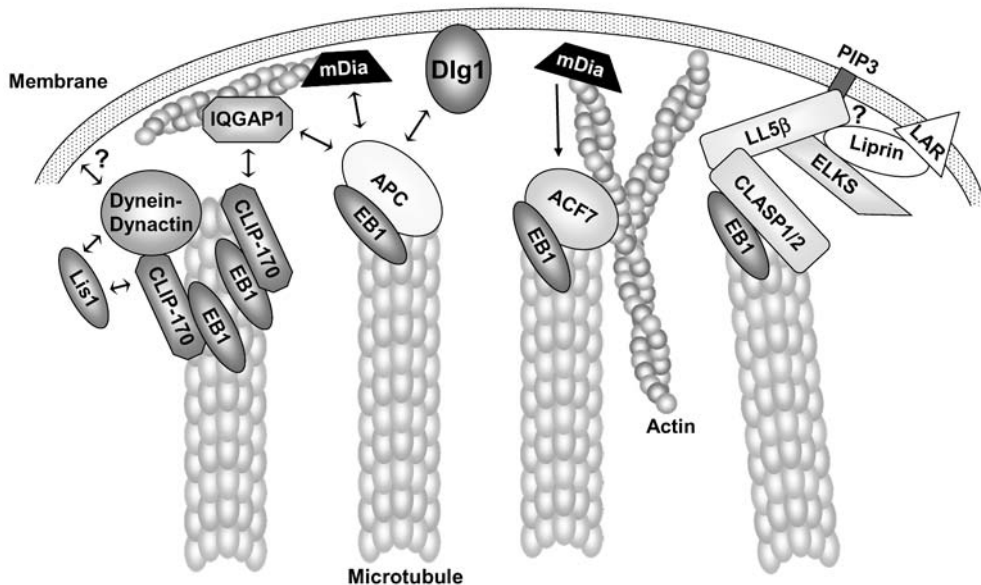


Figure 3: Cortical array of mammalian cells: Mammalian cell cortex during interphase. MTs are targeted to the cortex through different mechanisms, in which actin plays an essential role. Rac1/Cdc42-activated IQGAP1 binds to actin filaments and recruits MT plus-ends bound to CLIP-170 or APC towards the cell margin (83-85, 87, 95, 96). The formin mDia is activated by RhoA, and is also able to connect with the APC/EB1-complex on MT plus-ends (21, 96). The cytoskeletal cross-linker ACF7 links actin with MTs by directly binding MT plus-ends and/or plus-end associated EB1 at the cell margin, possibly also in mDia-regulated fashion (18, 88). APC attaches MT ends to the membrane also in an actin-independent manner, by binding to the large PDZ domain-containing protein Dlg1 (86). Another mechanism of cortical MT capture can be established via CLASP1/2. With the aid of EB1, CLASPs stabilize MTs at the cell cortex, where they form a complex with LL5β and ELKS. This complex can be anchored to the membrane via the pleckstrin homology (PH) domain of LL5β, which binds PIP3, or by binding the Liprin/LAR-complex (Chapter 5 & 6). Dynein-dynactin complex, attached to the cortex by as yet poorly elucidated mechanisms can cause MT sliding along the membrane and exert pulling forces on the MT network (60). CLIP-170 contributes to dynein localization at the tips (32, 34). CLIP-170-dynactin association, as well as dynein activity, can be regulated by Lis1 (32, 93).

and APC, were analyzed in the same system suggests these proteins act differently, as only a subset of CLASP-decorated MTs bears APC clusters (80).

Similar to budding yeast, also in mammals cytoplasmic dynein is involved in MT-cortex interactions (60). Dynein is implicated in centering the centrosome in interphase cells and in positioning the mitotic spindle, as it can pull the plus-ends of cortically attached MTs (Fig. 3b) (60, 89-91). Lis1 and CLIP-170 contribute to this aspect of dynein function, because, as shown in this thesis and other studies, they regulate dynactin association with the microtubule tips (32, 92, 93). Lis1 and dynactin are also believed to regulate dynein

motor activity (93, 94). The nature of the actual link between dynein and the plasma membrane is not yet entirely clear. It may involve dynactin interaction with spectrin (97, 98). In mitotic cells astral MTs are positioned by a complex of dynein-dynactin with NuMa, acting in concert with the mitotic regulator LGN (the mammalian Pins orthologue) and several other polarity factors, such as Inscuteable and Par3 (99). This complex is localized to the cell cortex via the G protein alpha subunit I (G α I). NuMa, bound to LGN and G α I, may be also acting on MTs directly (100). Until now, there are no indications that the dynein-dynactin pathway directly depends on MT stabilizers such as CLASPs, APC or spectraplakins, but this issue deserves further attention.

S. cerevisiae	S. pombe	Plants	Flies	Vertebrates
Bni1p	For3p	Formin-family members	Dia	mDia
Bud6p	Bud6p	x	x	x
Bud14p	Tea4p	x	x	x
Kel1p/Kel2p	Tea1p	x	x	x
Kar9p	x	x	dAPC1, E-APC	APC
Bim1p	Mal3p	EB1	EB1	EB1
Bik1p	Tip1p	x	D-CLIP-190	CLIP-170
Nip100p	Ssm4p	x	Glued	p150Glued
Dyn1	Dhc1	x	Dhc64C	Dynein HC
Pac1p	x	LIS1-like (At5g67320)	LIS1	LIS1
Stu1p	x	CLASP	Orbit/ MAST	CLASP1,2
x	x	x	CG30336	ELKS/CAST
x	x	x	x	LL5 β
x	x	x	Pins / Raps	LGN
x	x	x	x	NuMa
x	x	x	Shot, Kakapo	ACF7/BPAG1
Stu2p	Dis1p	Mor1	Msp	XMAP215/ch-TOG
PLD-1/Spo14	SPAC2F7.16c	PLD	PLD	PLD 1-4
x	x	SPR1	x	x
x	x	MAP-65	x	x

Table 1: Overview of comparable proteins that control the MT cortical array in at least one of the depicted species; yeasts (*S. cerevisiae* & *S. pombe*), Plants (*Arabidopsis thaliana* & *Nicotiana tabacum*), flies (*Drosophila melanogaster*) and Vertebrates (*Xenopus laevis*, *Homo sapiens*, *Mus musculus*). "X" means absence of clear homologues.

There are many other protein candidates that are likely to link MTs to membranes. For instance, CLIPR-59 is a protein belonging to the CLIP family, which associates with lipid rafts and the *trans*-Golgi network (101, 102). Also protein 4.1, an abundant component of human erythrocytes, stabilizes the spectrin-actin network and anchors it to the plasma membrane. It also has a MT binding domain and seems to be involved in MT organization, although its role in this process may be confined to the centrosome rather than the plasma membrane (103, 104). Given the multiplicity of potential cortical attachment factors in the mammalian system, the main challenge now is to characterize their relative importance and functional interplay in different processes, such as cell migration or mitosis.

7.5 Cortical MT arrays in plants.

Except for the mitotic spindle, which is similar in all species, the cytoskeleton of plant cells has a different organization compared to animal cells (105). Dividing plant cells entering the G₂ phase of the cell cycle possess a preprophase band (PPB) that consists of interconnected MTs and microfilaments encircling the nucleus. The PPB predicts the mitotic division plane. Late in mitosis the phragmoplast is formed, which is composed of opposing sets of parallel MTs and microfilaments. This cytoskeletal structure is responsible for the transport of Golgi-derived vesicles to the equatorial region. It forms a network filled with cell wall precursors for separating the two daughter cells. During interphase, MTs form cortical spiral arrays that are perpendicular to the growth direction and very closely apposed to the plasma membrane (106). The cortical MT array controls the directional expansion of plant cells, as well as the deposit of cellulose microfibrils that form the plant-specific cell wall (107-110). Plant cells have centrosomes without centrioles, instead MTs are thought to nucleate at the cortex in a pathway described by the ‘branching’ model (105, 111). According to this model, MT-nucleating templates are produced with the help of katanin by severing MT minus-ends with a γ -tubulin ring complex. These templates are transported by kinesins along the MTs to serve as new MT nucleating sites. Through this way plant cells are guaranteed a continual supply of cortical MTs, which are essential for cell growth. Because of the close proximity of the whole MT array to the plasma membrane, protein complexes at MT plus-ends of plant cells play a less significant role in the control of MT capture, compared to animal or yeast cells. The different cytoskeletal arrays within plant cells are therefore mainly regulated by specific MAPs that bind the whole MT lattice, instead of the +TIPs at MT plus-ends (112-114).

Higher plant cells seem to have several mechanisms to link cortical MTs with the plasma membrane (Fig. 4). MOR1 (MT organization 1) is the *Arabidopsis thaliana*

homologue of the TOGp/XMAP215/Dis1 family, and is involved in the organization and stabilization of the cortical MT array during plant interphase (105, 115, 116). Mutations in MOR1 display a disruption of the cortical MT array, suggesting a possible role for MOR1 in anchoring MTs to the membrane (115). Interestingly, the *Dictyostelium* homologue of MOR1 (DdCP224) is required for the interaction of MT plus-ends with the cell cortex (117). The budding yeast homologue Stu2p affects the dynamics of MT plus-ends and also plays a role in MT interactions with cortical sites in a Kar9p-dependent manner (64, 118). However, the question remains whether MOR1 really anchors MTs at the cortex in plants, and how does it achieve it. The molecular mechanisms involved may be quite diverse in different systems: for example, in *Dictyostelium* DdCP224 acts together with cytoplasmic dynein (117), while *Arabidopsis* lacks dynein-encoding genes altogether.

Another interesting protein found in tobacco (*Nicotiana tabacum*) is the 90-kDa phospholipase D (PLD), which interacts with MTs and the plasma membrane (119). PLDs are also found in *Arabidopsis thaliana*, yeast and mammals, and contain several domains that interact with phospholipids and phosphoinositides in the plasma membrane (e.g. Ca^{2+} -dependent C2 lipid binding domain (only in plants), pleckstrin homology (PH) domain, and a Phox (PX) domain) (119-121). They function as enzymes that catalyze the initial step of

Plant cortex (during interphase)

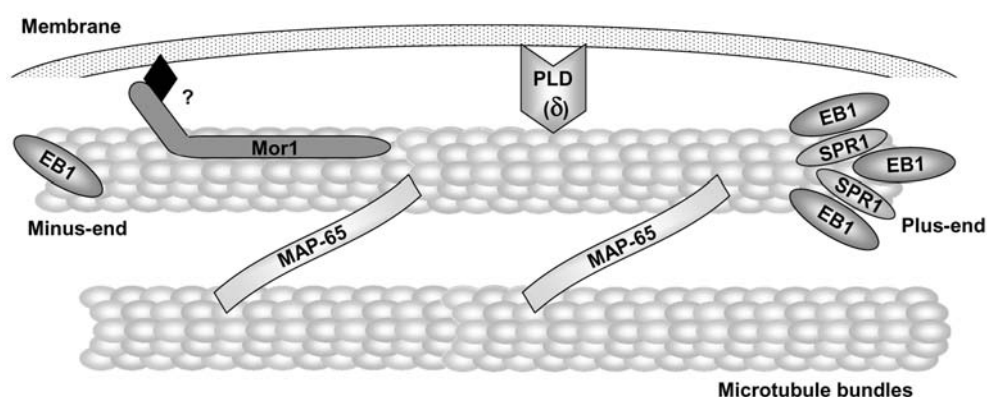


Figure 4: Cortical MT arrays in plants

Combined display of the interphase cortical arrays from different plants. MTs are arranged in spiral arrays in close proximity to the plasma membrane and perpendicular to the growth direction (106). MAP-65 family members are MT bundlers and form cross-bridges that space MTs ~30 nm apart (130). EB1 family members predominantly associate with MT plus-ends together with the plant-specific SPIRAL1 (SPR1), but can also be found at MT minus ends (128, 129, 131, 132). The XMAP215-like Mor1 stabilizes cortical MTs and possibly forms a link with the plasma membrane (105, 115). Also the plant phospholipase D δ (PLD- δ) associates with cortical MTs and contains specific domains to bind the plasma membrane and serve as an anchor protein (119-121, 127, 132). Because of the spiral array of cortical MTs, MAPs play a more prominent role in MT capture compared to +TIPs.

lipid hydrolysis, which produces phosphatidic acid (PA) and free head groups. PA thereby acts as a lipid messenger that is involved in several processes, like secretion, cytoskeleton rearrangement and several signalling pathways (122, 123). It is known that some PLDs directly interact with the cytoskeleton via tubulin or actin, which thereby influence the activity of PLD (124-126). In plants, membrane-associated PLDs appear to form a link with MTs, which is disconnected upon PLD-activation and may induce cytoskeletal reorganization (119, 127). It still remains to be elucidated which form of plant PLD is responsible for linking MTs to the membrane (127).

Similar to yeasts and animals, plants also have proteins that associate specifically with growing MT ends (113). In *Arabidopsis thaliana* three EB1 genes (AtEB1a, AtEB1b and AtEB1c) were identified as the first plant +TIPs, which bind MT ends, cortical MT-nucleation sites, as well as internal membrane organelles (Fig.4) (128, 129). CLIP family members have not been found in plants yet, and at least some plants, such as *Arabidopsis*, completely lack dyneins. However, one CLASP homologue is present in the *Arabidopsis* genome, although there is no indication whether this AtCLASP behaves like a +TIP (78).

Plant genomes encode a whole group of kinesins, some of which are likely to behave as +TIPs (133). These include the minus end directed kinesin-14 ATK5, which tracks the growing MT tips and is distantly related to *S.cerevisiae* Kar3p, a protein responsible for linking shrinking MT ends to the cortex (63, 134). Some plant kinesins are related to the budding yeast Kip2p and Kip3p and the fission yeast Tea2p, which in yeasts are involved in the mechanism of MT-cortex targeting (133, 135). In addition, two *Arabidopsis* kinesins belong to the kinesin-13 family (133). This family comprises proteins with an internal motor, which act as MT destabilizers and can bind to polymerizing MT ends (40, 136). The real function of plant kinesins still needs to be characterized, but considering their homology they will likely resemble their counterparts from other eukaryotes.

In general, the proteins discussed above play overlapping roles in shaping MT arrays and MT targeting to the cell cortex. Although the MT organization varies between different species, many proteins are conserved in evolution and form comparable complexes (Fig. 2, 3, Table 1). However, some proteins are absent in particular species, like CLIP-family members in plants, whereas their binding partners are present. With full knowledge of multiple genomic sequences and extensive proteomic characterization of MT-bound complexes, it seems unlikely that we are missing many MT tip-binding factors and associated components. Still, the mechanistic aspects underlying their function remain elusive, mostly due to the difficulties in reconstructing MT plus-end tracking *in vitro*.

Among all +TIPs, EB1 family members seem to be the most central players. They are multi-functional proteins, which regulate MT dynamics as well as the delivery of diverse

+TIPs to MT plus-ends. The COOH-terminal region of EB1 shares similarities with that of α -tubulin, suggesting that at least some proteins (like the members of the CAP-Gly family) may recognize EBs and tubulin through comparable mechanisms. One could also imagine that while EBs, present at the MT tips, create a sterical hindrance for MT binding by other +TIPs, their tails might form additional accessible binding sites, similar to those of tubulin subunits. Conversely, binding of various COOH-terminal partners may relieve EB auto-inhibition and promote tubulin/MT binding and EB-induced MT polymerization. How the EB1 binding by its multiple partners is regulated remains to be examined. Obviously, phosphorylation is a likely candidate, since EB1 possesses several potential phosphorylation sites including the COOH-terminal tyrosine. In agreement with this notion, in fission yeast only the dephosphorylated form of the EB1 homologue Mal3p can interact with the CLIP-170 homologue Tip1p (12). Moreover, the acidic tail of EB1 is strikingly similar to the tail of α -tubulin and therefore can possibly be detyrosinated by a tubulin carboxypeptidase. This would influence the interaction of EB1 with some partners such as CAP-Gly family members, which require the last tyrosine of EB1 for efficient binding.

Taken together, the existing data suggest that in many (if not all) species EB proteins form the core of the MT tip-associated complexes and may be the key to unravelling the mechanisms of their action on the MT structure and dynamics and their broader role in cellular architecture.

References

1. Kirschner M, Mitchison T. Beyond self-assembly: from microtubules to morphogenesis. *Cell* 1986;45(3):329-42.
2. Mimori-Kiyosue Y, Tsukita S. "Search-and-capture" of microtubules through plus-end-binding proteins (+TIPs). *J Biochem (Tokyo)* 2003;134(3):321-6.
3. Schuyler SC, Pellman D. Microtubule "plus-end-tracking proteins": The end is just the beginning. *Cell* 2001;105(4):421-4.
4. Galjart N, Perez F. A plus-end raft to control microtubule dynamics and function. *Curr Opin Cell Biol* 2003;15(1):48-53.
5. Carvalho P, Tirnauer JS, Pellman D. Surfing on microtubule ends. *Trends Cell Biol* 2003;13(5):229-37.
6. Akhmanova A, Hoogenraad CC. Microtubule plus-end-tracking proteins: mechanisms and functions. *Curr Opin Cell Biol* 2005;17(1):47-54.
7. Tirnauer JS, Bierer BE. EB1 proteins regulate microtubule dynamics, cell polarity, and chromosome stability. *J Cell Biol* 2000;149(4):761-6.
8. Morrison EE, Wardleworth BN, Askham JM, Markham AF, Meredith DM. EB1, a protein which interacts with the APC tumour suppressor, is associated with the microtubule cytoskeleton throughout the cell cycle. *Oncogene* 1998;17(26):3471-7.
9. Rogers SL, Rogers GC, Sharp DJ, Vale RD. *Drosophila* EB1 is important for proper assembly, dynamics, and positioning of the mitotic spindle. *J Cell Biol* 2002;158(5):873-84.
10. Tirnauer JS, O'Toole E, Berrueta L, Bierer BE, Pellman D. Yeast Bim1p promotes the G1-specific dynamics of microtubules. *J Cell Biol* 1999;145(5):993-1007.
11. Tirnauer JS, Grego S, Salmon ED, Mitchison TJ. EB1-microtubule interactions in *Xenopus* egg extracts: role of EB1 in microtubule stabilization and mechanisms of targeting to microtubules. *Mol Biol Cell* 2002;13(10):3614-26.
12. Busch KE, Brunner D. The microtubule plus end-tracking proteins mal3p and tip1p cooperate for cell-end targeting of interphase microtubules. *Curr Biol* 2004;14(7):548-59.
13. Su LK, Burrell M, Hill DE, Gyuris J, Brent R, Wiltshire R, Trent J, Vogelstein B, Kinzler KW. APC binds to the novel protein EB1. *Cancer Res* 1995;55(14):2972-7.
14. Korinek WS, Copeland MJ, Chaudhuri A, Chant J. Molecular linkage underlying microtubule orientation toward cortical sites in yeast. *Science* 2000;287(5461):2257-9.
15. Lee L, Tirnauer JS, Li J, Schuyler SC, Liu JY, Pellman D. Positioning of the mitotic spindle by a cortical-microtubule capture mechanism. *Science* 2000;287(5461):2260-2.
16. Bu W, Su LK. Characterization of functional domains of human EB1 family proteins. *J Biol Chem* 2003;278(50):49721-31.
17. Honnappa S, John CM, Kostrewa D, Winkler FK, Steinmetz MO. Structural insights into the EB1-APC interaction. *Embo J* 2005;24(2):261-9.
18. Slep KC, Rogers SL, Elliott SL, Ohkura H, Kolodziej PA, Vale RD. Structural determinants for EB1-mediated recruitment of APC and spectraplakins to the microtubule plus end. *J Cell Biol* 2005;168(4):587-98.

19. Nakamura M, Zhou XZ, Lu KP. Critical role for the EB1 and APC interaction in the regulation of microtubule polymerization. *Curr Biol* 2001;11(13):1062-7.
20. Zumbunn J, Kinoshita K, Hyman AA, Nathke IS. Binding of the adenomatous polyposis coli protein to microtubules increases microtubule stability and is regulated by GSK3 beta phosphorylation. *Curr Biol* 2001;11(1):44-9.
21. Wen Y, Eng CH, Schmoranz J, Cabrera-Poch N, Morris EJ, Chen M, Wallar BJ, Alberts AS, Gundersen GG. EB1 and APC bind to mDia to stabilize microtubules downstream of Rho and promote cell migration. *Nat Cell Biol* 2004;6(9):820-30.
22. Rogers SL, Wiedemann U, Hacker U, Turck C, Vale RD. Drosophila RhoGEF2 associates with microtubule plus ends in an EB1-dependent manner. *Curr Biol* 2004;14(20):1827-33.
23. Subramanian A, Prokop A, Yamamoto M, Sugimura K, Uemura T, Betschinger J, Knoblich JA, Volk T. Shortstop recruits EB1/APC1 and promotes microtubule assembly at the muscle-tendon junction. *Curr Biol* 2003;13(13):1086-95.
24. Mimori-Kiyosue Y, Grigoriev I, Lansbergen G, Sasaki H, Matsui C, Severin F, Galjart N, Grosveld F, Vorobjev I, Tsukita S, Akhmanova A. CLASP1 and CLASP2 bind to EB1 and regulate microtubule plus-end dynamics at the cell cortex. *J Cell Biol* 2005;168(1):141-53.
25. Akhmanova A, Hoogenraad CC, Drabek K, Stepanova T, Dortland B, Verkerk T, Vermeulen W, Burgering BM, De Zeeuw CI, Grosveld F, Galjart N. Clasps are CLIP-115 and -170 associating proteins involved in the regional regulation of microtubule dynamics in motile fibroblasts. *Cell* 2001;104(6):923-35.
26. Maiato H, Khodjakov A, Rieder CL. Drosophila CLASP is required for the incorporation of microtubule subunits into fluxing kinetochore fibres. *Nat Cell Biol* 2005;7(1):42-7.
27. Hayashi I, Ikura M. Crystal structure of the amino-terminal microtubule-binding domain of end-binding protein 1 (EB1). *J Biol Chem* 2003;278(38):36430-4.
28. Galjart N. CLIPs and CLASPs and cellular dynamics. *Nat Rev Mol Cell Biol* 2005;6(6):487-98.
29. Ligon LA, Shelly SS, Tokito M, Holzbaur EL. The microtubule plus-end proteins EB1 and dynactin have differential effects on microtubule polymerization. *Mol Biol Cell* 2003;14(4):1405-17.
30. Askham JM, Vaughan KT, Goodson HV, Morrison EE. Evidence that an interaction between EB1 and p150(Glued) is required for the formation and maintenance of a radial microtubule array anchored at the centrosome. *Mol Biol Cell* 2002;13(10):3627-45.
31. Hayashi I, Wilde A, Mal TK, Ikura M. Structural Basis for the Activation of Microtubule Assembly by the EB1 and p150(Glued) Complex. *Mol Cell* 2005;19(4):449-60.
32. Lansbergen G, Komarova Y, Modesti M, Wyman C, Hoogenraad CC, Goodson HV, Lemaitre RP, Drechsel DN, van Munster E, Gadella TW, Jr., Grosveld F, Galjart N, Borisy GG, Akhmanova A. Conformational changes in CLIP-170 regulate its binding to microtubules and dynactin localization. *J Cell Biol* 2004;166(7):1003-14.
33. Komarova YA, Akhmanova AS, Kojima S, Galjart N, Borisy GG. Cytoplasmic linker proteins promote microtubule rescue in vivo. *J Cell Biol* 2002;159(4):589-99.

34. Goodson HV, Skube SB, Stalder R, Valetti C, Kreis TE, Morrison EE, Schroer TA. CLIP-170 interacts with dynactin complex and the APC-binding protein EB1 by different mechanisms. *Cell Motil Cytoskeleton* 2003;55(3):156-73.
35. Dzhindzhev NS, Rogers SL, Vale RD, Ohkura H. Distinct mechanisms govern the localisation of *Drosophila* CLIP-190 to unattached kinetochores and microtubule plus-ends. *J Cell Sci* 2005;118(Pt 16):3781-90.
36. Komarova Y, Lansbergen G, Galjart N, Grosveld F, Borisy GG, Akhmanova A. EB1 and EB3 Control CLIP Dissociation from the Ends of Growing Microtubules. *Mol Biol Cell* 2005.
37. Carvalho P, Gupta ML, Jr., Hoyt MA, Pellman D. Cell cycle control of kinesin-mediated transport of Bik1 (CLIP-170) regulates microtubule stability and dynein activation. *Dev Cell* 2004;6(6):815-29.
38. Badin-Larcon AC, Boscheron C, Soleilhac JM, Piel M, Mann C, Denarier E, Fourest-Lieuvin A, Lafanechere L, Bornens M, Job D. Suppression of nuclear oscillations in *Saccharomyces cerevisiae* expressing Glu tubulin. *Proc Natl Acad Sci U S A* 2004;101(15):5577-82.
39. Erck C, Peris L, Andrieux A, Meissirel C, Gruber AD, Vernet M, Schweitzer A, Saoudi Y, Pointu H, Bosc C, Salin PA, Job D, Wehland J. A vital role of tubulin-tyrosine-ligase for neuronal organization. *Proc Natl Acad Sci U S A* 2005;102(22):7853-8.
40. Mennella V, Rogers GC, Rogers SL, Buster DW, Vale RD, Sharp DJ. Functionally distinct kinesin-13 family members cooperate to regulate microtubule dynamics during interphase. *Nat Cell Biol* 2005;7(3):235-45.
41. Chen CR, Chen J, Chang EC. A conserved interaction between Moe1 and Mal3 is important for proper spindle formation in *Schizosaccharomyces pombe*. *Mol Biol Cell* 2000;11(12):4067-77.
42. Rehberg M, Graf R. Dictyostelium EB1 is a genuine centrosomal component required for proper spindle formation. *Mol Biol Cell* 2002;13(7):2301-10.
43. Busch KE, Hayles J, Nurse P, Brunner D. Tea2p kinesin is involved in spatial microtubule organization by transporting tip1p on microtubules. *Dev Cell* 2004;6(6):831-43.
44. Chen XP, Yin H, Huffaker TC. The yeast spindle pole body component Spc72p interacts with Stu2p and is required for proper microtubule assembly. *J Cell Biol* 1998;141(5):1169-79.
45. Popov AV, Karsenti E. Stu2p and XMAP215: turncoat microtubule-associated proteins? *Trends Cell Biol* 2003;13(11):547-50.
46. van Breugel M, Drechsel D, Hyman A. Stu2p, the budding yeast member of the conserved Dis1/XMAP215 family of microtubule-associated proteins is a plus end-binding microtubule destabilizer. *J Cell Biol* 2003;161(2):359-69.
47. Shirasu-Hiza M, Coughlin P, Mitchison T. Identification of XMAP215 as a microtubule-destabilizing factor in *Xenopus* egg extract by biochemical purification. *J Cell Biol* 2003;161(2):349-58.
48. Holmfeldt P, Stenmark S, Gullberg M. Differential functional interplay of TOGp/XMAP215 and the KinI kinesin MCAK during interphase and mitosis. *Embo J* 2004;23(3):627-37.

49. Noetzel TL, Drechsel DN, Hyman AA, Kinoshita K. A comparison of the ability of XMAP215 and tau to inhibit the microtubule destabilizing activity of XKCM1. *Philos Trans R Soc Lond B Biol Sci* 2005;360(1455):591-4.
50. Raviv U, Needleman DJ, Li Y, Miller HP, Wilson L, Safinya CR. Cationic liposome-microtubule complexes: Pathways to the formation of two-state lipid-protein nanotubes with open or closed ends. *Proc Natl Acad Sci U S A* 2005.
51. Huisman SM, Segal M. Cortical capture of microtubules and spindle polarity in budding yeast - where's the catch? *J Cell Sci* 2005;118(Pt 3):463-71.
52. Liakopoulos D, Kusch J, Grava S, Vogel J, Barral Y. Asymmetric loading of Kar9 onto spindle poles and microtubules ensures proper spindle alignment. *Cell* 2003;112(4):561-74.
53. Maekawa H, Usui T, Knop M, Schiebel E. Yeast Cdk1 translocates to the plus end of cytoplasmic microtubules to regulate bud cortex interactions. *Embo J* 2003;22(3):438-49.
54. Maekawa H, Schiebel E. Cdk1-Clb4 controls the interaction of astral microtubule plus ends with subdomains of the daughter cell cortex. *Genes Dev* 2004;18(14):1709-24.
55. Miller RK, Matheos D, Rose MD. The cortical localization of the microtubule orientation protein, Kar9p, is dependent upon actin and proteins required for polarization. *J Cell Biol* 1999;144(5):963-75.
56. Huisman SM, Bales OA, Bertrand M, Smeets MF, Reed SI, Segal M. Differential contribution of Bud6p and Kar9p to microtubule capture and spindle orientation in *S. cerevisiae*. *J Cell Biol* 2004;167(2):231-44.
57. Segal M, Bloom K, Reed SI. Kar9p-independent microtubule capture at Bud6p cortical sites primes spindle polarity before bud emergence in *Saccharomyces cerevisiae*. *Mol Biol Cell* 2002;13(12):4141-55.
58. Sheeman B, Carvalho P, Sagot I, Geiser J, Kho D, Hoyt MA, Pellman D. Determinants of *S. cerevisiae* dynein localization and activation: implications for the mechanism of spindle positioning. *Curr Biol* 2003;13(5):364-72.
59. Lee WL, Oberle JR, Cooper JA. The role of the lissencephaly protein Pac1 during nuclear migration in budding yeast. *J Cell Biol* 2003;160(3):355-64.
60. Dujardin DL, Vallee RB. Dynein at the cortex. *Curr Opin Cell Biol* 2002;14(1):44-9.
61. Farkasovsky M, Kuntzel H. Cortical Num1p interacts with the dynein intermediate chain Pac11p and cytoplasmic microtubules in budding yeast. *J Cell Biol* 2001;152(2):251-62.
62. Knaus M, Cameroni E, Pedruzzi I, Tatchell K, De Virgilio C, Peter M. The Bud14p-Glc7p complex functions as a cortical regulator of dynein in budding yeast. *Embo J* 2005;24(17):3000-11.
63. Maddox PS, Stemple JK, Satterwhite L, Salmon ED, Bloom K. The minus end-directed motor Kar3 is required for coupling dynamic microtubule plus ends to the cortical shmoo tip in budding yeast. *Curr Biol* 2003;13(16):1423-8.
64. Miller RK, Cheng SC, Rose MD. Bim1p/Yeb1p mediates the Kar9p-dependent cortical attachment of cytoplasmic microtubules. *Mol Biol Cell* 2000;11(9):2949-59.
65. Martin SG, Chang F. New End Take Off: Regulating Cell Polarity during the Fission Yeast Cell Cycle. *Cell Cycle* 2005;4(8).
66. Browning H, Hackney DD. The EB1 homolog Mal3 stimulates the ATPase of the kinesin Tea2 by recruiting it to the microtubule. *J Biol Chem* 2005;280(13):12299-304.

67. Browning H, Hackney DD, Nurse P. Targeted movement of cell end factors in fission yeast. *Nat Cell Biol* 2003;5(9):812-8.
68. Feierbach B, Verde F, Chang F. Regulation of a formin complex by the microtubule plus end protein tea1p. *J Cell Biol* 2004;165(5):697-707.
69. Snaith HA, Sawin KE. Fission yeast mod5p regulates polarized growth through anchoring of tea1p at cell tips. *Nature* 2003;423(6940):647-51.
70. Martin SG, McDonald WH, Yates JR, 3rd, Chang F. Tea4p links microtubule plus ends with the formin for3p in the establishment of cell polarity. *Dev Cell* 2005;8(4):479-91.
71. Glynn JM, Lustig RJ, Berlin A, Chang F. Role of bud6p and tea1p in the interaction between actin and microtubules for the establishment of cell polarity in fission yeast. *Curr Biol* 2001;11(11):836-45.
72. Castagnetti S, Behrens R, Nurse P. End4/Sla2 is involved in establishment of a new growth zone in *Schizosaccharomyces pombe*. *J Cell Sci* 2005;118(Pt 9):1843-50.
73. Sun Y, Kaksonen M, Madden DT, Schekman R, Drubin DG. Interaction of Sla2p's ANTH domain with PtdIns(4,5)P₂ is important for actin-dependent endocytic internalization. *Mol Biol Cell* 2005;16(2):717-30.
74. Dong Y, Pruyne D, Bretscher A. Formin-dependent actin assembly is regulated by distinct modes of Rho signaling in yeast. *J Cell Biol* 2003;161(6):1081-92.
75. Ge W, Chew TG, Wachtler V, Naqvi SN, Balasubramanian MK. The Novel Fission Yeast Protein Pal1p Interacts with Hip1-related Sla2p/End4p and Is Involved in Cellular Morphogenesis. *Mol Biol Cell* 2005.
76. Inoue YH, do Carmo Avides M, Shiraki M, Deak P, Yamaguchi M, Nishimoto Y, Matsukage A, Glover DM. Orbit, a novel microtubule-associated protein essential for mitosis in *Drosophila melanogaster*. *J Cell Biol* 2000;149(1):153-66.
77. Lemos CL, Sampaio P, Maiato H, Costa M, Omel'yanchuk LV, Liberal V, Sunkel CE. Mast, a conserved microtubule-associated protein required for bipolar mitotic spindle organization. *Embo J* 2000;19(14):3668-82.
78. Gardiner J, Marc J. Putative microtubule-associated proteins from the Arabidopsis genome. *Protoplasma* 2003;222(1-2):61-74.
79. Yin H, You L, Pasqualone D, Kopski KM, Huffaker TC. Stu1p is physically associated with beta-tubulin and is required for structural integrity of the mitotic spindle. *Mol Biol Cell* 2002;13(6):1881-92.
80. Wittmann T, Waterman-Storer CM. Spatial regulation of CLASP affinity for microtubules by Rac1 and GSK3{beta} in migrating epithelial cells. *J Cell Biol* 2005;169(6):929-39.
81. Paravitane V, Coadwell WJ, Eguinoa A, Hawkins PT, Stephens L. LL5beta is a phosphatidylinositol (3,4,5)-trisphosphate sensor that can bind the cytoskeletal adaptor, gamma-filamin. *J Biol Chem* 2003;278(2):1328-35.
82. Reilein A, Nelson WJ. APC is a component of an organizing template for cortical microtubule networks. *Nat Cell Biol* 2005;7(5):463-73.
83. Tirnauer JS. A new cytoskeletal connection for APC: linked to actin through IQGAP. *Dev Cell* 2004;7(6):778-80.
84. Watanabe T, Wang S, Noritake J, Sato K, Fukata M, Takefuji M, Nakagawa M, Izumi N, Akiyama T, Kaibuchi K. Interaction with IQGAP1 links APC to Rac1, Cdc42, and actin filaments during cell polarization and migration. *Dev Cell* 2004;7(6):871-83.

85. Noritake J, Watanabe T, Sato K, Wang S, Kaibuchi K. IQGAP1: a key regulator of adhesion and migration. *J Cell Sci* 2005;118(Pt 10):2085-92.
86. Etienne-Manneville S, Manneville JB, Nicholls S, Ferenczi MA, Hall A. Cdc42 and Par6-PKC{zeta} regulate the spatially localized association of Dlg1 and APC to control cell polarization. *J Cell Biol* 2005;170(6):895-901.
87. Fukata M, Watanabe T, Noritake J, Nakagawa M, Yamaga M, Kuroda S, Matsuura Y, Iwamatsu A, Perez F, Kaibuchi K. Rac1 and Cdc42 capture microtubules through IQGAP1 and CLIP-170. *Cell* 2002;109(7):873-85.
88. Kodama A, Karakesisoglou I, Wong E, Vaezi A, Fuchs E. ACF7: an essential integrator of microtubule dynamics. *Cell* 2003;115(3):343-54.
89. Gomes ER, Jani S, Gundersen GG. Nuclear movement regulated by Cdc42, MRCK, myosin, and actin flow establishes MTOC polarization in migrating cells. *Cell* 2005;121(3):451-63.
90. Gonczy P. Mechanisms of spindle positioning: focus on flies and worms. *Trends Cell Biol* 2002;12(7):332-9.
91. Xiang X. LIS1 at the microtubule plus end and its role in dynein-mediated nuclear migration. *J Cell Biol* 2003;160(3):289-90.
92. Coquelle FM, Caspi M, Cordelieres FP, Dompierre JP, Dujardin DL, Koifman C, Martin P, Hoogenraad CC, Akhmanova A, Galjart N, De Mey JR, Reiner O. LIS1, CLIP-170's key to the dynein/dynactin pathway. *Mol Cell Biol* 2002;22(9):3089-102.
93. Tai CY, Dujardin DL, Faulkner NE, Vallee RB. Role of dynein, dynactin, and CLIP-170 interactions in LIS1 kinetochore function. *J Cell Biol* 2002;156(6):959-68.
94. King SJ, Schroer TA. Dynactin increases the processivity of the cytoplasmic dynein motor. *Nat Cell Biol* 2000;2(1):20-4.
95. Muresan V, Stankewich MC, Steffen W, Morrow JS, Holzbaur EL, Schnapp BJ. Dynactin-dependent, dynein-driven vesicle transport in the absence of membrane proteins: a role for spectrin and acidic phospholipids. *Mol Cell* 2001;7(1):173-83.
96. Holleran EA, Ligon LA, Tokito M, Stankewich MC, Morrow JS, Holzbaur EL. beta III spectrin binds to the Arp1 subunit of dynactin. *J Biol Chem* 2001;276(39):36598-605.
97. Lechler T, Fuchs E. Asymmetric cell divisions promote stratification and differentiation of mammalian skin. *Nature* 2005;437(7056):275-80.
98. Du Q, Macara IG. Mammalian Pins is a conformational switch that links NuMA to heterotrimeric G proteins. *Cell* 2004;119(4):503-16.
99. Gundersen GG. Microtubule capture: IQGAP and CLIP-170 expand the repertoire. *Curr Biol* 2002;12(19):R645-7.
100. Fukata M, Nakagawa M, Kaibuchi K. Roles of Rho-family GTPases in cell polarisation and directional migration. *Curr Opin Cell Biol* 2003;15(5):590-7.
101. Perez F, Pernet-Gallay K, Nizak C, Goodson HV, Kreis TE, Goud B. CLIPR-59, a new trans-Golgi/TGN cytoplasmic linker protein belonging to the CLIP-170 family. *J Cell Biol* 2002;156(4):631-42.
102. Lallemand-Breitenbach V, Quesnoit M, Braun V, El Marjou A, Pous C, Goud B, Perez F. CLIPR-59 is a lipid raft-associated protein containing a cytoskeleton-associated protein glycine-rich domain (CAP-Gly) that perturbs microtubule dynamics. *J Biol Chem* 2004;279(39):41168-78.
103. Perez-Ferreiro CM, Vernos I, Correas I. Protein 4.1R regulates interphase microtubule organization at the centrosome. *J Cell Sci* 2004;117(Pt 25):6197-206.

104. Hoover KB, Bryant PJ. The genetics of the protein 4.1 family: organizers of the membrane and cytoskeleton. *Curr Opin Cell Biol* 2000;12(2):229-34.
105. Wasteneys GO. Microtubule organization in the green kingdom: chaos or self-order? *J Cell Sci* 2002;115(Pt 7):1345-54.
106. Lloyd C, Chan J. Helical microtubule arrays and spiral growth. *Plant Cell* 2002;14(10):2319-24.
107. Baskin TI. On the alignment of cellulose microfibrils by cortical microtubules: a review and a model. *Protoplasma* 2001;215(1-4):150-71.
108. Baskin TI, Beemster GT, Judy-March JE, Marga F. Disorganization of cortical microtubules stimulates tangential expansion and reduces the uniformity of cellulose microfibril alignment among cells in the root of *Arabidopsis*. *Plant Physiol* 2004;135(4):2279-90.
109. Lloyd C, Chan J. Microtubules and the shape of plants to come. *Nat Rev Mol Cell Biol* 2004;5(1):13-22.
110. Wasteneys GO, Galway ME. Remodeling the cytoskeleton for growth and form: an overview with some new views. *Annu Rev Plant Biol* 2003;54:691-722.
111. Cyr R. How and Y plant microtubules branch. *Nat Cell Biol* 2005;7(10):927-9.
112. Hashimoto T. Dynamics and regulation of plant interphase microtubules: a comparative view. *Curr Opin Plant Biol* 2003;6(6):568-76.
113. Bisgrove SR, Hable WE, Kropf DL. +TIPs and microtubule regulation. The beginning of the plus end in plants. *Plant Physiol* 2004;136(4):3855-63.
114. Sedbrook JC. MAPs in plant cells: delineating microtubule growth dynamics and organization. *Curr Opin Plant Biol* 2004;7(6):632-40.
115. Whittington AT, Vugrek O, Wei KJ, Hasenbein NG, Sugimoto K, Rashbrooke MC, Wasteneys GO. MOR1 is essential for organizing cortical microtubules in plants. *Nature* 2001;411(6837):610-3.
116. Gard DL, Becker BE, Josh Romney S. MAPping the eukaryotic tree of life: structure, function, and evolution of the MAP215/Dis1 family of microtubule-associated proteins. *Int Rev Cytol* 2004;239:179-272.
117. Hestermann A, Graf R. The XMAP215-family protein DdCP224 is required for cortical interactions of microtubules. *BMC Cell Biol* 2004;5(1):24.
118. Kosco KA, Pearson CG, Maddox PS, Wang PJ, Adams IR, Salmon ED, Bloom K, Huffaker TC. Control of microtubule dynamics by Stu2p is essential for spindle orientation and metaphase chromosome alignment in yeast. *Mol Biol Cell* 2001;12(9):2870-80.
119. Gardiner JC, Harper JD, Weerakoon ND, Collings DA, Ritchie S, Gilroy S, Cyr RJ, Marc J. A 90-kD phospholipase D from tobacco binds to microtubules and the plasma membrane. *Plant Cell* 2001;13(9):2143-58.
120. Wang X. Multiple forms of phospholipase D in plants: the gene family, catalytic and regulatory properties, and cellular functions. *Prog Lipid Res* 2000;39(2):109-49.
121. Wang X. Phospholipase D in hormonal and stress signaling. *Curr Opin Plant Biol* 2002;5(5):408-14.
122. Wang X. Lipid signaling. *Curr Opin Plant Biol* 2004;7(3):329-36.
123. Banno Y, Takuwa Y, Akao Y, Okamoto H, Osawa Y, Naganawa T, Nakashima S, Suh PG, Nozawa Y. Involvement of phospholipase D in sphingosine 1-phosphate-induced activation of phosphatidylinositol 3-kinase and Akt in Chinese hamster ovary cells overexpressing EDG3. *J Biol Chem* 2001;276(38):35622-8.

124. Lee S, Park JB, Kim JH, Kim Y, Shin KJ, Lee JS, Ha SH, Suh PG, Ryu SH. Actin directly interacts with phospholipase D, inhibiting its activity. *J Biol Chem* 2001;276(30):28252-60.
125. Chae YC, Lee S, Lee HY, Heo K, Kim JH, Suh PG, Ryu SH. Inhibition of muscarinic receptor-linked phospholipase D activation by association with tubulin. *J Biol Chem* 2005;280(5):3723-30.
126. Kusner DJ, Barton JA, Qin C, Wang X, Iyer SS. Evolutionary conservation of physical and functional interactions between phospholipase D and actin. *Arch Biochem Biophys* 2003;412(2):231-41.
127. Dhonukshe P, Laxalt AM, Goedhart J, Gadella TW, Munnik T. Phospholipase d activation correlates with microtubule reorganization in living plant cells. *Plant Cell* 2003;15(11):2666-79.
128. Chan J, Calder GM, Doonan JH, Lloyd CW. EB1 reveals mobile microtubule nucleation sites in Arabidopsis. *Nat Cell Biol* 2003;5(11):967-71.
129. Mathur J, Mathur N, Kernebeck B, Srinivas BP, Hulskamp M. A novel localization pattern for an EB1-like protein links microtubule dynamics to endomembrane organization. *Curr Biol* 2003;13(22):1991-7.
130. Chan J, Mao G, Smertenko A, Hussey PJ, Naldrett M, Bottrill A, Lloyd CW. Identification of a MAP65 isoform involved in directional expansion of plant cells. *FEBS Lett* 2003;534(1-3):161-3.
131. Nakajima K, Furutani I, Tachimoto H, Matsubara H, Hashimoto T. SPIRAL1 encodes a plant-specific microtubule-localized protein required for directional control of rapidly expanding Arabidopsis cells. *Plant Cell* 2004;16(5):1178-90.
132. Sedbrook JC, Ehrhardt DW, Fisher SE, Scheible WR, Somerville CR. The Arabidopsis sku6/spiral1 gene encodes a plus end-localized microtubule-interacting protein involved in directional cell expansion. *Plant Cell* 2004;16(6):1506-20.
133. Reddy AS, Day IS. Kinesins in the Arabidopsis genome: a comparative analysis among eukaryotes. *BMC Genomics* 2001;2(1):2.
134. Ambrose JC, Li W, Marcus A, Ma H, Cyr R. A minus-end-directed kinesin with plus-end tracking protein activity is involved in spindle morphogenesis. *Mol Biol Cell* 2005;16(4):1584-92.
135. Schuyler SC, Pellman D. Search, capture and signal: games microtubules and centrosomes play. *J Cell Sci* 2001;114(Pt 2):247-55.
136. Moore AT, Rankin KE, von Dassow G, Peris L, Wagenbach M, Ovechkina Y, Andrieux A, Job D, Wordeman L. MCAK associates with the tips of polymerizing microtubules. *J Cell Biol* 2005;169(3):391-7.



Appendixes

Appendix A

Mass Spectrometry results for Bio-GFP-CLASP2 α (Q-TOF)

Identified proteins	Molecular weight (D)	NCBI GI number	Mascot Score	Identified Peptides
KIAA0467	59124	55960666	37	1
NEDD5 protein, Septin2	42886	23274163	41	1
KIAA0002, chaperonin containing TCP1, subunit 8	59035	1136741	412	8
TCP1 protein, t-complex 1	60819	12653759	56	2
Zinc finger CCH type antiviral protein 1	68717	16550682	190	6
Cortactin	71599	21707902	57	1
Serine/threonine protein kinase, MARK2	83524	7446398	96	3
Hypothetical protein FLJ23790	66060	21450643	96	2
Hect domain and RLD 5, HECT E3 ubiquitin ligase	118199	7705931	49	1
Actinin alpha	104358	4501893	44	1
Epidermal Langerhans cell protein LCP1	66552	7662274	71	2
NIMA-related kinase	108849	4885695	48	1
Rab6 interacting protein 2 (ELKS, ERC1, CAST2)	108840	14149661	73	3
LL5 beta protein	142813	27650425	317	8
Microtubule-vesicle linker CLIP-170 - human	157440	420071	755	19
CENPJ, Centromere protein J	154120	19923548	43	1
CLIP-associating protein 2, CLASP2	145046	7513045	2275	45
GRIP coiled-coil protein GCC185 isoform a	196873	31563507	459	15
CH-TOG protein (XMAP 215 homologue)	227076	3121951	88	3
Dystonin isoform 1, bullous pemphigoid antigen 1	632532	34577047	673	27
Plectin 1	515332	41322908	587	21
KIAA0754	123177	20521149	92	2

Mass Spectrometry results for Bio-GFP-ELKS α (Q-TOF)

Identified proteins	Molecular weight (D)	NCBI GI number	Mascot Score	Identified Peptides
Transcription factor NF-AT 45K chain	44898	1082855	82	1
Flotillin 1	47554	5031699	45	1
Novel protein HSPC117	55688	4468866	51	1
Cytoplasmic chaperonin hTRiC5 (gamma subunit of CCT chaperonin)	60862	609308	71	2
Growth regulated nuclear 68 protein	67394	226021	69	3
DDX17 protein, DEAD (Asp-Glu-Ala-Asp) box polypeptide 17, RNA helicase	72953	12653635	58	2
Zinc finger CCCH type antiviral protein 1	68717	16550682	434	6
Fragile X mental retardation syndrome protein, FMRP	70325	457237	98	2
HnRNA-binding protein M4	77897	479852	72	2
DEAD/H (Asp-Glu-Ala-Asp/His) box polypeptide 3	73625	13514817	67	1
KIAA1321, FMRP Interacting RNA binding protein	78137	7243023	163	4
Rab6 interacting protein 2 (ELKS, ERC1, CAST2)	108840	14149661	1450	36
Hect domain and RLD 5	118199	7705931	52	1
Liprin-beta1, protein-tyrosine phosphatase-interact. protein	113632	3309539	61	1
LL5 beta protein	142813	27650425	1332	25
LL5 alpha, KIAA0638, pleckstrin homology-like domain	152923	20521113	181	8
CAST1, KIAA0378 (cytomatrix protein p110, CAZ-associated structural protein)	112200	20521019	44	4

Mass Spectrometry results for Bio-GFP-LL5 β (Q-TOF)

Identified proteins	Molecular weight (D)	NCBI GI number	Mascot Score	Identified Peptides
Chromosome 19 open reading frame 21	75482	27735067	80	3
Hypothetical protein FLJ23790	66060	21450643	90	3
Alpha actinin	102661	2804273	77	2
Rab6 interacting protein 2 epsilon (ELKS, ERC1, CAST2)	128236	38045898	1296	30
Desmoglein2 preproprotein	123050	4503403	35	2
CLIP-associating protein 2, CLASP2	145046	7513045	93	2
Multiple aster 1, CLASP1	142315	7513102	88	2
Clathrin heavy chain 1	193260	4758012	42	1
LL5 beta protein	142813	27650425	2569	54
Ubiquitin specific protease 9	292860	11641423	93	3
Plectin 1 isoform 11	517822	41322923	1932	50
Plectin 1 isoform 6	533462	41322916	1907	51

The tables show proteins identified in pull downs with streptavidin beads from extracts of HeLa cells co-expressing biotin ligase BirA and Biotin-tagged GFP-CLASP2, ELKS α or LL5 β . The lists are corrected for background proteins, which were identified in a control pull-down using extracts of HeLa cells expressing BirA only. For each identified protein, the lists are filtered for duplicates and show only the hits with the highest Mascot score and most identified peptides.

Appendix B

Mass Spectrometry results for Bio-GFP-LL5 β -C (Q-TOF)

Identified proteins	Molecular weight (D)	NCBI GI number	Mascot Score	Identified Peptides
GTP-binding protein Rab8 / H-ray	22891	2144600	44	1
14-3-3 protein zeta (YWHAZ)	27899	55631158	190	4
Nascent polypeptide-associated complex alpha chain	23370	4092060	292	3
Lung cancer oncogene 7, GTP-binding regulatory protein	38378	37724561	201	6
Calponin-2	33943	6226844	51	1
GTP-binding regulatory protein beta-2 chain	38048	40032497	80	2
CPNE5, Copine V, Ca ⁺⁺ -dep. membrane binding protein	32781	31753190	41	1
Zyxin (Focal adhesion)	61238	7513441	21	1
PDE4D protein (Phosphodiesterase 4D, cAMP-specific)	24413	32306513	22	1
Transportin 2 (Importin 3, karyopherin beta 2b)	101909	19923142	112	2
Importin beta subunit b	98062	5107670	42	1
Programmed cell death 6 interacting protein	97395	22027538	34	1
Neurabin II, spinophilin, protein phosphatase-1	89629	13928136	134	4
Liprin beta 1, Protein Tyrosin Phosphatase Receptor Type F interacting protein	113641	3309539	148	3
Protein kinase N2 (EC 2.7.1.-) PRK2	112834	56204512	49	1
RAB6 interacting protein 2 (ELKS, ERC1, CAST2)	113966	38045898	33	1
LL5 beta protein (including peptides end. LL5 beta)	142813	27650425	450	10
Leucine-rich PPR motif-containing protein	159023	31074371	263	7
Liprin alpha, LAR-interacting protein, PPFIA1 protein	136135	21707845	106	4
Coatomer complex alpha chain homolog	139810	1002369	70	1
MAPK/ERK kinase kinase kinase 4	142767	29427585	53	2
LAR; Receptor-type tyrosine-protein phosphatase F precursor	212929	125978	50	3
High density lipoprotein-binding protein	141990	345882	38	1
Scribble isoform a	175809	18032008	124	4
Hypothetical protein FLJ20035 (dead-domain, DNA-replication, helicase)	199729	23958712	125	4

IQGAP1, Ras GTPase activating protein-related protein	191936	62089472	97	3
KIAA1728 protein, Tanc	181171	12698001	43	1
Talin 1	257920	55859707	63	3
Filamin B	276765	53791217	53	2

The table shows proteins identified in a pull down with streptavidin beads from an extract of formaldehyde cross-linked HeLa cells co-expressing biotin ligase BirA and Biotin-tagged GFP-LL5 β -C. The list is corrected for background proteins, which were identified in a control pull-down using extracts of HeLa cells expressing BirA only. For each identified protein, the lists are filtered for duplicates and show only the hits with the highest Mascot score and most identified peptides.



Summary

Summary:

The cytoskeleton of eukaryotic cells consists of three main types of structures: actin filaments, intermediate filaments and microtubules. This thesis is focused on microtubules and in particular on proteins that specifically bind to microtubules. Microtubules have a polarized structure. They are made up of α/β -tubulin heterodimers that polymerize in a head-to-tail fashion into linear protofilaments. Generally, 13 protofilaments associate laterally and with the same polarity to shape a hollow tube with a diameter of 20-25 nm, the microtubule. Microtubules have a slow growing minus-end and a fast growing plus-end, where the tubulin heterodimers can be incorporated. Since microtubules can grow (polymerize) or shrink (depolymerize), the cell is able to re-arrange its microtubule network very rapidly. When a microtubule shifts from a growing phase to a shrinking phase, this is called catastrophe. The opposite transition, when a microtubule starts growing again after a phase of shrinking, is called rescue. The process of switching between these different microtubule states is called dynamic instability. In many cell types, microtubules are nucleated at the centrosome, or the microtubule organizing centre (MTOC) and remain attached to it with their minus-ends, while the plus-ends grow towards the cell periphery. While growing, microtubules can search and capture diverse targets in a three-dimensional cytoplasmic space. This process can be random, but it may also be regulated by specific proteins that guide microtubules to certain contact sites. The plus ends of microtubules interact with specific microtubule plus-end binding proteins (also known as plus-end tracking proteins, or +TIPs). Since many +TIPs can associate with each other, a variety of protein complexes can be formed on microtubule tips. This thesis focuses on the functional analysis of the protein interactions at the microtubule plus-ends.

Chapter 2 shows how the +TIP CLIP-170 (cytoplasmic linker protein of 170 kDa) regulates its association with microtubules by changing its conformation. CLIP-170 contains two CAP-Gly domains at the NH₂ terminus that interact with microtubules, and two metal-binding domains at the COOH terminus to interact with various partners. The NH₂ terminus of CLIP-170 interacts directly with the COOH terminus via its first metal-binding domain. Other binding partners such as the dynactin subunit p150^{Glued} and LIS1 also interact with the COOH terminus of CLIP-170, but depend on the second metal-binding domain. Microtubule association of CLIP-170 is inhibited by its folded head-to-tail conformation, which in addition interferes with the binding of dynactin and LIS1 to the CLIP-170 COOH terminus.

Chapter 3 describes the functional relationship of CLIP-170 and CLIP-115 with the three EB family members EB1, EB2 and EB3. Several biochemical assays demonstrated that CLIPs directly interact with the COOH terminus of the EB proteins. This interaction is essential for the normal localization of CLIP-170 and enhances its intrinsic affinity for growing microtubule ends.

CLIP-associating proteins, CLASP1 and CLASP2 are two +TIPs that play redundant roles in regulating the density, stability and dynamics of interphase microtubules. Chapter 4 demonstrates that CLASPs stabilize microtubules at the cell periphery, possibly by forming a complex with EB1 at microtubule tips. CLASPs associate with the cortex in a microtubule-independent manner and mediate interactions between microtubule tips and the plasma membrane. Since CLASPs lack membrane-binding domains, their cortical localization depends on membrane-bound partners. Chapter 5 describes the identification of two novel cortical partners of CLASP1 and CLASP2 by using pull down assays coupled to mass spectrometry. These partners, LL5 β and ELKS, are required for normal cortical CLASP accumulation and microtubule organisation. Since LL5 β contains a PIP3-binding pleckstrin homology (PH) domain it is proposed that LL5 β and ELKS can form a PIP3-regulated cortical platform, to which CLASPs attach distal microtubule ends.

Chapter 6 reports an optimized procedure to identify components of membrane-bound protein complexes with the use of mass spectrometry. For the cortical protein LL5 β , which is involved in attaching microtubules to the membrane, it is shown that at least one of the isolated potential partners, liprin- α 1, is indeed a component of the LL5 β clusters at the margin of HeLa cells. The identified connection between LL5 β and liprins requires further biochemical and functional analysis, which will be a subject of future studies.

The data described in the experimental chapters of this thesis are further discussed in Chapter 7 in the context of related studies on microtubule plus end binding proteins in other animal systems as well as in plants and in fungi.

Samenvatting:

Dit proefschrift beschrijft de functie van verschillende eiwitten die betrokken zijn bij de werking van het cytoskelet. Wat is nou zo'n cytoskelet? Planten en dieren zijn allemaal opgebouwd uit cellen, die op hun beurt weer organen vormen, zoals een blad aan een plant of een lever in een mens. Er zijn heel veel verschillende soorten cellen met elk hun specifieke functie en uiterlijk; denk bijvoorbeeld aan zenuwcellen, bloedcellen, epitheelcellen, enz. Cellen bevatten het genetische materiaal in de vorm van DNA en maken daarmee eiwitten aan die fungeren als bouwstenen, werkuitvoerders of boodschapper-signalen. Het DNA van mensen bevat zo'n 25.000 genen, die naar schatting meer dan 250.000 verschillende eiwitten coderen. Bepaalde eiwitten, zoals tubuline, binden aan elkaar d.m.v. een kop-staart verbinding en vormen zo een lange kabel of draad. Cellen maken op deze manier verschillende type draden, ook wel filamenten genoemd, die samen een stevig netwerk vormen; het cytoskelet (zie hoofdstuk 1, fig. 2).

Het cytoskelet is betrokken bij een aantal essentiële processen van de cel. Ten eerste biedt het stevigheid aan de cel zoals onze botten het skelet vormen van ons lichaam en voorkomen dat we niet in elkaar zakken. Aangezien het cytoskelet heel dynamisch is kan het er voor zorgen dat bepaalde cellen zich kunnen bewegen. Daarnaast worden de filamenten gebruikt als een soort lopende band of roltrap waarover actief transport kan plaatsvinden van plek A naar plek B binnen de cel. Dit gebeurt met speciale motoreiwitten die over de filamenten lopen met hun te transporteren lading. Een andere belangrijk proces waar het cytoskelet een rol speelt is celdeling. Wanneer een cel zich gaat delen wordt het genetische materiaal eerst gekopieerd om vervolgens te worden gescheiden over twee nieuwe dochtercellen. Mechanisch gezien moet het gekopieerde DNA dus uit elkaar getrokken worden, hetgeen gebeurt door de filamenten van het cytoskelet (zie hoofdstuk 1, fig. 4).

Voor het normaal functioneren van cellen is het cytoskelet dus essentieel. Het is dan ook te begrijpen dat wanneer er een foutje optreedt dit ernstige gevolgen kan hebben voor de cel. Zo kan een opeenhoping van het cytoskelet-bindende eiwit Tau in hersencellen leiden tot de ziekte van Alzheimer. Ook kan het cytoskelet bewust worden aangetast waarmee o.a. de celdeling wordt stopgezet om bijvoorbeeld tumoren te bestrijden.

Zoals gezegd kent het cytoskelet verschillende filamenten; de intermediaire filamenten, actine filamenten en de microtubuli. Dit onderzoek concentreert zich op microtubuli, buisvormige filamenten met een diameter van 25 micrometer en opgebouwd uit twee type bouwstenen ofwel eiwitten; α en β tubuline. Eén uiteinde (min-einde) van de microtubuli is stabiel en wordt vastgehouden bij het centrosoom in het midden van de cel. Aan het andere uiteinde (plus-einde) kunnen telkens tubuline bouwstenen worden ingebouwd waardoor de microtubuli langer wordt, en vallen er tubuline bouwstenen vanaf waardoor het korter wordt. Het is te vergelijken met het bouwen van een toren die telkens weer een stukje in elkaar stort om vervolgens weer opgebouwd te worden. Dit mechanisme zorgt voor het dynamische karakter van microtubuli. In de meeste cellen groeien microtubuli van het midden uit naar de rand van de cel. Om ervoor te zorgen dat de gebouwde toren niet

in elkaar stort kan het uiteinde gestabiliseerd worden door speciale eiwitten; microtubuli plus-eind bindende eiwitten. Deze groep van eiwitten binden dus aan microtubuli uiteinden, maar kunnen ook onderling een interactie aangaan. Zo kunnen er diverse eiwitcomplexen, verschillend in samenstelling, binden aan microtubuli uiteinden en daarmee de dynamiek van microtubuli reguleren. Een uitgebreidere introductie van het cytoskelet wordt beschreven in hoofdstuk 1. Dit proefschrift concentreert zich op de functionele analyse van eiwit interacties aan de plus-uiteinden van microtubuli.

In hoofdstuk 2 wordt beschreven hoe de binding van het microtubuli plus-eind bindende eiwit CLIP-170 met microtubuli is gereguleerd. Om aan microtubuli te binden heeft CLIP-170 een specifiek domein aan de kop-kant, echter kan dit domein naast microtubuli ook aan de eigen staart van CLIP-170 binden. Wanneer de kop-kant van CLIP-170 direct met de staart-kant verbonden is, dan is er een cirkelvormige conformatie waarbij de kop niet meer in staat is om aan microtubuli te binden. Ook andere eiwitten, zoals p150^{Glued} en LIS1, die normaal aan de staart van CLIP-170 zouden kunnen binden, worden nu gehinderd door deze conformatie.

Hoofdstuk 3 laat vervolgens zien dat CLIP-170 en CLIP-115 een directe interactie aan kunnen gaan met de staart-kant van EB-familie eiwitten (EB1, EB2 en EB3). De verbinding tussen deze eiwitten speelt een belangrijke rol voor de lokalisatie van CLIP-170 en verhoogt de affiniteit voor groeiende microtubuli uiteinden.

CLASP1 en CLASP2 zijn andere microtubuli plus-eind bindende eiwitten en reguleren de stabiliteit, dynamiek en dichtheid van microtubuli voornamelijk aan de randen van de cel. Dit wordt beschreven in hoofdstuk 4. Deze CLASPs blijken ook een complex te kunnen vormen met EB1 aan de uiteindes van microtubuli. Doordat CLASPs zich nabij het plasma membraan bevinden kunnen ze microtubuli plus-eindes binden en daarmee de dichtheid vergroten van microtubuli aan de randen van de cel.

In hoofdstuk 5 wordt de vondst beschreven van twee nieuwe bindingspartners van CLASP1 en CLASP2 m.b.v. massaspectrometrie; LL5 β en ELKS. Beiden zijn betrokken bij de normale, microtubuli-onafhankelijke, lokalisatie van CLASPs nabij het plasma membraan. LL5 β heeft een special domein waarmee het zich kan vastankeren aan het membraan. Naast dit domein blijkt er echter nog een andere factor of eiwit bij betrokken te zijn, welke is getracht te identificeren in hoofdstuk 6.

Hoofdstuk 6 beschrijft een geoptimaliseerde procedure voor het identificeren van membraan gebonden eiwitten m.b.v. massaspectrometrie. Hiermee is een potentiële bindingspartner van LL5 β geïsoleerd, liprin- α 1, welke mogelijkwerwijs betrokken is bij de vastankering van LL5 β aan het plasma membraan.

Tot slot geeft hoofdstuk 7 een overzicht van de microtubuli plus-eind bindende eiwitten in verschillende organismen zoals gisten, planten en zoogdieren. EB1 wordt als centraal eiwit beschouwd welke interacties kan aangaan met veel verschillende type eiwitten. Hierdoor zou EB1 een sleutelfunctie kunnen hebben voor het ontrafelen van werkingsmechanismen van de structuur en dynamiek van microtubuli en hun rol in de architectuur van de cel.

Curriculum Vitae

Name: Gideon Willebrordus Adrianus Lansbergen
Born: 8 August 1978, Rotterdam, The Netherlands

October 2001 – October 2005

PhD, Department of Cell Biology and Genetics,
Erasmus University Medical Centre Rotterdam
Functional Analysis of Protein Interactions at Microtubule Tips.
Prof.dr. F. Grosveld (promotor) and Dr. A. Akhmanova (co-promotor)

September 1997 – September 2001

Master of Science, Faculty of Biology, University of Utrecht.

- Traineeship 1: Research Institute of Toxicology (RITOX), Utrecht
Effects of organotin compounds and diindolyl-methane's on CYPs, involved in estradiol synthesis and metabolism, in H295R human adrenocortical carcinoma cells and MCF-7 breast cancer cells.
Prof.dr. M. van den Berg and Prof.dr. W. Seinen
- Traineeship 2: Experimental Urology, Erasmus University Rotterdam.
Mechanism of androgen-independent growth of PC-346C human prostate cancer cells.
Prof.dr. F. Schröder and Dr. J.C. Romijn
- Graduation paper: Physiological Chemistry, University of Utrecht
Protein kinase B signalling pathway and the biology of ageing.
Prof.dr. B. Burgering and Prof.dr. J. Bos

1991 – 1997

Athenaeum at City College St. Franciscus, Rotterdam

Publications:

Yulia Komarova , **Gideon Lansbergen** , Niels Galjart , Frank Grosveld , Gary G. Borisy and Anna Akhmanova

EB1 and EB3 control CLIP dissociation from the ends of growing microtubules.

Mol Biol Cell 2005 Nov;16(11): 5334-5345.

Mimori-Kiyosue Y, Grigoriev I, **Lansbergen G**, Sasaki H, Matsui C, Severin F, Galjart N, Grosveld F, Vorobjev I, Tsukita S, Akhmanova A.

CLASP1 and CLASP2 bind to EB1 and regulate microtubule plus-end dynamics at the cell cortex.

J Cell Biol. 2005 Jan 3;168(1):141-53.

Lansbergen G, Komarova Y, Modesti M, Wyman C, Hoogenraad CC, Goodson HV, Lemaitre RP, Drechsel DN, van Munster E, Gadella TW Jr, Grosveld F, Galjart N, Borisy GG, Akhmanova A.

Conformational changes in CLIP-170 regulate its binding to microtubules and dynactin localization.

J Cell Biol. 2004 Sep 27;166(7):1003-14..

Stepanova T, Slemmer J, Hoogenraad CC, **Lansbergen G**, Dortland B, De Zeeuw CI, Grosveld F, van Cappellen G, Akhmanova A, Galjart N.

Visualization of microtubule growth in cultured neurons via the use of EB3-GFP (end-binding protein 3-green fluorescent protein).

J Neurosci. 2003 Apr 1;23(7):2655-64.

Sanderson, J.T., Boerma, J., **Lansbergen, G.W.A.**, van den Berg M.

Induction and inhibition of aromatase (CYP19) activity by various classes of pesticides in H295R human adrenocortical carcinoma cells.

Toxicol Appl Pharmacol. 2002 Jul 1;182(1):44-54.

Sanderson, J.T., Slobbe, L., **Lansbergen, G.W.A.**, Safe, S. and Van Den Berg, M.,

2,3,7,8-Tetrachlorodibenzo-p-dioxin and Diindolylmethanes Differentially Induce Cytochrome P450 1A1, 1B1, and 19 in H295R Human Adrenocortical Carcinoma Cells.

Toxicol Sci. 2001 May;61(1):40-48.

Dankwoord:

Het tot stand brengen van een proefschrift heeft vanzelfsprekend heel wat voeten in aarde en is iets wat je alles behalve alleen doet. Naast het vier jaar lang pipetteren en gieten van ruim 1000 SDS-PAGE gels hebben heel veel mensen mij op verschillende wijze geholpen en gesteund om tot dit eindresultaat te komen. Ik wil dan ook beginnen met iedereen te bedanken die in welke vorm dan ook hun steentje hebben bijgedragen aan de totstandkoming van dit proefschrift. Bepaalde mensen wil ik nog in het bijzonder bedanken.

Allereerst mijn promotor Frank, van wie ik goede sturing en advies heb gekregen gedurende mijn promotie. De informele werkbeprekingen bij jou op de bank waren zeer leerzaam en hebben mij voldoende inspiratie gegeven voor mijn onderzoek. Bedankt hiervoor.

Mijn co-promotor Anna, zonder jou had ik dit niet bereikt. Van jou heb ik zo ontzettend veel mogen leren wat betreft het pipetteerwerk, het opzetten van experimenten, het interpreteren van resultaten, het presenteren, en ga zo maar door. Jij wist altijd precies de juiste experimenten te verzinnen en had gauw door wanneer iets gedoemd was te mislukken. Deze efficiënte manier van wetenschap bedrijven heeft mede geleid tot mooie publicabele resultaten en daarmee ook dit boekje. Bedankt ook voor al het geduld en tijd die je voor me had, en de mogelijkheid om bij jou te kunnen promoveren als eerste AIO. Was het heel erg?

Verder wil ik Gerard bedanken voor de interessante werkbeprekingen op de 12^e. Jammer eigenlijk dat de groep te groot werd waardoor we niet meer met elkaar op je kamer konden zitten. Fijn dat je bereid was om deel te nemen in de kleine commissie als secretaris. Hierbij wil ik tevens de overige leden van de promotiecommissie bedanken voor het lezen en bekritisieren van mijn proefschrift; Niels, Dies, Sjaak en Roland.

Dit proefschrift bevat ook data die verkregen zijn door andere mensen en door samenwerkingen met andere internationale labs. Om te beginnen wil ik Yulia Komarova en Yuko Mimori-Kiyosue bedanken voor de vele experimenten en metingen die zij verricht hebben die mede hebben bijgedragen aan dit proefschrift. Hierbij noem ik ook de betrokkene Gary Borisy, Holly Goodson, David Drechsel, Erik van Munster, Theodorus Gadella, Hiroyuki Sasaki, Chiyuki Matsui, Fedaor Severin, Ivan Vorobjev, Shoichiro Tsukita en Toshihisa Ohtsuka. Claire Wyman bedankt voor het maken van de prachtige Scanning Force Microscopy plaatjes van CLIP-170. Mauro Modesti bedankt voor alle medewerking betreffende de eiwitexpressies, Baculovirus-technieken en alle hulp bij de FRET-metingen. Casper Hoogenraad bedankt voor de goede samenwerking en alle advies. Het is toch bijzonder dat ik met de mass spec een eiwit oppik waar jij juist aan gewerkt hebt. Wat betreft al het mass spec werk wil ik Jeroen en Karel heel erg bedanken voor de vele gels die jullie gerund hebben over de Q-TOF. We moeten trouwens nog steeds eens uitzoeken of al die keratines nou van mij of van jullie waren!

Dan wil ik alle mensen van lab1063 en 1030 in het bijzonder bedanken voor alle gezelligheid binnen en buiten de werktijden. Jullie hebben mij een leuke tijd bezorgd waar

ik goede herinneringen aan zal blijven houden. Ik ben blij dat ik jullie toch een stukje Jazz-kennis heb mee mogen geven door constant Arrow Jazz Fm aan te zetten in het lab (sorry Niels). Wie heeft trouwens die batterijen van de afstandsbediening?

Uiteraard wil ik mijn labgenoot en bench-buurman Daniël bedanken, je bent een gezellige kameraad om mee samen te werken en je hebt een goed gevoel voor humor. Dagelijks “Jensen in de middag”, alle verhalen over je wilde poezen thuis en bijna standaard 17:00 uur telefoon voor mij van het thuisfront (mis je het al?). Fijn dat je mijn Lambda-Pst taak zo graag over wilde nemen. Voor eventuele vragen kun je beter bij Michiel terecht denk ik. Succes in het Russische lab en bedankt dat je mijn paranimf wilt zijn.

Ilya, it was a surprise that we share our birthday on the 8th of August once we both arrived with cake on the same day. In addition we share the same hobby photography, and so you gave me enough inspiration and interesting tips about Photoshop. Thanks for all your help and assistance concerning the quantification measurements and statistical analyses.

Marja, met jou ben ik ongeveer tegelijkertijd begonnen en we zaten dus zo’n beetje in hetzelfde schuitje (en dezelfde zitkamer). De congressen en workshops waren altijd reuze gezellig, zeker wanneer ook de aanhang werd overgevoegen. Lekker stofrijden met de huurauto in Nice. Wanneer gaan we weer eens mountainbiken in Gosau tegen de berg op? Voel je niks van! Bedankt voor de gezellige tijd en veel succes met het afronden van je eigen promotie. Leuk dat je mijn paranimf wilt zijn.

Marco, geen groter genot dan een western blot! Ik zal de Huub Hangop-CD achterlaten zodat je kunt blijven genieten van dat “leke reddingsvest” en Nol. Ook nog bedankt namens “mijn vrouw”, voor de gelegenheid tot het vullen van je blauwe puntjes!

Jeffrey, wanneer er weer een BBQ in Tiel komt dan hoor ik dat graag. Ook voor Hollandse tegeltjes met spreuken houd ik me aanbevolen. Wellicht gaan we nog eens naar ‘t North Sea Jazz, of een concert van Treble; kijken of ze weer uit de maat slaan als ze naar ons kijken.... Trouwens sorry dat bijna de hele afdeling je Flipje noemde.

Frank, jouw eerste week op het lab zal ik niet snel vergeten, dat spontane luide geloei en wolvengejank. Jouw lab-video’s, week-CDs, week-trofee’s, de ontdekking van het “Rottûrdamse fenotype”, je muzikale(?) inbreng, en niet te vergeten Mabel, maakte je een bijzondere labgenoot. Mocht je nog een panoramafoto willen maken dan weet je me wel te vinden.

Suzanne de M&M-koningin, bedankt voor je soms heerlijke naïviteit. Wanneer je nog eens met Marco en mij mee wilt naar de Apenheul om 6 uur ’s morgens (tegen de mensenstroom in want dan heb je alle apen voor jezelf) dan moet je het maar zeggen. Sorry nog voor het maken van die succesvolle Suzanne-CD.

Ook bedank ik Nanda, Michael, Katharina, Xenia, Helen, Laura, Michiel en natuurlijk niet te vergeten Phebe, Rick, en Bjorn.

Verder ook dank aan de EDC-medewerkers (Ed, Ron, Esther), alle dames uit de spoelkeuken, de deskundige heren van de computers, Arthur, en natuurlijk mijn speciale dank aan Melle met wie ik voor sommige een heel bijzondere band had (je wist vaak mijn

pakjes persoonlijk af te geven op mijn bench). Marike en Jasperina bedankt voor de administratieve hulp en gezelligheid, we spreken elkaar nog wel op een van de concerten van Trijntje Oosterhuis. Ook bedankt Tom de Vries Lentsch voor de grafische ondersteuning aan dit proefschrift en alle tijd die je hierin hebt gestoken.

Uiteraard wil ik ook mijn ouders, (schoon)familie en vrienden bedanken voor hun steun en interesse in mijn onderzoek. Het viel niet altijd mee om uit te leggen wat ik nou precies aan het doen was, toch iets met cellen en eiwitten? Wellicht geeft dit proefschrift wat meer duidelijkheid.

Tot slot natuurlijk mijn grote dank naar mijn lieve vrouw Marieke voor alle warmte liefde, steun en advies van de afgelopen jaren en al het geduld dat je met me hebt gehad (“wanneer kan ik nou achter de computer?”). Je bent een kanjer!

Hora Est!